بسم الله الرحمن الرحيم

Sudan University of Science and Technology

Collage of Graduate Studies and

Scientific Research

Synthesis, Characterization and Biological activity of Some Amino Acid and Mixed Amino Acid Complexes with Some Transition Metals

تخليق وتوصيف والنشاط البيولوجي لبعض الاحماض الامينية وخليط من الاحماض الامينية لبعض

معقدات العناصر الانتقالية

A Thesis Submitted in Fulfillment Requirements of Doctor of Philosophy in chemistry

By:

Afra Murtada Yassin Mustafa

(B.Sc, H. Diploma, M.Sc Chemistry)

Supervisor:

Dr. Abdalslam Abdalla Dafalla

September 2019

بسم الله الرحمن الرحيم

استهلال

قال تعالى:

يَا أَيُّهَا الَّذِينَ آمَنُوا إِذَا قِيلَ لَكُمْ تَفَسَّحُوا فِي الْمَجَالِسِ فَافْسَحُوا يَفْسَحِ اللَّهُ لَكُمْ وَإِذَا قِيلَ انشُزُوا فَانشُزُوا يَرْفَعِ اللَّهُ الَّذِينَ آمَنُوا مِنكُمْ وَالَّذِينَ أُوتُوا الْعِلْمَ دَرَجَاتٍ وَاللَّهُ بِمَا تَعْمَلُونَ خَبِيرٌ ﴿١١﴾

صدق الله العظيم

سورة المجادلة الآية رقم (11)

Dedication

To:

My parents, Murtada Yassin and wafa Mohamed.

My brothers, Mohamed and Ahmed, and my sister Esra.

My husband, Mohamed Osman and my daughter, Aryam.

Acknowledgement

ABSTRACT

Fourteen Amino acid complexes, eight complexes $[M(L)_2]Cl$ type of Co (II) ion with glycine, serine, arginine, aspartic acid, Cu (II) and Fe (III) ions with glycine, Zn (II) ion with cysteine, and Ni (II) ion with leucine, five mixed amino acid complexes $[M(L)(L´)]Cl$ type of Au (III) ion with (glycine+ asparagine) , and (Serine+ Cysteine), Fe (III) ion with (Arg+Asp), Ni (II) ion with (cysteine+leucine), and Zn (II) ion with (asparagine+lucien), and one mixed amino acid complex $[M(L)(L´)(L´´)]$ type of Fe(III) ion (Arg +Asp+Ser), have been synthesized and characterized using EDX, FTIR, UV/Vis, TGA, XRD, spectra and conductivity measurements.

All amino acid ligands with metal ions have been found to act as bidentate chelating agents coordinating through COO^- and NH_2, to form octahedral geometry for Co (II), Cu (II), Ni (II) and Fe (III) complexes, squire planer geometry for gold (III) complexes, tetrahedral geometry for Zn (II) complexes.

The antibacterial activity of amino acid complexes were evaluated against five bacterial strains, three kinds of Gram positive (*Staphylo coccus aureas, Entero coccus feacalis, Klebsiella pneumonia*), and two kinds of Gram negative (*Escherichia coli, Pseudomonas aeruginosa*). The metal ions complexes were found to have good and varied degree of inhibitory effect against test bacteria.

مستخلص البحث

تم تخليق اربعة عشر معقدا حمض امينى، ثمانية معقدات خلقت من تفاعل نوع واحد من الاحماض الامينية مع ملح الايون بنسبة 1:1 وهم ملح ايون الكوبالت ثنائي التكافؤ مع الجلايسين، السيرين، الارجنين، وحمض الاسبارتيك، وملح ايون النحاس ثنائى التكافؤ وملح ايون الحديد ثلاثى التكافؤ مع الجلايسين، ملح ايون الزنك ثنائى التكافؤ مع السيستين، وملح ايون النيكل ثنائى التكافؤ مع الليوثين، خمسة معقدات احماض امينية خلقت من تفاعل نوعين مختلفين من الاحماض الامينية مع ملح الايون بنسبة 1:2 وهم ملح ايون الذهب ثلاثى التكافؤ مع (جلاسين+اسبرجين) و (سيستين+سيرين)، ملح ايون الحديد ثلاثى التكافؤ مع (حمض الاسبارتيك+الارجنين)، ملح ايون الزنك ثنائى التكافؤ مع (اسبرجين+ليوسين)، وملح ايون النيكل ثنائى التكافؤ مع (سيستين+ليوسين)، ومعقد واحد خلق من تفاعل ثلاثة انواع مختلفة من الاحماض الامينية بنسبة 1:1:1 من ملح ايون الجديد ثلاثى التكافؤ مع (سيرين+ارجنين+حمض الاسبارتيك)، وتم التعرف عليهم بواسطة اجهزة التحليل المختلفة وهى جهاز مطيافية تشتت الطاقة بالاشعة السينية ومطيافية الاشعة تحت الحمراء ومطياف الاشعة المرئية وفوق البنفسجية والتحليل الحراري الوزني وحيود الاشعة السينية وقياس التوصيلية الكهربائية. وتم التوصل الي ان الاحماض الامينية الاربعة تعمل كعوامل مخلبية ثنائية التنسيق مع الايونات. وتم تقييم النشاط الحيوي للمعقدات كمضادة للبكتريا مقابل خمسة سلالات بكتيرية، ثلاثة انواع من الجرام ايجابية ، ونوعان من الجرام سالبة ، ووجد ان لها خاصية كابح ضد البكتريا بصورة جيدة وبدرجات متفاوتة.

Table of contents

List of Tables

List of Figures

List of Abbreviations

AAS: Atomic Apsorbtion spectra.

AD: Alzheimer's disease.

ADMA: asymmetric dimethylarginine.

Ala: Alanine.

ALA: Amino levulinic Acid.

ALS: Amyotrophic Lateral Sclerosis.

AMP: Adenosine monophosphate

ANPS: 2-amino-4-nitrophenol-N-salicylidene.

AR grade: Grade Analytical reagents.

Arg or R: Arginine.

Asn or N: Asparagine.

Asp or D: Aspartic acid.

ATP: Adenosine triphosphate.

BCAAs: branched chain amino acids

BC: British Columbia.

Bipy: 2,2'-bipiridyl.

BS: bovine serum.

BSE: back scattered electrons.

Bzdtc: Benzyldithiocarbamate.

CA: Candida albicans.

CC_{50}: 50% cytotoxic concentration.

CFU: Colony-forming Unit.

CT: charge transfer.

Cys: Cysteine

Cysme: cysteine methyl ester.

DDAH: Dimethylearginine dimethyle aminohydrolase.

DiPrdtp: Dibenzyldithiophosphate.

DMF: Dimethylformamide.

DMSO: Dimethyl sulfoxide.

DNA: Deoxyribonucleic acid.

DTA: Differential Thermal Analysis.

E. coli: Escherichia coli

EC 1.1.1.95: Phosphoglycerate dehydrogenase.

EC 2.6.1.52: A pyridoxal-phosphate protein.

EC 3.1.3.3: Phosphoserine phosphatases.

ECM: Cell biology molecule

EDTA: Ethylenediamietetraacidic acid.

ER: Endoplasmic reticulum.

FDA: Food and Drug Administration.

FNB: Food and Nutrition Board.

GC-MS: Gass chromorography-mass spectrometry.

Gly or G: Glycine.

His: Histidine.

Hisme: Histidine methyl ester.

HMB-CoA: β-hydroxy β-methylbutyryl-CoA

HMG-CoA: hydroxymethylglutaryl-CoA

HS: High senstivity.

Ibs: Pound singular.

IgE,G,M: immunoglobulin E, G, M.

iNTD: International Working Group on Neurotransmitter Related Disorders.

IPSP: Inhibitory postsynaptic potential.

IR spetra: Infrared spectra.

LC_{50}: lethal concentration.

LDH: Lactate dehydrogenase.

Leu: leucine.

Lys: lysine.

MC-CoA: β-methylcrotonyl-CoA.

MDA: malondialdehyde.

MDBK: Madin-Darby boving kidney

Met: Methionine.

MIBK: methyl iso butyl ketone.

MIC: minimum inhibitory concentration.

ML: Magnatic momentum.

MLCT: Metal-ligand charge transfer.

MNC: maximal nontoxic concentration.

MRSA: Methicillin Resistant Staphylococcus aureus.

MS: Meduim senstivity.

MTC: Ministerio de Transport and Communication

mTHF: methylenetetrahydrofolate.

mTOR: mechanistic Target Of Rapamycin.

M.wt: Molecular weight.

NADH: Nicotinamide adenine dinucleotide.

n: Number of mole.

NAC: N-acetyl-cysteine.

NASA: The National aeronautics and Space Administration.

NAD: Nicotinamide adenine dinucleotide.

N-MeCHdtc: N-Methylcyclohexyldithiocarbamate.

NMDA: N-Methyle-D-aspartic acid

NMDAR: N-Methyle-D-aspartate reseptor.

NMR: Nuclear magnetic resonance.

NOS: Nitric oxide synthase.

PAD: Protein arginine deiminases.

PCEDX: Power Consumption Energy Dispersive X-ray fluorescence.

pH: Acidity or basicty of an aquose solution.

Phe: phenylalanine.

pKa: Acid dissociation constant.

PLP: Product Longevity program.

Ppm: Part per melion.

Pro: proline.

r: Corrilation coffeition.

R: Ressisstant.

RDAs: Recommended Dietary Allowances.

S: Spin multiplicity.

S. aureus: Staphylococcus aureus.

SDS-PAGE: Sodium dodecyl sulfate-polyacrylamide gel electrophoresis.

SD: Stander deviation.

Ser or S: serine.

SHMT: serine transhydroxymethylase.

SS: Small senstivity.

SOD: superoxide dismutase.

TGA: Thermogravemetric analysis.

TGD: Thermogravimetry differential.

THF: Tetrahydrofuran.

Thr: threonine.

tRNA: Transfer ribonucleic acid.

Tyr: Tyrosine.

UL: upper intake level.

USAMV: Universty of Agronomic Sciences and Veterinary Medicine of Bucharest.

USP: United States Pharmacopeia.

UV-Vis spetra: Ultraviolate-visble spectra.

WHO: World Health Organization.

Wt(g): Weight per gram.

XRD: X-ray diffractometry.

Δ_o: Spillting energy.

α-KIC: α-ketoisocaproate.

ΔGo: change of Gibbs free energy.

ΔHo: change of enthalpy.

ΔSo: change entropy.

εmax: extinction coefficient.

λmax: Maximum wavelength.

μl: Microleter.

δ3: Three stander deviations of the mean.

Chapter One

INTRODUCTION

INTRODUCTION

1.1 Background

The microbial resistance represent a problem and the outlook for the use of antimicrobial drugs in the future is still uncertain. Therefore, it must be taken measures to reduce this problem, for example, to control the use of antibiotic, develop research to better understand the genetic mechanisms of resistance, and to continue studies to develop new drugs, either synthetic or natural. The ultimate goal is to offer appropriate and efficient antimicrobial drugs to the patient.[1] for centuries, people have used cobalt and other ions to inhibit the growth of harmful microbes.

Coordination complexes of transition metals have been widely studied for their antibacterial, antifungal and potential cytotoxic chemotherapeutic agents. They have been evaluated against several pathogenic fungi and bacteria with promising results. One of the approaches to increases the efficacy of the drugs consists in their modification of physical and chemical factors. In addition to its ability to combat infection or neoplastic disease, these new agents must exhibit selective toxicity, chemical stability, and optimum rates of bio-transformation and elimination[2].

The chemistry of gold has attracted increasing attention in antitumor chemotherapy [3,4]. Complexes of gold (III) with bidentate ligands presented a number of important applications in chemotherapy, diagnostics, catalysis and surface chemistry[5,6]. Some gold complexes have been used as injections to reduce the pain and swelling of rheumatoid arthritis and tuberculosis[7]. Amino acids are well known of their biological importance as structure units that build up proteins, and their common use in nutritional supplements, fertilizers and food technology[8-10]. Amino acids and their metal complexes are important compounds in many biological, industrial and agricultural aspects[11,12]. Mixed ligand complexes play an important role in biological activities against pathogenic microorganism[13].

In recent years transition metals amino acid complexes have received much attention because the proved to be useful antibacterial agent applied against *staphylococcus aureus*, *Escherichia coli*, and nutritive supplies for humans and animals[14]. Twenty natural amino acids comprise the building block of proteins, which are chemical species indispensable to perform a large number of biological functions[15]. From these twenty amino acid, eight are essential and cannot be products by human body. Complexes of transition metal with amino acids in proteins and peptides are utilized in numerous biological processes, such as oxygen conveyer, electron transfer and oxidation. In these processes the enzymatic active site which is very specific, forms complexes with divalent metal ions[16].

When minerals such as zinc, copper, iron and others are chemically bonded to amino acids with at least two bonds from each amino acid, rings of atoms attached to the minerals result and chelation has occurred. Chelation occurs naturally in the body to facilitate transport of minerals across the intestinal wall as part of digestion[17,18]. Numerous papers have been published on metal complexation of amino acids during the past years because they proved to be useful chelation agents, as anti-inflammatory agents, as antibacterials applied against Escherichia coli and Streptococcus pyogenes[19].

1.2 Literature review

1.2.1 Antibiotics

1.2.1.1 Overview

Periodontal illnesses, as a group of illnesses that are caused by a combination of bacteria and oral variable bacterial flora, require local treatment at dental clinics, and, in special cases, are also associated with oral antibiotic combinations, with systemic action. According to oral pathologies, only one antibiotic or a combination of antibiotics may be prescribed. The whole difference between these two forms of recipes exists in the dosages of antibiotics. When prescribing a single antibiotic, we prefer a dose of 500 mg, but for two antibiotic prescriptions, dosages are reduced to 250 mg for each antibiotic in the combined group of antibiotics. Antibiotic combinations are preferred to be used with the intention of hitting the bacterial flora according to its characteristics aerobic, anaerobic, gram-negative, and gram-positive with certain antibiotics acting on certain bacteria. Each of the selected antibiotics is effective only in the case when the total periodontal curettage is completed; otherwise, it can gradually be passed to the diagnosis of refractory periodontitis. According to a study on the effects of combined antibiotics, amoxicillin and metronidazole are given after complete curettage; the application of antibiotics leads to much better clinical results compared to the periodontal treatment with mechanical curettage alone. According to the same study, this combination of antibiotics fights T. forsythia in a manner that prevents recolonization for up to 6 months after treatment. This element provides stability through the impairment expectancy of this periodontal treatment[20]. In addition combination of periodontal microbiology and antibiotic therapy qualifies as a normal extension of periodontal treatment, followed by a proper clinical diagnosis[21.]

1.2.1.2 Side Effects of Antibiotics Prescribed in Periodontal Recipes:

Data, preferably expressed in percentages, were collected from literature on the side effects of some antibiotics which are most frequently prescribed in periodontal recipes. These data are listed according to the prescribed antibiotic.

1.2.1.3 Penicillin's

During the application, amoxicillin causes hypersensitivity, manifesting in cross reaction and sensitivity towards degradation products with alkaline hydrolysis. Allergic reactions to penicillin are as frequent as 5–8% of cases, in contrast to penicillin anaphylactic shock, which occurs in the interval of 0.05% [22]. Nephritis, eosinophilia, and hemolytic anemia are other side effects that may be associated with typical oral lesions. Nausea, vomiting, diarrhea, and gastrointestinal problems appear in the case of the application of oral doses. Vaginal candidiasis is often caused by the application of ampicillin and amoxicillin. For penicillin, these are the efficiencies registered: anaphylactic allergic reaction, immunoglobulin E (IgE) 10%, urticarial rash; nontoxic antibiotic; eosinophilia 1–2%, 6–9%, late reaction of IgG/IgM: 1–5%; nephritis, fever, eosinophilia, hematuria: 1–2%; hematological reactions, hemolytic anemia, immune thrombocytopenia, leukopenia 1–5%; nervous system: epileptogenic action, encephalopathy; gastrointestinal system: diarrhea, pseudomembranous colitis, dysbacteriosis; cross allergy 10%; problems in the balance of electrolytes (Na, K). Broad spectrum antibiotics are not intended for epileptic women, or for those who use oral contraceptives[23].

1.2.1.4 Cephalosporin's

Cephalosporins may cause patient hyper sensibility with the same frequency as penicillin's. Their chemical structure somewhat differs from penicillin's, and penicillin allergic patients may not exhibit hypersensitivity to cephalosporin's. Allergic reactions occur in 5–10% of cases. For cephalosporin's, the following data have been registered: non-toxic, side effects 1–10%; allergies, hives, morbilliformsigns, eosinophilia, 1–2%; gastrointestinalproblems4%; 2%hematological reactions; intolerance to alcohol; nephrotoxicity, allergic interstitial nephritis. They are indicated in cases of female genital organ infections, meningitis, urinary tract infections, infections of the skin, and for surgical prophylaxis. Interaction with drugs: theophylline, streptomicin.

1.2.1.5 Tetracyclines

Tetracycline has gastrointestinal side effects, nausea, vomiting, and diarrhea. Tetracycline modifies the normal intestinal flora, inhibiting coliform organisms and allowing the overproduction of Pseudomonas, Proteus, and Clostridium. Vaginal candidiasis is associated with taking tetracycline[24]. Tetracycline is fixed to the structure of newly formed teeth, if it is taken during certain periods of pregnancy, such as at the fetal development stage. Liver toxicity occurs in cases where patients have previously had hepatic insufficiency, or when tetracycline is given intravenously. Tetracycline renal toxicity occurs when it is given together with diuretics, after nitrogen retention products. Local tissue toxicity appears with venous

thrombosis, and sensitivity to light is another side effect. Nausea and dizziness occur in 35–70% percent of cases[24].

1.2.1.6 Macrolides

Macrolides have gastrointestinal effects, such as gastrointestinal intolerance, which is related to the stimulation of bowel motility. They may cause acute hepatitis with fever and jaundice. The state of most patients can be improved after discontinuing the drug, but the symptoms may reappear after resuming its administration. Allergicreactionsincludefever, eosinophilia, and rash. Macrolides may increase serum concentrations of many drugs, such as theophylline, oral anticoagulants, cyclosporin, and metilprednizolon. Erythromycin increases plasma concentrations of oral digoxin, increasing its bioavailability[24]. Azithromycin differs from erythromycin and from claritromycina due to its pharmacokinetic characteristics. A dose of 500 mg of azithromycin provide slower plasma concentrations of 0.4 micro g/mL Azithromycin penetrates well into most tissues except the brain fluid, at concentrations 10–100 times higher than plasma concentrations. The tissue half-life is 2–4 days and ensures an elimination half-life of approximately 3 days. These properties allow azithromycin to be taken once a day and with a shorter duration of therapy. It should be taken 1 or 2 h before meals. It does not interact with other drugs, unlike erythromycin and clarithromycin [24]. Erythromycin has the following side effects: gastrointestinal problems occur in 3–4% of cases; skin allergies (1–2%); problems of the central nervous system (1–2%). It is indicated in cases of patients allergic to penicillin. It shows interaction with other medications such as theophylline.

1.2.1.7 Metronidazole

Antiprotozoal, as metronidazole, has a more powerful antibacterial activity against anaerobes, such as Clostridium. The 250 mg oral dose penetrates into the cerebrospinal fluid. Metronidazole is metabolized in the liver. Bacterial vaginosis is well treated with metronidazole. Nausea, diarrhea, stomatitis, and neutropenia are the most frequent side effects. Metronidazole offers dentists a good degree of efficiency, several advantages, and relatively minor side effects. It is the antibiotic against which suspects are still in the clinical development of resistance[21]. Based on the data provided by the literature, it appears that tetracycline causes discoloration of the teeth, gastrointestinal disorders, rare allergy, photosensitivity, nitrogen retention, and progressive uremia. It shows interactions with coumarin.

1.2.1.8 Clindamycin

Clindamycin has side effects like neutropenia, diarrhea, nausea, and enterocolitis. Clindamycin is displayed with the following information: skin allergy occurs in 10% of cases, while gastrointestinal

disturbances occur in about 11% of cases. Indicated in the case of patients allergic to penicillin, erythromycin is the postsecondary opportunity. It is indicated for the treatment of acne and osteomyelitis. It shows interactions with theophylline. Simultaneously giving the diuretic furosemide or other antibiotics, such as vancomycin, should be avoided because they empower nephrotoxicity. Side effects are auditory damage, vertigo, ataxia and loss of balance, and others. Given alone, side effects appear as follows: it affects the gastrointestinal system, with consequences such as nausea, vomiting, and diarrhea, as well as the nervous system, causing peripheral neuropathy, encephalopathy, hallucinations, etc.; intolerance to alcohol, associated with the emergence of an unpleasant metal taste in the mouth, and the brown coloration of urine.

1.2.1.9 Carbapenem

Carbapenem displays the following side effects: gastrointestinal disturbances, vomiting, nausea (4%), diarrhea (3%); pseudomembranous colitis (0.16%); appearance of skin allergy, to the extent of 2.7%; nervous system disturbances occur in 3% of cases; hematological problems appear in 0.3%. Side effects are estimated at the time of the analysis of antibiotic therapy indications, with indications for the purpose for therapy or for prophylaxis. Side effects are caused because antibiotics are foreign materials in the body. They have chemical structures that can cause toxic effects. They can cause allergies through the IgE. As foreign material in the body, the biological effects are also expressed in the body.

1.2.1.10 Discussion

When granting antibiotics, it is best to rely on microbiology diagnostics. This means that the sensitivity of certain bacteria to antibiotics must be found. Thus, we are convinced that the antibiotic effect will be adequate. Plaque and biofilm must be mechanically removed before giving antibiotics[25]. If antibiotics are not selected properly, higher pathogenicity is allowed through the transfer of genetic material for increased virulence and antibiotic resistance in oral microflora[26]. In cases of periodontal treatment, this type of control is difficult because the laboratory conditions for planting and microbiology diagnostics of oral bacterial flora are incomplete. The prescription of antibiotics is carried out on the basis data obtained from the periodontal clinical examination of the patient. Clinical examination reveals the presence of certain bacteria, such as plaque color change. It is known that the typical color of plaque changes depending on what bacteria or bacterial compound are included in the plaque structure. The color ranges from white to yellow, orange, green, cherry, or coffee. These color fluctuations show the presence of bacteria expressing the specific layer that gives color. Knowing the characteristics of bacteria and comparing the sensitivity, doctors can also prescribe a combination of

antibiotics. We strive for a broad-spectrum antibiotic to combine with narrow-spectrum antibiotics, and, further, for a field with the element fighting both aerobes and anaerobes. However, after an oral antibiotic is taken, its absorption causes a reaction in the system throughout the organs; that is the road that takes this hematological antibiotic to the gingiva and other organs. Doses of certain antibiotics express their concentration in area of gums. Besides the positive effect of the antibiotic, side effects may also be encountered expressed in organs and other systems of the body. Based on the above data about the side effects of antibiotics applied in the treatment of periodontal diseases, the obtained results show that patients are at the risk of:

- Allergy (5%),

- Nephritis (3%),

- Hematological problems (2–2.5%),

- Gastrointestinal problems (5.5%),

- Disturbance in the nervous system (2%),

- Signs of allergy on the skin (5.5%),

- Problems with electrolytes displayed in lower percentages.

Allergies against drugs are expressed as main and primary complications in 5% of cases. The hematologic system, gastrointestinal system, nervous system, cardiovascular system, and kidneys all appear in a list of issues that manifest as side effects. Interaction with different medications is present. The influence on the body systems is 4% in total, the maximum value of which is expressed on the skin, and the minimum value of which is expressed in the nervous system. Jaundice is a side effect that occurs as result allergic reactions in other organs, with the added value of IgG-IgM complexes (non-IgE). Most antibiotics are associated with disorders in the normal function of platelets and red blood cells. They affect intestinal flora, necessary for the absorption of vitamin K, and can lead to bleeding problems. In this sense, the percentage of gastrointestinal disorders (5.5%) affects the percentage of hematological problems (2.5%). It should be noted that those impacts are proportional. Taking antibiotics affects the effects of other drugs that patients take, in the context of binding proteins for transport. We stress that the nervous system disturbances are present in lower percentages and only in the cases of overdose of antibiotics. With the termination of treatment with the antibiotic, everything returns to normal. Side effects are divided by the class and proximity of antibiotics with each other; this is linked to the similarity in their chemical structure. The percentage of bacterial resistance to the antibiotic classes is not reflected in the results. This is because the purpose of the study was a simple analysis of values of

percentages of side effects only, and not the effects on bacterial strains. So, when giving a prescription, we balance between the percentage of side effects, the percentage of bacterial resistance, and the percentage of success based on the recommended dose of antibiotics. Local drug delivery as an active treatment or maintenance therapy depends on clinical findings, responses to treatment described in the literature, desired clinical outcomes, and patients' dental and medical histories, including their past usage of antimicrobials[27]. A meta-analytic study demonstrated that statistically significant though not clinically substantial improvement could be achieved in cases of chronic periodontitis when local delivery of tetracycline was used as an adjunct to scaling and root planning[28]. Tetracycline fiber therapy along with scaling and root planning improves the healing outcome, namely, the reduction in pocket depth and gain in clinical attachment level, when compared to scaling and root planning alone[29]. Studies addressing metronidazole utilization in a variety of clinical conditions demonstrate that its routine use does not enhance root planning[10]. We conclude that systemic metronidazole given 250 mg for 7 days in conjunction with debridement of the tooth surfaces can significantly reduce the need for periodontal surgery compared to the standard regimen which included only debridement[30]. These latest data, based on published studies, point out once again that any treatment with antibiotics, systemic or local, only reaches its maximum periodontal healing effect, if applied after the removal of bacterial plaque from the affected teeth. The healing effects at periodontal structures are balanced by the side effects of antibiotic therapy.

1.3 Coordination Chemistry:

Coordination compounds, as the tern is usually used in inorganic chemistry, include compounds composed of a metal atom or ion and one or more ligands (atoms, ions, or molecules) that formally donatc clcctrons to the metal. This definition includes compounds with metal-carbon bonds, called organometallic compounds.

The name coordination compound comes from the coordinate covalent bond, which historically was considered to form by donation of a pair of electrons from one atom to another. Because these compounds are usually formed by donation of electron pairs of ligands to metals, the name is appropriate. Coordinate covalent bonds are identical to covalent bonds formally Iormed by combining one electron from each atom; only the formal electron counting distinguishes them. Coordination compounds are also acid-base adducts, and are frequently called complexes or, if charged, complex ions.

1.3.1 History:

Although the history of bonding and the interpretation of reactions of coordination compounds really begins with Alfred Werner (1866-1919), coordination compounds were known much earlier. Many coordination compounds have been used as pigments since antiquity. Examples still in use include Prussian blue ($KFe[Fe(CN)_6]$), aureolin ($K_3[Co_2(NO_2)_6].6H_2O$, yellow), and alizarin red dye (the calcium aluminum salt of 1,2-dihydroxy-9,10-anthraquinone.The striking colors of compounds such as these and their color changes on reaction were described in very early documents and provided impetus for further studies. The ion known today as tetraamminecopper (I1) (actually $[Cu(NH_3)_4(H_2O)_2]^{2+}$ in solution), which has a striking royal blue color, was certainly known in prehistoric times. With the gradual development of analytical methods, the formulas of many of these compounds became known late in the 19th century, and theories of structure and bonding became possible.

Inorganic chemists tried to use the advances in organic bonding theory and the simple ideas of ionic charges to explain bonding in coordination compounds, but found that the theories were inadequate. In a compound such as hexaammine cobalt (I11) chloride, $[Co(NH_3)_6]Cl_3$, the early bonding theories allowed only three other atoms to be attached to the cobalt (because of its "valence" of 3). By analogy with ordinary salts, such as $FeCl_3$, the chlorides were assigned this role. This left the six ammonia molecules with no means of participating in bonding, and it was necessary to develop new ideas to explain the structure. One theory, proposed first by C. W. Blomstrand[31] (1826-1894) and developed further by S. M. Jørgensen[32] (1837-1914), was that the nitrogens could form chains much like those of carbon (and thus could have a valence of 5) as shown in Table (1.1), and that chloride ions attached directly to cobalt were bonded more strongly than those bonded to nitrogen. Alfred Werner[33] (1866-1919) proposed instead that all six ammonias could bond directly to the cobalt ion. Werner allowed for a looser bonding of the chloride ions; we now consider them as independent ions. The series of compounds in Table (1.1) illustrates how both the chain theory and Werner's coordination theory predict the number of ions to be formed by a series of cobalt complexes. Blomstrand's theory allowed dissociation of chlorides attached to ammonia but not of chlorides attached directly to cobalt. Werner's theory also included two kinds of chlorides. The number of chlorides attached to the cobalt (and therefore unavailable as ions) plus the number of ammonia molecules totaled six. The other chlorides were considered less firmly bound and could therefore form ions in solution. We now consider them to be ions in the solid state as well.

Table (1.1) Comparison of Blomstrand's Chain Theory and.Werners Coordination theory

Werner Formula (Modern Form)	Number of Ions Predicted	Blomstrand Chain Formula	Number of Ions Predicted
$[Co(NH_3)_6]Cl_3$	4	$Co \begin{cases} NH_3-Cl \\ NH_3-NH_3-NH_3-NH_3-Cl \\ NH_3-Cl \end{cases}$	4
$[Co(NH_3)_5Cl]Cl_2$	3	$Co \begin{cases} NH_3-Cl \\ NH_3-NH_3-NH_3-NH_3-Cl \\ Cl \end{cases}$	3
$[Co(NH_3)_4Cl_2]Cl$	2	$Co \begin{cases} Cl \\ NH_3-NH_3-NH_3-NH_3-Cl \\ Cl \end{cases}$	2
$[Co(NH_3)_3Cl_3]$	0	$Co \begin{cases} Cl \\ NH_3-NH_3-NH_3-Cl \\ Cl \end{cases}$	2

Figure (1.1) Cis and Trans Isomers.

Except for the last compound in the table, the predictions match, and the ionic behavior does not distinguish between them. Even with the last compound, problems with purity and conductance measurements left some ambiguity. The argument between Jergensen and Werner continued for many years, with each presenting data and explanations favoring his own position. This case illustrates some of the good features of such controversy. Werner was forced to develop his theory further and synthesize new compounds to test his ideas because Jergensen defended the earlier theory so vigorously.

Werner proposed an octahedral structure for compounds such as those in Table (1.1). He prepared and characterized many isomers, including both green and violet forms of $[Co(H_2NC_2H_4NH_2)_2Cl_2]^{1+}$ aimed that these compounds had the chlorides arranged **trans** (opposite each

9

other) and cis (adjacent to each other) respectively, in an overall octahedral geometry, as in Figure (1.1). Jergensen offered alternative isomeric structures but finally conceded defeat in 1907, when Werner succeeded in synthesizing the green *trans* and the violet *cis* isomers of $[Co(NH_3)_4Cl_2]^{1+}$ w, hich there were no counterparts in the chain theory. However, even synthesis of tlxs compound and the later discovery of optically active coordination compounds did not completely convince all chemists, although such compounds could not be explained directly by the chain theory. It was argued that Werner's optically active compounds still contained carbon, and that their chirality could be due to the carbon atoms. Finally, Werner resolved the compound $[Co(Co(NH_3)(OH)_2)_3]Br_6$ Figure (1.2), initially prepared by Jergensen, into its two optically active forms, using d- and 1-a-bromocamphor-T-sulfonate as the resolving agents. With this final proof of optical activity without carbon, the validity of Werner's theory was finally accepted. Pauling [34] extended the theory in terms of hybrid orbitals, and later theories[35] have adapted arguments first used for electronic structures of ions in crystals to coordination compounds.
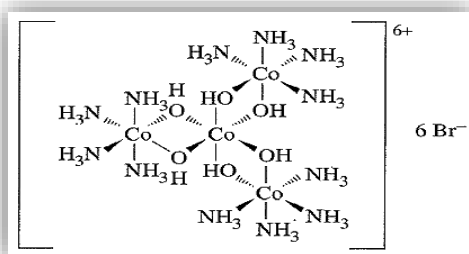
Figure (1.2) Werner's Totally Inorganic Optically Active Compound, $[Co(Co(NH_3)_4(OH)_2)]Br_6$

The Werner theory of coordination compounds was based on a group of compounds that is relatively slow to react in solution and thus easier to study. For this reason, many of his examples were compounds of Co (III), Rh (III), Cr (III), Pt (II), and Pt (IV), which are kinetically inert or slow to react. Examination of more reactive compounds over the years has confirmed their similarity to those originally studied, so we will include examples of both types of compounds in the descriptions that follow.

Werner's theory required two kinds of bonding in the compound: a primary one in which the positive charge of the central metal ion is balanced by negative ions in the compound, and a secondary one in which molecules or ions (known collectively as ligands) are attached directly to the transition metal ion. The secondary bonded unit has been given many different names, such as the complex ion or the

coordination sphere, and the formula is written with this part in brackets. Current practice considers this coordination sphere the more important, so the words primary and secondary no longer bear the same significance. In the examples in Table (1.1), the coordination sphere acts as a unit; the ions outside the brackets balance the charge and are free ions in solution. Depending on the nature of the metal and the ligands, the metal can have from one up to at least 16 atoms attached to it, with 4 and 6 the most common numbers.[36] Additional water molecules may be added to the coordination sphere when the compound is dissolved in water. We should include the water molecules specifically in the description of the compound, but in some cases they are omitted in order to concentrate on the other ligands. The discussion that follows concentrates on the coordination sphere; the other ions associated with it can frequently vary without changing the bonding between ligands and the central metal.

Werner used compounds with four or six ligands in developing his theories, with the shapes of the coordination compounds established by the synthesis of isomers. For example, he was able to synthesize only two isomers of the $[Co(NH_3)_4Cl_2]^{1+}$ T he possible structures with six ligands are octahedral, trigonal prismatic, trigonal antiprismatic, and hexagonal (either planar or pyramidal). Because there are two possible isomers for the octahedral shape and three for each of the others, as shown in figure (1.2), Werner claimed that the structure was octahedral. Such an argument cannot be conclusive, because a missing isomer may simply be difficult to synthesize or isolate. However, later experiments confirmed the octahedral shape, with *cis* and *trans* isomers as shown in figure (1.2). Werner's synthesis and separation of optical isomers proved the octahedral shape conclusively, because none of the other six-coordinate geometries could have similar optical activity.

In a similar way, other experiments were consistent with square-planar Pt (I1) compounds, with the four ligands at the corners of a square. Only two isomers are found for $[Pt(NH_3)_2Cl_2]$. Although the two could have had different shapes (tetrahedral and square-planar, for example), Werner assumed that they had the same overall shape and, because only one tetrahedral structure is possible for this compound, he argued that they must have square-planar shapes with *cis* and *Trans* geometries. Again, his arguments were correct, although the evidence he presented could not be conclusive. The possible structures are shown in Figure (1.3).

After Werner's evidence for the octahedral and square-planar natures of many complexes, it was clear that any acceptable theory needed to account for bonds between ligands and metals and that the number of bonds required was more than that commonly accepted at that time. Transition metal compounds with six ligands, for example, cannot fit the simple Lewis theory with eight electrons around each atom, and

even expanding the shell to 10 or 12 electrons does not work in cases such as $[Fe(cN)_6]^{4-}$, with a total of *18* electrons to accommodate. In fact, the 18-electron rule is sometimes useful in accounting for the bonding in many coordination compounds in a simple way; the total number of valence electrons around the central atom is counted, with 18 as a common result.

Pauling[37] used his valence bond approach to explain differences in magnetic behavior among coordination compounds by use of either 3d or 4d orbitals of the metal ion. Griffith and 0rgel[38] developed and popularized the use of ligand field theory, derived from the crystal field theory of Bethe[39] and Van Vleck[40] on the behavior of metal ions in crystals and from the molecular orbital treatment of Van V1eck[41].
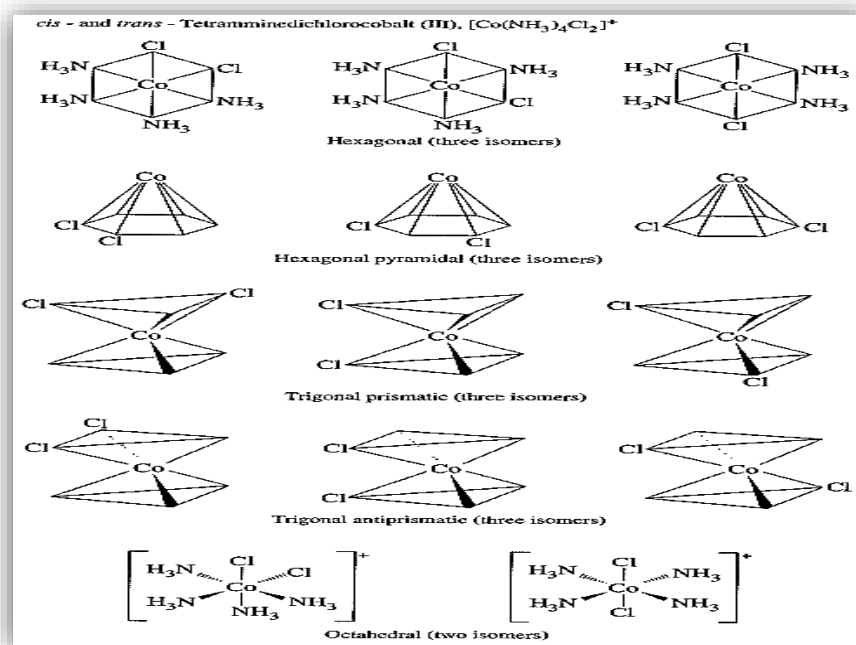
Figure (1.3) Possible Isomers for Hexacoordinate Complexes
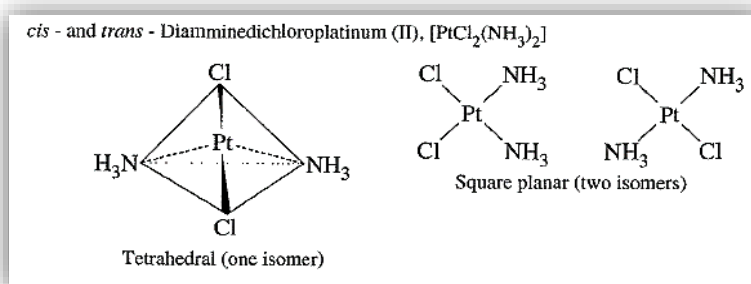
Figure (1.4) Possible Structures for Tetracoordinate Complexes.

1.3.2 Theories of electronic structure:

1.3.2.1 Terminology:

Different names have been used for the theoretical approaches to the electronic structure of coordination complexes, depending on the prcferences of the authors. The labels we will use are described here, in order of their historical development:

Valence bond theory. This method describes bonding using hybrid orbitals and electron pairs, as an extension of the electron-dot and hybrid orbital methods used for simpler molecules. Although the theory as originally proposed is seldom used today, the hybrid notation is still common in discussing bonding.

Crystal field theory. This is an electrostatic approach, used to describe the split in metal d-orbital energies. It provides an approximate description of the electronic energy levels that determine the ultraviolet and visible spectra, but does not describe the bonding.

Ligand field theory. This is a more complete description of bonding in terms of the electronic energy levels of the frontier orbitals. It uses some of the terminology of crystal field theory but includes the bonding orbitals. However, most descriptions do not include the energy of these bonding orbitals.

Angular overlap method. This is a method of estimating the relative magnitudes of the orbital energies in a molecular orbital calculation. It explicitly takes into account the bonding energy as well as the relative orientation of the frontier orbitals.

In the following pages, the valence bond theory and the crystal field theory are described very briefly to set more recent developments in their historical context. The rest of the chapter describes the ligand field theory and the method of angular overlap, which can be used to estimate the orbital energy levels. These two supply the basic approach to bonding in coordination compounds for the remainder of the book.

1.3.2.2 Historical background

Valence bond theory

The valence bond theory, originally proposed by Pauling in the 1930s, uses the hybridization ideas for octahedral complexes[42], d^2sp^3 hybrids of the metal orbitals are required. However, the d orbitals used by the first-row transition metals could be either 3d or 4d. Pauling originally described the structures resulting from these as covalent and ionic, respectively. He later changed the terms to "hyperligated" and "hypoligated," and they are also known as inner orbital (using 3d) and outer orbital (using 4d) complexes. The number of unpaired electroas, measured by [he magnetic behavior of the compounds, determines which d orbitals are used. Low spin and high spin are now used as more descriptive labels

for the two configurations possible for d^4 through d^7 ions. Fe (III) has five unpaired electrons as an isolated ion, one in each of the 3d orbitals.

In octahedral coordination compounds, it may have either one or five unpaired electrons. In complexes with one unpaired electron, the ligand electrons force the metal d electrons to pair up and leave two 3d orbitals available for hybridization and bonding.

In complexes with five unpaired electrons, the ligands do not bond strongly enough to force pairing of the 3d electrons. Pauling proposed that the 4d orbitals could be used for bonding in such cases, with the arrangement of electrons shown in Figure (1.4). When seven electrons must be provided for, as in Co (II), there are either one or three unpaired electrons. In the low-spin case with one unpaired electron, the seventh electron must go into a higher orbital (unspecified by Pauling, but presumed to be 5S)[43].

In the high-spin case with three unpaired electrons, the 4d or outer orbital hybrid must be used for bonding, leaving the metal electrons in the 3d levels. Similar arrangements are necessary for eight or nine electrons [Ni (II) and Cu (II)], although they frequently change geometry to either tetrahedral or square-planar structures. This illustrated in Figure (1.5).

The valence bond theory was of great importance in the development of bonding theory for coordination compounds, but it is rarely used today except when discussing the hybrid orbitals used in bonding. Although it provided a set of orbitals for bonding, the use of the very high energy 4d orbitals seems unlikely, and the results do not lend themselves to a good explanation of the electronic spectra of complexes. Because much of our experimehtal data are derived from electronic spectra, this is a serious shortcoming.
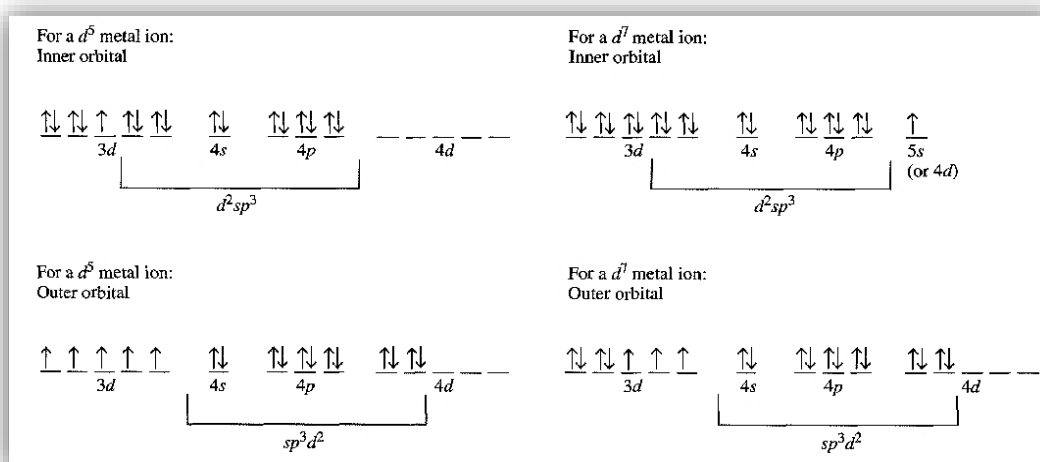
Figure (1.5) Inner and Outer Orbital Complexes. In each case, ligand electrons fill the d2sp3 bonding orbitals. The remaining orbitals contain the electrons from the metal.

Crystal field theory

As originally developed, crystal field theory[44], was used to describe the electronic structure of metal ions in crystals, where they are surrounded by oxide ions or other anions that create an electrostatic field with sylninetry depcndent on the crystal structure. The energies of the d orbitals of the metal ions are split by the electrostatic field, and approximalt: values for thcse energies can be calculated. No attempt was made to deal with covalent bonding, because the ionic crystals did not require it. Crystal field theory was developed[45] in the 1930s. Shortly afterward, it was recognized that the same arrangement of charged or neutral electron pair donor species around a metal ion existed in crystals and in coordination complexes, and a more complete molecular orbital theory was developed.[45] However, neither was widely used until the 1950s, when interest in coordination chemistry increased.

1.3.3 Structures of coordination compounds[46,p(577-581)]

Coordination compounds are also known as coordination complexes, complex compounds, or simply complexes. The essential feature of coordination compounds is that coordinate bonds form between electron pair donors, known as the ligands, and electron pair acceptors, the metal atoms or ions. The number of electron pairs donated to the metal is known as its coordination number. Although many complexes exist in which the coordination numbers are 3, 5, 7, or 8, the majority of complexes exhibit coordination numbers of 2, 4, or 6.

In order for a pair of electrons to be donated from a ligand to a metal ion, there must be an empty orbital on the metal ion to accept the pair of electrons. This situation is quite different from that where covalent bonds are being formed because in that case, one electron in a bonding pair comes from each of the atoms held by the bond. One of the first factors to be described in connection with the formation of coordinate bonds is that of seeing what type(s) of orbitals are available on the metal. If the metal ion is Zn^{+2}, the electron configuration is $3d^{10}$. Therefore, the $4s$ and $4p$ orbitals are empty and can be hybridized to give a set of four empty $sp3$ hybrid orbitals. This set of hybrid orbitals could accommodate four pairs of electrons donated by ligands with the bonds pointing toward the corners of a tetrahedron. Accordingly, it should be expected that $[Zn(NH_3)_4]^{+2}$ would be tetrahedral, and that is correct.

In 1893, Alfred Werner proposed a theory to explain the existence of complexes such as $CoCl_3.6NH_3$, $CoCl_3.4NH_3$, $PtCl_2.2NH_3$, and $Fe(CN)_3.3KCN$. He began by assuming that a metal ion has two kinds of valence. The fi rst, the primary valence, is satisfied by negative groups that balance the charge on the metal. For example, in $CoCl_3.6NH_3$ the +3 valence of cobalt is satisfied by three Cl^- ions. A secondary valence is used to bind other groups that are usually specifi c in number. In the case here,

the six NH_3 molecules satisfy the secondary valence of cobalt, so the coordination number of cobalt is 6. As a result of the NH_3 molecules being bonded directly to the cobalt ion, the formula is now written as $[Co(NH_3)_6]Cl_3$ where the square brackets are used to identify the actual complex that contains the metal and the ligands bound directly to it.

In a complex such as $CoCl_3.4NH_3$, the coordination number of 6 for cobalt is met by the four NH_3 molecules and two Cl^- ions being bonded directly to the cobalt. That leaves one Cl^- ion that satisfies part of the primary valence, but it is not bonded directly to the cobalt ion by means of a secondary valence. The formula for this coordination compound is written as $[Co(NH_3)4Cl_2]Cl$. Support for these ideas is provided by dissolving the compounds in water and adding a solution containing Ag^+. In the case of $CoCl_3.6NH_3$ or $[Co(NH_3)_6]Cl_3$, all of the chloride is immediately precipitated as AgCl. For $CoCl_3.4NH_3$ or $[Co(NH_3)_4Cl_2]Cl$, only one third of the chloride precipitates as AgCl because two chloride ions are bound to the cobalt ion by coordinate bonds, the secondary valence. Two Cl^- ions satisfy both primary and secondary valences of cobalt, but one Cl^- satisfies only a primary valence. For a solution of the compound $[Co(NH_3)_3Cl_3]$, none of the chloride ions precipitate when Ag^+ is added because all of them are bound to the cobalt ion by coordinate bonds.

The electrical conductivity of solutions containing the complexes just described provides additional confirmation of the correctness of this view. For example, when $[Co(NH_3)_3Cl_3]$ is dissolved in water, the compound behaves as a nonelectrolyte. There are no ions are present because the Cl^- ions are part of the coordinate structure of the complex. On the other hand, $[Co(NH_3)_6]Cl_3$, $[Co(NH_3)_5Cl]Cl_2$, and $[Co(NH_3)_4Cl_2]Cl$ behave as 1:3, 1:2, and 1:1 electrolytes, respectively. A similar situation exists for $[Pt(NH_3)_4Cl_2]Cl_2$, which behaves as a 1:2 electrolyte and has only half of the chloride ions precipitated when Ag^+ is added to a solution of the complex. A large number of compounds like $FeCl_3.3KCl$ are known, and they are often called *double salts* because they consist of two complete formulas linked together. Many of the compounds are actually coordination compounds with formulas like $K_3[FeCl_6]$. As will be shown later, there are many complexes that have coordination numbers of 2 (linear complexes such as $[Ag(NH_3)_2]^+$), 4 (tetrahedral complexes such as $[CoCl4]^{-2}$ or square planar complexes such as $[Pt(NH_3)_4]^{+2}$) or 6 (octahedral complexes such as $[Co(NH_3)_6]^{+3}$). A considerably smaller number of complexes having coordination numbers of 3 (trigonal planar), 5 (trigonal bipyramid or squarebased pyramid), 7 (pentagonal bipyramid or capped trigonal prism), or 8 (cubic or anticubic, which is also known as Archimedes antiprism) are also known. These structures are shown in Figure (1.6).
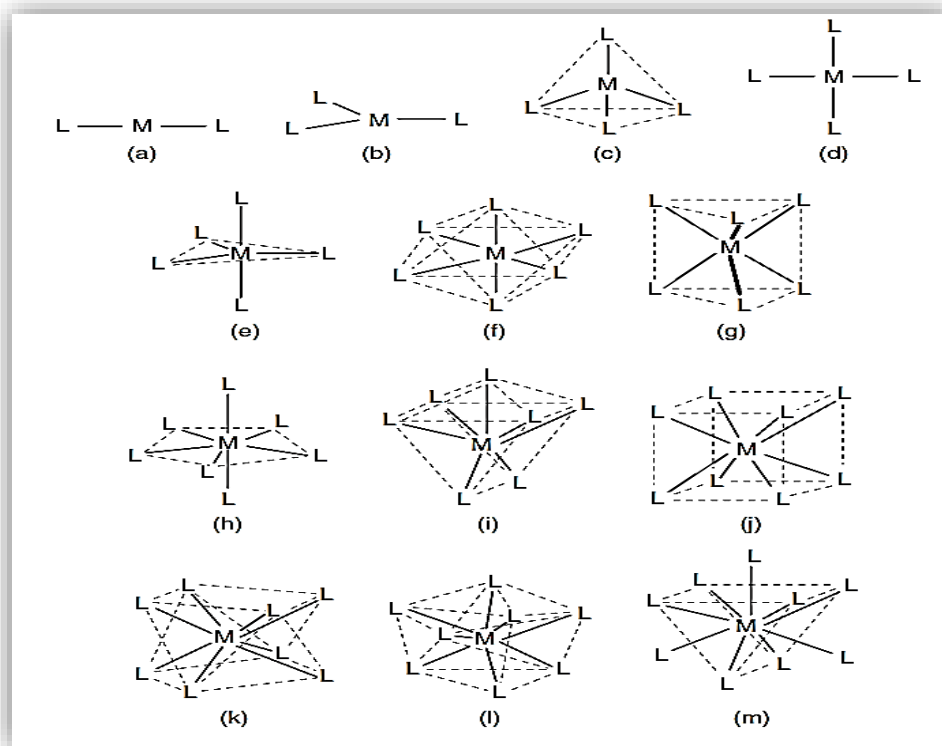
Figure (1.6) Some of the most common structures for coordination compounds: (a) linear; (b) trigonal planar; (c) tetrahedron; (d) square plane; (e) trigonal pyramid; (f) octahedron; (g) trigonal prism; (h) pentagonal bipyramid; (i) single-capped trigonal prism; (j) cubic; (k) Archimedes (square) antiprism; (l) dodecahedron; (m) triple capped trigonal prism.

In a tetrahedral structure, all of the positions around the central atom are equivalent, so there is no possibility of geometrical or cis/trans isomerism. If all four groups bonded to the metal are different.

Alfred Werner[33] isolated these two isomers, which showed conclusively that the complex is square planar rather than tetrahedral. The *cis* isomer is now known by the trade name *cisplatinol* or *cisplatin*, and it is used in treating certain forms of cancer.

If a complex has a coordination number of 6, there are several ways to place the ligands around the metal. A completely random arrangement is not expected because chemical bonds do not ordinarily form that way. Three regular types of geometry are possible for a complex containing six ligands.

The six groups could be arranged in a planar hexagon (analogous to benzene) or the ligands could be arranged around the metal in a trigonal prism or in an octahedral structure. For a complex having the formula MX_4Y_2, these arrangements lead to different numbers of isomers as shown in Figure (1.7).
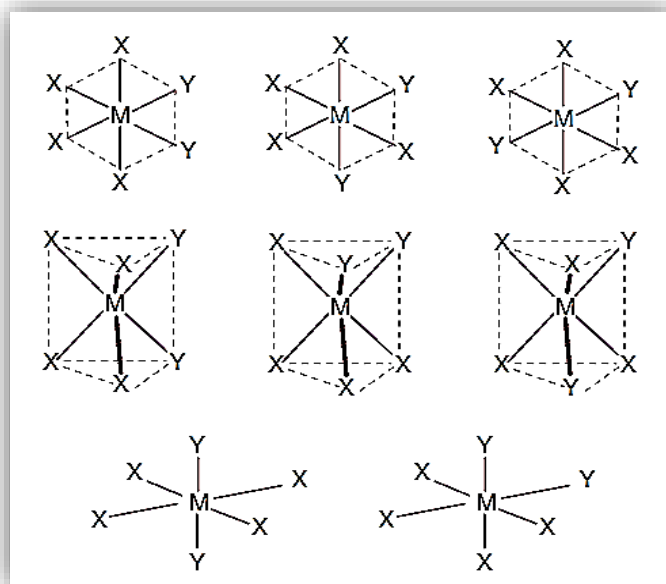
Figure (1.7) Geometrical isomers for MX_4Y_2 complexes having planar hexagonal, trigonal prism, and octahedral structures

With the availability of modern experimental techniques, the structure of a compound can be established unequivocally. However, more than 100 years ago only chemical means were available for structure elucidation. The fact that only two isomers could be isolated was a good *indication* that a complex having the formula MX_4Y_2 has an octahedral structure. The argument could be made that the synthetic chemist was not able to prepare a third possible isomer or that it exists but was so unstable that it could not be isolated.

Although the majority of complexes have structures that are linear, tetrahedral, square planar, or octahedral, a few compounds have a trigonal bipyramid structure. Most notable of these are $Fe(CO)_5$, $[Ni(CN)_5]^{-3}$, and $[Co(CN)_5]^{-3}$. Some complexes having a coordination number of 5 have the squarebase pyramid structure, including $[Ni(CN)_5]^{-3}$. Although it is not particularly common, the coordination number 8 is found in the complex $[Mn(CN)_8]^{-4}$, which has a cubic structure with CN^- ions on the corners.

Because the coordinate bonds are the result of Lewis acid-base interactions, the number of species that can form complexes with metal ions is large. Lewis bases such as H_2O, NH_3, F^-, Cl^-, Br^-, I^-, CN^-, SCN, and NO^{2-} all form a wide range of coordination compounds. Added to these are compounds such as amines, arsines, phosphines, and carboxylic acids that are all potential ligands. The ethylenediamine molecule, $H_2NCH_2CH_2NH_2$, is a ligand that forms many very stable complexes because each nitrogen atom has an unshared pair of electrons that can be donated to a metal ion. This results in the

18

ethylenediamine molecule being attached to the metal ion at two sites, giving a ring with the metal ion being one of the members. A ring of this type is known as a chelate (pronounced "key-late") ring (from the Greek word chelos, meaning "claw"). A complex that contains one or more chelate rings is called a chelate complex or simply a chelate. There are many other groups, known as chelating agents, which can bind to two sites.

1.3.4 A Simple valence bond description of coordination bonds[46,p(592-597)]

One of the goals in describing any structure on a molecular level is to interpret how the bonding arises by making use of atomic orbitals. In the area of coordination chemistry, a simple valence-bond approach is successful in explaining some of the characteristics of the complexes. In this approach, the empty orbitals on the metal ions are viewed as hybrid orbitals in sufficient number to accommodate the number of electron pairs donated by the ligands. It is generally true that first-row transition metals form complexes that in many cases contain six coordinate bonds. This especially true if the charge on the metal ion is +3. The reason for this is that a +3 metal ion has a high charge-to-size ratio that exerts a strong attraction for pairs of electrons. If the metal ion has a +2 charge, it is sometimes found that only four ligands will bind to the metal ion, but it also depends on the availability of empty orbitals on the metal ion. In this case, the charge-to-size ratio is considerably smaller (the charge is only 67% as high and the size is usually larger), so the metal ion has a much smaller affi nity for electron pairs. This is the case for +2 ions such as Cu^{+2} and Zn^{+2}, which form many complexes in which the coordination number is 4, although as we shall see there are other factors involved.

Table (1.2) Hybrid Orbital Types in Coordination Compounds.

Atomic Orbitals	Hybrid Type	Number of Orbitals	Structure
s,p	sp	2	linear
s,d	sd	2	linear
s,p,p	sp^2	3	trigonal planar
s,p,p,p	sp^3	4	tetrahedral
s,d,d,d	sd^3	4	tetrahedral
d,s,p,p	dsp^2	4	square planar
d,s,p,p,p	dsp^3	5	trigonal bipyramid
s,p,p,d,d	sp^2d^2	5	square-base pyramid
d,d,s,p,p	d^2sp^3	6	octahedral
s,p,p,p,d,d	sp^3d^2	6	octahedral
s,p,d,d,d,d	spd^4	6	trigonal prism
s,p,p,p,d,d,d	sp^3d^3	7	pentagonal bipyramid
s,p,p,p,d,d,d,d	sp^3d^4	8	dodecahedron
s,p,p,p,d,d,d,d	sp^3d^4	8	Archimedes antiprism
s,p,p,p,d,d,d,d,d	sp^3d^5	9	capped trigonal prism
In dsp^2 the $d_{x^2-y^2}$ orbital is used. In sp^2d^2 and d^2sp^3 the $d_{x^2-y^2}$ and d_{z^2} orbitals are used.			

The simplified problems in describing the structure of complexes becomes one of deciding what hybrid orbital type will accommodate the number of electron pairs donated by the ligands and also correspond to the known structure of the complex. Some of the structures associated with specific types of hybrid orbitals were presented in Figure (1.8), but there are other cases that apply to complexes of metal ions. In addition to regular geometrical structures, there are numerous complexes that have irregular structures. In some cases, Jahn-Teller distortion causes the structure to deviate from ideal geometry. In spite of the diffi culties, it is useful to know the hybrid orbital types associated with complexes having various structures. Table (1.2) gives a summary of the major hybrid orbital types that are applicable to complexes.

When Zn^{+2} forms a complex such as $[Zn(NH_3)_4]^{+2}$, it is easy to rationalize the bonding in terms of hybrid orbitals. Zn^{+2} have a d^{10} confi guration, but the $4s$ and $4p$ orbitals are empty. Therefore, a set of four empty sp^3 hybrids can result. As shown next, four orbitals can accept four pairs of electrons that are donated by the ligands.
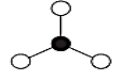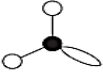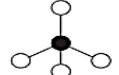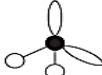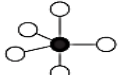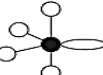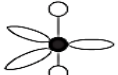
20

Figure (1.8) Molecular structure based on hybrid orbital type.

Likewise, it is easy to rationalize how Ag^+ (a d^{10} ion) can form a linear complex with two ligands like NH_3.
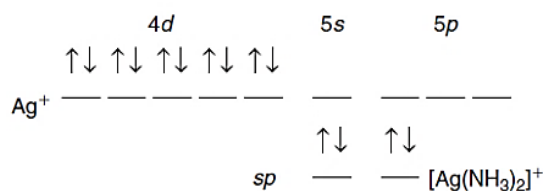
When the scheme above is examined, it is easy to see that if two of the $5p$ orbitals are used, a set of sp^2 hybrid orbitals could be produced that would accommodate pairs of electrons from three ligands. It is not surprising that only a few complexes are known in which Ag^+ exhibits a coordination number of 3.

If all of the 5p orbitals were used in the hybrids, the resulting sp^3 hybrids could accommodate four pairs of electrons, and a tetrahedral complex could result. Although complexes like $[Ag(CN)_3]^{-2}$ and $[Ag(CN)_4]^{-3}$ have been identifi ed in solutions where the concentration of CN^- is high, such complexes

are unusual and of low stability. The vast majority of complexes of Ag⁻ have a coordination number of 2 and linear structures. Part of the reason for this is that the silver ion is relatively large and has a low charge, which results in a low charge density. Such an ion does not assimilate the electron density from added ligands as readily as do those for which the charge density is high.

For metal ions having confi gurations d^0, d^1, d^2, or d^3, there will always be two of the d orbitals empty to form a set of d^2sp^3 hybrids. Therefore, we expect complexes of these metal ions to be octahedral in which the hybrid orbital type is d^2sp^3. If we consider Cr^{+3} as an example, the formation of a complex can be shown as follows:
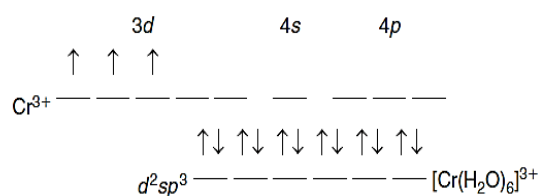
In an octahedral complex, the coordinate system is set up so that the ligands lie on the axes. The d orbitals that have lobes lying along the axes are the dz^2 and the d x^2+y^2. The dxy, dyz, and $d$xz orbitals directed between the axes are considered to be nonbonding. It should not be inferred that only octahedral complexes are produced by Cr^{+3}. Although tetrahedral complexes would not be expected in solutions that contain Cr^{+3} because of its high charge density, solid [PCl₄][CrCl₄] contains the tetrahedral CrCl₄⁻ ion. With the 4 s and 4 p orbitals being empty, it is easy to see how sp^3 hybrids are obtained.

When the number of electrons in the d orbitals is four, as in the case of Mn^{+3}, there exists more than one possible type of hybrid orbital. For example, if the electrons remain unpaired in the d orbitals, there is only one orbital in the set that is empty. As a result, if an octahedral complex is formed, making use of two d orbitals requires that the 4 d orbitals be used so that sp^3d^2 hybrid orbitals would be used by the metal. This case can be shown as follows:
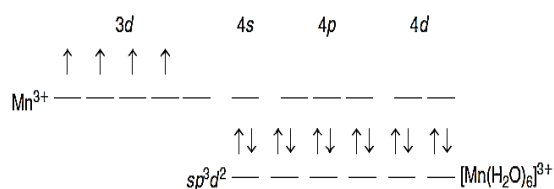
This bonding arrangement results in four unpaired electrons in the 3d orbitals, but with some ligands, the situation is different. In those cases, two of the 3d orbitals are made available to form a set of hybrid orbitals by means of electron pairing. When this occurs, the bonding arrangement can be shown as follows:
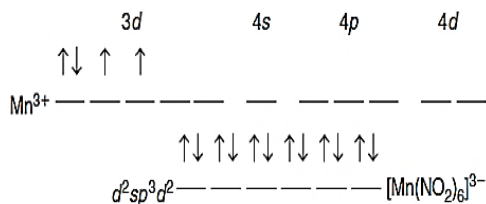
Only two unpaired electrons are present in this complex, and as will be shown in the next section, the two types of manganese complexes can be distinguished by means of their magnetic character.

In $[Mn(H_2O)_6]^{+3}$, the 4d orbitals used to form hybrids are those outside the usual valence shell that consists of 3d , 4s , and 4p orbitals. Consequently, such a complex is often referred to as an outer orbital complex. To identify the hybrid orbitals, the symbol sp $3d^2$ is used to indicate that the d orbitals are part of the shell with n = 4 and they follow the s and p orbitals in fi lling. In $[Mn(NO_2)_6]^{-3}$, the d orbitals are those in the valence shell so the complex is called an inner orbital complex and the hybrid orbital type is designated as d^2sp^3 to show that the principal quantum number of the d orbitals is lower than that of the s and p orbitals. Another way in which the two types of complexes are distinguished is by the terms high spin and *low spin*. In $[Mn(H_2O)_6]^{+3}$, there are four unpaired electron spins, whereas in $[Mn(NO_2)_6]^{-3}$, there are only two unpaired electrons. Therefore, the former is referred to as a highspin complex, and the latter is designated a low-spin complex.

For a d^5 ion such as Fe^{+3} , the fi ve electrons may be unpaired in the set of five *d* orbitals, or they may be present as two orbitals occupied by pairs of electrons and one orbital having single occupancy. A complex such as $[Fe(H_2O)_6]^{+3}$ is typical of the fi rst bonding mode (fi ve unpaired electrons, high spin,outer orbital), whereas $[Fe(CN)_6]^{-3}$ is typical of the second (one unpaired electron, low spin, inner orbital). Three orbitals can accommodate six electrons, so a d^6 ion such as Co^{+3} should form two series of complexes in which the six electrons occupy all fi ve orbitals with two in one orbital and one in each of the others. This results in four unpaired electrons being found in the outer-orbital, highspin complex $[CoF_6]^{-3}$. On the other hand, a low-spin, inner-orbital complex such as $[Co(NH_3)_6]^{+3}$ has no unpaired electrons because all six of the 3d electrons are paired in three of the orbitals.

When the d^7 and d^8 electron confi gurations are considered, there are additional possibilities for forming bonding orbitals. With seven or eight electrons in the five orbitals, there is no possibility of having two of the 3d orbitals vacant so if an octahedral complex is formed, it must be of the high-spin, outer-orbital type. Both Co^{+2} (d^7) and Ni+2 (d^8) form many complexes of this type. With all of the 3d orbitals being populated (not necessarily filled), the possibility exists for using the 4s and 4p orbitals in forming tetrahedral complexes and $[CoCl_4]^{-2}$ and $[Ni(NH_3)_4]^{+2}$ have tetrahedral structures. Although it is

23

not possible to have two of the 3d orbitals vacant, it is certainly possible to have one empty, so the possibility of the dsp^3 hybrid orbital type exists. With regard to the orbitals used, the Co^{+2} ion behaves as follows:
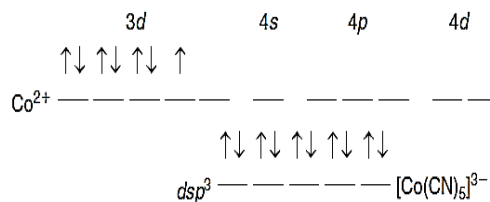
For the $d\,8$ Ni^{2+} ion, the orbitals and bonding can be shown as follows:
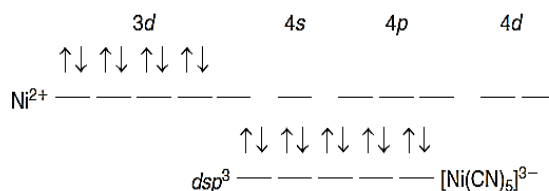
If a complex having a coordination number of 4 is produced, only two of the 4p orbitals are used and the hybrid orbital type is dsp^2, which is characteristic of a square planar complex. For Ni^{+2}, this is illustrated by the following scheme:
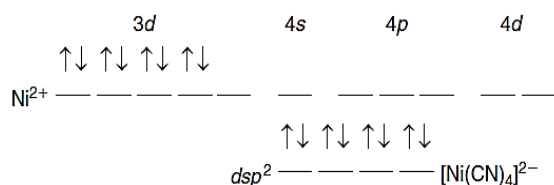
Co^{+2} and Ni^{+2} also have the ability to make use of 4s, 4p, and 4d orbitals in another way by forming sp^{2}d^2 hybrids in the formation of complexes having a square-based pyramid structure. In fact, trigonal bipyramid and square-based pyramid structures are both observed for [Ni(CN)$_5$]$^{-3}$.

1.3.5 Synthesis of coordination compounds[46,p(695-701)]

Coordination compounds have been produced by a variety of techniques for at least two centuries. Zeise's salt, K[Pt(C$_2$H$_4$)Cl$_3$], dates from the early 1800s, and Werner's classic syntheses of cobalt complexes were described over a century ago. Synthetic techniques used to prepare coordination compounds range from simply mixing the reactants to employing nonaqueous solvent chemistry. In this section, a brief overview of some types of general synthetic procedures will be presented. The organometallic chemistry of transition metals will be presented, and additional preparative methods for complexes of that type will be described there.

1.3.5.1 Reaction of a Metal Salt with a Ligand

One of the techniques for producing coordination compounds is to simply combine the reactants. Some reactions may be carried out in solution, but others may involve adding a liquid or gaseous ligand directly to a metal compound. Some reactions of this type are the following:

$$NiCl_2.6H_2O_{(s)} + 3\ en_{(l)} \rightarrow [Ni(en)_3]Cl_2.2H_2O(s) + 4\ H_2O$$

$$Cr_2(SO_4)_{3(s)} + 6\ en_{(l)} \rightarrow [Cr(en)_3]_2(SO_4)_{3(s)}$$
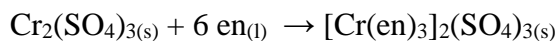
The product obtained during the second reaction, $[Cr(en)_3]_2(SO_4)_3$ (s), is a solid mass. It has been found advantageous to dissolve ethylenediamine in an inert liquid that has a high boiling point such as toluene. Refl uxing this solution while adding solid $Cr_2(SO_4)_3$ slowly gives a fi nely divided product that is easier to separate by fi ltration and is easy to purify. This technique can be applied to the preparation of numerous other types of complexes. In this case, changing the reaction medium gives a product that is more convenient to use in subsequent work. An example of a synthesis utilizing a nonaqueous solvent is a common procedure that is used to prepare $[Cr(NH_3)_6]Cl_3$. The reaction is

$$CrCl_3 + 6\ NH_3 \xrightarrow{\text{liq NH3}} [Cr(NH_3)_6]Cl_3$$
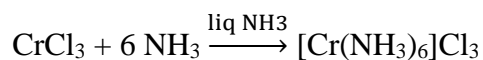
It has been found that this reaction is catalyzed by sodium amide, $NaNH2$. The function of the catalyst appears to involve the replacement of Cl^- by NH^{-2}, which is the stronger nucleophile. Once the NH^{-2} ion is attached to Cr^{+3}, it quickly removes a proton from a solvent molecule to be transformed into a coordinated NH_3 molecule. As will be shown later in this chapter, this type of behavior is also characteristic of coordinated OH^- in aqueous solutions.

Some alkenes will react with metal salts to give complexes that involve electron donation from the double bond. A classic case of this type is the formation of Zeise's salt. However, if the alkene has more than one potential donor site, bridged complexes may result. One such ligand is butadiene, which forms an interesting bridged structure with CuCl. The reaction is carried out at -10 °C with CuCl being added directly to liquid butadiene.

$$2\ CuCl + C_4H_6 \rightarrow [ClCuC_4H_6CuCl]$$
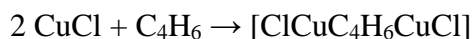
Acetylacetone (2,4-pentadione) undergoes a tautomerization that can be shown as
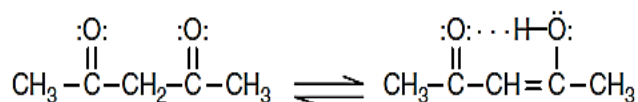
And the equilibrium is strongly solvent dependent. When a small amount of ammonia is present, the proton in the OH groups is removed to form the anion,

$$CH_3-\overset{\displaystyle :O:}{\overset{\displaystyle \|}{C}}-CH=\overset{\displaystyle :\overset{..}{O}:^-}{\overset{\displaystyle |}{C}}-CH_3$$
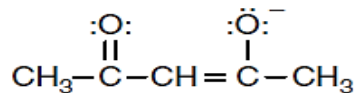
Which is an excellent chelating agent. The anion, abbreviated as acac, will react with many metal ions to form stable complexes. An example of this type of reaction is

$$CrCl_3 + 3\ C_5H_8O_2 + 3\ NH_3 \rightarrow Cr(C_5H_7O_2)_3 + 3\ NH_4Cl$$
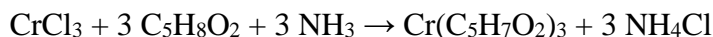
Complexes containing acac are especially stable because they exist as neutral complexes such as $M(acac)_3$ and $M(acac)_2$ when the metal is +3 and +2, respectively. Many other reactions have been carried out in which the ligand reacts with a metal compound. In many cases, it is preferable to start with an anhydrous metal compound, and dehydration can sometimes be accomplished by a reaction with $SOCl_2$.

1.3.5.2 Ligand Replacement Reactions

The replacement of one ligand by another is the most common type of reaction of coordination compounds, and the number of reactions of this type is enormous. Some are carried out in aqueous solutions, some in nonaqueous media, and others can be carried out in the gas phase. One such reaction is

$$Ni(CO)_4 + 4\ PCl_3 \rightarrow Ni(PCl_3)_4 + 4\ CO$$
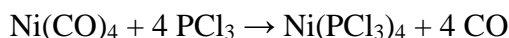
When an octahedral complex such as $[Cr(CO)_6]$ reacts with pyridine, only three CO ligands are replaced. In the product $[Cr(CO)_3(py)_3]$, the CO and py ligands are *trans* to each other. Replacement reactions are important because frequently one type of complex is easily prepared and then can be converted to another that cannot be obtained easily. Gaseous butadiene will react with an aqueous solution of $K_2[PtCl_4]$ to give a bridged complex in which Cl ligands are displaced.

$$2\ K_2[PtCl_4] + C_4H_6 \rightarrow K_2[Cl_3PtC_4H_6PtCl_3] + 2\ KCl$$
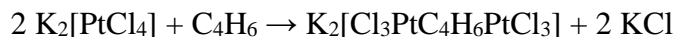
A large number of syntheses involve replacement reactions.

1.3.5.3 Reaction of Two Metal Compounds

Several synthetic processes involve the reaction of two metal salts. A well-known example of this type is the following.

$$2\ AgI + HgI_2 \rightarrow Ag_2[HgI_4]$$
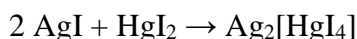
This reaction has been induced in several ways, but one novel procedure involves the action of ultrasound on a suspension of the two solid reactants in dodecane. The ultrasonic vibrations create cavities in the liquid that implode, driving particles of the solid together at high velocity. Under these

conditions, the solids react in much the same way as if they were heated, but in cases where an unstable product is formed, it is not thermally decomposed.

A variation of this type of reaction occurs when a metal complex already containing ligands reacts with a simple metal salt to give a redistribution of the ligands. For example,

$$2 \ [Ni(en)_3]Cl_2 + NiCl_2 \rightarrow 3 \ [Ni(en)_2]Cl_2$$

1.3.5.4 Oxidation-Reduction Reactions

Many coordination compounds can be prepared when a compound of the metal is either reduced or oxidized in the presence of a ligand. Oxalic acid is a reducing agent, but it also serves as a source of the oxalate ion, which is a good chelating agent. An interesting reaction of this type involves the reduction of dichromate by oxalic acid as shown by the following equation:

$$K_2Cr_2O_7 + 7 \ H_2C_2O_4 + 2 \ K_2C_2O_4 \rightarrow 2 \ K_3[Cr(C_2O_4)_3].3H_2O + 6 \ CO_2 + H_2O$$
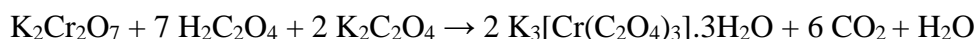
In other reactions, the metal may be oxidized as the complex is formed. Numerous complexes of Co (III) have been prepared by the oxidation of solutions containing Co(II). This technique is particularly useful in the case of cobalt because Co^{+3} is a strong oxidizing agent that reacts with water if it is not stabilized by complexation. In the following reactions, en is ethylenediamine, $H_2NCH_2CH_2NH_2$:

$$4 \ CoCl_2 + 8 \ en + 4 \ en.HCl + O_2 \rightarrow 4 \ [Co(en)_3]Cl_3 + 2 \ H_2O$$

$$4 \ CoCl_2 + 8 \ en + 8 \ HCl + O_2 \rightarrow 4 \ trans\text{-}[Co(en)_2Cl_2]Cl.HCl + 2 \ H_2O$$
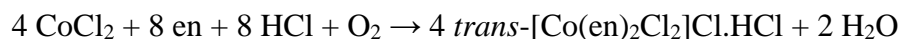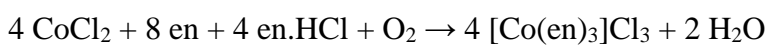
Heating the product of the second reaction yields *trans*-[Co(en)₂Cl₂]Cl by the loss of HCl. Dissolving *trans* [Co(en)₂Cl₂]Cl in water and evaporating the solution by heating results in the formation of *cis* - [Co(en)₂Cl₂]Cl as the result of an isomerization reaction.

1.3.5.5 Partial Decompositions

Reactions in which volatile ligands such as H_2O and NH_3 are lost as a result of heating lead to the formation of other complexes. Generally, these reactions involve solids, and some such processes will be described later in this chapter. As a volatile ligand is driven off, another group can enter the coordination sphere of the metal. In other cases, there may be a change in bonding mode of a ligand that is already present. For example, SO_4^{-2} may become bidentate to complete the coordination sphere of the metal. The synthesis of $[Co(NH_3)5H_2O]Cl_3$ (s) is rather straightforward, and after it is obtained, it is converted when heated to $[Co(NH_3)_5Cl]Cl_2$ (s) by the reaction

$$[Co(NH_3)_5H_2O]Cl_3(s) \rightarrow [Co(NH_3)_5Cl]Cl_2(s) + H_2O(g)$$

Other compounds containing different anions are obtained by the following reaction:

$$[Co(NH_3)_5Cl]Cl_2 + 2\ NH_4X \rightarrow [Co(NH_3)_5Cl]X_2 + 2\ NH_4Cl$$
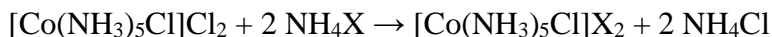
This metathesis reaction can be carried out in aqueous solutions as a result of differences in solubility. Two additional reactions representing partial decomposition are the following:

$$[Cr(en)_3]Cl_{3(s)} \rightarrow cis\text{-}[Cr(en)_2Cl_2]Cl_{(s)} + en_{(g)}$$

$$[Cr(en)_3](SCN)_{3(s)} \rightarrow trans\text{-}[Cr(en)_2(NCS)_2]SCN_{(s)} + en_{(g)}$$
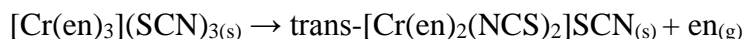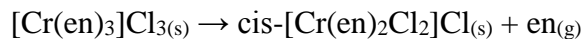
These reactions have been known for almost 100 years and they have been extensively studied. The reactions are catalyzed by the corresponding ammonium salt in each case, although other protonated amines function as catalysts. It appears that the function of the catalyst is to supply H^+, which helps to force an end of the ethylenediamine molecule away from the metal.

1.3.5.6 Precipitation Making Use of the Hard-Soft Interaction Principle

As a consequence of the hard-soft interaction principle, ions of similar size and magnitude of charge interact best. That interaction includes the formation of precipitates. It is possible to make use of this principle when isolating complex ions that are relatively unstable. A well known case of this type is the isolation of the $[Ni(CN)_5]^{-3}$ ion, which results when aqueous solutions containing Ni^{+2} also contain an excess of CN^-. Attempts to isolate $[Ni(CN)_5]^{-3}$ by adding K^+ were not successful because what was obtained was $K_2[Ni(CN)_4]$ and KCN. It was only when a large cation having a +3 charge was utilized that the pentacyanonickelate (II) ion was obtained in a solid product. The large +3 cation used was $[Cr(en)_3]^{-3}$. With that cation, the solid product was $[Cr(en)_3][Ni(CN)_5]$. The following equations describe the process:

$$Ni^{+2} + 4\ CN \rightarrow [Ni(CN)_4]^{-2}$$

$$[Ni(CN)_4]^{2-} + CN^- \longrightarrow [Ni(CN)_5]^{3-}$$

$$K^+ \swarrow \qquad \searrow [Cr(en)_3]^{3+}$$

$$K_2[Ni(CN)_4] + KCN \qquad [Cr(en)_3][Ni(CN)_5]$$
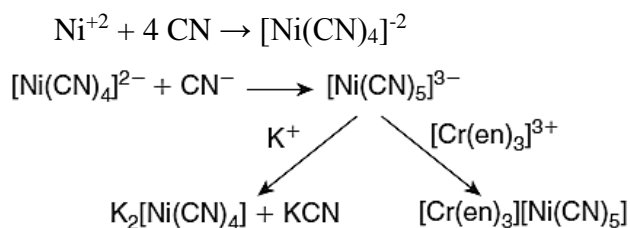
In many parts of this book, the utility of the hard-soft interaction principle has been described. In the situation described, the choice of an appropriate cation makes possible the isolation of a relatively unstable complex ion by providing a crystal environment that helps to stabilize the complex. The application of basic principles that relate to structure and stability can also be useful in synthetic chemistry.

1.3.5.7 Reactions of Metal Compounds with Amine Salts

Many years ago, L. F. Audrieth studied numerous reactions of amine hydrochloride salts. These compounds contain a cation that is a protonated amine that can function as a proton donor.

Consequently, the molten salts are acidic and they undergo many reactions in which they function as acids. This behavior is also characteristic of ammonium chloride as well as pyridine hydrochloride (or pyridinium chloride). Numerous metal oxides and carbonates react readily with the molten amine salts, as illustrated by the following equation:

$$NiO(s) + 2\ NH_4Cl_{(l)} \rightarrow NiCl2_{(s)} + H_2O_{(l)} + 2\ NH_{3(g)}$$

Hydrothiocyanic acid (also known by the archaic name rhodanic acid), HSCN, is a strong acid, so it is easy to prepare stable amine hydrothiocyanate salts such as that of piperidine, $C_5H_{11}N$ (abbreviated as pip). In this reaction, the less volatile base, piperidine, replaces the volatile weak base, NH_3.

$$NH_4SCN_{(s)} + pip_{(l)} \rightarrow pipH^+SCN^-_{(s)} + NH_{3(g)}$$
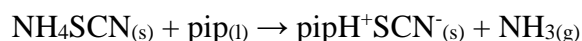
The salt pipHSCN, known as piperidinium thiocyanate or piperidine hydrothiocyanate, has a melting point of 95°C. When metal compounds are added to this molten salt, thiocyanate complexes of the metals are produced. For example, the following reactions can be carried out at 100°C in the presence of an excess of the amine hydrothiocyanate:

$$NiCl_2 + 6H_2O_{(s)} + 6\ pipHSCN_{(l)} \rightarrow (pipH)_4[Ni(SCN)_6]_{(s)} + 2\ pipHCl_{(l)} + 6\ H_2O_{(g)}\ CrCl_3.6H_2O_{(s)} + 6$$
$$pipHSCN_{(l)} \rightarrow (pipH)_3[Cr(NCS)_6]_{(s)} + 3\ pipHCl_{(l)} + 6\ H_2O_{(g)}$$
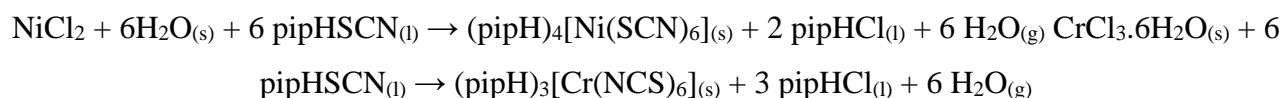
In some cases, the metal complex contains both piperidine and thiocyanate as ligands, as illustrated by the following equation:

$$CdCO_{3(s)} + 2\ pipHSCN_{(l)} \rightarrow [Cd(pip)_2(SCN)_2]_{(l)} + CO_{2(g)} + H_2O_{(g)}$$
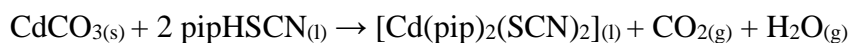
In addition to the reactions just described using molten pipHSCN, several reactions have been carried out at low temperature by sonicating mixtures of metal salts and pipHSCN (House, 1998). The use of ultrasound results in products of higher purity than when the molten salt is used. This is probably due to the fact that some of the products are not very stable at the temperature of the molten salt (100°C) and mixtures result under those conditions. In carrying out the reactions, the amine hydrothiocyanate and the metal compound were suspended in dodecane and pulsed ultrasound was applied. The following reactions are typical of preparations of this type:

$$MnCO_{3(s)} + 6\ pipHSCN_{(s)} \rightarrow (pipH)_4[Mn(NCS)_6]_{(s)} + 2\ pip_{(l)} + CO_{2(g)} + H_2O_{(l)}$$
$$MnCl_2.4H_2O_{(s)} + 4\ pipHSCN_{(s)} \rightarrow (pipH)_2[Mn(NCS)_4]_{(s)} + 2\ pipHCl + 4\ H_2O_{(l)}$$
$$Fe_2O_{3(s)} + 12\ pipHSCN_{(s)} \rightarrow 2\ (pipH)_3[Fe(NCS)_6]_{(s)} + 6\ pip_{(l)} + 3\ H_2O_{(l)}$$
$$NiCO_{3(s)} + 4\ pipHSCN_{(s)} \rightarrow (pipH)_2[Ni(NCS)_4]_{(s)} + 2\ pip_{(l)} + CO_{2(g)} + H_2O_{(l)}$$
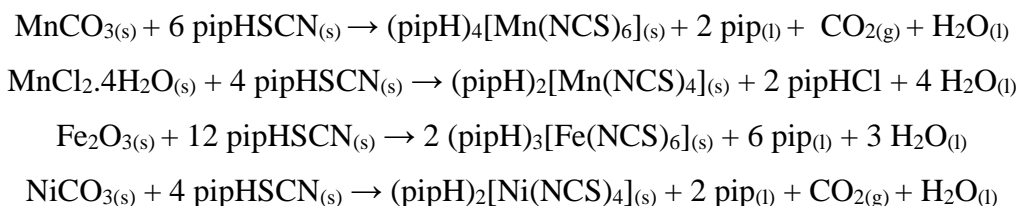
In every case, the products were obtained in high purity in this convenient, one-step synthesis. Although ultrasound has not been used extensively in inorganic chemistry, it is a well-known technique in organic synthesis.

1.3.6 Electronic spectra:[46,p(645-650)]

Perhaps the most striking aspect of many coordination compounds of transition metals is that they have vivid colors. The dye Prussian blue, for example, has been used as a pigment for more than two centuries (and is still used in blueprints); it is a complicated coordination compound involving iron(ll) and iron(lll) coordinated octahedrally by cyanide. Many precious gems exhibit colors resulting from transition metal ions incorporated into their crystalline lattices. For example, emeralds are green as a consequence of the incorporation of small amounts of chromium (II1) into crystalline $Be_3Al_2Si_6O_{18}$; amethysts are violet as a result of the presence of small amounts of iron (II), iron (III), and titanium (1V) in an A1203 lattice; and rubies are red because of chromium (III), also in a lattice of $A1_2O_3$. The color of blood is caused by the red heme group, a coordination compound of iron present in hemoglobin. Most readers are probably familiar with blue $CuSO_4.5H_2O$, a compound often used to demonstrate the growing of large, highly symmetric crystals.

It is desirable to understand why so many coordination compounds are colored, in contrast to most organic compounds, which are transparent, or nearly so, in the visible spectrum. We will first review the concept of light absorption and how it is measured.

The ultraviolet and visible spectra of coordination compounds of transition metals involve transitions between the d orbitals of the metals. Therefore, we will need to look closely at the energies of these orbitals and at the possible ways in which electrons can be raised from lower to higher energy levels. The energy levels of d electron configurations (as opposed to the energies of *individual* electrons) are somewhat more complicated than might be expected, and we need to consider how electrons in atomic orbitals can interact with each other.

For many coordination compounds, the electronic absorption spectrum provides a convenient method for determining the magnitude of the effect of ligands on the d orbitals of the metal. Although in principle we can study this effect for coordination compounds of any geometry, we will concentrate on the most common geometry, octahedral, and will examine how the absorption spectrum can be used to determine the magnitude of the octahedral ligand field parameter Δ_o, for a variety of complexes.

1.3.6.1 Electronic spectra of coordination compounds

We can now make the connection between electron-electron interactions and the absorption spectra of coordination compounds. For example, a d^2 configuration gives rise to five free-ion terms, ^3F, ^3P, ^1G, ^1D, and ^1S, with the ^3F term of lowest energy. Absorption spectra of coordination compounds in most cases involve the d orbitals of the metal, and it is consequently important to know the free-ion terms for the possible d configurations. Determining the microstates and free-ion terms for configurations of three or more electrons can be a tedious process. For reference, therefore, these are listed for the possible d electron configurations in Table (1.3). In the interpretation of spectra of coordination compounds, it is often important to identify the lowest-energy term. A quick and fairly simple way to do this is given here, using as an example a d^3 configuration in octahedral symmetry.

1. Sketch the energy levels, showing the d electrons.

2. Spin multiplicity of lowest-energy state = number of unpaired electrons $+1 \equiv 2S+1$

3. Determine the maximum possible value of M_L (=sum of m_l values) for the configuration as shown. This determines the type of free-ion term (e.g., S, P, D)

4. Combine results of Steps 2 and 3 to get the ground term.

Step 3 deserves elaboration. The maximum value of m_l for the first electron would be 2 (the highest value possible for a d electron). Because the electron spins are parallel, the second electron cannot also have $m_l = 2$ (it would violate the exclusion principle); the highest value it can have is $m_l = 1$. Finally, the third electron cannot have $m_l = 2$ or 1, because it would then have the same quantum numbers as one of the first two electrons; the highest ml value this electron could have would therefore be 0. Consequently, the maximum value of $M_L = 2+1+0=3$.

Table (1.3) free ion trems for d^n configuration

Configuration	Free-ion Terms					
d^1	^2D					
d^2		$^1S\,^1D\,^1G$	$^3P\,^3F$			
d^3	^2D		$^4P\,^4F$	$^2P\,^2D\,^2F\,^2G\,^2H$		
d^4	^5D	$^1S\,^1D\,^1G$	$^3P\,^3F$	$^3P\,^3D\,^3F\,^3G\,^3H$	$^1S\,^1D\,^1F\,^1G\,^1I$	
d^5	^2D		$^4P\,^4F$	$^2P\,^2D\,^2F\,^2G\,^2H$	$^2S\,^2D\,^2F\,^2G\,^2I$	$^4D\,^4G$ ^6S
d^6	Same as d^4					
d^7	Same as d^3					
d^8	Same as d^2					
d^9	Same as d^1					
d^{10}	^1S					

NOTE: For any configuration, the free-ion terms are the sum of those listed; for example, for the
d^2 configuration, the free-ion terms are $^1S + {}^1D + {}^1G + {}^3P + {}^3F$.

31

With this review of atomic states, we may now consider the electronic states of coordination compounds and how transitions between these states can give rise to the observed spectra. Before considering specific examples of spectra, however, we must also consider which types of transitions are most probable and, therefore, give rise to the most intense absorptions.

1.3.6.2 Splitting of spectroscopic states

As we have seen, an understanding of spin-orbit coupling is necessary to determine the spectroscopic states that exist for various electron confi gurations, d^n. Because they will be needed frequently in this chapter, the spectroscopic states that result from spin-orbit coupling in d^n ions that have degenerate d orbitals are summarized in Table (1.4).

The spectroscopic states shown in Table (1.4) are those that arise for the so-called free or gaseous ion. When a metal ion is surrounded by ligands in a coordination compound, those ligands generate an electrostatic field that removes the degeneracy of the d orbitals. The result is that eg and t2g subsets of orbitals are produced. Because the d orbitals are no longer degenerate, spin-orbit coupling is altered so that the states given in Table (1.4) no longer apply to a metal ion in a complex. However, just as the d orbitals are split in terms of their energies, the spectroscopic states are split in the ligand field. The spectroscopic states are split into components that have the same multiplicity as the free ion states from which they arise. A single electron in a d orbital gives rise to a ^2D term for the gaseous ion, but in an octahedral field the electron will reside in a t2g orbital, and the spectroscopic state for the t_2g^1 configuration is ^2T_2g. If the electron were excited to an eg orbital, the spectroscopic state would be ^2Eg. Thus, transitions between ^2T_2g and ^2Eg states would not be spin forbidden because both states are doublets. Note that lowercase letters are used to describe orbitals, whereas capital letters describe spectroscopic states.

Table (1.4) Spectroscopic States for Gaseous Ions Having d^n Electron Configurations[a].

Ion	Spectroscopic states
d^1, d^9	^2D
d^2, d^8	$^3F, ^3P, ^1G, ^1D, ^1S$
d^3, d^7	$^4F, ^4P, ^2H, ^2G, ^2F, 2^2D, ^2P$
d^4, d^6	$^5D, ^3H, ^3G, 2^3F, ^3D, 2^3P, ^1I, 2^1G, ^1F, 2^1D, 2^1S$
d^5	$^6S, ^4G, ^4F, ^4D, ^4P, ^2I, ^2H, 2^2G, 2^2F, 3^2G, 3^2D, ^2P, ^2S$
$^a 2^3F$ means two distinct ^3F terms arise, etc.	

Table (1.5) Splitting of Spectroscopic States in a Ligand Field^a

Gaseous Ion spectroscopic state	Components in an octahedral field	Total degeneracy
S	A_{1g}	1
P	T_{1g}	3
D	$E_g + T_{2g}$	5
F	$A_{2g} + T_{1g} + T_{2g}$	7
G	$A_{1g} + E_g + T_{1g} + T_{2g}$	9
H	$E_g + 2 T_{1g} + T_{2g}$	11
I	$A_{1g} + A_{2g} + E_g + T_{1g} + 2 T_{2g}$	13
^{a}Ligand field states have the same multiplicity as the spectroscopic state from which they arise.		

A gaseous ion having a d^2 configuration gives rise to a ^3F ground state as a result of spin-orbit coupling. Although they will not be derived, in an octahedral ligand field the t_2g^2 configuration gives three different spectroscopic states that are designated as ^3A_2g, ^3T_1g, and ^3T_2g. These states are often referred to as ligand field states. The energies of the three states depend on the strength of the ligand field, but the relationship is not a simple one. The larger the ligand field splitting, the greater the difference between the ligand field states of the metal. For the time being, we will assume that the function is linear, but it will be necessary to refine. Table (1.5) shows a summary of the states that result from splitting the gaseous state terms of metal ions in an octahedral field produced by six ligands. Figure (1.9) shows the approximate energies of the ligand field spectroscopic states as a function of the field strength for all d n ions. In the drawings, the states are assumed to be linear functions of Δ_o, but this is not correct over a wide range of field strength. For the d1 ion, the ^2D ground state is split into ^2T_2g and

^{2}Eg states in the ligand field. As the fi eld strength, Δ_o, increases, a center of energy is maintained for the energies of the ^{2}T$_2$g and ^{2}Eg states in exactly the same way that a center of energy is maintained by the t$_2$g and eg orbital subsets. Therefore, in order to give no net change in energy, the slope of the line for the ^2Eg state is -(3/5) Δ_o, whereas that of the ^2T_2g state is -(2/5) Δ_o.

Note that the ground-state terms for d^n ions (except for d^5) are all either D or F terms and that the state splitting occurs so that the center of energy is maintained. For the ligand fi eld states that are produced by splitting the ^{3}F term (which results from a d^2 configuration), the center of energy is also preserved even though there are three states in the ligand field. By looking at table (1.5), it can be seen that all of the states that arise from splitting the D and F ground states for the gaseous ions have T, E, or A designations. When describing the splitting of the d orbitals in an octahedral field, the "t" orbitals were seen to be triply degenerate, whereas the "e" orbitals were doubly degenerate. We can consider the spectroscopic states in the ligand field to have the same degeneracies as the orbitals, which makes it possible to preserve the center of energy. From the diagrams shown in Figure (1.8), it can be seen that the splitting pattern for a d^4 ion is like that for d^1 ion except for being inverted and the states having the appropriate multiplicities. Likewise, the splitting pattern for a d^3 ion is like that for d^2 except for being inverted and the multiplicity being different. The reason for this similarity is the "electron-hole" behavior that is seen when the spectroscopic states for confi gurations such as p^1 and p^5 are considered. Both give rise to a ^{2}P spectroscopic state, and only the J values are different. It should be apparent from the diagrams shown in Figure (1.8) that the ligand field splitting pattern is the same for d^1 and d^6, d^2 and d^7, and so forth, except for the multiplicity. In fact, it is easy to see that this will be true for any d^n and d^{5+n} configurations. It is also apparent that the singly degenerate "A" states that arise from the S states for d^5 and d^{10} confi gurations are not split in the ligand field. All of the ligand fi eld components and their energies in an octahedral field are summarized in Table (1.6).
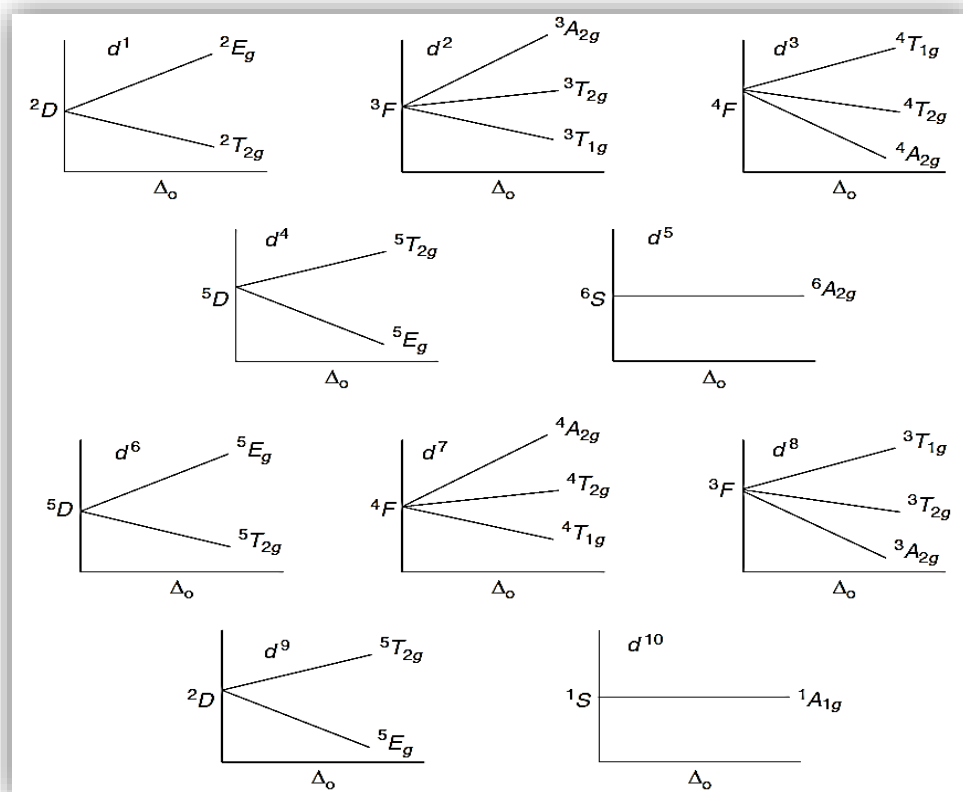
Figure (1.9) Splitting patterns for ground-state *D* and *F* terms in an octahedral field.

Table (1.6) Energies of Octahedral Ligand Field States in Terms of Δ_o.

Ion	State	Octahedral field states	Energies in octahedral field
d^1	^2D	$^2T_{2g} + {}^2E_g$	$-(2/5)\Delta_o, + (3/5)\,\Delta_o$
d^2	^3F	$^3T_{1g} + {}^3T_{2g} + {}^3A_{2g}$	$-(3/5)\Delta_o, + (1/5)\Delta_o, + (6/5)\Delta_o$
d^3	^4F	$^4A_{2g} + {}^4T_{2g} + {}^4T_{1g}$	$-(6/5)\Delta_o, -(1/5)\Delta_o, + (3/5)\Delta_o$
d^4	^5D	$^5E_g + {}^5T_{2g}$	$-(3/5)\Delta_o, + (2/5)\Delta_o$
d^5	^6S	$^6A_{1g}$	0
d^6	^5D	$^5T_{2g} + {}^5E_g$	$-(2/5)\Delta_o, + (3/5)\Delta_o,$
d^7	^4F	$^4T_{1g} + {}^4T_{2g} + {}^2A_{2g}$	$-(3/5)\Delta_o, + (1/5)\Delta_o, + (6/5)\Delta_o$
d^8	^3F	$^3A_{2g} + {}^3T_{2g} + {}^3T_{1g}$	$-(6/5)\Delta_o, -(1/5)\Delta_o, + (3/5)\Delta_o$
d^9	^2D	$^2E_g + {}^2T_{2g}$	$-(3/5)\Delta_o, + (2/5)\Delta_o$
d^{10}	^1S	^1A_g	0
Ligand field state of lowest energy given first, and energies are listed in the same order.			

When a transition metal ion is surrounded by ligands that generate a tetrahedral field, the splitting pattern of the d orbitals is inverted when compared to that in an octahedral field. As a result, the e orbitals lie lower than the t^2 set (note that there is no subscript "g" because a tetrahedron does not have a center of symmetry). A further consequence is that the energies of the ligand field spectroscopic states shown in Table (1.6) are also reversed in order compared to their order in octahedral fi elds. For example, in an octahedral fi eld, the d^2 ion gives the states (in order of increasing energy) ^3T_1g, ^3T_2g, and ^3A_2g as shown in Table 18.3. In a tetrahedral fi eld, the order of increasing energy for the states arising from a d^2 ion would be $^3A_2$, $^3T_2$, and $^3T_1$. For a specific d^n electron confi guration, there are usually several spectroscopic states that correspond to energies above the ground state term. However, they may not have the same multiplicity as the ground state. When the spectroscopic state for the free ion becomes split in an octahedral field, each ligand field component has the same multiplicity as the ground state. Transitions between spectroscopic states having different multiplicities are spin forbidden. Because the T2g and Eg spectroscopic states in a ligand fi eld have the same multiplicity as the ground states from which they arise, it can be sees that the T2g → Eg transition is the only spin-allowed transition for ions that have D ground states. In cases where the ground state is an F term, there is a P state of higher energy that has the same multiplicity. That state gives a T1g state (designated as T1g (P)) having the same multiplicity as the groundstate T1g term. Accordingly, spectroscopic transitions are possible from the ground state in the ligand field to the T state that arises from the P term. Therefore, for ions having T and A ground states, the spin-allowed transitions in an octahedral field are as follows in Table (1.7).

Table (1.7) spin-allowed transitions in an octahedral field

Octahedral Field			
For *T* ground states:		**For *A* ground states:**	
ν_1	$T_{1g} \rightarrow T_{2g}$	ν_1	$A_{2g} \rightarrow T_{2g}$
ν_2	$T_{1g} \rightarrow A_{2g}$	ν_2	$A_{2g} \rightarrow T_{1g}$
ν_3	$T_{1g} \rightarrow T_{1g}(P)$	ν_3	$A_{2g} \rightarrow T_{1g}(P)$

The spin-allowed transitions for ions having *T* and *A* ground states in tetrahedral fields are as follows in Table (1.8).

Table (1.8) spin-allowed transitions in tetrahedral fields

Tetrahedral Field			
For T ground states:		**For A ground states:**	
ν_1	$T_1 \rightarrow T_2$	ν_1	$A_2 \rightarrow T_2$
ν_2	$T_1 \rightarrow A_2$	ν_2	$A_2 \rightarrow T_1$
ν_3	$T_1 \rightarrow T_1(P)$	ν_3	$A_2 \rightarrow T_1(P)$

As shown, for both octahedral and tetrahedral complexes, three absorption bands are expected. Many complexes do, in fact, have absorption spectra that show three bands. However, charge transfer absorption makes it impossible in some cases to see all three bands, so spectral analysis must often be based on only one or two observed bands[47,p(645-650)].

1.4 Amino acid:

1.4.1 Overview:

Although more than 300 different amino acids have been described in nature, only 20 are commonly found as constituents of mammalian proteins. [Note: These are the only amino acids that are coded for by DNA, the genetic material in the cell] Each amino acid (except for proline, which has a secondary amino group) has a carboxyl group, a primary amino group, and a distinctive side chain (R-group) bonded to the α-carbon atom (Figure 1.9A). At physiologic pH (approximately pH 7.4), the carboxyl group is dissociated, forming the negatively charged carboxylate ion (–COO⁻), and the amino group is protonated (–NH$_3^+$). In proteins, almost all of these carboxyl and amino groups are combined through peptide linkage and, in general, are not available for chemical reaction except for hydrogen bond formation (Figure 1.1B). Thus, it is the nature of the side chains that ultimately dictates the role an amino acid plays in a protein. It is, therefore, useful to classify the amino acids according to the properties of their side chains, that is, whether they are nonpolar (have an even distribution of electrons) or polar (have an uneven distribution of electrons, such as acids and bases; Figures (1.10)[48].
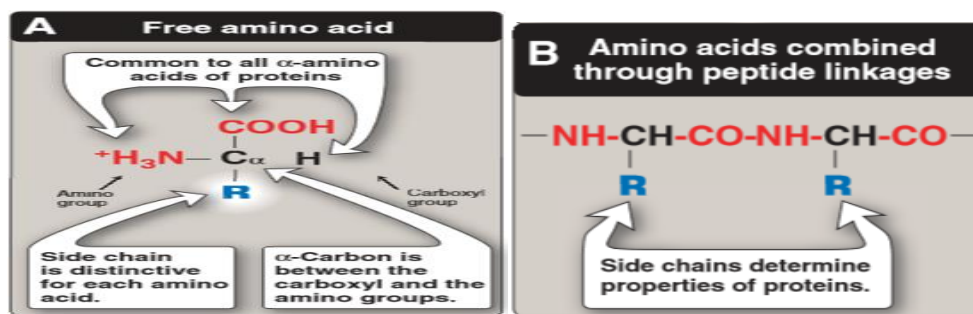
Figure (1.10) Structural features of amino acids (shown in their fully protonated form).

1.4.2 Classification of amino acids:

There are five ways of classifying amino acids depending on the:

1. Chemical nature of the amino acid in the solution

2. Structure of the side chain of the amino acids

3. Nutritional requirement of amino acids

4. Metabolic product of amino acids

5. Nature or polarity of the side chain of the amino acids. These illustrated in Table (1.9).

Table (1.9): The 20, L-α-amino acids (standard amino acids) found in proteins

Name	Symbol	Structural formula
Aliphatic side chain		
Glycine	Gly (G)	$H-CH-COO^-$ with NH_3^+
Alanine	Ala (A)	$CH_3-CH-COO^-$ with NH_3^+
Valine	Val (V)	CH_3, CH_3 >$CH-CH-COO^-$ with NH_3^+
Leucine	Leu (L)	H_3C, H_3C >$CH-CH_2-CH-COO^-$ with NH_3^+
Isoleucine	Ile (I)	CH_3, CH_2, CH_3 >$CH-CH-COO^-$ with NH_3^+
Hydroxylic (OH) group containing side chains		
Serine	Ser (S)	$CH_2-CH-COO^-$ with OH and NH_3^+
Threonine	Thr (T)	$CH_3-CH-CH-COO^-$ with OH and NH_3^+
Tyrosine	Tyr (Y)	See aromatic group containing side chain amino acids

Sulfur containing side chains

Cysteine	Cys (C)	CH_2—CH—COO$^-$ SH NH$_3^+$
Methionine	Met (M)	CH_2—CH_2—CH—COO$^-$ S—CH_3 NH$_3^+$

Side chains containing acidic groups (–COOH) and their amides

Aspartic acid	Asp (D)	COO$^-$—CH_2—CH—COO$^-$ NH$_3^+$
Aspargine	Asn (N)	H_2N—C—CH_2—CH—COO$^-$ ‖O NH$_3^+$
Glutamic acid	Glu (E)	$^-$OOC—CH_2—CH_2—CH—COO$^-$ NH$_3^+$
Glutamine	Gln (Q)	NH_2—C—CH_2—CH_2—CH—COO$^-$ ‖O NH$_3^+$

Basic groups containing side chains

Arginine	Arg (R)	H—N—CH_2—CH_2—CH_2—CH—COO$^-$ C=NH$_2^+$ NH$_3^+$ NH_2
Lysine	Lys (K)	CH_2—CH_2—CH_2—CH_2—CH—COO$^-$ NH$_3^+$ NH$_3^+$
Histidine	His (H)	CH_2—CH—COO$^-$ NH$_3^+$ (imidazole ring HN / N)

Aromatic group containing side chains

Histidine	His (H)	See above
Phenylalanine	Phe (F)	(benzene ring)—CH_2—CH—COO$^-$ NH$_3^+$
Tyrosine	Tyr (Y)	OH—(benzene ring)—CH_2—CH—COO$^-$ NH$_3^+$
Tryptophan	Trp (W)	(indole ring)—CH_2—CH—COO$^-$ NH$_3^+$

Imino acids

Proline	Pro (P)	CH_2———CH—COO$^-$ CH_2 NH CH_2

1.4.2.1 Classification Based on Chemical Nature of the Amino Acid in Solution

According to this type of classification, amino acids are classified as follows:

i. Neutral amino acids

ii. Acidic amino acids

iii. Basic amino acids.

1.4.2.2 Classification Based on Chemical Structure of Side Chain of the Amino Acid

According to this type of classification, amino acids are classified as:

1. Aliphatic amino acids

2. Hydroxy amino acids

3. Sulfur containing amino acids

4. Dicarboxylic acid and their amides

5. Diamino acids

6. Aromatic amino acids

7. Imino acids or heterocyclic amino acids.

1.4.2.3 Nutritional Classification of Amino Acids

On the basis of nutritional requirement, amino acids are classified into two groups:

i. Essential or indispensable amino acids

ii. Nonessential or dispensable amino acids.

1.4.2.4 Metabolic Classification of Amino Acids

On the basis of their catabolic end products, the twenty standard amino acids are divided in three groups

i. **Glucogenic amino acids:** Those which can be converted into glucose. Fourteen out of the twenty standard amino acids are glucogenic amino acids

ii. **Ketogenic amino acids:** Those which can be converted to ketone bodies. Two amino acids **leucine** and **lysine** are exclusively ketogenic.

iii. **Both glucogenic and ketogenic:** Those which can be converted to both glucose and ketone bodies. Four amino acids **isoleucine, phenylalanine, tryptophan** and **tyrosine** are glucogenic and ketogenic.

1.4.2.5 Classification Based on Nature or Polarity of Side Chain of Amino Acid

According to this type of classification, amino acids are classified into two major classes, Figure (1.11):

i. Hydrophilic or polar amino acids.

ii. Hydrophobic or nonpolar amino acids[49].
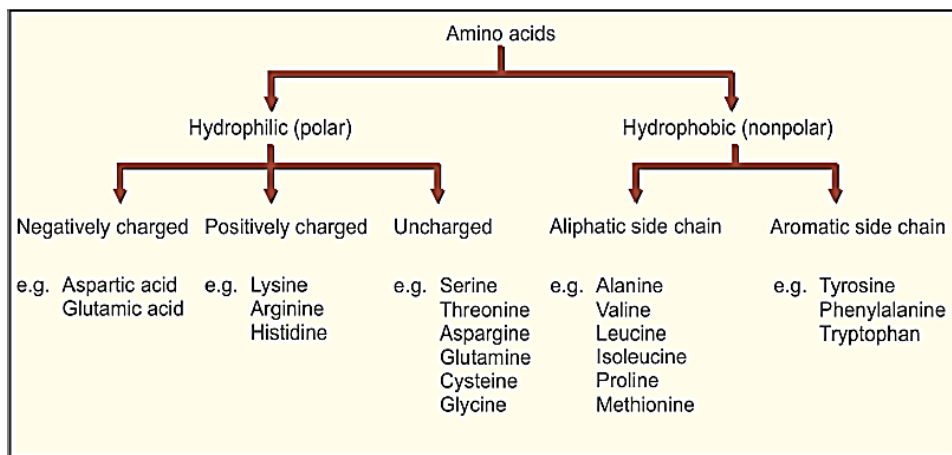
Figure (1.11) Classification of amino acids based on polarity

1.4.3 Properties of the function groups of amino acid:

Amino Acids May Have Positive, negative, or Zero net Charge In aqueous solution, the charged and uncharged forms of the ionizable weak acid groups ´COOH and ´NH^{3+} exist in dynamic protonic equilibrium:

$$R - COOH \rightleftarrows R - COO^- + H^+$$
$$R - NH_3^+ \rightleftarrows R - NH_2 + H^+$$
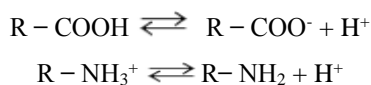
While both R´COOH and R´NH$_3^+$ are weak acids, R´COOH is a far stronger acid than R´NH$_3^+$. Thus, at physiologic pH (pH 7.4), carboxyl groups exist almost entirely as R´COO$^-$ and amino groups predominantly as R´NH$_3^+$. The imidazole group of histidine and the guanidino group of arginine exist as resonance hybrids with positive charge distributed between two nitrogens (histidine) or three nitrogen's (arginine) Figure (1.12) illustrate the effect that the pH of the aqueous environment has on the charged state of aspartic acid and lysine, Figures (1.13) and (1.14), respectively.
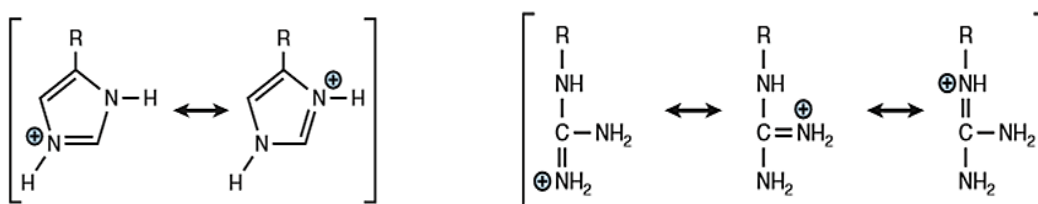
Figure (1.12) Resonance hybrids of the protonated R groups of histidine (light) and arginine (right)
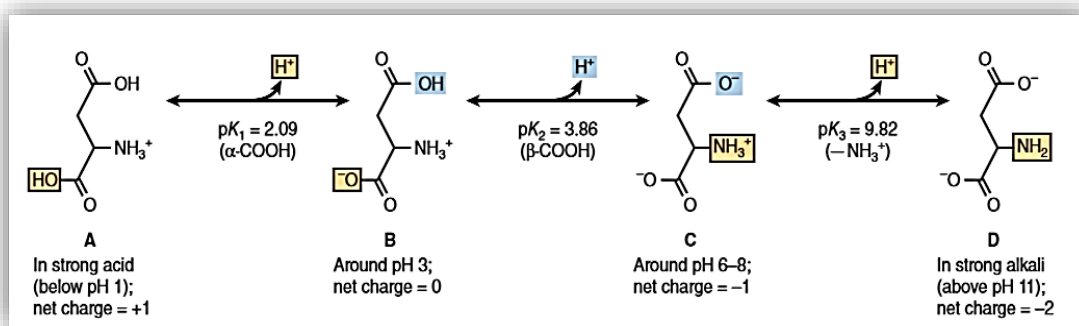
Figure (1.13) Protonic equilibria of aspartic acid
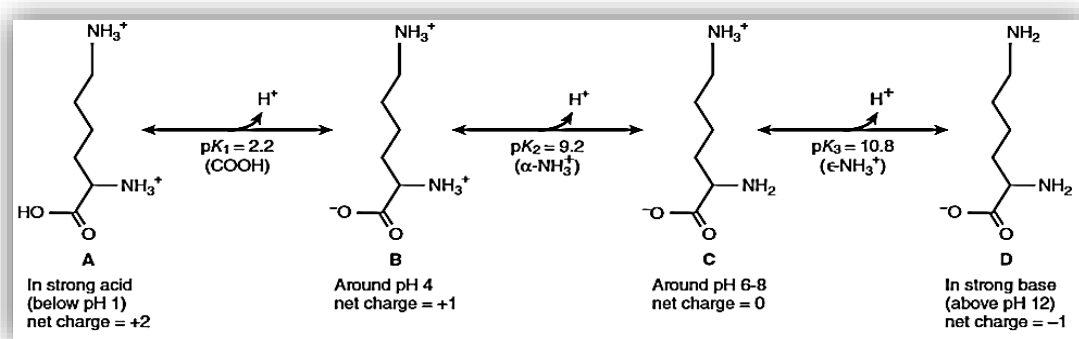
Figure (1.14) Protonic equilibria of lysine

Molecules that contain an equal number of positively and negatively charged groups bear no net charge. These ionized neutral species are termed zwitterions. Amino acids in blood and most tissues thus should be represented as in, Figure (1.15) A.
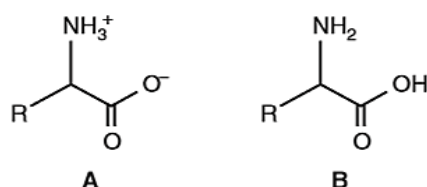
Figure (1.15) Zwitterions of amino acid species

Structure B cannot exist in aqueous solution because at any pH low enough to protonate the carboxyl group, the amino group would also be protonated. Similarly, at any pH sufficiently high for an uncharged amino group to predominate, a carboxyl group will be present as $R´COO^-$. The uncharged representation B is, however, often used when diagramming reactions that do not involve protonic equilibria.

42

1.4.4 The (R) groups determine the properties of amino acids:

Each functional group of an amino acid exhibits all of its characteristic chemical reactions. For carboxylic acid groups, these reactions include the formation of esters, amides, and acid anhydrides; for amino groups, acylation, amidation, and esterification; and for ´OH and ´SH groups, oxidation and esterification. Since glycine, the smallest amino acid, can be accommodated in places inaccessible to other amino acids, it often occurs where peptides bend sharply. The hydrophobic R groups of alanine, valine, leucine, and isoleucine and the aromatic R groups of phenylalanine, tyrosine, and tryptophan typically occur primarily in the interior of cytosolic proteins. The charged R groups of basic and acidic amino acids stabilize specific protein conformations via ionic interactions, or salt bridges. These interactions also function in "charge relay'' systems during enzymatic catalysis and electron transport in respiring mitochondria. Histidine plays unique roles in enzymatic catalysis. The pKa of its imidazole proton permits histidine to function at neutral pH as either a base or an acid catalyst without the need for any environmentally induced shift. The primary alcohol group of serine and the primary thioalcohol (´SH) group of cysteine are excellent nucleophiles, and can function as such during enzymatic catalysis. The pK3 of selenocysteine, 5.2, is 3 units lower than that of cysteine, so that it should, in principle, be the better nucleophile. However, the secondary alcohol group of threonine, while a good nucleophile, is not known to fulfill an analogous role in catalysis. The ´OH groups of serine, tyrosine, and threonine frequently serve as the points of covalent attachment for phosphoryl groups that regulate protein function[50].

1.4.5 Glycine

Glycine (symbol Gly or G;[51] glaısi:n/)[52] is the amino acid that has a single hydrogen atom as its side chain. It is the simplest possible amino acid. The chemical formula of glycine is NH_2-CH_2-$COOH$. Glycine is one of the proteinogenic amino acids. Glycine is a colorless, sweet-tasting crystalline solid. It is the only achiral proteinogenic amino acid. It can fit into hydrophilic or hydrophobic environments, due to its minimal side chain of only one hydrogen atom. The acyl radical is glycyl.

1.4.5.1 History and etymology

Glycine was discovered in 1820 by the French chemist Henri Braconnot when he hydrolyzed gelatin by boiling it with sulfuric acid.[53] He originally called it "sugar of gelatin", [54,55] but the French chemist Jean-Baptiste Boussingault showed that it contained nitrogen.[56] The American scientist Eben Norton Horsford, then a student of the German chemist Justus von Liebig, proposed the name "glycocoll";[57,58] however, the Swedish chemist Berzelius suggested the simpler name "glycine".[59,60] The name comes

from the Greek word γλυκύς "sweet tasting"[61] (which is also related to the prefixes glyco- and gluco-, as in glycoprotein and glucose). In 1858, the French chemist Auguste Cahours determined that glycine was an amine of acetic acid.[62]

1.4.5.2 Production

Although glycine can be isolated from hydrolyzed protein, this is not used for industrial production, as it can be manufactured more conveniently by chemical synthesis.[16] The two main processes are amination of chloroacetic acid with ammonia, giving glycine and ammonium chloride,[63] and the Strecker amino acid synthesis,[64] which is the main synthetic method in the United States and Japan.[65] About 15 thousand tonnes are produced annually in this way.[66] Glycine is also cogenerated as an impurity in the synthesis of EDTA, arising from reactions of the ammonia coproduct.[67]

1.4.5.3 Acid-base properties
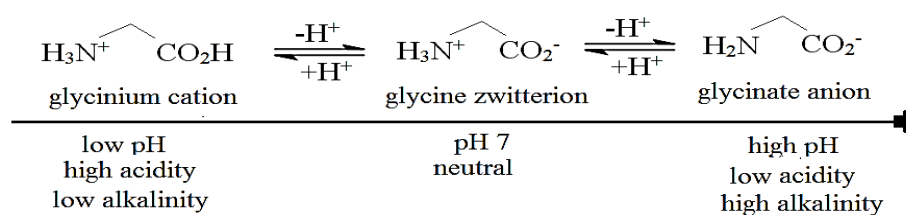
Figure (1.16) effect of pH in glycine

In aqueous solution, Figure (1.16), glycine itself is amphoteric: at low pH the molecule can be protonated with a pK_a of about 2.4 and at high pH it loses a proton with a pK_a of about 9.6 (precise values of pK_a depend on temperature and ionic strength).

1.4.5.4 Metabolism

Biosynthesis

Glycine is not essential to the human diet, as it is biosynthesized in the body from the amino acid serine, which is in turn derived from 3-phosphoglycerate, but the metabolic capacity for glycine biosynthesis does not satisfy the need for collagen synthesis.[68] In most organisms, the enzyme serine hydroxymethyltransferase catalyses this transformation via the cofactor pyridoxal phosphate:[69]

$$\text{Serine} + \text{tetrahydrofolate} \rightarrow \text{glycine} + N^5,N^{10}\text{-Methylene tetrahydrofolate} + H_2O$$
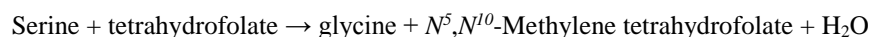
In the liver of vertebrates, glycine synthesis is catalyzed by glycine synthase (also called glycine cleavage enzyme). This conversion is readily reversible.[69]

$$CO_2 + NH_4^+ + N^5,N^{10}\text{-Methylene tetrahydrofolate} + NADH + H^+ \rightleftharpoons \text{Glycine} + \text{tetrahydrofolate} + NAD^+$$
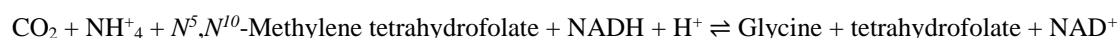
Degradation

Glycine is degraded via three pathways. The predominant pathway in animals and plants is the reverse of the glycine synthase pathway mentioned above. In this context, the enzyme system involved is usually called the glycine cleavage system:[69]

$$\text{Glycine+tetrahydrofolate+NAD}^+ \rightleftharpoons \text{CO}_2\text{+NH}^+_4\text{+ } N^5,N^{10}\text{-Methylene tetrahydrofolate + NADH + H}^+$$
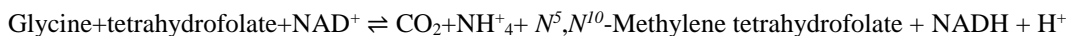
In the second pathway, glycine is degraded in two steps. The first step is the reverse of glycine biosynthesis from serine with serine hydroxymethyl transferase. Serine is then converted to pyruvate by serine dehydratase.[69] In the third pathway of glycine degradation, glycine is converted to glyoxylate by D-amino acid oxidase. Glyoxylate is then oxidized by hepatic lactate dehydrogenase to oxalate in an NAD^+-dependent reaction.[69] The half-life of glycine and its elimination from the body varies significantly based on dose. In one study, the half-life varied between 0.5 and 4.0 hours.[70]

Physiological function

The principal function of glycine is as a precursor to proteins. Most proteins incorporate only small quantities of glycine, a notable exception being collagen, which contains about 35% glycine due to its periodically repeated role in the formation of collagen's helix structure in conjunction with hydroxyproline.[69,71]

As a biosynthetic intermediate

In higher eukaryotes, δ-aminolevulinic acid, the key precursor to porphyrins, is biosynthesized from glycine and succinyl-CoA by the enzyme ALA synthase. Glycine provides the central C_2N subunit of all purines.[69]

As a neurotransmitte

Glycine is an inhibitory neurotransmitter in the central nervous system, especially in the spinal cord, brainstem, and retina. When glycine receptors are activated, chloride enters the neuron via ionotropic receptors, causing an Inhibitory postsynaptic potential (IPSP). Strychnine is a strong antagonist at ionotropic glycine receptors, whereas bicuculline is a weak one. Glycine is a required co-agonist along with glutamate for NMDA receptors. In contrast to the inhibitory role of glycine in the spinal cord, this behaviour is facilitated at the (NMDA) glutamatergic receptors which are excitatory.[72] The LD_{50} of glycine is 7930 mg/kg in rats (oral),[73] and it usually causes death by hyperexcitability.

1.4.5.5 Uses

In the US, glycine is typically sold in two grades: United States Pharmacopeia ("USP"), and technical grade. USP grade sales account for approximately 80 to 85 percent of the U.S. market for glycine.

Where the customer's purity requirements exceed the minimum required under the USP standard, for example for some pharmaceutical applications such as intravenous injections, pharmaceutical grade glycine, often produced to proprietary specifications and typically sold at a premium over USP grade glycine, may be used. Technical grade glycine, which may or may not meet USP grade standards, is sold at a lower price for use in industrial applications, e.g., as an agent in metal complexing and finishing.[74]

Animal and human foods

USP glycine has a wide variety of uses, including as an additive in pet food and animal feed, in foods and pharmaceuticals as a sweetener/taste enhancer, or as a component of food supplements and protein drinks.

Two glycine molecules in a dipeptide form (Diglycinate) are sometimes used as a way to enhance the absorption of mineral supplementation since, only when bound to a dipeptide, can be absorbed through a different set of transporters.[75]

Cosmetics and miscellaneous applications

Glycine serves as a buffering agent in antacids, analgesics, antiperspirants, cosmetics, and toiletries. A variety of industrial and chemical processes use glycine or its derivatives, such as the production of fertilizers and metal complexing agents.[76]

Chemical feedstock

Glycine is an intermediate in the synthesis of a variety of chemical products. It is used in the manufacture of the herbicide glyphosate.[77]

Laboratory research

Glycine is a significant component of some solutions used in the SDS-PAGE method of protein analysis. It serves as a buffering agent, maintaining pH and preventing sample damage during electrophoresis. Glycine is also used to remove protein-labeling antibodies from Western blot membranes to enable the probing of numerous proteins of interest from SDS-PAGE gel. This allows more data to be drawn from the same specimen, increasing the reliability of the data, reducing the amount of sample processing, and number of samples required. This process is known as stripping.

Industrial Use

It is widely used as an intermediate of the medicine such as thiamphenicol, as an intermediate in the production of glyphosate, as a solvent for removing carbon dioxide (CO_2) in the fertilizer industry, and as the galvanizing solution in electroplating.[78,79]

1.4.5.6 Presence in space

The presence of glycine outside the earth was confirmed in 2009, based on the analysis of samples that had been taken in 2004 by the NASA spacecraft Stardust from comet Wild 2 and subsequently returned to earth. Glycine had previously been identified in the Murchison meteorite in 1970.[80] The discovery of cometary glycine bolstered the theory of panspermia, which claims that the "building blocks" of life are widespread throughout the Universe.[81] In 2016, detection of glycine within Comet 67P/Churyumov-Gerasimenko by the Rosetta spacecraft was announced.[82] The detection of glycine outside the solar system in the interstellar medium has been debated.[83] In 2008, the Max Planck Institute for Radio Astronomy discovered the glycine-like molecule aminoacetonitrile in the Large Molecule Heimat, a giant gas cloud near the galactic center in the constellation Sagittarius.[84] which summarized in Table (1.10).

Table (1.10) Presence of glycin in foods[85]

Food	g/100g
Snacks, pork skins	11.04
flour (low fat)Sesame seeds	3.43
Beverages, Protein powder soy based	2.37
Seeds, safflower seed meal, partially defatted	2.22
Meat, bison, beef and others (various parts)	1.5-2.0
Gelatin desserts	1.96
Seeds, pumpkin and squash seed kernels	1.82
Turkey, all classes, back, meat and skin	1.79
Chicken, broilers or fryers, meat and skin	1.74
Pork, ground, 96% lean / 4% fat, cooked, crumbles	1.71
Bacon and beef sticks	1.64
Peanuts	1.63
spiny lobsterCrustaceans	1.59
Spices, mustard seed, ground	1.59
Salami	1.55

Nuts, butternuts, dried	1.51
Fish, salmon, pink, canned, drained solids	1.42
Almonds	1.42
Fish, mackerel	0.93
Cereals ready-to-eat, granola, homemade	0.81
, (bulb and lower-leaf portion), freeze-driedLeeks	0.7
Cheese, parmesan (and others), grated	0.56
, green, cooked, boiled, drained, without saltSoybeans	0.51
Bread, protein (includes gluten)	0.47
Egg, whole, cooked, fried	0.47
Beans, white, mature seeds, cooked, boiled, with salt	0.38
Lentils, mature seeds, cooked, boiled, with salt	0.37

1.4.6 Serine

Serine (symbol Ser or S)[86,87] is an α-amino acid that is used in the biosynthesis of proteins. It contains an α-amino group (which is in the protonated $-NH_3^+$ form under biological conditions), a carboxyl group (which is in the deprotonated $-COO^-$ form in physiological conditions), and a side chain consisting of a hydroxymethyl group, classifying it as a polar amino acid. It can be synthesized in the human body under normal physiological circumstances, making it a nonessential amino acid.

1.4.6.1 Occurrence

This compound is one of the naturally occurring proteinogenic amino acids. Only the L-stereoisomer appears naturally in proteins. Figure (1.17), It is not essential to the human diet, since it is synthesized in the body from other metabolites, including glycine. Serine was first obtained from silk protein, a particularly rich source, in 1865 by Emil Cramer[88]. Its name is derived from the Latin for silk, *sericum*. Serine's structure was established in 1902.[89]
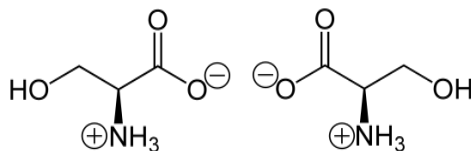
Figure (1.17) L-Stereoisomer of serine in proteins

1.4.6.2 Biosynthesis

The biosynthesis of serine, Figure (1.18) starts with the oxidation of 3-phosphoglycerate (an intermediate from glycolysis) to 3-phosphohydroxypyruvate and NADH by phosphoglycerate dehydrogenase (EC 1.1.1.95). Reductive amination (transamination) of this ketone by phosphoserine transaminase (EC 2.6.1.52) yields 3-phosphoserine (O-phosphoserine) which is hydrolyzed to serine by phosphoserine phosphatase (EC 3.1.3.3).[90] In bacteria such as *E. coli* these enzymes are encoded by the genes serA (EC 1.1.1.95), serC (EC 2.6.1.52), and ser B (EC 3.1.3.3).
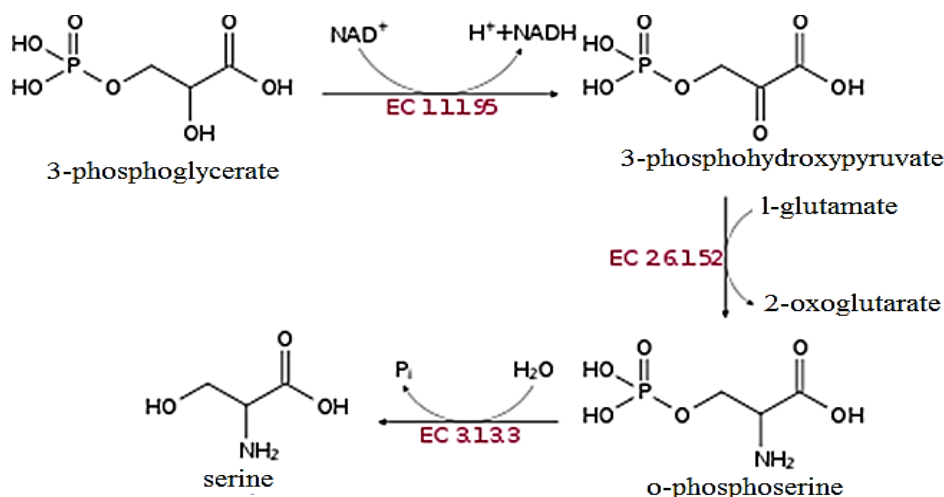
Figure (1.18) Serine biosynthesis

Glycine biosynthesis: Serine hydroxymethyltransferase (SHMT = serine transhydroxymethylase) also catalyzes the reversible conversions of L-serine to glycine (retro-aldol cleavage) and 5,6,7,8-tetrahydrofolate to 5,10-methylenetetrahydrofolate (mTHF) (hydrolysis).[91] SHMT is a pyridoxal phosphate (PLP) dependent enzyme. Glycine can also be formed from CO_2, NH_4^+, and mTHF in a reaction catalyzed by glycine synthase.[89]

1.4.6.3 Synthesis and industrial production

Industrially, L-serine is produced by fermentation, with an estimated 100-1000 tonnes per year produced.[92] In the laboratory, racemic serine can be prepared from methyl acrylate via several steps, Figure (1.19).[93]
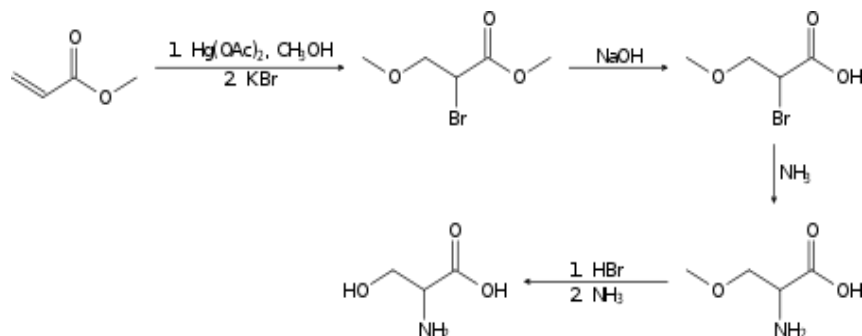
Figure (1.19) serine production

1.4.6.4 Biological function

Metabolic

Serine is important in metabolism in that it participates in the biosynthesis of purines and pyrimidines. It is the precursor to several amino acids including glycine and cysteine, as well as tryptophan in bacteria. It is also the precursor to numerous other metabolites, including sphingolipids and folate, which is the principal donor of one-carbon fragments in biosynthesis.

Structural role

- Serine plays an important role in the catalytic function of many enzymes. It has been shown to occur in the active sites of chymotrypsin, trypsin, and many other enzymes. The so-called nerve gases and many substances used in insecticides have been shown to act by combining with a residue of serine in the active site of acetylcholine esterase, inhibiting the enzyme completely.

- Serine sidechains are often hydrogen bonded; the commonest small motifs formed are ST turns, ST motifs (often at the beginning of alpha helices) and ST staples (usually at the middle of alpha helices).

- As a constituent (residue) of proteins, its side chain can undergo *O*-linked glycosylation, which may be functionally related to diabetes.

- It is one of three amino acid residues that are commonly phosphorylated by kinases during cell signaling in eukaryotes. Phosphorylated serine residues are often referred to as phosphoserine.

- Serine proteases are a common type of protease.

Signaling

D-Serine, synthesized in neurons by serine racemase from L-serine (its enantiomer), serves as a neuromodulator by coactivating NMDA receptors, making them able to open if they then also bind glutamate. D-serine is a potent agonist at the glycine site (NR1) of the NMDA-type glutamate receptor (NMDAR). For the receptor to open, glutamate and either glycine or D-serine must bind to it; in

addition a pore blocker must not be bound (e.g. Mg^{2+} or Zn^{2+}).[94] In fact, D-serine is a more potent agonist at the glycine site on the NMDAR than glycine itself. D-serine was thought to exist only in bacteria until relatively recently; it was the second D amino acid discovered to naturally exist in humans, present as a signaling molecule in the brain, soon after the discovery of D-aspartate. Had D amino acids been discovered in humans sooner, the glycine site on the NMDA receptor might instead be named the D-serine site.[95] Apart from central nervous system, D-serine plays a signaling role in peripheral tissues and organs such as cartilage,[96] kidney[97] and corpus cavernosum.[98]

Clinical significance

Serine deficiency disorders are rare defects in the biosynthesis of the amino acid L-serine. At present three disorders have been reported: 3-phosphoglycerate dehydrogenase deficiency, 3-phosphoserine phosphatase deficiency and Phosphoserine aminotransferase deficiency. These enzyme defects lead to severe neurological symptoms such as congenital microcephaly and severe psychomotor retardation and in addition in patients with 3-phosphoglycerate dehydrogenase deficiency to intractable seizures. These symptoms respond to a variable degree to treatment with L-serine, sometimes combined with glycine.[99,100] Response to treatment is variable and the long-term and functional outcome is unknown. To provide a basis for improving the understanding of the epidemiology, genotype/phenotype correlation and outcome of these diseases their impact on the quality of life of patients, as well as for evaluating diagnostic and therapeutic strategies a patient registry was established by the noncommercial International Working Group on Neurotransmitter Related Disorders (iNTD).

1.4.6.5 Research for therapeutic use

D-Serine is being studied in rodents as a potential treatment for schizophrenia[101] and L-serine is in a FDA-approved human clinical trial as a possible treatment for Amyotrophic Lateral Sclerosis ALS (ClinicalTrials.gov identifier: NCT01835782).[102] A 2011 meta-analysis found adjunctive sarcosine to have a medium effect size for negative and total symptoms.[103] D-Serine has also been described as a potential biomarker for early Alzheimer's disease (AD) diagnosis, due to a relatively high concentration of it in the cerebrospinal fluid of probable AD patients.[104]

1.4.7 Arginine

Arginine, also known as L-arginine (symbol Arg or R)[51], is an α-amino acid that is used in the biosynthesis of proteins.[105] It contains an α-amino group, an α-carboxylic acid group, and a side chain consisting of a 3-carbon aliphatic straight chain ending in a guanidino group. At physiological pH, the carboxylic acid is deprotonated ($-COO^-$), the amino group is protonated ($-NH_3^+$), and the guanidino

group is also protonated to give the guanidinium form ($-C-(NH_2)_2^+$), making arginine a charged, aliphatic amino acid.[106] It is the precursor for the biosynthesis of nitric oxide. In humans, arginine is classified as a semiessential or conditionally essential amino acid, depending on the developmental stage and health status of the individual.[107] Preterm infants are unable to synthesize or create arginine internally, making the amino acid nutritionally essential for them.[108] Most healthy people do not need to supplement with arginine because it is a component of all protein-containing foods[109] and can be synthesized in the body from glutamine via citrulline.[110]

1.4.7.1 History

Arginine was first isolated in 1886 from lupin and pumpkin seedlings by the German chemist Ernst Schulze[111] and his assistant Ernst Steiger.[112] In 1897, Ernst Schulze and Ernst Winterstein (1865–1949) determined the structure of arginine.[113] Schulze and Winterstein synthesized arginine from ornithine and cyanamide in 1899,[114] but some doubts about arginine's structure lingered[115] until Sørensen's synthesis of 1910.[116]

1.4.7.2 Sources

Dietary sources

Arginine is a conditionally essential amino acid in humans and rodents,[117] as it may be required depending on the health status or lifecycle of the individual. For example, while healthy adults can supply their own requirement for arginine, immature and rapidly growing individuals require arginine in their diet,[118] and it is also essential under physiological stress, for example during recovery from burns, injury, and sepsis,[118] or when the small intestine and kidneys, which are the major sites of arginine biosynthesis, have been damaged.[117] It is, however, an essential amino acid for birds, as they do not have a urea cycle.[119] For some carnivores, for example cats, dogs[120] and ferrets, arginine is essential,[117] because after a meal, their highly efficient protein catabolism produces large quantities of ammonia which need to be processed through the urea cycle, and if not enough arginine is present, the resulting ammonia toxicity can be lethal.[121] This is not a problem in practice, because meat contains sufficient arginine to avoid this situation.[121] Animal sources of arginine include meat, dairy products, and eggs,[122,123] and plant sources include seeds of all types, for example grains, beans, and nuts.[123]

Biosynthesis

Arginine is synthesized from citrulline in arginine and proline metabolism by the sequential action of the cytosolic enzymes argininosuccinate synthetase and argininosuccinate lyase. This is an energetically costly process, because for each molecule of argininosuccinate that is synthesized, one molecule of

adenosine triphosphate (ATP) is hydrolyzed to adenosine monophosphate (AMP), consuming two ATP equivalents.

Citrulline can be derived from multiple sources:

- from arginine itself via nitric oxide synthase, as a byproduct of the production of nitric oxide for signaling purposes
- from ornithine through the breakdown of proline or glutamine/glutamate
- from asymmetric dimethylarginine via DDAH

The pathways linking arginine, glutamine, and proline are bidirectional. Thus, the net use or production of these amino acids is highly dependent on cell type and developmental stage.

On a whole-body basis, synthesis of arginine occurs principally via the intestinal–renal axis: the epithelial cells of the small intestine produce citrulline, primarily from glutamine and glutamate, which is carried in the bloodstream to the proximal tubule cells of the kidney, which extract citrulline from the circulation and convert it to arginine, which is returned to the circulation. This means that impaired small bowel or renal function can reduce arginine synthesis, increasing the dietary requirement.

Synthesis of arginine from citrulline also occurs at a low level in many other cells, and cellular capacity for arginine synthesis can be markedly increased under circumstances that increase the production of inducible NOS. This allows citrulline, a byproduct of the NOS-catalyzed production of nitric oxide, to be recycled to arginine in a pathway known as the citrulline-NO or arginine-citrulline pathway. This is demonstrated by the fact that, in many cell types, NO synthesis can be supported to some extent by citrulline, and not just by arginine. This recycling is not quantitative, however, because citrulline accumulates in NO-producing cells along with nitrate and nitrite, the stable end-products of NO breakdown.[124]

1.4.7.3 Function

Arginine plays an important role in cell division, wound healing, removing ammonia from the body, immune function,[125] and the release of hormones.[107,126,127] It is a precursor for the synthesis of nitric oxide (NO),[128] making it important in the regulation of blood pressure.[129-131]

Proteins

Arginine's side chain is amphipathic, because at physiological pH it contains a positively charged guanidinium group, which is highly polar, at the end of a hydrophobic aliphatic hydrocarbon chain. Because globular proteins have hydrophobic interiors and hydrophilic surfaces,[132] arginine is typically

found on the outside of the protein, where the hydrophilic head group can interact with the polar environment, for example taking part in hydrogen bonding and salt bridges.[133] For this reason, it is frequently found at the interface between two proteins.[134] The aliphatic part of the side chain sometimes remains below the surface of the protein.[133] Arginine residues in proteins can be deiminated by PAD enzymes to form citrulline, in a post-translational modification process called citrullination.This is important in fetal development, is part of the normal immune process, as well as the control of gene expression, but is also significant in autoimmune diseases.[135,275] another post-translational modification of arginine involves methylation by protein methyltransferases.[135,176]

Precursor

Arginine is the immediate precursor of NO, an important signaling molecule which can act as a second messenger, as well as an intercellular messenger which regulates vasodilation, and also has functions in the immune system's reaction to infection.

Arginine is also a precursor for urea, ornithine, and agmatine; is necessary for the synthesis of creatine; and can also be used for the synthesis of polyamines (mainly through ornithine and to a lesser degree through agmatine, citrulline, and glutamate. The presence of asymmetric dimethylarginine (ADMA), a close relative, inhibits the nitric oxide reaction; therefore, ADMA is considered a marker for vascular disease, just as L-arginine is considered a sign of a healthy endothelium.

1.4.7.4 Structure
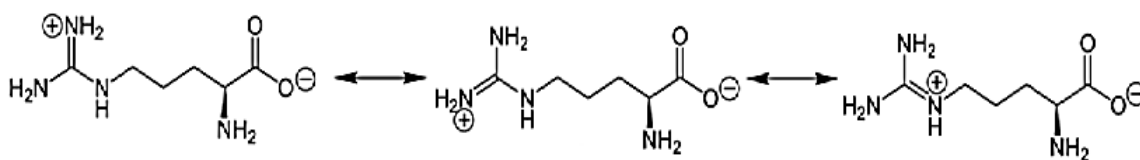
Figure (1.20) Delocalization of charge in guanidinium group of L-Arginine

The amino acid side-chain of arginine consists of a 3-carbon aliphatic straight chain, the distal end of which is capped by a guanidinium group, Figure (1.20). Which has a pK_a of 12- 48, and is therefore always protonated and positively charged at physiological pH. Because of the conjugation between the

double bond and the nitrogen lone pairs, the positive charge is delocalized, enabling the formation of multiple hydrogen bonds.

1.4.7.5 Research

Growth hormone

Intravenously administered arginine is used in growth hormone stimulation tests[136] because it stimulates the secretion of growth hormone.[137] A review of clinical trials concluded that oral arginine increases growth hormone, but decreases growth hormone secretion, which is normally associated with exercising.[138] However, a more recent trial reported that although oral arginine increased plasma levels of L-arginine it did not cause an increase in growth hormone.[139]

High blood pressure

A meta-analysis showed that L-arginine reduces blood pressure with pooled estimates of 5.4 mmHg for systolic blood pressure and 2.7 mmHg for diastolic blood pressure.[130] Supplementation with L-arginine reduces diastolic blood pressure and lengthens pregnancy for women with gestational hypertension, including women with high blood pressure as part of pre-eclampsia. It did not lower systolic blood pressure or improve weight at birth.[140]

1.4.8 Aspartic acid:

Aspartic acid (symbol Asp or D;[141] the ionic form is known as aspartate), is an α-amino acid that is used in the biosynthesis of proteins.[142] Similar to all other amino acids it contains an amino group and a carboxylic acid. Its α-amino group is in the protonated $-NH_3^+$ form under physiological conditions, while its α-carboxylic acid group is deprotonated $-COO^-$ under physiological conditions. Aspartic acid has an acidic side chain (CH_2COOH) which reacts with other amino acids, enzymes and proteins in the body.[142] Under physiological conditions (pH 7.4) in proteins the side chain usually occurs as the negatively charged aspartate form, $-COO^-$.[142] It is a non-essential amino acid in humans, meaning the body can synthesize it as needed. D-Aspartate is one of two D-amino acids commonly found in mammals.[141] In proteins aspartate sidechains are often hydrogen bonded to form asx turns or asx motifs, which frequently occur at the N-termini of alpha helices. The L-isomer of Asp is one of the 22 proteinogenic amino acids, i.e., the building blocks of proteins. Aspartic acid, like glutamic acid, is classified as an acidic amino acid, with a pK_a of 3.9, however in a peptide this is highly dependent on the local environment, and could be as high as 14. Asp is pervasive in biosynthesis.

1.4.8.1 Discovery

Aspartic acid was first discovered in 1827 by Auguste-Arthur Plisson and Étienne Ossian Henry[143] by hydrolysis of asparagine, which had been isolated from asparagus juice in 1806.[144] Their original method used lead hydroxide, but various other acids or bases are more commonly used instead.

1.4.8.2 Forms and nomenclature

There are two forms or enantiomers of aspartic acid. The name "aspartic acid" can refer to either enantiomer or a mixture of two.[145] Of these two forms, only one, "L-aspartic acid", is directly incorporated into proteins. The biological roles of its counterpart, "D-aspartic acid" are more limited. Where enzymatic synthesis will produce one or the other, most chemical syses will produce both forms, "DL-aspartic acid", known as a racemic mixture.

Biosynthesis

Because Aspartate can be synthesized by the body it is classified as a non-essential amino acid. In the human body, aspartate is most frequently synthesized through the transamination of oxaloacetate. The biosynthesis of aspartate is facilitated by an aminotransferase enzyme: the transfer of an amine group from another molecule such as alanine or glutamine yields aspartate and an alpha-keto acid.[142] Aspartate also plays an important role in the urea cycle.

Chemical synthesis

Racemic aspartic acid can be synthesized from diethyl sodium phthalimidomalonate, $(C_6H_4(CO)_2NC(CO_2Et)_2)$.[146] The major disadvantage of the above technique is that equimolar amounts of each enantiomer are made. Using biotechnology it is now possible to use immobilised enzymes to create just one type of enantiomer owing to their stereospecificity.

1.4.8.3 Metabolism

  - In plants and microorganisms, aspartate is the precursor to several amino acids, including four that are essential for humans: methionine, threonine, isoleucine, and lysine. The conversion of aspartate to these other amino acids begins with reduction of aspartate to its "semialdehyde", $O_2CCH(NH_2)CH_2CHO$.[147] Asparagine is derived from aspartate via transamidation:

$$-O_2CCH(NH_2)CH_2CO_2- + GC(O)NH_3+ O_2CCH(NH_2)CH_2CONH_3+ + GC(O)O$$
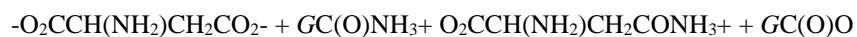
(Where GC (O)NH_2 and GC(O)OH are glutamine and glutamic acid, respectively)

- In the urea cycle, aspartate and ammonia donate amino groups leading to the formation of urea.

- Aspartate has many other biochemical roles. It is a metabolite in the urea cycle and participates in gluconeogenesis. It carries reducing equivalents in the malate-aspartate shuttle, which utilizes the ready interconversion of aspartate and oxaloacetate, which is the oxidized (dehydrogenated) derivative of malic acid. Aspartate donates one nitrogen atom in the biosynthesis of inosine, the precursor to the purine bases. In addition, aspartic acid acts as a hydrogen acceptor in a chain of ATP synthase.

- Aspartate (the conjugate base of aspartic acid) stimulates NMDA receptors, though not as strongly as the amino acid neurotransmitter L-glutamate does.[148]

1.4.9 Leucine

Leucine (symbol Leu or L)[51] is an essential amino acid that is used in the biosynthesis of proteins. Leucine is an α-amino acid, meaning it contains an α-amino group (which is in the protonated $-NH_3^+$ form under biological conditions), an α-carboxylic acid group (which is in the deprotonated $-COO^-$ form under biological conditions), and a side chain isobutyl group, making it a non-polar aliphatic amino acid. It is essential in humans, meaning the body cannot synthesize it: it must be obtained from the diet. Human dietary sources are foods that contain protein, such as meats, dairy products, soy products, and beans and other legumes. Like valine and isoleucine, leucine is a branched-chain amino acid. The primary metabolic end products of leucine metabolism are acetyl-CoA and acetoacetate; consequently, it is one of the two exclusively ketogenic amino acids, with lysine being the other.[149] It is the most important ketogenic amino acid in humans.[150 p.101] Leucine and β-hydroxy β-methylbutyric acid, a minor leucine metabolite, exhibit pharmacological activity in humans and have been demonstrated to promote protein biosynthesis via the phosphorylation of the mechanistic target of rapamycin (mTOR).[151,152]

1.4.9.1 Dietary leucine

As a food additive, L-leucine has E number E641 and is classified as a flavor enhancer.[153]

Requirements

The Food and Nutrition Board (FNB) of the U.S. Institute of Medicine set Recommended Dietary Allowances (RDAs) for essential amino acids in 2002. For leucine, for adults 19 years and older, 42 mg/kg body weight/day.[154]

Sources

Table (1.11) food sources of leucine [155]

Food	g/100g
concentrate, dry powderWhey protein	10.0-12.0

concentrate, dry powderSoy protein	7.5-8.5
, mature seeds, roasted, saltedSoybeans	2.87
seed, hulledHemp	2.16
, round, top round, rawBeef	1.76
Peanuts	1.67
, salmon, pink, rawFish	1.62
Wheat germ	1.57
Almonds	1.49
, broilers or fryers, thigh, rawChicken	1.48
, yolk, rawChicken egg	1.40
Oats	1.28
(soybeans, green, raw)Edamame	0.93
Beans, pinto, cooked	0.78
, cookedLentils	0.65
, cookedChickpea	0.63
, yellowCorn	0.35
, whole, 3.25% milk fatCow milk	0.27
, brown, medium-grain, cookedRice	0.19
, human, mature, fluidMilk	0.10

1.4.9.2 Health effects

As a dietary supplement, leucine has been found to slow the degradation of muscle tissue by increasing the synthesis of muscle proteins in aged rats.[156] However, results of comparative studies are conflicted. Long-term leucine supplementation does not increase muscle mass or strength in healthy elderly men.[157] More studies are needed, preferably ones based on an objective, random sample of society. Factors such as lifestyle choices, age, gender, diet, exercise, etc. must be factored into the analyses to isolate the effects of supplemental leucine as a standalone, or if taken with other branched chain amino acids (BCAAs). Until then, dietary supplemental leucine cannot be associated as the prime reason for muscular growth or optimal maintenance for the entire population. Both L-leucine and D-leucine protect mice against seizures.[12] D-leucine also terminates seizures in mice after the onset of seizure activity, at least as effectively as diazepam and without sedative effects.[158] Decreased dietary intake of L-leucine promotes adiposity in mice.[159] High blood levels of leucine are associated with insulin resistance in humans, mice, and rodents.[160] This might be due to the effect of leucine to stimulate mTOR signaling.[161] Dietary restriction of leucine and the other BCAAs can reverse diet-induced obesity

in wild-type mice by increasing energy expenditure, and can restrict fat mass gain of hyperphagic rats.[162,163]

1.4.9.3 Safety

Leucine toxicity, as seen in decompensated maple syrup urine disease, causes delirium and neurologic compromise, and can be life-threatening.

A high intake of leucine may cause or exacerbate symptoms of pellagra in people with low niacin status be it interferes with the conversion of L-tryptophan to niacin.[164]

Leucine at a dose exceeding 500 mg/kg/d was observed with hyperammonemia.[165] As such, unofficially, a tolerable upper intake level (UL) for leucine in healthy adult men can be suggested at 500 mg/kg/d or 35 g/d under acute dietary conditions.[165,166]

1. 4.9.4 Pharmacodynamics

Leucine is a dietary amino acid with the capacity to directly stimulate myofibrillar muscle protein synthesis.[167] This effect of leucine arises results from its role as an activator of the mechanistic target of rapamycin (mTOR),[166] a serine-threonine protein kinase that regulates protein biosynthesis and cell growth. The activation of mTOR by leucine is mediated through Rag GTPases,[168-170] leucine binding to leucyl-tRNA synthetase,[168,169] leucine binding to sestrin 2,[171-173] and possibly other mechanisms.

1.4.9.5 Metabolism in humans
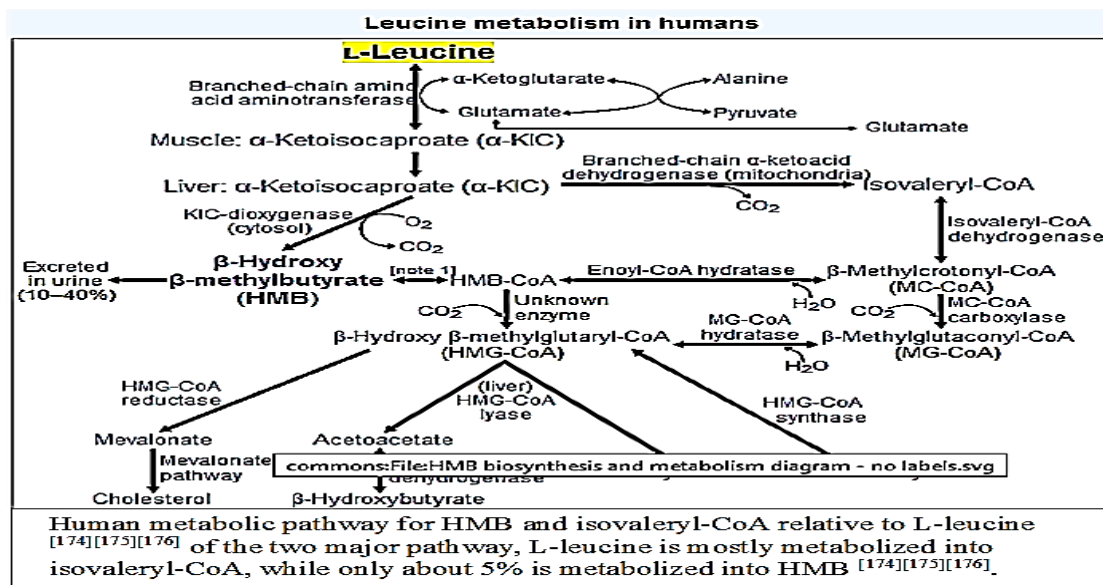
Figure (1.21) leucine metabolisum in human

Leucine metabolism occurs in many tissues in the human body in figure (1.20), however, most dietary leucine is metabolized within the liver, adipose tissue, and muscle tissue. Adipose and muscle

tissue use leucine in the formation of sterols and other compounds, combined leucine use in these two tissues is seven times greater than in the liver.[177] In healthy individuals, approximately 60% of dietary L-leucine is metabolized after several hours, with roughly 5% (2–10% range) of dietary L-leucine being converted to β-hydroxy β-methylbutyric acid (HMB).[175,34,176] Around 40% of dietary L-leucine is converted to acetyl-CoA, which is subsequently used in the synthesis of other compounds.[176]

The vast majority of L-leucine metabolism is initially catalyzed by the branched-chain amino acid aminotransferase enzyme, producing α-ketoisocaproate (α-KIC).[175,176] α-KIC is mostly metabolized by the mitochondrial enzyme branched-chain α-ketoacid dehydrogenase, which converts it to isovaleryl-CoA.[175,176] Isovaleryl-CoA is subsequently metabolized by isovaleryl-CoA dehydrogenase and converted to MC-CoA, which is used in the synthesis of acetyl-CoA and other compounds.[176] Duringbiotin deficiency, HMB can be synthesized from MC-CoA via enoyl-CoA hydratase and an unknown thioesterase enzyme,[178,179,180] which convert MC-CoA into HMB-CoA and HMB-CoA into HMB respectively.[179] A relatively small amount of α-KIC is metabolized in the liver by the cytosolic enzyme 4-hydroxyphenylpyruvate dioxygenase (KIC dioxygenase), which converts α-KIC to HMB.[175,176,181] In healthy individuals, this minor pathway, which involves the conversion of L-leucine to α-KIC and then HMB – is the predominant route of HMB synthesis.[175,176]

A small fraction of L-leucine metabolism – less than 5% in all tissues except the testes where it accounts for about 33% is initially catalyzed by leucine aminomutase, producing β-leucine, which is subsequently metabolized into β-ketoisocaproate (β-KIC), β-ketoisocaproyl-CoA, and then acetyl-CoA by a series of uncharacterized enzymes.[176,182]

The metabolism of HMB is catalyzed by an uncharacterized enzyme which converts it to β-hydroxy β-methylbutyryl-CoA (HMB-CoA).[178,176] HMB-CoA is metabolized by either enoyl-CoA hydratase or another uncharacterized enzyme, producing β-methylcrotonyl-CoA (MC-CoA) or hydroxymethylglutaryl-CoA (HMG-CoA) respectively.[175,176] MC-CoA is then converted by the enzyme methylcrotonyl-CoA carboxylase to methylglutaconyl-CoA (MG-CoA), which is subsequently converted to HMG-CoA by methylglutaconyl-CoA hydratase.[175,176,182] HMG-CoA is then cleaved into acetyl-CoA and acetoacetate by HMG-CoA lyase or used in the production of cholesterol via the mevalonate pathway.[175,176]

1.4.9.6 Synthesis in non-human organisms

Leucine is an essential amino acid in the diet of animals because they lack the complete enzyme pathway to synthesize it *de novo* from potential precursor compounds. Consequently, they must ingest it, usually as a component of proteins. Plants and microorganisms synthesize leucine from pyruvic acid with a series of enzymes:[183]

- Acetolactate synthase.
- Acetohydroxy acid isomeroreductase.
- Dihydroxyacid dehydratase.
- α-Isopropylmalate synthase.
- α-Isopropylmalate isomerase.
- Leucine aminotransferase.

1.4.10 Asparagine

Asparagine (symbol Asn or N[51]), is an α-amino acid that is used in the biosynthesis of proteins. It contains an α-amino group (which is in the protonated $-NH^+_3$ form under biological conditions), an α-carboxylic acid group (which is in the deprotonated $-COO^-$ form under biological conditions), and a side chain carboxamide, classifying it as a polar (at physiological pH), aliphatic amino acid. It is non-essential in humans, meaning the body can synthesize it. A reaction between asparagine and reducing sugars or other source of carbonyls produces acrylamide in food when heated to sufficient temperature. These products occur in baked goods such as French fries, potato chips, and toasted bread.

1.4.10.1 History

Asparagine was first isolated in 1806 in a crystalline form by French chemists Louis Nicolas Vauquelin and Pierre Jean Robiquet (then a young assistant) from asparagus juice,[184,185] in which it is abundant, hence the chosen name. It was the first amino acid to be isolated. Three years later, in 1809, Pierre Jean Robiquet identified a substance from liquorice root with properties which he qualified as very similar to those of asparagine,[186] and which Plisson identified in 1828 as asparagine itself.[187,188]

The determination of asparagine's structure required decades of research. The empirical formula for asparagine was first determined in 1833 by the French chemists Antoine François Boutron Charlard and Théophile-Jules Pelouze; in the same year, the German chemist Justus Liebig provided a more accurate formula.[189,190] In 1846 the Italian chemist Raffaele Piria treated asparagine with nitrous acid, which removed the molecule's amine ($-NH_2$) groups and transformed asparagine into malic acid.[191] This revealed the molecule's fundamental structure: a chain of four carbon atoms. Piria thought that asparagine was a diamide of malic acid;[192] however, in 1862 the German chemist Hermann Kolbe

showed that this surmise was wrong; instead, Kolbe concluded that asparagine was an amide of an amine of succinic acid.[193] In 1886, the Italian chemist Arnaldo Piutti (1857–1928) discovered a mirror image or "enantiomer" of the natural form of asparagine, which shared many of asparagine's properties, but which also differed from it.[194] Since the structure of asparagine was still not fully known the location of the amine group within the molecule was still not settled [195] Piutti synthesized asparagine and thus determined its true structure.[196]

1.4.10.2 Structural function in proteins

Since the asparagine side-chain can form hydrogen bond interactions with the peptide backbone, asparagine residues are often found near the beginning of alpha-helices as asx turns and asx motifs, and in similar turn motifs, or as amide rings, in beta sheets. Its role can be thought as "capping" the hydrogen bond interactions that would otherwise be satisfied by the polypeptide backbone.

Asparagine also provides key sites for N-linked glycosylation, modification of the protein chain with the addition of carbohydrate chains. Typically, a carbohydrate tree can solely be added to an asparagine residue if the latter is flanked on the C side by X-serine or X-threonine, where X is any amino acid with the exception of proline.[197]

1.4.10.3 Sources

Dietary sources

Asparagine is not essential for humans, which means that it can be synthesized from central metabolic pathway intermediates and is not required in the diet.

Asparagine is found in:
- Animal sources: dairy, whey, beef, poultry, eggs, fish, lactalbumin, seafood
- Plant sources: asparagus, potatoes, legumes, nuts, seeds, soy, whole grains

Biosynthesis

The precursor to asparagine is oxaloacetate. Showed in Figure (1.22) Oxaloacetate is converted to aspartate using a transaminase enzyme. The enzyme transfers the amino group from glutamate to oxaloacetate producing α-ketoglutarate and aspartate. The enzyme asparagine synthetase produces asparagine, AMP, glutamate, and pyrophosphate from aspartate, glutamine, and ATP. In the asparagine synthetase reaction, ATP is used to activate aspartate, forming β-aspartyl-AMP. Glutamine donates an ammonium group, which reacts with β-aspartyl-AMP to form asparagine and free AMP.
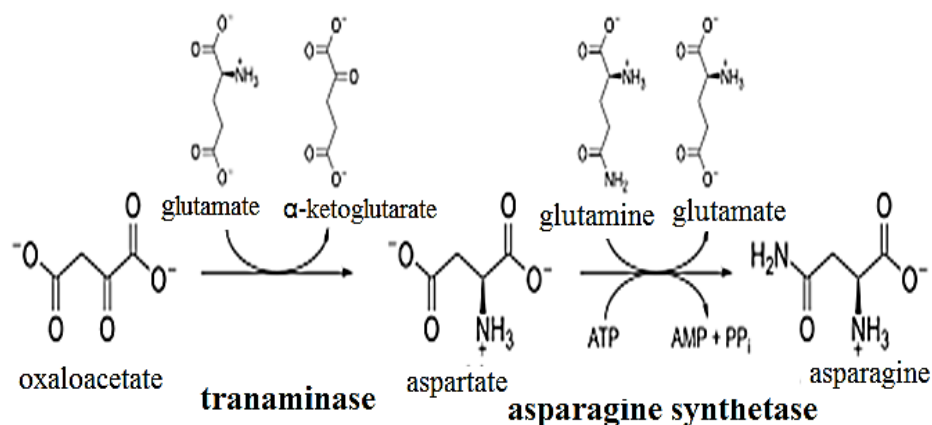
Figure (1.22) Biosynthesis of asparagine from oxaloacetate

1.4.10.4 Degradation

Asparagine usually enters the citric acid cycle in humans as oxaloacetate. In bacteria, the degradation of asparagine leads to the production of oxaloacetate which is the molecule which combines with citrate in the citric acid cycle (Krebs cycle). Asparagine is hydrolyzed to aspartate by asparaginase. Aspartate then undergoes transamination to form glutamate and oxaloacetate from alpha-ketoglutarate.

1.4.10.5 Function

Asparagine is required for development and function of the brain.[198] It also plays an important role in the synthesis of ammonia. The addition of N-acetylglucosamine to asparagine is performed by oligosaccharyltransferase enzymes in the endoplasmic reticulum.[199] This glycosylation is important both for protein structure[200], and protein function.[201]

1.4.11 Cysteine

Cystine is the oxidized dimer form of the amino acid cysteine and has the formula $(SCH_2CH(NH_2)CO_2H)_2$. It is a white solid that is slightly soluble in water. It serves two biological functions: a site of redox reactions and a mechanical linkage that allows proteins to retain their three-dimensional structure.[202]

1.4.11.1 Formation and reactions

It is common in many foods such as eggs, meat, dairy products, and whole grains as well as skin, horns and hair. It was not recognized as being derived of proteins until it was isolated from the horn of a cow in 1899.[203] Human hair and skin contain approximately 10–14% cystine by mass.[204] It was discovered in 1810 by William Hyde Wollaston.

It is formed from the oxidation of two cysteine molecules, via the formation of a disulfide bond. In cell biology, cystine (found in proteins) can only exist in non-reductive (oxidative) organelles, such as the secretory pathway (ER, Golgi, lysosomes, vesicles and ECM). Under reductive conditions (in the cytoplasm, nucleus, etc.) cysteine is predominant. The disulfide link is readily reduced to give the corresponding thiol cysteine. Typical thiols for this reaction are mercaptoethanol and dithiothreitol:

$$(SCH_2CH(NH_2)CO_2H)_2 + 2\,RSH \rightarrow 2\,HSCH_2CH(NH_2)CO_2H + RSSR$$
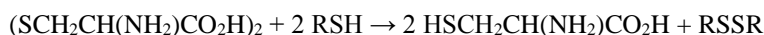
Because of the facility of the thiol-disulfide exchange, the nutritional benefits and sources of cystine are identical to those for the more-common cysteine. Disulfide bonds cleave more rapidly at higher temperatures.[205]

1.4.11.2 Cystine-based disorders

The presence of cystine in urine is often indicative of amino acid reabsorption defects. Cystinuria has been reported to occur in dogs.[206] In humans the excretion of high levels of cystine crystals can be indicative of cystinosis, a rare genetic disease.

1.4.11.3 Biological transport

Cystine serves as a substrate for the cystine-glutamate antiporter. This transport system, which is highly specific for cystine and glutamate, increases the concentration of cystine inside the cell. In this system, the anionic form of cystine is transported in exchange for glutamate. Cystine is quickly reduced to cysteine. Cysteine prodrugs, e.g. acetylcysteine, induce release of glutamate into the extracellular space.

1.4.11.4 Cystine hair nutritional supplements

Cysteine supplements are sometimes marketed as anti-aging products with claims of improved skin elasticity. Cysteine is more easily absorbed by the body than cystine, so most supplements contain cysteine rather than cystine. N-acetyl-cysteine (NAC) is better absorbed than other cysteine or cystine supplements.

1.5 Trace elements

The term trace elements refer to chemical elements present in a natural material at very small amounts. In analytical chemistry, a trace element is an element in a sample that has an average concentration of <100 parts per million (ppm) measured in atomic count or <100 μg/g. In biochemistry, a trace element is a dietary mineral that is needed in very minute quantities for the proper growth, development, and physiology of the organism[207].

Trace elements have several important roles in human bodies, some are essential for enzymes reactions where they attract and facilitate conversion of substrate molecules to specific end products. Moreover, some of them donate or accept electrons in redox reactions that are of primary importance in the generation and utilization of metabolic energy. Some of them have structural roles and responsible for the stability of important biological molecules. Furthermore, some trace elements have important actions throughout biological processes, for example, ıron (Fe) which can bind, transport, and release oxygen in the body[208,209]. In fact, although the trace elements are essential components of biological activities, the excessive levels of these elements can be toxic for the body health and may lead to many fatal diseases, such as cancers. In this review article, we will describe the properties and biological important of a variety of trace elements.

1.5.1. Zinc (Zn)

Zn is a chemical element with symbol Zn and atomic number 30. It is the first element of group 12 of the periodic table. This element was discovered by German chemist Andreas Sigismund Marggraf in 1746 at Germany[210]. It has an atomic weight of 65.4. Zn is the second metal present in the human body (about 2.5 g), after Fe (about 4 g) but before copper (Cu) (about 0.2 g). It is found throughout the entire body system, with half in the muscle tissue[211]. The established recommended daily amount (RDA) for Zn is 8 mg/day for women and 11 mg/day for men[212]. In fact, Zn is found in wheat, brown rice, oats, lentils, soybeans, dried peas, black-eyed peas, lima beans, walnuts, peanuts, cashews, brazil nuts, many cheeses, any kind of liver, and animal flesh such as beef, lamb, chicken, turkey, and various fish and seafood. It is also found in most vitamin mineral supplements as sulfate, citrate, or oxide and these are inexpensive and bioavailable sources[212-214].

Zn is an essential trace element that functions as a cofactor for certain enzymes involved in metabolism and cell growth, it is found in nearly 300 specific enzymes[215-217]. As a component of many enzymes, Zn is involved in the metabolism of proteins, carbohydrates, lipids, and energy. Zn is vital for the healthy working of many of the body's systems; it plays an essential role in numerous biochemical pathways. It is particularly important for healthy skin and is essential for a healthy immune system and resistance to infection. Zn plays a crucial role in growth and cell division where it is required for protein and DNA synthesis, in insulin activity, in the metabolism of the ovaries and testes, and in liver function[215,218].

Zn deficiency may occur due to insufficient dietary intake. It was reported that nearly two billion people in the developing world are deficient in Zn [216]. Zn deficiency is a serious problem in many developing

countries. Zn deficiency is ranked as the 5th leading risk factor in causing disease, especially diarrhea and pneumonia in children, which can lead to high mortality rates in these underdeveloped regions. Other severe deficiency symptoms include stunted growth and impaired development of infants, children, and adolescents. Early Zn deficiency also leads to impaired cognitive function, impaired immune function, behavioral problems, memory impairment, and problems with spatial learning and neuronal atrophy. Public health programs involving Zn supplementation and food fortification could help overcome these problems[219,220]. In more severe cases, Zn deficiency causes hair loss, delayed sexual maturation, impotence, hypogonadism in males, and eye and skin lesions, weight loss, delayed healing of wounds, taste abnormalities, and mental lethargy can also occur [221-223].

The World Health Organization (WHO) advocates Zn supplementation for severe malnutrition and diarrhea. Zn supplements help prevent disease and reduce mortality, especially among children with low birth weight or stunted growth[224].

1.5.2. Copper (Cu)

Cu is a chemical element with symbol Cu and atomic number 29. It is in the top of group 11, of the periodic table, above silver and gold. It has an atomic weight of 63.5. Cu is a reddish metal with a face-centered cubic crystalline structure. It reflects red and orange light and absorbs other frequencies in the visible spectrum. It is malleable, ductile, and an extremely good conductor of both heat and electricity (second only to silver in electrical conductivity) [225,226]. The discovery of Cu dates from pre-historic times, where it was known to some of the oldest civilizations on record. It has a history of use that is at least 10,000 years old, a Cu pendant was found in northern Iraq that dates to 8700 BC[227].

Cu is an essential trace element in plants and animals. The human body only contains about 150 mg of this vital mineral. The established RDA for Cu in normal healthy adults is 2 mg/day[228]. Cu is absorbed in the gut and then transported to the liver bound to albumin. After processing in the liver, Cu is distributed to other tissues in a second phase. Cu transport in liver involves the protein ceruloplasmin, which carries the majority of Cu in blood. Ceruloplasmin also carries Cu that is excreted in milk and is particularly well absorbed as a Cu source[229-231]. The best dietary sources of Cu to human body include wheat, barley, sunflower seeds, almonds, pecans, walnuts, peanuts, cashews, prunes, raisins apricots, various dried beans, mushrooms, chicken, and most fish[232].

Cu is an essential constituent of several enzymes such as cytochrome oxidase, monoamine oxidase, catalase, peroxidase, ascorbic acid oxidase, lactase, tyrosinase, and superoxide dismutase (SOD). Moreover, due to its presence in a wide variety of enzymes, Cu is involved in many metabolic reactions.

For example, the presence of Cu in the SOD helps in the conversion of superoxide to oxygen and hydrogen peroxide[233,234]. Cu is an essential micronutrient necessary for the hematologic and neurologic systems. It is necessary for the growth and formation of bone, formation of myelin sheaths in the nervous systems, helps in the incorporation of Fe in hemoglobin, assists in the absorption of Fe from the gastrointestinal tract, and in the transfer of Fe from tissues to the plasma[235].

Cu deficiency is rare among healthy people, but it may occur among infants. The most common symptoms of Cu deficiency include fatigue, anemia, and a decreased number of white blood cells. Sometimes, osteoporosis develops or nerves are damaged. Nerve damage can cause tingling and loss of sensation in the feet and hands. Muscles may feel weak. Some people become confused, irritable, and mildly depressed. It has been found that the most common cause of Cu deficiency is the remote gastrointestinal surgery, such as gastric bypass surgery, due to malabsorption of Cu. On the other hand, Menkes disease is a genetic disorder of Cu deficiency involving a wide variety of symptoms that is often fatal[236,237]. Acquired Cu deficiency is mainly attributable to nutritional deficiency and may be seen in malnourished low-birth weight infants, newborns, and small infants. Cu deficiency has also been reported to develop after intractable diarrhea and prolonged parenteral or enteral nutrition. However, since Cu supplementation of intravenous and enteral nutritional formulas was made mandatory, the incidence of Cu deficiency has decreased dramatically[238-240].

1.5.3. Iron (Fe)

Fe is a chemical element with symbol Fe and atomic number 26 and has been known since the beginning of time. It is by mass the most common element on Earth, forming much of Earth's outer and inner core. It is the fourth most abundant elements after oxygen, silicon, and aluminum, respectively. It has an atomic weight of 55.8. Fe is the most abundant metal in the human body. Body Fe content is approximately 3-4 g, which almost corresponds to a concentration of 40-50 mg of Fe per kilogram of body weight[241]. The established RDA for Fe in normal healthy adults is 8 mg/day for men and post-menopausal women and 18 mg/day for menstruating women[242] (this is due to lose a lot of blood during their monthly period).

The rich sources of dietary Fe include red meat, liver, lentils, beans, peas, nuts, seeds, poultry, fish, seafood, leaf vegetables, watercress, tofu, chickpeas, black-eyed peas, blackstrap molasses, fortified bread, and fortified breakfast cereals. It is also found in low amounts in molasses, teff, and farina. It has been found that Fe in meat is more easily absorbed than Fe in vegetables[232].

The majority of Fe in the body is contained within hemoglobin, an erythrocyte protein that transfers oxygen from the lungs to the tissues. The Fe contained in hemoglobin is also responsible for the red color of blood[239]. Fe is an essential component of myoglobin, a protein that provides oxygen to muscles[243]. Fe is also necessary for growth, development, normal cellular functioning, and synthesis of some hormones and connective tissue[243,244].

In the case that the body supply of available Fe is too low, this lead to a condition known as Fe deficiency. Fe deficiency is the most common nutritional deficiency in the world. People with Fe deficiency cannot produce an adequate amount of hemoglobin to meet their body's oxygen transport needs. When the deficiency becomes severe, the condition is diagnosed as Fe-deficiency anemia[245,246]. The WHO estimates that approximately half of the 1.62 billion cases of anemia worldwide are due to Fe deficiency[247]. The most common symptoms of Fe-deficiency anemia are tiredness and weakness due to the inadequate oxygen supply to the body's cells and paleness in the hands and eyelids due to the decreased levels of oxygenated hemoglobin. The other symptoms include fatigue, dizziness, hair loss, twitches, irritability, brittle or grooved nails, impaired immune function, pagophagia, and restless legs syndrome[245,248,249]. It has been observed that the deficiency in Fe level usually associated with increase possibility of exposure to toxoplasmosis in women[250]. Fe-deficiency anemia can be treated using Fe supplements[245]. Most of vitamin/mineral supplements have Fe in them as common sulfates, fumarates, and gluconates.

1.5.4. Nickel (Ni)

Ni is a chemical element with symbol Ni and atomic number 28. Ni is a silvery-white metal, hard, malleable, and ductile metal. It is of the Fe group and it is a fairly good conductor of heat and electricity. It has an atomic weight of 58.7. Ni is a naturally occurring element that is present in soil, water, air, and biological materials. It is a natural component of earth's crust and is present in igneous rocks[251]. Natural sources of nickel include dusts from volcanic emissions and the weathering of rocks and soils[252].

Inorganic fertilizers particularly phosphate fertilizers have variable levels of nickel[253]. Ni was discovered by the Swedish chemist Axel Fredrik Cronstedt in the mineral niccolite, in 1751[254]. Today, it is known that the most important use of nickel is in making alloys, especially in stainless steel.

It is well accepted that nickel is as essential ultra-trace nutrient in plants, animals, and humans. It has been reported that the nickel is essential for the active synthesis of urease in plant cells. In several species of higher plants such as jack beans, soybeans, rice, and tobacco, it is required for effective urea metabolism and urease synthesis[255,256]. Although the biological function of nickel is still somewhat

unclear in human body, however, nickel is found in the body in highest concentrations in the nucleic acids, particularly RNA, and is thought to be somehow involved in protein structure or function. It has been speculated that nickel may play a role, as a cofactor, in the activation of certain enzymes related to the breakdown or utilization of glucose. Ni may aid in prolactin production and thus be involved in human breast milk production[257-260]. More research is needed to reveal the properties of this interesting mineral in the human body.

There is no RDA has been established for nickel. Nevertheless, it has been reported that the estimated daily intake of nickel from food and water worldwide is 80-130 μg/day[232]. Ni is contained in many foods such as, beans, chocolate, soybeans, lentils, split, green peas, oats, buckwheat, barley, and corn. Nuts, such as walnuts and hazelnuts, are the best sources of nickel. Many vegetables and some fruits, such as bananas and pears, have moderate amounts of nickel[261].

It has been found that humans may be exposed to nickel during breathing air, eating food, or smoking cigarettes. Skin contact with nickel-contaminated soil or water may also result in nickel exposure. In fact, small quantities of nickel are essential for the body, but when the uptake is too high it can be a danger to human health. Studies have shown that acute exposure of human body to nickel may cause several health problems such as liver, kidney, spleen, brain and tissue damage, vesicular eczema, lung, and nasal cancer [259,262].

It has been observed that the exposure to nickel (especially, nickel in jewelry) may result in the development of a dermatitis known as "nickel allergy" in sensitized individuals. The first symptom is usually itching, before skin eruption occurs. Ni is an important cause of contact allergy, partly due to its use in jewelry intended for pierced ears [263,264]. Furthermore, it has been demonstrated that acute exposure to nickel carbonyl, a carcinogenic gas that results from the reaction of nickel with heated carbon monoxide, can cause symptoms such as frontal headaches, nausea, vomiting, or vertigo. Long-term nickel inhalation may cause serious health problems, including cancer [265].

Ni deficiency has not been shown to be a concern in humans, despite this it may cause biochemical changes, such as reduced Fe resorption that leads to anemia. It can disturb the incorporation of calcium into skeleton and lead to parakeratosis-like damage, which finds expression in disturbed Zn metabolism. It has found that nickel deficiency particularly affects carbohydrate metabolism [258]. More researches are required to see the benefits of, and what effects nickel deficiency can cause on the human body.

1.5.5. Cobalt (Co)

Co is a chemical element with symbol Co and atomic number 27. It has an atomic weight of 58.9. Co was first discovered in 1739 by the chemist Georg Brandt of Swedish. Co is hard, shiny, crisp, bluish-gray metal. It is a very stable metal that is not affected by air or water. Co is one of the three magnetic minerals (in addition to Fe and nickel) that is often used in magnet alloys. It has considerable industrial applications. It is used in paints and dyes, where it has been used since the middle ages in the production of a blue colored glass (smalt) [266]. The radioactive counterpart Co-60 is a powerful gamma ray source that used in medical applications, such as radiotherapy trace and cancer fighter. It is also used for sterilization of medical supplies and medical waste [267].

Co is an essential trace element for the human body, where it is a key constituent of cobalamin (the scientific name of vitamin B12). It also has a substantial role in the formation of amino acids and neurotransmitters. Human body can get Co ions through several pathways: With food, by the respiratory system, by the skin, and as a component of biomaterials. The cobalt ions enter the body through any of the above routes and bind with proteins within the bloodstream and get transported with blood to be deposited in tissues and cells [268,269]. The largest source of exposure to cobalt for the general population is the food supply. The estimated intake from food is 5-40 μg/day, most of which is inorganic cobalt. Green vegetables and fresh cereals are the richest sources of cobalt, whereas dairy products, refined cereals, and sugar contain the least cobalt. Inorganic forms of cobalt are toxic to the human body, and the longer they stay in the body, the more the detrimental effects they cause in cells [270].

It has been found that the cobalt deficiency is associated with disturbances in vitamin B12 synthesis. It might cause anemia and hypothyroidism, as well as increase the risk of developmental abnormalities and failure in infants [271]. The excess level of this metal in the human body might cause hypothyroidism and overproduction of erythrocytes, fibrosis in lungs and asthma [272].

1.6 The previous studies

There are many previous studies that dealt with the study of the study in the theoretical framework, and some of them did not address these topics directly. The researcher benefited from them in the theoretical framework, and some of these studies:

Study of Mikkat Zaghlool Hamdi and co-worker[273]

The study aimed to synthesize a mixed ligand complexes of gold (III) with some amino acids and dithiocarbamates or dithiophosphates, which was summarized to Complexes of the type [Au (L)(L′ or L″)]Cl were prepared [L≡ deprotonated glycine (Gly), Alanine (Ala), Valine(Val) or Methionine (Met), L′ = N-Methylcyclohexyldithiocarbamate (N-MeCHdtc) or Benzyldithiocarbamate (Bzdtc) anion and L″

≡ 0,0-Dipropyldithiophosphate (DiPrdtp) or 0,0- Dibenzyldithiophosphate (DiBzdtp) anion were synthesized and characterized by molar conductivity, IR and UV-Vis spetra, for the complexes. The gold(III) complexes were all square planar with the dithiocarbamates or dithiophosphates acted as bidentate ligands coordinated through the two sulfur atoms and the aminoacid anions coordinated through N and O except for the methionine ligand which coordinate through S and N atoms.

The method of work followed by the researcher in this study, Preparation of [Au (N-MeCHdtc)(Gly)]Cl, [Au(NMeCHdtc) (Val)] Cl, [Au(N-MeCHdtc)(Ala)] Cl, [Au (NMeCHdtc) (Met)] Cl, [Au (Bzdtc) (L)] Cl, [Au(L)(DiPrdtp)] Cl, and [Au(L) (DiBzdtp)] Cl as cited in the literature [274,275]. A solution of sodium aurrate Na(AuCl4) (prepared by adding aqueous solution of NaHCO3 to a solution of HAuCl4.4H2O in water to PH~7.0) was added with stirring to a solution mixture of Na N-MeCHdtc in water and aqueous solution of sodiumglycinate, NaGly, (prepared by dissolving of glycine in water followed by the addition of aqueous solution of NaOH to PH~7.5). The resulting precipitate was filtered, washed several times with water and dried in air. For [Au (N-MeCHdtc)(Gly)]Cl complex, The following complexes were prepared using the same method with the same number of moles but using the appropriate weight for each complex.

From the characterized of the complexes found, the molar conductivity of the dithiocarbamate complexes were measured in dimetylformamide (10^{-3}M) solvent indicate that theses complexes are 1:1 electrolyte [276]. The corresponding dithiophosphate complexes [Au (L)(DiPrdtp)] Cl and [Au (L)(DiBzdtp)] Cl, are partially soluble in warm DMF(~40°C) but insoluble in THF, cyanomethane, benzene, dichloromethane, chloroform, DMSO, DMF+DMSO mixture and ethanol. Accordingly, the conductivity of the dithiophosphate, were measured in the solid state and the results obtain, indicate their 1:1 electrolytic nature. The electronic spectra for diamagnetic gold(III) complexes are similar to their isoelectronic counter part platinum(II) complexes expected to possess three spin allowed transitions in the field of square planar geometry represented by The electronic spectra of the prepared gold(III) complexes gave three absorption bands. These bands Can be assigned to $^1A_{1g} \rightarrow {}^1A_{2g}$ (ν_1), $^1A_{1g} \rightarrow {}^1B_{1g}$ (ν_2), and $^1A_{1g} \rightarrow {}^1E_g$ (ν_3) transition respectively, the position of these bands are in agreement with low-spin square planar geometry for gold (III) complexes [276]. Bands at values higher than 30000cm^{-1} were assigned to charge transfer. The significant IR spectra data of the ligands and their gold (III) complexes with were recorded, the ν(C-S) band in the IR spectra of the two dithiocarbamate ligands shown at 957 and 990 cm^{-1} shifted to lower region (cm^{-1}) in the IR spectra of their complexes. The shift together with the presence of one ν(C-S) band only suggest the bidentate coordination of the dithiocarbamate in their

complexes. The ν(C-N) band position which is usually taken as a measure of the thioureide form to the structure of dithiocarbamate compounds[278], appeared in the IR spectra of the two dithiocarbamate ligands (N-MeCHdtc and Bzdtc) at 1454 and 1469cm^{-1}, respectively. These positions were shifted to higher frequency values (1487-1508 cm^{-1}) on complex formation. It has been proved that this band undergoes blue shift, when the dithiocarbamate act as bidentate chelating ligand[279,280]. These observation tend to further support the bidentate nature of the dithiocarbamates in their gold (III) complexes. The free dithiophosphate ligands exhibit ν_s (P-S) band appeared at 538 and 563 cm^{-1}. These bands were shifted to lower frequencies upon complex formation (517-558cm^{-1}). On the other hand the ν_{as} (P-S) ir bands for the two dithiophosphate ligands located at 617 and 619 cm^{-1} were shifted to higher frequencies in the range 622-644cm^{-1} upon the formation of gold (III) complexes. These observation indicate the bidentate coordination of the dithiophosphate ligands in their complexes[281,282]. The ν (P-O) band appear at 985,993cm^{-1} in the free dithiophosphate ligands, were shifted to lower frequencies (958-977cm^{-1}) upon complex formation. The observed shift of ν (P-O) support the bonding of the two sulfur atoms to gold (III) because the observed shift is an indication of electron drainage form theP-O towards P-S[283]. The values of ν_{as} (COO$^-$) and ν_s (COO$^-$) for the amino acid ligands. The corresponding values for the gold(III) complexes indicate that the ν_s (COO$^-$) values were shifted to lower wave numbers while the ν_{as} (COO$^-$) frequencies were shifted to higher wave numbers [expect for the methionine complexes [Au(N-MeCHdtc)(Met)]Cl, [Au(Bzdtc)(Met)]Cl, [Au(DiPrdtp)(Met)]Cl, and [Au (DiBzdtp) (Met)]Cl) . The values of Δ [ν_{as}(COO$^-$)_ν_s(COO$^-$)] for the complexes are (230-272cm^{-1}) indicate the involvement of the carboxylate anion in bonding as monodentate ligand. The values of Δ [ν_{as}(COO$^-$)_ν_s(COO$^-$)] for the methionine complexes were (202-204cm^{-1}) suggesting that the carboxylate is not involved in bonding[284].

The N-H vibration observed at (2956-3164cm^{-1}) in the free amino acids were shifted to higher wave numbers (2996-3234cm^{-1}) in the IR spectra of the complexes suggesting coordination of the amino group[285]. The ν (C-S) in the methionine ligand appears at 1316 cm^{-1} were shifted to higher number (1335-1338cm^{-1}) on complex formation (complex [Au (N-MeCHdtc)(Met)]Cl, [Au(Bzdtc)(Met)]Cl, [Au(DiPrdtp)(Met)]Cl, and [Au (DiBzdtp) (Met)]Cl), indicating the participation of methionine sulfur in bonding[286]. The ir spectra of the complexes showed the appearance of non ligand bands observed at (466-498cm^{-1}) which were assigned to ν (Au-N). The appearance of bands at (565-576cm^{-1}) in the ir spectra of the complexes, with the exception of (complexes [Au(N-MeCHdtc)(Met)]Cl, [Au (Bzdtc)(Met)]Cl, [Au (DiPrdtp)(Met)]Cl, and [Au (DiBzdtp)(Met)]Cl), were assigned to ν (Au-O).

The result of the characterized of this study Concluded of a mixed ligand complexes of gold(III) with four aminoacids (Gly, Ala, Val and Methionine) and two dithiocarbamates (N-MeCHdtc and Bzdtc) or two dithiophosphates (DiPrdtp and DiBzdtp) were successfully prepared by simple mixing of a queous solution of the three components. The results were square planar complexes of Au(III) with the dithiocarbamate and dithiophosphate ligands behaved as bidentate coordinated through the two sulfur atoms. The aminoacid anions coordinated through the nitrogen atom of the amino group in all complexes and through the oxygen of the carboxylate group with the exception of the methionine complexes ([Au (N-MeCHdtc)(Met)]Cl, [Au(Bzdtc)(Met)]Cl, [Au(DiPrdtp)(Met)]Cl, and [Au (DiBzdtp)(Met)]Cl)) where the sulfur atom replaces the carboxylate oxygen.

Study of P. Rabindra Reddy and co-worker[287]

The study aimed to Synthesis and characterization of mixed ligand complexes of Zn(II) and Co(II) with amino acids: Relevance to zinc binding sites in zinc fingers, which was summarized to mixed ligand complexes of Zn(II) and Co(II) with cysteine, histidine, cysteine methyl ester, and histidine methyl ester have been synthesized and characterized by elemental analysis, conductivity measurements, and infrared, and TGA. In these complexes, histidine, and histidine methyl ester act as bidentate ligands involving amino and imidazole nitrogens in metal coordination. Similarly, cysteine, and cysteine methyl ester also act as bidentate ligands coordinating through thiol sulphur and amino nitrogen. Tetrahedral geometry has been proposed for Zn(II) and Co(II) complexes based on experimental evidence.

The method of work followed by the researcher in this study, The four complexes $[Zn(Cys)(His)]^-$ (1), $[Co(Cys)(His)]^-$ (2) $[Zn(Cysme)(Hisme)]^+$ (3) and $[Co(Cysme)(Hisme)]^+$ (4) were synthesized by mixing an aqueous solution containing equimolar ratios of ligands which were added simultaneously and independently to equimolar concentrations of zinc chloride, and cobalt chloride, under refluxed until the complex is precipitated.

From the characterized of the complexes found, the analytical data corresponding to the 1, 2, 3 and 4 complexes are in equimolar stoichiometric 1:1:1 ratio. The presence or absence of chloride ions in the above complexes was determined by Mohr's method. No evidence was found for the presence of chloride ions in the coordination sphere of the complexes. The conductivity values in DMSO correspond to non electrolytes for the complexes[288].

In 1 and 2 complexes, the IR spectra showed characteristic bands in the region 3300–3000 cm^{-1} which is lower in comparison with free NH$_2$. Hence, it can be concluded that the nitrogen of the amino group is involved in metal coordination. No shift was observed in the asymmetric and symmetric

stretching vibrations of carboxylate groups, this supports the non-involvement of carboxylate groups in metal coordination. The spectra also showed shifting of ν imidazole in plane to 1050 cm^{-1}, indicating the coordination of imidazole nitrogen with the metal. The peak due to νS–H is lost in the spectra of the mixed ligand complexes, due to deprotanation of the S–H group on binding with the metal. The spectra did not show any broad band in the range 3400 cm^{-1} to 3100 cm^{-1}, indicating the non coordination of water molecules. Other low intensity bands observed in the far IR region in the range 460–500 cm^{-1} were assigned to ν (M−N) stretching and 400 cm^{-1} to ν (M−S) stretching vibrations. The peak due to ν (M−Cl) at ~280 cm^{-1} was not observed, indicating the non coordination of chloride in complexes. Thus from the IR spectra of the mixed ligand complexes it is clear that histidine binds to metal ions through imidazole and amino nitrogen's and cysteine binds through thiol sulphur and amino nitrogen. In the ternary complexes, the IR spectra showed characteristic bands in the region 3300–3000 cm^{-1} which is lower in comparison with free ν NH$_2$ (3500–3300 cm^{-1}). Hence, it can be concluded that the nitrogen of the amino group is involved in coordination with metal. This is also confirmed by the absence of a peak at 2000 cm^{-1} in the spectrum of metal complexes, due to binding of NH$_2$ to the metal ion. No shift was observed in the stretching vibration of ester carbonyl group, this supports the noninvolvement of ester group in metal coordination. The spectra also showed shifting of u imidazole band to ~1050 cm^{-1}, indicating the coordination of imidazole nitrogen with the metal. The peak due to ν S–H was not seen in the spectra of the mixed ligand complexes, due to deprotonation of the S–H group on binding with the metal. The spectra did not show a broad band in the range 3400 cm^{-1} to 3100 cm^{-1}, indicating the non-coordination of water molecules. Other low intensity bands observed in far IR region in the range 480–500 cm^{-1} were assigned to ν (M–N) stretching and at 400 cm^{-1} to ν (M–S) stretching vibrations. The peak due to ν (M–Cl) at ~280 cm^{-1} was not observed, indicating the non-coordination of chloride ions in the complexes. Thus from IR spectra of the mixed ligand complexes it is clear that histidine methyl ester binds to metal ions with imidazole and amino nitrogen's and cysteine methyl ester binds through the thiolsulphur and the amino nitrogen atom. The reflectance spectra of the complexes 1 and 2 showed multiple bands at 28820 cm^{-1}, 32790 cm^{-1} and 35210 cm^{-1}, which were assigned to charge transfer (CT) bands in the complexes. However, an additional band at 15380 cm^{-1} was observed in [Co(Cys)(His)] complex, which was assigned to d–d transition, $^4A_2 \rightarrow {}^4T_1(P)$. Accordingly, tetrahedral geometry was proposed for the cobalt complex. The reflectance spectra of the complexes 3 and 4 showed multiple bands at 28820 cm^{-1}, 32790 cm^{-1} and 35340 cm^{-1}, which were assigned to charge transfer (CT) bands in the complexes. However, an additional band at 15580 cm^{-1} was observed in [Co(Cysme)(Hisme)]$^+$

complex, which was assigned to d–d transition, $^4A_2 \rightarrow {}^4T_1(P)$. Accordingly, tetrahedral geometry was proposed for the cobalt complex. The TGA curve of 1 complex, showed the absence of water molecules, as sudden weight loss was observed at 300°C. The total weight loss was 50%. The weight loss at 447°C was 47·9%, which corresponds to a weight loss of molecular weight 160 units. Similarly, the TGA curve of 2 complexes, showed absence of water molecules and the total % weight loss is 60·73%, and the weight loss at 891°C was 54.24%, which corresponds to a weight loss of molecular weight of 179 units. The TGA curve of 3 complex showed sudden weight loss at 300°C, indicating the absence of water molecules in the coordination sphere of the complex. The total weight loss was 77·48% and the weight loss at 891°C was 70.15%, which corresponds to a weight loss of molecular weight 257 units. Similarly, the TGA curve of 4 complex showed the absence of water molecules and the total weight loss was 58·83%, and the weight loss at 891°C was 53.23%, which corresponds to a weight loss of molecular weight of 193 units, implied in a 1:1:1 complex in accordance with the analytical data. The thermogravimetric analysis (TGA) provides authentic information regarding the absence of water molecules in the coordination sphere of the complex. Further, the electronic, magnetic, IR and NMR spectral data confirm tetrahedral geometry for all the complexes studied. Based on these conclusions, the structure 2 is proposed for these ternary complexes.

Study of M. M. Alam and co-worker[289]

The study aimed to Simultaneous Preparation of Facial and Meridional Isomer of Cobalt-Amino acid Complexes and their Characterization, which was summarized to Preparation and characterization of various complexes of cobalt (III)-amino acid system, especially cobalt (III) glycinato and cobalt (III) alaninato complexes are reported. The identification of the various isomers of these complexes is also reported. The various isomers are separated from their mixture by fractional crystallization. Each of these complexes has been characterized by observing physical characteristics, chemical analysis, UV-visible spectroscopy and IR-spectroscopy. The direct impact of geometry of the complexes to IR stretching frequencies and UV-visible spectral data of amino and carboxyl group in the complexes provided sufficient information about the geometry. A prediction about the geometries of the synthesized has also been focused.

The method of work followed by the researcher in this study, Potassium hydrogencarbonate water is cooled in an ice bath with mechanical stirring. Adding cobalt (II) chloride 6-hydrate solution prepared at 30°C in water. The mixture is allowed to stand in an ice bath, and hydrogen peroxide is then added at a rate of one drop every 5 second, with mechanical stirring at 0-5°C, followed by suction filtration. The

glycine is added to the resulting green filtrate of potassium tri(carbonato)cobalt(III).The mixture is heated at 60-70°C until the color of the resulting solution is changes from green to dark blue to violet. Then 6N acetic acid is added slowly at a rate of 1 drop every 5 seconds with mechanical stirring. The solution is stirred vigorously until the evolution of carbon dioxide ceases and the color of the solution has becomes reddish violet.

$$10 \, KHCO_3 + 2 \, CoCl_2.6H_2O + H_2O_2 \rightarrow 2K_3[Co(CO_3)_3] + 4CO_2 \uparrow + 4KCl + 18H_2O$$

$$K_3[Co(CO_3)_3] + 3H_2NCH_2COOH + 3HC_2H_3O_2 \rightarrow fac. \, and \, mer. \, [Co(H_2NCH_2COO)_3] + 3C_2H_2O_2 + 3CO_2\uparrow + 3H_2O$$
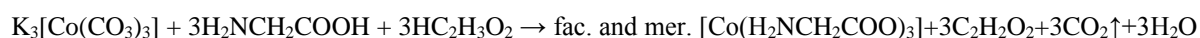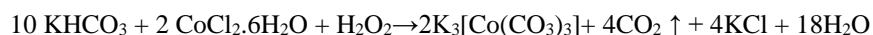
The deposited reddish pink crystals of the soluble facial isomer are collected by suction filtration. The filtrate is concentrated in a rotary evaporator until violet crystals of the more soluble meridional isomer are deposited. The molecular structures of both isomers are presented in Figures (1.23) and (1.24)[290].
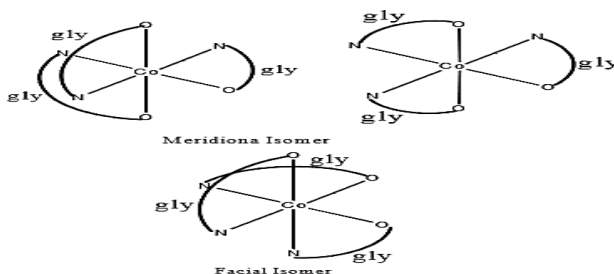
Figure (1.23) Meridional and facial isomer of Co(gly)₃ complex
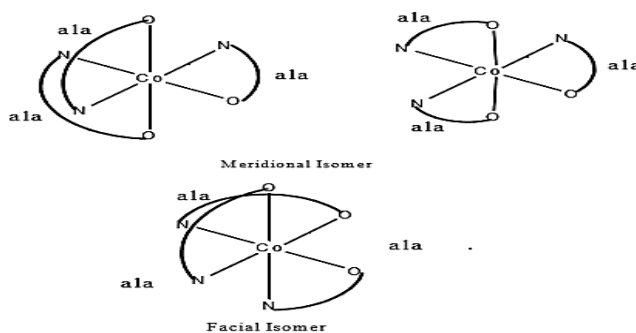
Figure (1.24) Meridional and facial isomer of Co(ala)₃ complex

Preparation of tris (Alaninato) cobalt (III) complex, the above procedure can be modified to prepare the corresponding complexes of other amino acids.

From the characterized of the complexes found, IR bands of various Co-amino acid complexes are shown peaks in the 3000 cm^{-1} region for the Co-Amino acid complexes reveal that the N-H stretching vibration is considerably changed on the formation of the nitrogen to metal bond. It is evident from the IR bands of Co-glycine system that both the symmetric and asymmetric stretching frequencies of NH$_3^+$(N-H) is increased. The N-H stretching frequency in glycine was assigned as 3107 cm^{-1}. This is increased to 3447.2 and 3229.2 cm^{-1} in facial isomer of [Co(gly)$_3$] and 3447.2 and 3136.6 cm^{-1} in meridional isomer. In Co-alanine system the asymmetric stretching is increased considerably than that of alanine due to creation of inductive effect on nitrogen atom and hence the stability of N-H bond also bond strength is increased. Therefore, the stretching frequency is increased[291]. In all Co-Amino acid complexes the asymmetric (–COO$^-$) stretching frequencies are increased and symmetric (–COO$^-$) stretching frequencies are decreased. The explanation of this observation is that when the –COO$^-$ bonded to metal ions lose or break down of symmetry of octahedral geometry occur.
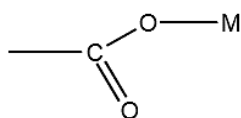
This is consistent with findings in the present study and the mode of chelation of the metal by the ligand may be suggested as[292,293].
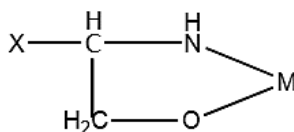
The UV-visible spectrum of starting material and (CoCl$_2$.6H$_2$O) and complexes are showed, two absorption bands of same absorbance obtained at the wavelength of 375 nm and 520 nm. The electronic absorption result for prepared complexes is consistent with the literature value [294,290]. By comparing the λ_{max} and ε_{max} of these prepared complexes and starting material, it is concluded that they are not same species. For all Co-amino acid complexes the value of ε_{max} are greater than that of CoCl$_2$.6H$_2$O. It was observed that ε_{max} value of meridional isomer is larger than that of facial isomers of all the complexes. This can be explained on the basis of symmetry. A simple general rule that complex contains symmetrical structure has pale color since splitting is restricted i.e. transition becomes less important and relatively less intense bands were observed. Visual distinction also supports this result. Facial isomer is reddish pink and the meridional isomer is violet. The transitions occurring in Co-amino acid complex are two types. One confined to the d-orbital of the Co atom (ligand field band), other is

incipient charge transfer (LMCT or MLCT)[295]. The π orbitals of each carboxylate group would overlap with only one of the three t_{2g} d-orbitals of the metal that is the π-orbitals of carboxylate group on the y–axis would overlap the dxy orbital of the Co_3^+ ion [296]. From these observations, it is concluded that when –COO$^-$ bonded to Co_3^+ ion, the loss or break of symmetry of octahedral geometry takes place[297]. These are consistent with reported work [298].

The result of the characterized of this study Concluded in a various isomers of glycine and alanine complexes of cobalt (III) are prepared in aqueous medium. Because of their solubility difference two isomers are separately crystallized from the solution. In both glycine and alanine cobalt (III) complexes, two types of geometrical isomer of different color is obtained. In facial isomer isomers, all of the amino groups of the amino acid molecules are adjacent, while in meridional isomer, two of these occupy opposite positions. By comparing the values of ε max in ultraviolet absorption spectra, it was concluded that the larger value is for meridional isomer. We observed the shifting of –COO$^-$ and –NH$_2$ stretching frequencies in the complexes compared to their corresponding ligands which indicate the coordination of ligands to metal ion. In the case of meridional and facial-tris-(glycino)-cobalt (III) isomers the infrared spectra reveal that the reddish pink isomers has the cis (1,2,3) configuration and the violet meridional isomers has the (1,2,6) structure. Although neither isomer possesses a center of symmetry, the greater number of bands observed for the compounds suggested that the configuration of the isomer has lower overall order of symmetry as would be expected for a (1,2,3) structure.

Study of Andreea Stanila and co-worker[299]

The study aimed to Antibacterial Activity of Copper and Cobalt Amino Acids Complexes, which was summarized to The antibacterial properties of differently copper and cobalt amino acids complexes on agar plates was investigated in the present study. The antibacterial activity of amino acid complexes was evaluated against on three bacteria strains (*Escherichia coli, Bacillus cereus, Micrococcus luteus*). Generally, the amino acids complexes were mainly active against gram-positive organisms, species like *Micrococcus luteus* being the most susceptible strain tested. It was registered a moderate antibacterial activity against *Bacillus cereus*. The microorganisms *Escherichia coli*, which are already known to be multi-resistant to drugs, were also resistant to the amino acids complexes but also to the free salts tested. *Escherichia coli* were susceptible only to the CoCl$_2$ and copper complex with phenylalanine. The complexes with leucine and histidine seem to be more active than the parent free ligand against one or more bacterial species. Moderate activity was registered in the case of complexes with methionine and phenylalanine. From the complexes tested less efficient antibacterial activity was noted in the case of

complexes with lysine and valine. These results show that cobalt and copper complexes have an antibacterial activity and suggest their potential application as antibacterial agents.

The method of work followed by the researcher in this study, There were synthesized six amino acids complexes with copper ions using as ligands methionine, phenylalanine, valine, leucine, lysine (Cu-Met, Cu-Phe, Cu-Val, Cu-Leu, respectively Cu-Lys) and five amino acids complexes with cobalt ions and methionine, phenylalanine, leucine, lysine as ligands (Co-Met, Co-Phe, Co-Leu, respectively Co- Lys). All amino acids were synthesized in the Chemistry and Biochemistry Department of USAMV. The purpose of the study was to obtain neutral complexes of $[Co(LH_2O)_2] \cdot nH_2O$ and $[Cu(LH_2O)_2]$ type at pH=8-10, in the presence of a strong basis (NaOH) to obtain the ionization conditions of the amino acid. The complexes were prepared following the procedure: 2 mmols of all ligands were dissolved in 20 ml distilled water and for deprotonation of the amino acids 0.33 ml 30% NaOH was added[300]. Then 1 mmol of the metal salts was dissolved in 2 ml of distilled water, and was added to the deprotonated amino acid solution under stirring for several minutes. The precipitate was filtered off, washed with water several times, and dried in air. For all the amino acids, the precipitation was instantaneous, and the colour was pink for cobalt complexes and blue for copper complexes. The compounds were found to be soluble in methanol, ethanol, DMSO or DMF. Microbial strains. The amino acids were tested against the following microorganisms: *Escherichia coli, Micrococcus luteus, Bacilus cereus*. Bacterial strains provided from MTC Romania, were cultured overnight at 37°C in agar. Preculture of test bacteria for 24 h with a 250 ml peptone broth (Difco Laboratories) produced a stock preparation containing a logphase cell density of approximately 107 colony forming units (CFU)/ml as evaluated initially by measurements of the optical density at 600 nm.

From the characterized of the complexes found, the elemental analysis measurements of the carbon, nitrogen, hydrogen and sulphur content, confirm that the composition corresponded to a metal: ligand ratio in all the Co (II) complexes was found to be 1:2. IR spectra demonstrate that amino acids act as bidental ligands by involving the amino and carboxyl groups in coordination with metallic ions. In the spectra of the ligand the ν (N-H) stretching vibrations appear at 3052 cm-1. This band appear to be shifted toward higher frequencies in the spectra of the complex with 55 cm^{-1} for copper complex proving the involvement of the -NH$_2$ group in the complex formation[301]. The ν(O-H) stretching vibration does not appear in the spectra ligand, but it do in spectra of the complex at 3421 cm^{-1}, suggesting the presence of the crystal and coordinated water in this compound. The absorption band at 1624 cm^{-1} was attributed to the ν(C=O) stretching vibration in the ligand spectrum and appears to be shifted to 1608

cm^{-1} for complex. The consecutive bands at 1600 and 1527 cm^{-1}, in the spectrum of the ligand were assigned to the symmetric and asymmetric bending vibrations of N-H bond. In the spectrum of the complex are shifted to 1578 cm^{-1} and 1584 cm^{-1}, which also indicates the involvement of this group in the metal- ligand bond formation. UV-Vis and electron spin resonance (EPR) spectra shows typical species monomer and tetrahedral symmetry for the copper complexes and octahedral for the cobalt[302,300]. The antibacterial activity of amino acids complexes was investigated against isolated grampositive strain (*Bacillus cereus, Micrococcus luteus*) and one standard gramnegative bacteria (*Escherichia coli*). Generally the amino acids complexes were mainly active against grampositive. The results of the antimicrobial screening by agar diffusion are showed, one of the microorganisms that showed a susceptibility to these amino acids complexes was *Micrococcus luteus*. It has been registered a moderate antibacterial activity against Bacillus cereus. Such results were not totally un- expected since these bacteria form resting spores and are more resistant to environmental conditions than any other tested bacteria. *Escherichia coli*, which are already known to be multi-resistant to drugs, were also resistant to the amino acids complexes but also to the free salts tested. *Escherichia coli* were susceptible only to the CoCl$_2$ and Cu-Phe. Such results are very interesting, because this bacterium was standard strain. The values for diameter of inhibition zone of the tested amino acids complexes ranged from 0 to 30 mm depending on the bacterial strain and the type of amino acid used for chelating the transitional metal. A difference in antibacterial activity has been observed for Bacillus cereus in the following order: Cu-Leu > Cu- His ≈ Cu-Cl$_2$ > Cu-Phe > Co-Phe ≈ Co-Leu ≈ CoCl$_2$ > Cu-Met> Co-Met > Cu-Val > Co-Lys, while for Microco- cus luteus the order was: Cu-Cl$_2$ ≈ CoCl$_2$ > Co-Phe ≈ Cu- His > Cu-Met > Cu-Leu ≈ Co-Met ≈ Co-Leu ≈ Co-Lys > Cu-Val ≈Cu-Val, based on the measurement diameter of inhibition zone. The results show a variable effect of amino acids complexes on the microorganisms. All complexes studied, presented moderate to high activity against *Micrococcus luteus* and *Bacillus cereus*. In most of the cases was registered a relation dose effect. Complexes with leucine and histidine seem to be more active than the parent free ligand against one or more bacterial species. Moderate activity was registered in the case of complexes with methionine and phenylalanine. From the complexes tested less efficient anti- bacterial activity was noted in the case of complexes with lysine and valine. Finally, regarding to effects of the antibiotics used as positive control, Bacillus cereus it has been registered a higher antibacterial meanwhile for the other two bacterial strains a moderate activity.

The result of the characterized of this study Concluded, The results show that amino acids complexes have inhibitory effect against *Micrococcus luteus* and Bacillus cereus and less efficient

against *Escherichia coli*. More in the case of Bacillus cereus antibacterial activity being much stronger than free salts. Therefore, the present results revealed the importance of amino acids complexes and can be associated with antibiotics, to control resistant bacteria, which are becoming a threat to human health. Furthermore, these amino acids complexes were active against bacteria under very low concentration, thus minimizing the possible toxic effects. These results show that cobalt and copper complexes have an antibacterial activity and suggest its potential application as potential antibacterial agents, in the field of disinfection, food packaging and piping of drinking water.

Study of Petia Genova and co-worker[303]

The study aimed to cytotoxicity of Co (III) complexes of arginine, which was summarized to The cytotoxicity of four Co (III) complexes of arginine on nontumour MDBK cells and on two cell lines derived from transplantable tumors, LSCC-SF(Mc29) and LSR-SF (SR), was evaluated comparatively. Based on the cytotoxic concentration required to inhibit cell surveillance by 50% (CC_{50}) it was bund that: (i) the cytotoxicity of complexes tested increases when the concentration decreased; (ii) the cell surveillance depends on both complex and cell specificities. The complex specificity was illustrated by the order $1 > 4 > 2 > 3$. The cell specific response was demonstrated by the fact that LSCC-SG (Mc29) cells were up to 60 times more sensitive to 1 while LSR-SF (SR) cells were up to 1000 times more sensitive to 2 as compared to MDBK cells. Furthermore, with the prolongation of action on nontumour cells the cytotoxicity of 4 decreased up to 300 times while for both tumour cells it was independent on the duration of action.

The method of work followed by the researcher in this study, the investigated complexes are ntethised according to the procedures published earlier for the complexes 1, 2 and 4 [304] and for the complex 3[305], this illustrated in Table (1.12).

Table (1.12) Co (III) complexes of arginine

Nr	Complex
1	L-/+/$_D$-*mer*-[Co(S-argH)$_3$](NO$_3$)$_3$2H$_2$O
2	D-/+/$_D$-*fac*-[Co(S-argH)$_3$](NO$_3$)3H$_2$0
3	D-(-)$_D$-*cis*(NO$_2$)-*trans*(N)-[Co(S-argH)$_2$(NO$_2$)$_2$]Cl0.5H$_2$O
4	(-)$_D$-*anti*(N)-D-*cis*(N),*cis*(O)-L-*cis*(N), *cis*(O)-[Co$_2$(s-argH)$_4$(OH)$_2$]Cl$_4$.4H$_2$0

Three cell lines were used in the experiments. The nontumour one was derived from bovine kidney cells, MDBK. The other two were derived fi'om transplantable tumor in rat induced by Rous sm'coma virus, sU'ain Schmidt- Ruppin, LSR-SF(SR) and in chicken induced by myeolocytomatosis Mc29 virus, LSC-SF(Mc29). Cells from all tepee lines were grown at 37°C in RPMI-1640 medium (GIBCO BILl,) supplemented with 10% bovine serum (BS) and antibiotics. Dtu'ing the experinaents the medium was supplemented with 5% BS. Methods of detecting the effect on cell viability, concentration required to inhibit cell viabili, by 50% (CC_{50}) and maximal nontoxic concentration (MNC). Co (III) complexes were first dissolved in DMSO till a concenta'ation of 1M was obtained. Dilutions were made in cell growth medium. Cells were seeded into 96 well tissue culture plates at a concenlxation of $1 \times l0^4$ cells/ml and cultured at 37°C in CO_2 atmosphere. Confluent monolaye were washed and covered with media modified with the appropriate compound in ten-fold dilutions starting from 10mM till 0.1M. Cytopathic effects were read on the 24h and 48h after culturing cells at 37°C by microscopy of unstained monolayers and by taipan blue exclusion test. The cell viability was calculated as a percent from the total number of cells per sample. The dose-response relationships were constituted by linearly regressing drug concentrations against the percent inhibition of stability values Ibr the cell control. The CC_{50} of the each compound was calculated from dose response curves. Each experiment was done in duplicate.

The result of this study Concluded to during experimentations it was found that the cytotoxicity of all four Co (III) complexes of arginine increased when the concentration decreased. Moreover, this phenomenon was independent on both complex and cell specificities. On the contrary, based on the data from CC_{50} it was found that the cell staveillance depended on both complex and cell specificities. Thus, complex specificities were manifested by the tact that 1 was the most cytotoxic complex out of fox" complexes tested. This could be due to a specific geometrical and absolute configuration of 1 that causes different ways of dissociation in the inner sphere of the complexes. Also, the tree guanidine groups of the arginine give the possibility to the complex for interactions with different biomolecules in the cell forming hydrogen bonds and other dipole - dipole interactions. In addition, the highest eytotoxicity of I could be also due to NO. Ions participating in the outer sphere, as it is known that the activity of anions decreases in the order $NO_3^- > C1 > NO_2^-$. This could be also the reason of the increased cytotoxicity of 2 for tumotu but not for nontumota cells.

Study of Masaaki Yokota and co-worker[306]

The study aimed to Cu (II) Complex of L-Leucine Favor a Different Type of Crystal Structure from Cu(II)-L-Val and Cu(II)-L-Ile, which was summarized to Crystallization behavior of Cu(II) complexes

of branched chain amino acids (BCAAs) has been studied. Mixing of Cu (II) and L-leucine in solution caused immediate precipitation of Cu (II)-L-Leu complex, while no precipitants were obtained when L-Val or L-Ile were used as ligands. These results are discussed based on structure differences among the precipitants.

The method of work followed by the researcher in this study, One of BCAAs (L-Val, L-Leu, L-Ile) was dissolved in distilled water. To the solution was added of CuOAC as solid followed by dissolution of CuOAC to form homogeneous solution. Complex formation was occurred in the homogeneous system and changes in the solution state was observed by naked eye. In this experimental, pH of the solution was not controlled and the solution was allowed for stand at 298 K. If the precipitation was occurred by only the mixing, resultant crystals were filtered and its structure was analyzed. In case of no precipitation, the solvent water was evaporated and crystallization was forced to occur. Structure of the formed crystals were determined by measuring powder XRD using Riga ku RINT 2200 (CuKα: λ = 1.5406 Å). Structure of the obtained crystals were estimated by comparing the calculated patters simulated using published crystallographic data[307-309].

From the characterized of the complexes found, only Cu(II)(L-Leu)$_2$ was precipitated as stable trans-form, while the others were formed metastable cis-forms. Why only L-Leu favor the trans-isomer. This is very interesting results because the three BCAAs used as ligands have similar molecular structures. Our guess for these results are as follows: Metastable cis-forms are kinetic products, while the stable trans-forms are thermodynamic products. In Cu(II)(BCAA)$_2$ crystals formation, the metastable forms must appear first, then the metastable forms transform into stable forms. In this transformation process, side chain effect of the BCAAs must appear.

The result of the characterized of this study Concluded to Cu(II) complex formation of L-Leucine leads to self-precipitation only by mixing the two reactants in the solution. On the other hand, no self-precipitation occurred when L-Val and L-Ile were used as ligands. These results may be explained only L-Leu favor stable trans conformation rather than unstable hydrated cis conformation. Using the phenomena found in this study, separation of BCAAs, which is difficult by usual crystallization, is expected.

Study of T. Rosu and co-worker[310]

The study aimed to complex compinations of transtional metals with mixed ligands, which was summarized to synthesis and characterization of ternary complex combinations of Zn(II) and Co(II) with Tyrosine and Cysteine as primary ligands and 2,2'-bipiridyl as secondary ligands. The type of complex

combinations form depends on pH. Complex combinations were characterized through IR-spectroscopy, electronic spectra, thermogravimetrycal analysis, electrical conductibility and elemental analysis. Analyzing the result we were able to determine the geometry of complex combinations that we obtained.

The method of work followed by the researcher in this study of synthesis of complexes [Zn(Tyr)(Bipy)], [Zn(Cys)(Bipy)], [Cu(Tyr)(Bipy)], and [Zn(Cys)(Bipy)], reacted between metal and ligands by 1:1:1 molar ratio. Bipy in HCl, and $ZnSO_4H_2O$, and $Co(NO_3)_2.6H_2O$ in HCl, separately. The mixture was stirred, heated, and cooled under energetic stirring, a solution of Tyr and Cys, separately, in solution of NaOH was added. The pH of the solution was adjusted to 4.5 using HCl. It was observed the formation of a color precipitate, which was filtered, washed with methanol and dried out.

For the characterization of complex combinations obtained were used: electronic spectra performed with spectrophotometer VSU-2P diffuse reflectance technique (using MgO), IR spectra (KBr) using Spekord M-80 Carl Zeiss Jena spectrometer, in the range 4000-400 cm^{-1}, elemental analysis for C,N using a Carlo-Erba LA 118 analyzer, and AAS-1N Carl-Zeiss-Jena spectrometer for Zn(II) and Co(II), thermo gravimetrical analysis using MQ-1500 derivatograph and molar conductance in nitrobenzene solution on Consort C-533 conduct meter. The electrical conductibility resulted showed that complex combination [Co(Try)$_2$(Bipy)] has a character of nonelectrolyte and the other two are electrolytes. Curve of the loss of weight TG and TGD for Co(II) complex: [Co(Tyr)(Bipy)(H$_2$O)$_2$]NO$_3$ green and [Co$_2$(Cys)(Bipy)$_2$(H$_2$O)$_2$](NO$_3$)$_2$ brown-red indicate a loss of weight from 130°-140°C corresponding to 2 molecules of water per mol of complex combination. Between 220-360°C the loss of weight is 32.20% with a maximum of temperature at 305°C for complex combination [Co(Tyr)(Bipy)(H$_2$O)$_2$]NO$_3$ and 38.18% with a maximum of temperature at 294°C for [Co$_2$(Cys)(Bipy)(H$_2$O)$_2$](NO$_3$)$_2$. For the green combination we observed the third loss of weight 37.30% with a maximum of temperature at 610°C corresponding of one mol of complex. For the brown-red combination between 494-635°C we have a loss of weight of 28.10% in two steps that indicates the elimination of one mol of Cys from two molecule of complex combination. We can presume that S-S bond is broken from Cys molecule and elimination of the two fragments took place in two steps. The final step of loss of weight 690-800°C, 694-810°C suggests that NO^{3-} is eliminated and the residue corresponds to Co$_2$O$_3$. The presented the loss of weight (TG and TGD) and the curve of differential analysis (ATD) which indicates the effect endo-exothermic that accompanies the loss of weight for complex combination: [Co$_2$(Cys)(Bipy)$_2$(H$_2$O)$_2$](NO$_3$)$_2$. The curve of thermo analysis for [Co(Tyr)$_2$(Bipy)] doesn't indicate the elimination of water molecules or NO^{3-} groups. Curve for loss of weight TG and TGD for complex

combination of Zn(II): [Zn(Tyr)(Bipy)$_2$]2SO$_4$ yellow-green [Zn$_2$(Cys)(Bipy)]SO$_4$ are characterized by three steps in the same ranges of temperature. For complex combinations [Zn$_2$(Cys)(Bipy)]SO$_4$ the loss of weight between 480-644°C took place in two steps, in [Zn$_2$(Cys)(Bipy)]SO$_4$ complex. In electronic spectra, three absorption bands appear, which are corresponding to stretching and bend frequencies (amino acid I, amino acid II) can be attributed to –NH$_2$ from Tyr are shifted to higher wave numbers in complex combination spectrum. This proves that the group –NH$_2$ is involved in coordination. The position of absorption bands corresponding to the same frequencies of Cys, from the complex combination IR spectrum, is unchanged. This behaviour indicates that, the –NH$_2$ group from amino acid is not involved in coordination. This confirms once again the information from literature[311]. If the synthesis of complex combination takes place at pH>4, in coordination are involved –COOH groups and atoms of sulfur. The frequency of vibrations HCOOH, attributed to the absorption bands from 1880 cm$^-$^{1}(Tyr) and 1730 cm^{-1} (Cys) are situated in the spectrum of complex combinations, to lower wave numbers. This fact indicates amino acids coordination to metal ions through –COO$^-$ in ionized form. The vibration frequencies HC-S and HS-S from IR spectrum of complex combination with Cys ligand are situated to lower wave numbers, indicating that the sulfur atoms are involved in the coordination, that are more polarizable than nitrogen atoms in the process of coordination. This frequency can be attributed to HOH given by water molecules coordinated. The presence of water molecules in complex combination composition is indicated also by thermo gravimetrical analysis.

From the data we presented so far we can consider that Tyr as ligand coordinates to metal ions through –COOH group ionized and through –NH$_2$ group and the Cys ligand is coordinated through –COOH group ionized and sulfur atoms only if the pH>4. We point out that, for all complex combination that we prepared, the band located at 1555 cm^{-1} disappears. The band from 1555 cm^{-1}, strong, is characteristic of C=N group from 2,2'-Bipyridil. This proves that nitrogen atoms from Bipyridinic unit are coordinated to metal ions. From the value of their transitions, from complex combination of Co, we determined the parameter Dq and B using the following relationships:[312]

$$^4A_2g\acute{I} \, ^4T1g=18Dq \quad ^4T_1g(P)\acute{I} \, ^4T_1g(F)=6Dq+15B$$

The calculated Dq and B values are specific to octahedral Co(II) complexes. Charge transfer bands, L Í M, were observed at 29000 and 31645 cm^{-1} in the UV-VIS spectra of Zn(II) complexes [312]. From experimental data we can suppose that the structures of ternary complex combination prepared in figure (1.22).
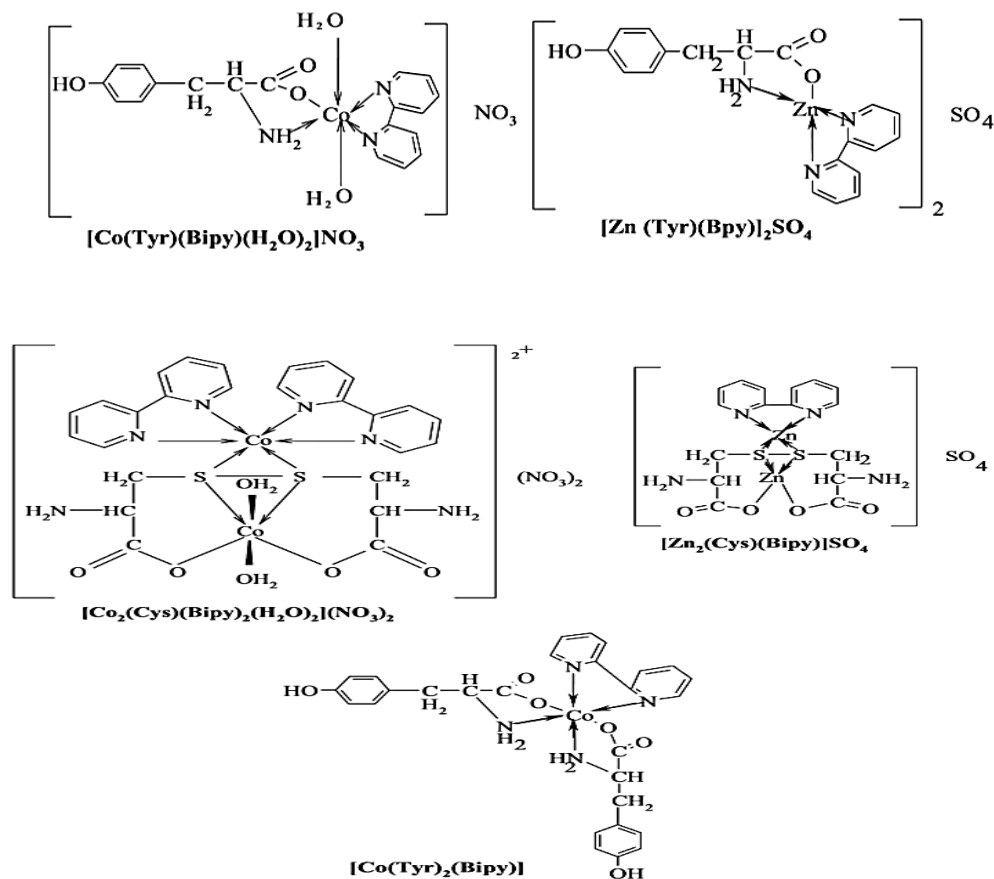
Figure (1.25) Structures of ternary complex combination

The result of the characterized of this study Concluded, the obtained ternary complex combination with Co(II) and Zn(II) using as primary ligands amino acids L-Tyrosine and L-Cysteine and 2,2'-Bipyridil as secondary . Depending on pH value, the coordination mode of L-Cysteine is different. Probable geometry of complex combination was attributed using experimental data.

Study of Devajani Boruah[313]

The study aimed to interaction of Cobalt(II) and Nickel(II) ions with Amino acids in Aqueous solution: A Spectrophotometric Study, which was summarized to The interactions of transition metals cobalt(II) and nickel(II) ions with the amino acids L-threonine(L-thr), L- proline(L-pro) and L-lysine(L-lys) in aqueous solution have been studied by using visible spectroscopic method. On addition of amino acids to the aqueous solution of the metal ions, a change in the visible spectra is observed due to the replacement of the water molecules from the coordination sphere of the aquo- complex $[M(H_2O)_6]^{2+}$ by the amino acid molecules.

$$[M\ (H_2O)_6]^{2+} + L = [M\ (H_2O)5L]^{2+} + H_2O$$

(where M = Co(II) and Ni(II); L = L-thr, L-pro and L-lys). The equilibrium constants and the change of Gibbs free energy ΔG_o of the water exchange process at room temperature have been determined. For Ni(II)-H_2O-amino acid systems the equilibrium constants have been determined for five variable temperatures (318-298 K) and the corresponding thermodynamic parameters ΔG_o, ΔH_o and ΔS_o have been calculated.

The method of work followed by the researcher in this study, the salts $CoCl_2.6H_2O$ and $NiCl_2.6H_2O$ used in this study were of AR grade which were purchased from E.Merck. The amino acids L-lysine, L-threonine and L-proline were purchased from Loba Chemie which were used as received. The metal and amino acid solutions were prepared just before each measurement by direct dissolution salts and amino acids in doubly distilled water. The concentration of the amino acids in the sample solutions were kept as low as possible. The visible spectra were recorded in aqueous solution by using 1 cm3 quartz cell in the range 800-360 nm on Shimadzu UV-240 spectrometer. The variable temperature (318-298 K) experiments were performed by using temperature regulated cell holder. The pH of the solutions was measured by using Elico Li-120 pH meter. The replacement process for Co(II)-L-lysine system can be represented on the basis of the report that only one water molecule has been replaced by the amino acid ligand from the coordination sphere of the metal ion[314].

From the characterized of the complexes found, The absorption peak for $[Co(H_2O)_6]^{2+}$ ion has been observed at 502 nm. The spectra of $[Ni(H_2O)_6]^{2+}$ ion shows three peaks at 392 nm, 656 nm and 736 nm respectively. The equilibrium constants for Ni(II) ions have been determined with respect to the sharper peak at 392 nm. The peaks of Ni(II) shifted towards blue to ~385 nm on addition of amino acids to their aquo-complexes. The both amino acids L-threonine and L-lysine are tridentate with the three coordination sites –COOH, –NH_2, –OH and COOH, –NH_2 –NH_2 respectively while L-proline has two viz., – COOH, –NH–. In aqueous solution Co(II) and Ni(II) ions exist as octahedral $[M\ (H_2O)_6]^{2+}$ [315] aquo ions. When amino acid is added to the aquo ion, replacement of water molecules by amino acids occur from the coordination sphere of the metal ions. The coordination mode of amino acids to the metal center depends on the pH of the solution. In solution amino acids exist as zwitter ion predominantly at pH $\leq$ 7 [316,317] and the amino acids behave as monodentate ligand coordination of the amino acids to the metal centre occurs through the oxygen atom of its carboxylate group. When the pH of the solution is 12, both the nitrogen and oxygen atoms take part in coordination with the metal ions[318].

The result of the characterized of this study Concluded, The interactions of cobalt(II) and nickel(II) ions with the amino acids L-threonine, L-proline and L-lysine in aqueous solution have been studied by visible spectroscopic method. The equilibrium constants for Ni(II)-amino acid complexes are found to be higher than the Co(II)-amino acid complexes. The equilibrium constants for the amino acids follow the fellowing order L-pro > L-thr > L-lys. Different thermodynamic parameters have been calculated. Stability of the metal-amino acid complexes have been compared.

Study of Ajay R. Patil and co-worker[319]

The study aimed to Synthesis, characterization and biological activity of mixed ligand Co (II) complexes of schiff base 2-amino-4-nitrophenol-n-salicylidene with some amino acids, which was summarized to Co (II) complexes of Schiff base 2-amino-4-nitrophenol-N-salicylidene with some amino acids were synthesized. The Schiff base and its mixed ligand complexes, in general, were non-hygroscopic and stable solids. The structural characterization of Schiff base and cobalt complexes were done on the basis of their melting point, solubility, elemental analyses, conductivity measurements, GC-MS, FTIR, UV-Visible spectroscopy, and X-ray diffraction studies. The morphology of mixed ligand Co (II) complexes was studied by scanning electron microscopy. The compounds were subjected to simultaneous thermogravimetric analysis to study their decomposition mechanism and thermal stability. The Schiff base and mixed ligand complexes were preliminary scanned against various strains of microbes to study their biological effect.

The method of work followed by the researcher in this study, the 2-amino-4-nitrophenol-N-salicylidene [ANPS] was synthesized as per procedure reported[320-322]. Solution of amino acids (viz. alanine, phenylalanine, valine, cysteine, leucine and glutamic acid) prepared in HCl were mixed with aqueous solution of Cobalt sulphate ($CoSO_4.7H_2O$) and warmed ethanoic solution of Schiff base by 1:1:1 molar ratio. The mixture was stirred vigorously. The pH of the reaction mass was adjusted to 10.0-11.0 by using NaOH solution. The dark brown colored precipitation occurred. The precipitate was then digested on water bath for 3h. The precipitate obtained was then cooled, filtered and washed with warm water followed by 50 % ethanol and dried in vacuo at 70-80°C.

From the characterized of the complexes found, The FTIR spectra of compounds were quite complex due to presence of numerous bands with varying intensities, making the task quite difficult. Attempt however had been made to assign some of important bands on the basis of reported spectra of several mixed ligand complexes [320,322,323]. The significant feature of the infrared spectra of ANPS was presence of band at 1642.07 cm^{-1} which was assign to frequency of C=N group[324]. This suggested the

formation of ANPS by reaction of salicylaldehyde and 2- amino-4-nitrophenol. The broad band observed at 3555.65 cm^{-1} in the spectrum of ANPS was assigned for stretching vibrations of –OH group. The presence of phenolic –OH was also confirmed by another band in the FTIR spectrum at 1377.49 cm^{-1}. The band observed at 1599.30 cm^{-1} was assigned for stretching vibrations of -NO$_2$ functional group in the ligand [323,324]. The FTIR spectrum of mixed ligand Co (II) complexes showed the broad and moderate band centered in the range 3428.10-3437.15 cm^{-1} due to –OH vibrations of the phenolic –OH group. These vibrations are reported to occur around 3500 cm^{-1} for the compounds containing free –OH functional group [324,325]. The appearance of –OH vibrations in Co (II) complexes were slightly lower than the vibrations of –OH in the spectrum of ANPS. This may be due to involvement of one of the –OH groups in the metal ligand bonding. The presence of one free phenolic – OH group was confirmed by another band observed in the range 1384.96-1397.31 cm^{-1}. This indicated that the ANPS form covalent bond with metal ion by deprotonation of one –OH group. The other two bands observed in the range 3069.05-3080.95 cm^{-1} and 3015.02-3069.95 cm^{-1} were assigned for –NH asymmetric and –NH symmetric stretching vibrations of –NH$_2$ group. For free amino acid these values are reported around 3040 cm^{-1} and around 2960 cm^{-1} respectively. These values were shifted to higher wave numbers in the spectra of Co (II) complexes, suggesting coordination of the amino group through nitrogen with the Co (II) ion [322,323,325].

Literature survey reveals that an asymmetric vibrations and symmetric vibrations due to free amino acid are observed at around 1590 cm^{-1} and 1400 cm^{-1} respectively. These values were shifted to higher wave numbers in the spectra of cobalt complexes i.e. υ_{asym}(COO$^-$) in the range 1732.85-1756.89 cm^{-1} and υsym (COO$^-$) in the range 1701.05- 1740.25 cm^{-1} indicating the covalent bond formation via deprotonation of the carboxylic acid group during the complexation[325].

The strong band observed in the range 1611.03-1617.47cm^{-1} was assigned for C=N vibrations. These vibrations were observed in the lower wave number as compared to the vibrations in the ANPS. This indicated the coordinate bond formations through the nitrogen atom of C=N group[323,325]. The band due to –NO $_2$ was observed at 1599.30 cm^{-1} in the spectrum of ANPS remain unchanged in the FTIR spectra of mixed Co(II) ligand complexes of Co(II) suggesting non involvment of –NO $_2$ group in the bonding. This band was obtained in the range 1574.74 – 1589.90 cm^{-1} in the IR spectra of Co (II) complexes [323,325].

The [Co(ANPS)(Cys)] complex show small weak band at 2569.80 cm^{-1} which is assigned for stretching frequency of -SH group in the cystein. The literature value for the -SH vibrations is in the

range of 2550-2590 cm^{-1}. Therefore in the [Co(ANPS)(Cys)] complex the band observed in this range was assigned for stretching frequency of -SH group.

In FTIR spectra of Co(II) complexes, some new bands of weak intensity observed in the regions around 645.80- 649.01 cm^{-1} and 515.18-516.32 cm^{-1} may be ascribed to the M-O and M-N vibrations respectively. It may be noted that these vibrational bands are absent in the infrared spectra of ANPS as well as the amino acids [322,325,326].

The electronic absorption spectrum of ANPS in DMSO solvent in the showed three peaks. The high intensity band was observed at 210 nm (47,619 cm^{-1}). The second of low intensity band was observed at 255 nm (39,215 cm^{-1}) and the third band was observed at 324 nm (30,864 cm^{-1}). The data obtained was compared with the literature data of several Schiff bases and their mixed ligand complexes[320]. The electronic absorption for ANPS in the DMSO may occur due to the transitions of the electrons from lower molecular orbital to higher molecular orbital. From the nature and position of the transition in the spectra, it was assigned for intra-ligand transitions.

The Shivankar et al has recorded the $\pi \rightarrow \pi^*$ at 48,543-38,760 cm^{-1}, for the aromatic chromophore in the ligand 8- hydroxyquinoline. In addition, the band observed in the UV-Visible spectrum of 8-hydroxyquinoline in the range 29,762-29,717 cm^{-1} was reported for

n $\rightarrow \pi^*$ transition[325]. For the present study, the frequency of first two bands was in range of 210-255 nm. Hence by comparing with the literature values, these transitions observed in the UV spectrum of ANPS were assigned for $\pi \rightarrow \pi^*$ transition for the aromatic chromophore in the ligand ANPS[320-329]. Similarly the third band observed at 324 nm (30,864 cm^{-1}) was assigned for n $\rightarrow \pi^*$ transition of C=N group in the ligand[316].

In the metal complexes, the inner ligand transitions were common due to presence of C=N and C=C groups in the ligand structures. These bands remain as it is, but new band in the range 370-377 nm was observed, supporting the formation of strong metal–ligand bonds. This band is reported for the charge transfer band[330]. In the solution, electronic absorption spectra of Co (II) complexes, the seven signals were observed. Out of which the three signals were indicative of intra ligand transitions of ANPS, while other three signals were indicative of D$_2$h symmetry for the Co (II) d^7 square planar complexes. A well defined strong band occurring in the range 657- 667 nm was assigned for the transitions ^{2}Ag $\rightarrow ^2$B$_1$g ($x^2 - y^2 \rightarrow$ xy) and the another band observed in the range 498-501 nm was assigned for ^{2}A$_g \rightarrow ^2$B$_{3g}$, (xz $\rightarrow$ xy). Another band around 400 nm and a shoulder around 370 nm were assigned for metal to ligand

charge transfer bands. These bands were assigned to the $^2A_g \rightarrow ^2B_{2u}$ $[xz \rightarrow L(\pi^*)]$ and $^2A_g \rightarrow ^3B_{3u}$ $[yz \rightarrow L(\pi^*)]$ transitions respectively. In general, Co(II) in square planer geometry absorb in the regions[330].

The thermograms (TG) of the compounds have been recorded in flowing nitrogen atmosphere at the heating rate of 10°C/min on approximately 10 mg samples. The Co (II) complexes investigated showed similar behavior in their TG and Differential Thermal Analysis (DTA) studies.

The ANPS undergo two step decomposition processes. The first step was started at 170°C and completed at 360°C showing weight loss of 40.584%. This was attributed to the loss of aldehyde moiety. While the second step occurred in the range 360-645°C corresponds to the weight loss 59.416%. This may be attributed to weight loss due to 2- amino-4-nitrophenol moiety. The thermogram of ANPS showed 100% weight loss.

The TG of Co (II) complexes showed that they were thermally more stable to varying degree. The complexes show the gradual loss in weight due to decomposition by fragmentation with increasing temperature up to certain extent, after that no significant weight loss was observed. This indicated that, expected decomposition product was cobalt oxide Co (II) in all the cases. The similar observations were recorded for all the Co (II) complexes indicating their high thermal stability[331], but for [Co(ANPS)(Ala)] and [Co(ANPS)(Leu)] the expected decomposition product was accompanied by some part of chelate structure. This observation indicated that, the [Co(ANPS)(Ala)] and [Co(ANPS)(Leu)] are thermally more stable than other cobalt complexes.

The [Co(ANPS)(Cys)] and [Co(ANPS)(Glu)] undergo two step decomposition process. The first step of decomposition process was started in the range 30-45°C and completed in the range 615-640°C which was accompanied by a weight loss in the range 29.618-32.022%. This may be attributed to the loss of some part of ANPS. The second step started in the range 615-640°C and completed in the temperature range 1010-1030°C which was accompanied by a weight loss of 48.040-50.432%. This may correspond to the combined weight loss due to remaining part of ANPS and amino acid moiety[331].

The [Co(ANPS)(Ala)], [Co(ANPS)(Phe)] and [Co(ANPS)(Val)] undergo three step decomposition process. The first step was started in the range 30-235°C and completed in the range 420-650°C which was accompanied by a weight loss in the range 23.408-38.240%. This may be attributed to the loss of some part of ANPS. The second step was observed starts in the range 420-650°C and completed in the range 750-820°C which was accompanied by a weight loss in the range 14.109-37.369%. This may corresponds to the loss of remaining fragment of ANPS. The third step of decomposition process was

started in the range 750-820°C and completed in the range 1040-1050°C which was accompanied by weight loss in the range 20.089-29.590%. This may correspond to the loss of amino acid moiety[332].

The [Co(ANPS)(Leu)] undergo four step decomposition process. The first step was started at 30°C and completed at 420°C which was accompanied by a weight loss of 18.757%. This may be attributed to the loss of some part of ANPS. The second step was started at 420°C and completed at 625°C which was accompanied by a weight loss of 14.941%. This may correspond to the loss of some part of amino acid. The third step of decomposition process occurred in the range 625-805°C which was accompanied by weight loss of 16.638%. This may correspond to the loss of remaining fragment of amino acid moiety[332]. The fourth step of decomposition process occurred in the range 805-1010°C which was accompanied by weight loss of 32.985%. This may corresponds to the loss of ANPS moiety. In general, the final decomposition product in all the Co (II) complexes was found to be their respective cobalt oxide accompanied. Therefore 100% weight loss was not observed for the Co (II) complexes[325]. This indicated that the thermal stability of increases on complex formation.

The X-ray diffractogram of the complexes of ANPS recorded in the range 0-80°. Each diffractor was well resolved into sharp reflux suggesting highly crystalline nature for the mixed ligand complexes[333-340]. The d-spacing of the crystalline part of the compounds was calculated using the Bragg equation. The width 'β' at half the maximum of crystalline peak was measured and the crystallite size was calculated using the Deby-Scherrer relation. The result showed that the crystallite size of the mixed ligand Co (II) complexes ranges from 5.38-36.44 A°. From the results, it is clear that, all mixed ligand complexes showed different crystallite size. The X-ray diffractogram of all mixed ligand complexes also showed that, the natures of peaks are well resolved, sharp, with very good intensity. No noticeable broadening area under the peaks was observed. Hence the all mixed ligand Co (II) complexes synthesized in present investigation were crystalline in nature.

The compound synthesized in the present investigation has been subjected to various antimicrobial screening programs based on their structural features so as to ascertain their activity against different microorganisms. The various screening programs conducted have been in the in vitro study by the serial tube dilution technique [325,322,341,342]. The solvent used was DMSO, and the sample concentrations were 200, 100, 50, 25, 12.5 ppm. Antibacterial and antifungal data for *ampiciline* and *Streptomycin* are also included in this table for the purpose of comparison. It has been observed that the compounds showed very good antibacterial and antifungal activity at 12.5, 25, 50, 100 and 200 ppm. The results have been expressed as percentage inhibition. The results of preliminary study on antimicrobial activity indicated

that most of the compounds were highly and few were moderate active against both organisms. In comparison with the activity of ANPS, activity of the metal complexes was more. This indicated that activity increases with introduction of metal ion. The activity of mixed ligand complexes with ligand 'phe' showed higher activity as compared to other complexes. The presence of bulky substituents may be responsible for the enhancement of biological activity[322-344]. Compared to standard compounds [345,346] *ampiciline* for antibacterial activities and Streptomycin for antifungal activities, the present compounds were similar effect against the selected strains of microorganisms.

Study of Faliah Hassan Ali Al-Jeboori and co-worker[347]

The study aimed to synthesis and investigation of complex formation between amino acid (glycine) and various metal ion by using spectroscopic methods, which was summarized to The solid complexes of [M(C 2H4O2N) 2 .H 2O] [where M: Mn^{+2} , Cu^{+2} , Co^{+2} , Ni^{+2} , Zn^{+2} , Cd^{+2} and Pb] were obtained from the reaction of chloride salt of cobalt (II), cupper (II), Nickel (II), Manganese (II), Zinc (II), Cd (II), and Pb(II), with the sodium salt of the amino acid glycine . The complexes characterized by mean infrared, microelemental analysis (C.H.N). The amino acid act as bidentate ligand with coordination involving the carboxylic oxygen and nitrogen atom of amino group. The V(C=O), V st (N-H) and Vb(N-H) vibration are shifted to higher frequencies for complexes comparable with ligand the atomic absorption spectroscopy and microelemental analysis, confirms the compounds stoichiometry. The compounds show poor solubility in water and in the common organic solvents. This behavior is consistent with a polymeric chain.

The method of work followed by the researcher in this study, The purpose of the study, was, to obtain, neutral, complexes, of $[M^{+2}$ (GLY $H_2O)_2$] [where M = metal ion : (Mn, Cu, Co, Ni, Zn, Cd and Pb) GLY = Glycine. Type at pH= (8-10), in the presence of a strong basic (NaOH) to obtain the ionization conditions of the amino acid Glycine. The complexes were prepared following procedure described in the literature[348]: 2 mmole of GLY were dissolved in distilled water and deprotonation of the amino acid by NaOH, then 1 mmole of metal salt of metal ions was dissolve in distilled water and was added to deprotonated amino acid solution under stirring for several minutes. The precipitate was filtered off, washed with water several times and dried in air.

From the characterized of the complexes found, For the synthesized copper, cobalt, Nickel, manganese, zinc, cadmium and lead Complexes the elemental analysis results confirm the 1:2 copper ion to ligand.

The vibrational frequencies related to Vas (Coo⁻) and Vs (Coo⁻) in glycine occur at (1611 and 1414) cm⁻¹, while for Mn (II) complex observed at (1634 and 1364) cm⁻¹, for Cu (II) complex at (1623 and 1384) cm⁻¹, for Co (II) complex observed at(1657 and 1422) cm⁻¹ for Ni (II) complex observed at (1627 and 1399) cm⁻¹ and for Zn (II) complex observed at (1680 and 1391) cm⁻¹. Two very well resolved bands at 1500 cm⁻¹ and broad at 3100 cm⁻¹ are an indication of the amino group to the metal ion (7). In the infrared spectrum of glycine the broad band at 3170-2529 cm⁻¹ and a medium band 1507 cm⁻¹ correspond to ν NH₂ stretching and bending vibration respectively for free ligand is shifted in the spectra of the complexes and appears at (3420 and 1438) cm⁻¹ for Mn(II) complex , (3344 and 1450) cm⁻¹ for Cu (II) complex , (3289 and 1850) cm⁻¹ for Co (II) complex , (3436 and 3640 (b)) cm⁻¹ for Ni (II) complex and (3413 (b) and 1507 (s)) cm⁻¹ for Zn (II) complex These shifted compared to those of the free ligand , which means that (–NH₂) group is involved in metal- ligand formation . The absence of d (NH³⁺) band at 2128 cm⁻¹ in the spectra of the complexes in comparison to the free as ligand, also constitute another valuable to the free ligand, also constitute another valuable proof of the involvement of NH₂ group coordination.

Infrared spectra of the complexes were also measured in the region 400-700 cm⁻¹ in order to identify frequencies related to M-O and M-N bands. The M-O frequencies for Mn (II), Cu (II), Co (II), Ni (II) and Zn (II) complexes were observed respectively at 527 cm⁻¹, 527 cm⁻¹, 531 cm⁻¹, 531 cm⁻¹, 570 cm⁻¹ and 620 cm⁻¹ respectively. While M — N frequencies were identified at rang (300 – 500) cm⁻¹. These results are in agreement with literature value, being similar to other metal complexes with amino acid[349].

The ν (O-H) stretching vibration do not appear in the ligand, Ni (II) complex and Zn (II) complex spectra, but they do in spectra of other complexes at range (3450 – 3750) cm⁻¹ suggesting the presence of the crystal and coordinated water in these compounds.

Study of I.P. Tripathi, and co-worker[350]

The study aimed to Synthesis, Characterization of Some Complexes of Copper (II) with L-Asparginine, L-Histidine, L-Lysine, which was summarized to Cu(II) complexes are interesting due to their biologically active and deliberated interest in the research due to their coordination properties. Because these complexes have high pharmacological potential and act as good chelating agents. A series of complexes of Cu(II) with essential amino acids, where L (L-Asparginine, L- Histidine, L-Lysine) and M (Cu²⁺), have been prepared with formula $[M(L)_2]^{2+}$. The complexes were synthesized and

characterized by elemental chemical analysis, electronic and infrared spectra.IR spectroscopy confirms the ligand coordination to the metal ions through carboxyl and amine groups.

The method of work followed by the researcher in this study, which generally known that a metal ion can bind two amino acids to form a complex. Therefore, amino acid-metal complexes were prepared in the deionized water by reacting the corresponding amino acid and metal ion in a 1:2 molar ratio. The $[Cu (L)_2]^{+2}$ complexes were prepared from four different salts of copper and amino acids (L-Asparginine, L-Histidine, L- Lysine) as ligand. In this process 2 mM of amino acid was added in 20 ml of aqueous solution which containing 2 mM of sodium acetate and allow it to a clear solution with continuous string. Then 2 ml aqueous solution of 1 mM of metal salt was added drop by drop into that solution with continuous string for 3 hours. A dark blue colored solution obtained which were transferred into petri dish for crystallization. After few days deep blue colored crystals obtained.

From the characterized of the complexes found, all the complexes are single colored, non-hygroscopic and thermally stable solids. The analytical data of these complexes were indicating metal-ligand bonding. The complexes are insoluble in common organic solvents but fairly soluble in H_2O and DMSO.

The symmetry around the metallic ions was determined comparing the amino acid and metallic complexes UV-Visible spectra. The electronic spectra of the complexes were recorded in DMSO. One representative ligand field spectra of $[Cu (his)_2]^{2+}$. Characteristic $\pi-\pi$ * transitions are observed in the spectrum of complexes at 257, 288, and 364 nm [351,352]. The electronic spectrum also exhibits a broad band at 815 nm attributable to d-d transitions, which strongly distorted the octahedral geometry around the Cu (II) ion[353]. The UV-Visible spectra of the complexes show absorption bands assigned to a large band around 634 nm. The presence of the later band mentions an octahedral stereochemistry for these complexes[354]. The absorption bands of the complexes corresponded to the n→σ*, n→π* and π*→π* transitions of -NH_2 and -COO, Shifts in these bands and the observed d-d transitions of the complexes, indicated coordination.

The IR spectrum of amino acids exhibits significant features in υNH_3 and υ C=O regions. The amino acids exist as zwitterions in solution and in solid state. The IR spectra of amino acids exhibited significant features in $\upsilon NH3$ and υ COO^- regions[355]. In histidine the peaks at 3130 cm^{-1}, 3009 cm^{-1} were ascribed to N-H symmetric and asymmetric stretching vibrations and 1588 cm^{-1} and 1413cm^{-1} for carboxylate group of histidine. The peak due to imidazole in plane was observed at ~964 cm^{-1}. NH^{3+} twisting and rocking and COO^- wagging frequencies were observed in the range 1200–600 cm^{-1}. In

coordination chemistry Infrared studies of the complexes of amino acids have shown that a useful tool in structural studies[356]. The spectra exhibited a marked difference between bands belonging to the stretching vibration of υ (N-H) of the amine group in the range between 3448-3383 cm^{-1}, suggesting the possibility of the coordination of ligand through the nitrogen atom at the amine group[356-358]. The N-H stretching vibration at 3119 cm^{-1}, in the complex was shifted to higher frequencies with the complexes, suggesting that the coordination of the metal ions with the ligand was via the nitrogen atom[359-361]. The infrared spectra of the complexes [Cu (his)$_2$]$^{2+}$, [Cu (asp)$_2$]$^{2+}$ and [Cu (his)$_2$]$^{2+}$. The absorption band at 1624 cm^{-1} was ascribed to the υ (C=O) stretching vibration in the spectrum. In the spectrum of the complexes are shifted to 1578cm^{-1} and 1584 cm^{-1}, which also indicates the involvement of this group in the metal-ligand bond formation.

The result of the characterized of this study Concluded, the Complexes of metal ions with amino acids can be assigned as a perfect models to study the pharmacological active effects of drugs and also lowering toxic effects. The considerable fact is interactions between transitional metal ions and amino acids are very interesting in the biological applications. A series of complexes of Cu(II) and amino acid i.e. L-Aspargine, L- Histidine and L-Lysine with formula [Cu(L)$_2$]$^{+2}$ have been synthesized and characterized on the basis of elemental chemical analysis, infrared spectra, UV- Visible and cyclic voltammetry measurements. The IR spectra indicated the presence of amino acid coordinated through nitrogen atom and the oxygen from the carboxylic group. The experimental data suggest that the ligands act as bidentate and adopt an octahedral stereochemistry.

Study of Muhammad Abdul Qadir and co-workers[362]

The study aimed to synthesis of metal complexes with amino acids for animal nutrition, which was summarized to Metal complexes of amino acids are important in the biological system, for both nutritive and catalytic chemical reactions. A series of metal (II) complexes have been synthesized by the reaction of chloride salts of magnesium, calcium, iron, cobalt, copper and zinc with amino acids DL-alanine, L-glutamic acid and leucine. Complex formation occurred at the proximal sites of the carboxyl moiety and the alpha amino nitrogen by 1:2 stoichiometric reactions which were also confirmed by elemental analysis and FTIR data. The metal complexes of DL-alanine and L-glutamic acid are water soluble while metal-leucine complex has solubility in DMSO. The purposed structures of complexes were confirmed by HNMR studies.

100 mL of equimolar quantities of each metal salt and amino acid (0.1M) were mixed in a flask fitted with a water condenser and a magnetic stirrer and a hot plate. The pH of the content was

maintained at 4-6 for Fe, Cu, Zn and Co, while for Ca and Mg the pH was 8-10. The contents of the flask were refluxed for 1-4 hrs and the change in color was noted. In order to isolate the complex, the contents of the flask were evaporated in a china dish to 15-25mL and cooled in a refrigerator for crystallization. Lumps of crystals were observed in different shapes and were washed with small amount of water and acetone mixture (1:4).

From the characterized of the complexes found, the magnesium, calcium, iron, cobalt, copper and zinc complexes with DL-Alanine, Leucine and L-Glutamic acid using equimolar concentration were synthesized. All the complexes Metal-Glutamic acid complexes are water soluble while Metal-Leucine has dimethylsulfoxide (DMSO) solubility, each metal complex has a definite crystal shapes. The metal to amino acid ratio was 1:2 confirmed by AAS. Most of the amino acid complexes were formed at a pH of 4-6, however calcium and magnesium complexes were formed at a pH of 8-10. All the complexes showed the prominent colors which absorb in visible region of spectrum, the absorption maximum (λ_{max}), well resolved bands in both UV and visible region and molar extinction coefficient (ϵ_{max}) using concentration of 8x10 M by using the cell with path length of 1cm. The formation of metal alanine complex is evidenced by the formation of five member lactones type structure. The FTIR Spectra of these compounds can thus be correlated to five member lactones. So the complex showing minimum transmittance in the range 1000-1300cm [C-O stretching (asymmetric & symmetric)] can be considered to have maximum chances of metal to alanine bonding. Fe in this regards show minimum transmittance of all metal alanine complexes in this region i.e. 1100 cm^{-1}. From this it can be concluded that Alanine has the maximum tendency for bonding with Fe and 79.7 % yield of Fe-Alanine complex prove our observation, on the other hand the maximum transmittance of Cu-Alanine complex at 1151 cm^{-1} exhibit the minimum tendency of alanine to bind with Cu and it is also evident from its yieldof only 15.4%. In other metal-alanine complexes the situation is in-between these two extremes as it is evidence by their % transmittances in the range of C-O stretching for lactones. The order of strength of metal-alanine bond for different metals is as follows: Fe>Co>Ca>Zn>Mg>Cu. The complex of metals with glutamic acid showing minimum transmittance in the range of 1000-1300 cm^{-1} [C-O stretching (asymmetric &symmetric)] can be considered to have maximum chances of metal to L-glutamic acid bonding. 18.2% transmission by Ca-glutamic acid at 1130 cm^{-1} showed the minimum transmittance among all metal-glutamic acid complexes. So glutamic acid have maximum tendency to bind with Ca and it is also evident from its 46.17% yield. On the other hand maximum transmittance is shown by Fe-glutamic acid complex which was 78.5% at 1205 cm^{-1}, thus exhibiting minimum tendency of glutamic acid to bind

with Fe and it is evident from its yield of 2.96% while the transmittance exhibit by other metal-glutamic acid complexes in-between these two extremes. The bond of different metals with leucine follow the order as Ca>Co>Cu>Zn>Mg>Fe. 1000-1300 cm^{-1} [C-O stretching (asymmetric & symmetric)] can be considered to have maximum chances of metal to leucine bonding because of showing minimum transmittance. In case of leucine, Zn showed the minimum transmittance of 1102 cm^{-1} with 23.01% transmittance among all other metal-leucine complexes in this region. So leucine have maximum tendency to bind with Zn and it is also evident from its 26.77% yield. On the other hand maximum transmittance is   shown by Mg-leucine complex which was 64.8% at1195 cm^{-1}, thus exhibiting minimum tendency of leucine to bind with Mg and it is evident from its 8.27% yield as well. In other metal-leucine complexes the transmission is in-between these two extremes following the binding order of Zn>Ca>Co> Cu>Fe>Mg. ^{1}HNMR assignments of detreated solution of amino acids and their metal complexes (DL-alanine and L-glutamic acid in DO while leucine in DMSO), The recorded spectra (H NMR, 400 MHz) for all the free ligands and their metal complexes, which were identified with help of literature cited, were found in their expected regions[363]. The chemical shift value of amino group and hydroxyl value was shifted to higher field region because of coordination bonding and deprotonation respectively which confirm the involvement of both groups in bonding. The groups which are away from metal in complex showed a little bit difference in their chemical shifts.

The result of the characterized of this study Concluded, The metal amino acid complexes are of extreme importance from nutritive point of view for both animal sand plants because of their easy absorption due to their smaller size. Their bonding strengths are strong enough for the molecules to remain intact through application and absorption, but not as strong as to resist breakdown for metabolic usage to the metal atoms because they are not synthetic or foreign to living system.

Study of Maria Hübner and co-workers[364]

The study aimed to spectroscopic studies of copper (II) complexes with some amino acid as ligand, which was summarized to Cooper-amino acids complexes: $[Cu(L_1)_2].H_2O$ (1), L_1 − hystidine; $[Cu(L_2)_2].H_2O$ (2), L_2 − methionine and $[Cu(L_3)_2].H_2O$ (3), L_3 − threonine have been synthesized and characterized by means elemental analysis, FT–IR, UV–VIS and ESR spectroscopies. The atomic elemental measurements confirm the 1:2 metal ions: amino acid ratio composition for the synthesized compounds. Through FT-IR spectroscopy were obtained information about the copper (II) ions coordination. In the FT-IR spectra of the ligand the vs(N–H) stretching vibration appears at 3082 cm^{-1} (L_1), 3146 cm^{-1} (L_2) and 3176 cm^{-1} (L_3) and is shifted in the spectra of the complexes (49 cm^{-1}, 83 cm-1,

35 cm^{-1} respectively) proving the involvement of the –NH$_2^-$ group in the complex formation. The ν(C=O) stretching vibrations is shifted in the complexes spectra confirming the involvement of the carboxylic group in the metal ions covalent bonding. The local symmetry of the copper ions was obtained by comparing the ligand UV-VIS spectra with those of amino acid complexes.

The method of work followed by the researcher in this study, the complexes were prepared following the procedure described in the literature[365]: 2mmol of the threonine were dissolved in warm distilled water. For the deprotonation of the amino acid 0.33 ml 30% NaOH was added. For all the complexes the precipitation was instantaneous, the copper – hystidine complex is blue-violet, has solubility in water and methanol and the decomposition temperature is 205 0C; the copper – methionine complex is grey-blue (ε= 99.8 %); the copper – threonine complex is blue (ε= 87.2%). The complexes were filtered, washed with ethanol and dried in desiccators under P4O10. Then, the complexes were recrystallized on methanol, dried and weight to establish the percent of complexation.

Elemental analysis results confirm the 1:2 ratio metal: ligand. Information about the metal ions coordination was obtained by comparing the IR frequencies of the ligand with those of the copper complexes. In the spectrum of the ligand L1 the ν (N–H) stretching vibration appears at 3082 cm^{-1} and is shifted toward higher wave numbers in the spectra of the complex proving the involvement of the –NH$_2^-$ group in the complex formation[366]. The δ (N-H) stretching vibration appears in the spectrum of the ligand 1570 cm^{-1} and 1571 cm^{-1} and is shifted toward lower wave numbers at 1568 cm^{-1} and 1561 cm^{-1} for 1 which involves the aminic group at the coordination[367]. The ν(C=O) stretching vibration emerge in the ligand spectrum at 1630 cm-1 and is shifted in the complexes spectra with 5 cm^{-1} (for 1) confirming the involvement of the carboxylic group in the metal ions covalent bonding[368]. The ν(OH) stretching vibrations does not emerge in the ligand L1 and complex 1 spectra suggesting the presence of coordination water molecules. The stretching vibration of the imidazole ring appears in the ligand spectrum at 829 cm^{-1} and is shifted with 23 cm-1 in the complex 1 spectrum suggesting the coordination of the imidazole nitrogen to the copper ion. In the spectrum of the ligand L$_2$, the ν(N-H) stretching vibration appears at 3146cm^{-1} and is shifted with 83 cm-1 in the complex 2 spectra proving the involvement of the –NH$_2^-$ group in the complex formation[367-369]. The absence of the δ$_{as}$ (NH3$^+$) vibration in the spectra of the complex also constitutes another valuable proof of the involvement of the NH$_2$ group coordination[370]. The CH$_2$-S and CH$_3$-S stretching vibrations appear as a sharp band at 2915 cm^{-1} in the ligand L$_2$ spectrum and are insignificant shifted in spectra of the complexes confirming the noninvolvement of these groups to the coordination. The absorption band at 1610 cm^{-1} was attributed to

the ν(C=O) stretching vibration in the spectrum of the ligand L_2 and appears to be shifted toward higher wave numbers in the spectra of 2, proving the involvement of the carboxylic group in the covalent bonding to the metal ion[371]. The ν (OH) stretching vibration does not appear in the spectra of the ligand L_2 and complex 2, suggesting the presence the crystal water in these compounds. Due to the δ (N-H) bending vibration shifting in the complexes spectra the involvement of $-NH_2^-$ group to the metal bonding formation was confirmed. In the ligand L_3 spectra the ν (N-H) stretching vibration appears splitted ($\approx 3176 cm^{-1}$, $\approx 3161 cm^{-1}$) and is shifted at ≈ 3141 cm^{-1}in the Cu(II) spectra proving the involvement of the $-NH_2^-$ group in the complex formation[367,368]. The absorption band from 1636 cm^{-1} in the ligand L_3 spectrum was attributed to the ν (C=O) stretching vibration and appears to be shifted toward lower wave numbers in the complexes spectra, which involves the carboxylic group in the covalent bonding to the metal ion[370]. Because the threonine molecule contains a hydroxyl group attached to a carbon atom a δ (C-H) vibration appears at 1345 cm^{-1} and 1416 cm^{-1} and a ν (C-C) vibration appears at 1416 cm^{-1}. The shifting of δ (C-H) vibrations is insignificant in the complex spectra, proving the noninvolvement of this group to the coordination. The ν (OH) stretching vibrations do not emerge in the ligand L_3 spectrum, but they appear in the complex 3 spectra at 3443 cm^{-1}, suggesting the presence of the crystallisation water within these complexes. Information about local symmetry of metal ions was obtained by comparing the ligand spectra with those of complexes with amino acids[371].

In the UV spectrum of the ligand L_1, the band from 225 nm was attributed to the $\pi \rightarrow \pi *$ transition. The same band is shifted in the complex spectra at 215 nm for 1, because of the π electrons transition of the imidazolic ring. The band from 275 nm in the UV spectrum of L_1 was attributed to the $n \rightarrow \pi *$ transition of C=O bond. This band is shifted toward lower wavelengths with 20 nm in the spectrum of 1, confirming the presence of the ligand within the complex and also the covalent nature of the metal-ligand bond. In visible domain a d-d transition appears at 632 nm in the spectrum of complex 1 and was assigned to the $^2T_2g \rightarrow 2Eg$ transition, specific for Cu (II) complexes with tetragonal distortion owing to the Jahn-Teller effect. The $n \rightarrow \pi *$ characteristic band assigned to the C=O bond appears at 267 nm in the ligand L2 spectrum and is shifted toward UV domain with 8 nm in the complex 2 spectra, proving the presence of the ligand within the complex [372] and the covalent nature of the metal ligand bond[372]. In the visible domain the spectrum of complex 2 show a large shoulder at 625 nm, assigned to the $^2T_2g \rightarrow$ ^2Eg transition, specific to Cu (II) complexes with tetragonal distortion due to the Jahn-Teller effect. The position of the band maxima and respective assignment for Co (II) complex with methionine is typical for octahedral geometries. The free ligand L_3 and the complex 3 exhibit similar spectra in the UV region

in relation to the number of absorption bands. The n→ π^* characteristic band in the UV spectra assigned to the C=O bond appear at 267.5 nm for threonine (Fig.7.a) and is shifted toward higher wave lengths with 7.5 nm for Cu-L$_3$, confirming the presence of the ligand in the complex[373] and the covalent nature of the metal ligand bond. In the visible domain a d-d transition appears between at 617 nm in the copper complex spectrum assigned to the $^2T_{2g} \rightarrow ^2Eg$ transition, specific for Cu (II) complexes with tetragonal distortion owing to the Jahn-Teller effect.

The result of the characterized of this study Concluded, Metallic complexes containing chelated amino acids have been subject to intense investigations, with most attention being paid to α-amino acid complexes. The atomic absorption spectroscopy and elemental measurements confirm the 1:2 metal ions: amino acid ratio composition for the synthesized compounds. The local symmetry of the copper ions was obtained by comparing the ligand UV-VIS spectra with those of amino acid complexes. For the copper complexes a octahedral or pseudotetrahedral arrangement is proposed on the basis of infrared spectra, electronic absorption and electronic spin resonance spectra. The obtained structural data allow us to propose the molecular formulas for the studied metal complexes which are shown in Figure (1.26).

(a) (b) (c)
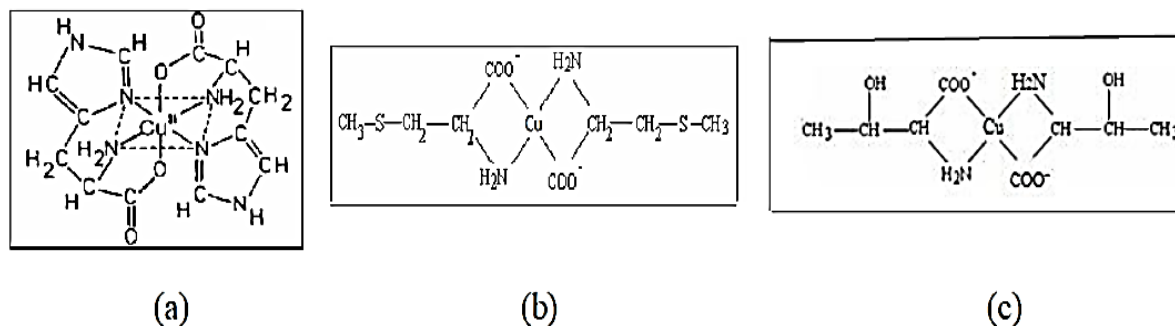
Figure (1.26) Structural formulas proposed for the synthesized complexes: [Cu(L$_1$)$_2$]·H$_2$O– hystidine (a), [Cu(L$_2$)$_2$]·H$_2$O – methionine (b) and [Cu(L$_3$)$_2$]·H$_2$O– threonine (c)

Study of THIAGO A.D. RODRIGUES1 and co-workers[374]

The study aimed to copper II - polar amino acid complexes: toxicity to bacteria and larvae of Aedes aegypti, which summarized to control strategies using insecticides are sometimes ineffective due to the resistance of the insect vectors. In this scenario new products must be proposed for the control of insect vectors. The complexes L-aspartate Cu (II) and L-glutamate-Cu (II) complexes were synthesized and characterized by elemental analysis, visible ultraviolet, infrared spectroscopy and potentiometric titration. The toxicity of these complexes was analyzed in *Aedes aegypti* (Diptera: Culicidae) larvae and Gram-negative and Gram-positive bacteria. The interaction between the ligands and the amino acid

balance and the distribution of the species as a function of pH were discussed. The lethal concentration median (LC_{50}) for *Ae. aegypti* larvae were: L-glutamic acid- Cu (II) – 53.401 mg L^{-1} and L-aspartate-Cu (II) – 108.647 mg L^{-1}. The minimum inhibitory concentration (MIC) required for *Staphylococcus aureus* and *Escherichia coli* was: L-glutamate-Cu (II) 500-2000 mg L^{-1} and L-aspartate-Cu (II) 1000-2000 mg L^{-1}. The concentrations demonstrated toxicity that evidence the potential of the complexes as bactericide and insecticide. Metal complexes formed by amino acids and transition metals are advantageous because of low environmental toxicity, biodegradability and low production cost.

The method of work followed by the researcher in this study available in the literature[375-377] (Rayms-Keller et al. 1998, Baran et al. 2000, Brumano 2008). The L-glutamate-Cu (II) was synthesized by mixing aqueous solutions of L-glutamic acid and copper (II) nitrate at 80°C, by stirring for 1 hour, followed by allowing the solution to stand for 24 hours in absolute ethanol to precipitate the complex L-glutamate-Cu (II). The precipitate was filtered using a filter paper, washed with absolute ethanol and then dried in vacuum desiccator for characterization. The same procedure was used for the synthesis of L-aspartate-Cu (II).

The infrared spectrum of the L-aspartate-Cu (II) and L-glutamate-Cu (II) showed that the most important for the analysis bands in the spectra are carboxylate (COO^-) and amino groups (NH_2). The spectra showed a significant shift, suggesting a possible role in the coordination of the carboxylate metal-ligand[376]. The resulting Vas ($-COO^-$) and Vs for L-aspartate-Cu (II) were 1585/1667 and 1407 cm^{-1}, respectively, and for L-glutamate-Cu (II) 1384/1400 and 1588 cm^{-1}, respectively.

This study was concerned in evaluation of bacterial activity using *Staphylococcus aureus* and *Escherichia coli, which was reach to,* The MIC for *S. aureus* ATCC 25923/L-glutamate-Cu (II) was 500 mg L^{-1} and *E. coli*/ATCC 25922/L-glutamate-Cu (II) was 2000 mg L-1, and for *S. aureus* ATCC 25923/L-aspartate-Cu (II) was 1000 mg L^{-1} and *E. coli* ATCC 25922/L-aspartate-Cu (II) was 2000 mg L^{-1}. The results showed that the metal complexes have different biological activity for Gram-positive (*S. aureus*) and Gram-negative (*E. coli*). This aspect could be related to formation of the bacterial cell wall. Gram-positive bacteria have a single wall that consists of peptidoglycan, whereas Gram-negative bacteria have three walls that are composed of polysaccharides, phospholipids and peptidoglycan. These different characteristics in the constitution of the cell wall results in increased resistance to antibiotics in Gram-negative bacteria[378], due to which MIC for *E. coli* is higher. Bacterial growth was not inhibited in the control.

The results from this study were concluded in the bactericidal effect suggests that the metal complexes can act in a comprehensive (multifunctional) way not only on the target organisms (mosquito larvae), but also on all the bacterial microbiota installed in the mosquito breeding sites. The larvae would come in contact with the metallic complex from the hatching, passing the entire larval stage in that condition. The decrease of the bacterial microbiota would cause food shortages, helping in larval mortality and consequently of the adults that developed in that breeding place.

Study of Temitayo Olufunmilayo Aiyelabola and co-workers[379]

The study aimed to Synthesis, characterization and antimicrobial activities of some metal (II) amino acids' complexes, which was summarized to metal (II) coordination compounds of glycine were synthesized and characterized using infrared and electronic spectroscopic, and magnetic susceptibility measurements. The complexes were tested for antimicrobial activity against *Bacillus subtilis*, *Staphylococcus aureus*, *Methicillin Resistant Staphylococcus aureus* (MRSA), *Escherichia coli, Pseudomonas aeruginosa, Proteus vulgaris* and *Candida albicans*. The stoichiometric reaction between the metal (II) ions and ligands in molar ratio M:L (1:3) [where M = Co, Ni, and Cu; L= glycine] resulted in the formation of five-coordinate square pyramidal dinuclear geometry for both copper complexes and six-coordinate octahedral geometry for the other complexes. The spectroscopic data suggested that the ligand coordinated via both their amino and carboxylate ion moieties. The complexes demonstrated better activities against one or more of the tested microbes than acriflavine, the standard drug used.

The method of work followed by the researcher in this study, the coordination compounds were prepared according to a modification of previously reported method[380] by the addition of appropriate metal salt for copper, nickel, and cobalt to a solution of the ligand dissolved with stirring in distilled water with the addition of Na_2SO_4. The mixture was then heated on a water bath for 2 h. An immediate precipitation was obtained for majority of the complexes, while some required further concentration and cooling. The products obtained were filtered, washed with methanol and dried *in vacuo* at 60°C.

From the characterization and evaluation of complexes found, the complexes showed a wide range of colors that were in agreement with those obtained for similar coordination compounds. Some of the compounds decomposed before melting. All the complexes were sparingly soluble in general organic solvents and therefore efforts at growing their single crystals for X-ray structural studies were unsuccessful. The electronic spectra of complexes showed, the absorption bands of the ligands appeared corresponded to the $n \rightarrow \sigma^*$, $n \rightarrow \pi^*$ and $\pi^* \rightarrow \pi^*$ transitions of -NH$_2$ and -COO$^-$, the major

chromophores, and -C_6H_5. Shifts in these bands and the observed *d-d* transitions of the compounds, indicated coordination.

In Glycinato complexes, The visible spectrum for this Cu(II) complex displayed bands at 620 and 632 nm assigned to $^2B_1g \rightarrow {}^2A_1g$ and $^2B_1g \rightarrow {}^2E_1g$ transitions, ascribed to a square pyramidal geometry[381]. Nickel (II) complexes are known to exhibit complicated equilibrium between coordination numbers six (octahedral) and four (square planar/tetrahedral)[382]. The absorption bands at 505, 523 and 544 nm were consistent with a six-coordinate octahedral geometry and were assigned to $^3A_2g(F) \rightarrow {}^3T_1g$ (F), $^3A_2g(F) \rightarrow {}^1Tg(F)$ and $^3A_2g(F) \rightarrow {}^1Eg$ transitions, respectively[383]. The Co(II) complex gave two well resolved absorption bands at 520 and 667 nm, which were assigned to $^4T_1g(F) \rightarrow {}^4A_2g(F)$ and $^4T_1g(F) \rightarrow {}^4T_1g(P)$ transitions, respectively consistent with a six coordinate octahedral geometry. The IR spectral showed The N-H stretching vibration at 3119 cm^{-1} in glycine was shifted to higher frequencies with the complexes, suggesting that the coordination of the metal ions with the ligand was via the nitrogen atom[384-386]. This was corroborated by similar shifts in the weak C-N stretching frequency of the ligand at 1127 cm^{-1} to higher frequencies in the complexes[387]. Infrared studies on coordination compounds of amino acids have shown that the carboxylate ion is affected by coordination, making it a useful tool in structural studies [385]. Similarly, the asymmetric stretching vibration at 1615 cm^{-1} for the carboxylate ion was shifted to higher frequencies with the complexes, confirming coordination via this functional group. For the symmetric stretch, sharp extended bands were observed instead of distinct bands. This has been reported to be due to the zwitterionic nature of the ligand in the crystalline form[385]. Sharp ex- tended bands at ~3480 - 3620 cm^{-1} in the complexes indicated intermolecular hydrogen bonding between the uncoordinated oxygen atom of the carboxyl group and the amino group of neighboring molecule. Broad bands at ~1340 cm^{-1} however confirmed the intramolecular hydrogen bonding[388]. New bands at 502 - 548 and 621 - 695 cm^{-1} were assigned to (M-N) and M-O bond stretching band frequencies, respectively and served as further evidence of coordination via the nitrogen and oxygen atoms of the ligand. The antimicrobial activities of the compounds are presented in Table (1.13).

Table (1.13) Zones of inhibition for the coordinated compounds (20 mg/ml)

Compounds	Zone of inhibition (mm)*						
	Gram (+)			Gram (−)			Fungus
	S. aureus	B. subtilis	MRSA	E. coli	Ps. aeruginosa	P. vulgaris	C. albicans
Na[Cd(L₁)₃]	13.0 ± 0.4	6.0	6.0	6.0	6.0	6.0	20.0 ± 0.4
Na[Ni(L₁)₃]	6.0	6.0	6.0	6.0	6.0	14.1 ± 0.3	6.0
Na[Co(L₁)₃]	13.0 ± 0.5	13.1 ± 1.0	12.0 ± 0.4	9.0 ± 0.3	20.2 ± 0.1	9.0 ± 0.2	6.0
Na[Mn(L₁)₃]	13.0 ± 0.5	6.0	6.0	13.1 ± 0.2	6.0	6.0	6.0
Na[Cd(L₂)₃]	22.0 ± 0.2	18.0 ± 0.2	20.2 ± 0.1	6.0	8.0 ± 0.3	13.0 ± 0.0	44.0 ± 0.4
Na[Ni(L₂)₃]	6.0	6.0	6.0	6.0	6.0	6.0	15.0 ± 0.7
Na[Co(L₂)₃]	6.0	15.0 ± 0.1	15.0 ± 0.0	6.0	21.0 ± 0.0	6.0	15.0 ± 0.0
Na[Mn(L₂)₃]	17.0 ± 0.4	8.0 ± 0.5	10.1 ± 0.5	8.1 ± 0.6	9.0 ± 0.3	8.0 ± 0.8	6.0
Acriflavine	20.0 ± 0.0	6.0	6.0	20.0 ± 0.0	6.0	15.0 ± 0.0	19.0 ± 6.0

*Zone size measured included the 6.0 mm size of the filter paper disc.

Study of DAN RUSU and co-workers[389]

The study aimed to Synthesis and Characterization of Some Cobalt (II) Complexes with Amino Acids Having Biological Activities, which was summarized to the Cobalt-amino acids complexes in aqueous solution: $[Co(L_1H_2O)_2]\times H_2O$ (1), (L₁=lysine), $[Co(L_2H_2O)_2]\times H_2O$ (2), (L₂=leucine) and $[Co(L_3H_2O)_2]\times 2H_2O$ (3), (L3=methionine) were synthesized and characterized by means of elemental, thermal and IR, and UV-VIS spectroscopic investigations, and biological measurements. The IR spectra show that amino acids act as bidentate ligands with coordination involving the carboxylic oxygen and the nitrogen atom of the amino group. The ν(C=O), ν(N-H), and δ(NH) vibrations are shifted toward higher frequencies for complexes comparable with ligands. And Visible electronic are typical for monomeric species with octahedric local symmetry around the metal ion. The biological testing of the synthesized complexes was done to see citotoxic activity that might show on cell cultures of Sacharomices cerevisiae and Candida albicans.

The method of work followed by the researcher in this study, the complexes were prepared following the procedure described in the literature[390]: 2 mmols of ligands were dissolved in 20 mL distilled water and for deprotonation of the amino acids 0.33 mL 30% NaOH was added. Then 1 mmol of the metal salt of CoCl₂ x6H₂O) was dissolved in 2 ml of distilled water, and was added to the deprotonated amino acid solution under stirring for several minutes. The precipitate was filtered off, washed with water several times, and dried in air.

Elemental analysis results of cobalt- amino acid complexes confirm the 1:2 cobalt ion to ligand composition. The analysis of thermal showed the curves of the complexes clearly indicates that the weight loss between 20-110°C corresponds to one crystal water molecule for first two complexes[391].

The endothermic peaks between 140 and 170˚C correspond to the loss of coordinated water molecules in two steps. The sharp endothermic peak occuring between 180-200˚C may be due to melting of the complexes without weight loss. In the temperature range 200-500˚C the exotermic peaks in the DTA curves indicated the succesive two decompositions steps. The exothermic peak at ~320˚C may be due to loss of two molecules of organic radicals (C_4H_{10}-izobutil, C_4H_8-NH_2-amino butyl and C_3H_7S-metylthioethyl) from the ligand. The second exothermic peak at ~ 470˚C, correspond to the pyrolysis of the amino acid rest. The complexes are stable up to ca. 320 beyond which they start decomposing. The final weights of the residues correspond to the metal oxides as end product[392]. FT-IR Spectroscopy gave information about the cobalt ion coordination was obtained by comparing the IR frequencies of the ligands with those of the cobalt complexes. In the spectra of the ligands, the ν (N-H) stretching vibrations appear at 3118 cm^{-1} for L_1, at 3052 cm-1 for L_1, and at 3146 for L_3. These bands appear to be shifted toward higher frequencies in the spectra of the complexes with 7 cm^{-1} for (1), 250 cm^{-1} and 55 cm^{-1} for (2), and 26 cm^{-1} for (3) proving the involvement of the –NH2 group in the complex formation[393]. The ν (O-H) stretching vibrations do not appear in the ligand spectra, but they do in spectra of their complexes at 3447 cm^{-1}, 3421 cm^{-1} and 3419 cm^{-1} respectively, suggesting the presence of the crystal and coordinated water in these compounds. The absorption band at 1624 cm^{-1} was attributed to the ν (C=O) stretching vibration in the L_1 spectrum and appears to be shifted to 1637 cm^{-1} for complex (1), at 1608 cm^{-1} in the L_2 spectrum and at 1639 cm^{-1} for complex (2), respectively. The same vibration appears in the L_3 spectrum at 1610 cm^{-1} which is shifted with 30 cm^{-1} toward higher frequencies in the spectrum of complex (3), displaying a well-resolved and high intensity signal, which involves the carboxylic group in covalent bonding to the cobalt ion[394]. The consecutive bands at 1600 and 1527 cm^{-1}, in the spectrum of the L_1 were assigned to the symmetric and asymmetric bending vibrations of N-H bond. In the spectrum of the complex (1) this band appears at 1559 cm^{-1}, shifted compared to those of the ligand, which means that –NH2 group is involved in metal-ligand formation. These vibrations in the L_2 and L_3 spectra appear at 1577 and 1510 cm^{-1} and at 1580, 1563 and 1508 cm^{-1}, respectively and are shifted to 1578 cm^{-1} and 1584 cm^{-1} in the corresponding spectra of the complexes (2) and (3). The band at 2904 cm^{-1} in the spectrum of complex (3) was attributed to the CH2-S and CH3-S bonds and is slightly shifted compared to that of the ligand (2915 cm^{-1}) which means that these groups were not involved in the coordination[395]. UV-VIS Spectroscopy showed bands in the range 200-370 nm can be assigned to n→π* / π→π* intra ligand transitions associated to amino acid[396]. Free ligands and complexes exhibit similar spectra in UV region in relation to the number of the absorption bands. A

common feature of these spectra is the presence of three absorption peaks. The two located at lower frequencies have been assigned to $\pi \rightarrow \pi^*$(~330 nm) and $n \rightarrow \pi^*$(~260 nm) transition and the additional peak found at higher frequencies corresponds to the $\pi \rightarrow \pi^*$(~210 nm) transition in a sequence of increasing energy. These bands are shifted to lower energy in the cobalt complexes at ~380 nm, ~275 nm and ~225 nm, respectively[397].

The visible spectra of the cobalt complexes exhibit add broad band at 550-450 nm, such a feature should be expected for a octahedral CoO_4N_2 chromophore and can be assigned to $^4T_1g(P) \rightarrow {}^4T_1g(F)$ transition. Moreover, the variation of the position of the above absorption band can be ascribed to perturbation energies arising from the inductive and delocalization effects of the substituents on the amino acids fragments.

Biological Activity results showed all the amino acids had an increased proliferation rate, but in different proportions, due to the concentrations of the complex or the free amino acid. Generally, copper complexes have similar proliferation rate with the corresponding amino acids. Cobalt complexes, especially Co-leucine have a proliferation rate increased with 50%. In this experiment it couldn't be established a relation dose-effect, but in general the supplementation with 10 μL/mL of 10-4 M amino acids complexes solutions in culture medium offer a good correlation with the tested compound. Leucine complexes with both metals have the higher proliferation rate.

Lactate dehydrogenase (LDH) can be used in cytotoxicity studies, as a marker of cell damage. The normal plasma membrane is impermeable to LDH, but damage of the cell membrane results in a change in the membrane permeability and subsequent leakage of LDH into the extracelular fluid. In vitro release of LDH from cells provides an accurate measure of cell membrane integrity and cell viability. LDH activity is the most used test and reliable for cytotoxicity. Level of LDH from extracellular medium is expressed in nm NADH/min/10000 cells. Because the level of LDH was under 0.15 nm NADH/min/ 10000 cells it can be concluded that the compounds are not cytotoxic. Lipid peroxidation is the oxidative deterioration of polyunsaturated fatty acids with the production of lipid hydroperoxides, conjugated diene, cyclic peroxides and finally fragmentation to ketones and aldehydes (including malondialdehyde MDA). For all the cobalt complexes the peroxidation level was very low (under 0.1 nmol MDA/mL solution) which means that these complexes have not a peroxidant effect. It can be concluded that both cobalt-amino acids complexes after three hours increase the proliferation rate in different proportion. After 8 h the inhibition rate for the cobalt-lysine was I8=1% in average for all three doses and for cobalt-methionine I8=2% (10-3 M), I8=4% (2.10-3 M), I8=4 % (3.10-3M). After 24 h the inhibition rates for

the tested complexes were: cobalt-lysine I24=9% (10-3), I24=13% (2.10-3), I24=13 % (3.10-3M); and for cobalt-methionine I24=8% (10-3), I24=13% (2.10-3), I24=14 % (3.10-3M). The cellular growth inhibition percents after 24 h are higher in all cases, meaning that these cobalt complexes with amino acids, especially those with methionine, are more efficient against *Candida albicans* on a long term, comparing with Heroral, whose inhibition decreased in time.

The results from this study were concluded in the cobalt amino acids complexes $[Co(L_1)2(H_2O)_2] \times H_2O$ (L_1 =lysine), $[Co(L_2)_2(H_2O)_2] \times H_2O$ (L_2= leucine) and $[Co(L_3)_2(H_2O)_2] \times 2H_2O$ (L_3= methionine) were synthesized in aqueous solution and analyzed by means of elemental analysis, thermogravimetric and differential analysis, , IR, and UV-VIS spectroscopies. The composition corresponded to a metal: ligand ratio in all the Co (II) complexes was found to be 1:2. The IR spectra show that the amino acids act as bidentate ligands with coordination involving the carboxyl oxygen and the nitrogen atom of amino group.

The electronic and EPR spectra confirm octahedral local symmetry for the cobalt ion. Cobalt complexes especially those with methionine were proved to have the higher activity against *Candida albicans* and *Saccaromices cerevisae*. These complexes are efficient against CA on long term because the higher inhibition of growth rate was after 24 h. The obtained structural data allow us to propose the following molecular formula for the studied cobalt complexes as shown in figure (1.26).

M= Co^{2+}
R = - $(CH_2)_4$-NH_2 for Co-lysine
R = - $(CH_2)_4$ for Co-leucine
R = - $(CH_2)_2$-S-CH_3 for Co-methionine
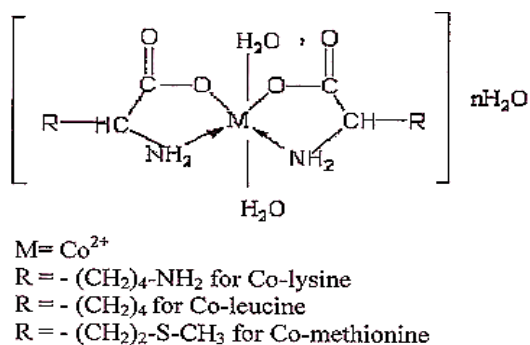
Figure (1.27) Molecular formula proposed for the cobalt amino acid complexes

Study of Mohammed Mansour Saleh Saif and co-workers[398]

The study aimed to antibacterial activity of selected plant (Aqueous and methanolic) extracts against some pathogenic bacteria, which was summarized to the development of new antibacterial agents from natural origins is of increasing interest. Therefore, the aim of this study is to evaluate 8 selected plants for their *in vitro* antibacterial activity against pathogenic bacteria isolated from infected wounds and burns. The plants were extracted with hot water and methanol. The antibacterial activity was determined

using the disc and agar-well diffusion methods. All the plant extracts demonstrated activity against the tested bacteria, with inhibition zone diameters ranging from 3-24.5 mm. The best results were obtained with those from aqueous extract of *Carissa edulis*. The phytochemical screening of the aqueous and methanol extracts indicated the presence of flavonoids, tannins, alkaloids, glycosides, and terpenoids, which might explain the activity of the extracts whereby they can be offering additive activity against the test bacterial strains. In conclusion, the results indicate the plant extracts contain important metabolites in the search for new effective antibacterial agents.

The method of work followed by the researcher in this study, the plants were collected and extracted the plan species by Parekh and Chand (2006)[399], aquose extraction method with some modifications, and methanol extraction method by Benlafya *et al*. (2014)[400]**, and** the plant extracts were screened for their antibacterial activity by using disc and agar-well diffusion methods described by CLSI (2015)[401].

The results of antibacterial activities achieved in this study, aqueous and methanol extracts of eight plants were screened against three bacterial isolates, namely *E. coli*, *S. aureus*, and *P. aeruginosa*. From the results presented in Table (1.14), it was observed that all extracts were active against the tested bacteria, either Gram-positive or Gram-negative bacteria, with inhibition zone diameters ranging from 3 - 24.5 mm. In general, the inhibitory effects of plant extracts using well diffusion method were found to be higher than that of disc diffusion method. This result was consistent with the previous studies on other plants[402,403]. Also, the aqueous and methanol extracts from the same plants showed different activities. There are no common rules for this, but in most cases, the organic extracts showed the same or greater activity than the aqueous extracts[404].

In this study, some of the antibacterial inhibition zone diameters were more than 20 mm. The highest antibacterial activity was achieved by the aqueous extract of *Carissa edulis* against *P. aeruginosa***,** with inhibition zone of 24.5 mm using agar-well diffusion method. Because of its high efficacy against *P. aeruginosa*, the extract of *C. edulis* may be effective in the treatment of infections resulted from this multi-resistant pathogenic bacterium. *P. aeruginosa* is known to develop resistance against multiple classes of antibacterial agents, even during the course of treating an infection[405].

The lowest antibacterial activity was recorded for aqueous extract of *Adenium obesum* against *S. aureus* (using agar-well diffusion method) and methanol extract of the same plant against *P. aeruginosa* (using disc diffusion method), with inhibition zone of 3 mm for each. In general, the aqueous extract of this plant showed the lowest antibacterial activities against all tested bacteria.

By using agar-well diffusion method, the highest antibacterial activities against *E. coli*, *S. aureus*, and *P. aeruginosa* were achieved by using aqueous extract of *C. edulis*, methanol extract of *Kanahia laniflora*, and aqueous extract of *C. edulis*, respectively, and the antibacterial values were 22.5, 19.5, and 24.5 mm, at the same order.

In comparison with agar-well diffusion method, the highest antibacterial activity against *E. coli* using disc diffusion method was 17.5 mm when aqueous extract of *Calotropis procera* was applied. For *S. aureus* and *P. aeruginosa*, the highest antibacterial activities using disc diffusion method were 20 and 22 mm, respectively, when methanol extract of *Syzygium aromaticum* was used.

Table (1.14): Antimicrobial activity of plant extracts against tested

| Plant species | Extract (0.5 g/ml) | Inhibition zone diameter (mm) | | | | | |
| | | E. coli | | S. aureus | | P. aeruginosa | |
		D	W	D	W	D	W
Adenium obesum	H₂O	5.5	4	6.5	3	8.5	4
	MeOH	5.5	3.5	7	10.5	3	6
Carissa edulis	H₂O	17	22.5	17.5	19	13.5	24.5
	MeOH	13.5	17	13.5	15	12	18
Calotropis procera	H₂O	17.5	18.5	15.5	16	16	19
	MeOH	12	17	12	14	11.5	17
Kanahia laniflora	H₂O	11.5	20	12.5	17.5	11	17.5
	MeOH	19	22	18	19.5	18	21.5
Origanum majorana	H₂O	6	9	14	11	15	17
	MeOH	7	9	9	10	14	15
Syzygium aromaticum	H₂O	5	7	15	16	11	13
	MeOH	12	11	20	18	22	20
Lepidium sativum	H₂O	6	8	11	11	10	14
	MeOH	7	8	11	13	10	11.5
Capparis spinosa	H₂O	7	10	10	11	10	12
	MeOH	6	7	7	9	9	12
Gentamicin (30 µg)	-	15	-	19	-	16	–
Vancomycin (10 µg)	-	0	-	22	-	0	–
Ciprofloxacin (30 µg)	-	11	-	11	-	8	–

H₂O, aqueous extract; MeOH, methanol extract; D, disc diffusion method; W, agar-well diffusion method

The results from this study were concluded in extracts of natural origin are a common starting point in the search for new antibacterial agents. From the results presented in this study, it is possible to conclude that some extracts of studied plants were have antibacterial activity against pathogenic bacteria isolated from burns and wounds infections higher than standard antibiotics using in this study. Furthermore, the obtained results demonstrate that these plants could represent a new source of antibacterial agents, less expensive than the imported antibiotics. In this respect, it will be very interesting to conduct a bioassay-oriented fractionation of the active extracts to isolate the pure compounds responsible for the antibacterial activities.

Study of Mohammad K. Islam and co-workers[406]

The study aimed to Synthesis, Characterization and Bioactivities of Some Novel Oxovanadium(IV) Glycinato Complexes, which was summarized to the novel oxovanadium(IV) complexes, $[VIVO(GlyH)(Gly)]^+ClO_4^-.H_2O$ (**1**), $[VIVO(GlyH)(Gly)]^+NO_3^-.H_2O$ (**2**), $[VIVO(GlyH)(Gly)]^+CH_3COO^-.H_2O$ (**3**) were synthesized and characterized by FTIR, UV-Vis and ^1H NMR spectroscopic measurements. The cumulative spectroscopic assessment envisaged that, the complexes adopt a square pyramidal structure, in which the two glycine ligands coordinate to vanadium (IV) center in bidentate fashions conforming a homoleptic structure. The amino nitrogen and a carboxylato oxygen atom coordinate the vanadium (IV) center from both sides making a five members chelate by each side. All the complexes are stable in amorphous state and in aerobic and anaerobic solution. Significantly, all the complexes have the antifungal activities against *Aspergillus Niger* and *Penicillium notatum* but ineffective against *Candida tropicalis*. No antibacterial activity was observed for the complexes against tested bacteria and unfortunately, they were found cytotoxic against brine shrimp bioassay.

The method of work followed by the researcher in this study, Oxovanadium (IV) sulfate was dissolved deaerated water. To this solution $Ba(ClO_4)_2$, $[Ba(NO_3)_2$ in case of the synthesis of compound **2** and $Ba(CH_3COO)_2$ in case of the synthesis of compound **3** respectively] was added and the mixture was stirred at ambient temperature (30±2 ℃) for 2 hours. Barium sulfate precipitated was filtered off. Then the antibacterial activity test was achieved by disc diffusion method.

The result of characterization for complexes involvement, Spectroscopic properties, Table (1.15) describe the infrared spectra of the complexes (1, 2 and 3) which exhibit vC-H bands at around 2960-2963 cm^{-1}, vC-N bands at around 1180-1263 cm-1 and the vC-O bands at around 1328-1344 cm^{-1}. The observed frequencies $v$asy(COO-) was at 1632 cm^{-1} and the $v$sy(COO-) at 1440 cm^{-1} are fairly in good agreement with the literature (Temitayo, et al., 2012)[407]. The absence of the uncoordinated vCOOH

(1730-1775 cm^{-1}) in the IR spectra indicate a clue for the coordination of the ligands to metal ions through the carboxylate anions[408]. The bands assigned due to the vV-N at 552-553 cm^{-1} are also fairly resembling to the literature[407]. The participation of the lone pairs of electrons on the N of the amino group in the ligand to the metals is supported by this band frequency[409,410] observed the chelation of the vanadium (IV) by the amino and carboxylate groups, while[411] have found that glycine seems to behave as a monodentate ligand. Though glycine can be coordinated to VO^{2+} ion in both monodentate or a bidentate fashions with the variations in function of H$^+$ concentrations[412,413], our present observation supports the later one. The characteristic bands due to vV=O appeared at 983-991 cm^{-1} are suggestive of square pyramidal geometries around vanadium[414-418]. The –NH stretching frequency at around 3170-3178 cm^{-1} reduced on coordination, attributable to the reduction in bond order on coordination[419]. All the three complexes show vOH stretching bands at around 3424-3432 cm^{-1} and vH-OH bending bands at around 1624-1632 cm^{-1} which eventually indicate the presence of lattice water molecule   The Cl-O stretching for the perchlorate anion for the complex [VIVO(GlyH)(Gly)]+ClO^{4-}.H$_2$O (**1**) appeared at 1121 and 614 cm^{-1} The perchlorate group is ionic in the complex, since there is no splitting of the perchlorate band around 1100 cm^{-1} [415,420,421]. The IR spectrum for the complex [VIVO(GlyH)(Gly)]$^+$NO$_3^-$.H$_2$O (**2**) exhibits bands at 772 and 1382 cm^{-1} support the presence of an ionic nitrate[420,421] and band at 1598 cm-1 is assigned for the presence of acetate ion for the complex [VIVO(GlyH)(Gly)]$^+$CH$_3$COO$^-$.H$_2$O.

Table (1.15): IR spectral data* (cm-1) for the complexes.

Complex No.	vC-H	vC-N	vC-O	vN-H	vCOO	vV=O	vOH	vH-OH	vV-O	vV-N	Other bands
1	2963 s	1263 m	1328 w	3178 vs	1632 m, 1440 m	983 m	3432 s	1638 s	690 w	553 vw	1121 vs, 614 s, vClO$_4$
2	2960 s	1221 m	1344 w	3168 s	1635 m, 1401 m	991 s	3424 s	1624 s	692 w	553 vw	772 m, 1382 vs, vNO$_3$
3	2962 s	1180 m	1329 w	3170 s	1625 m, 1406 m	984 s	3431 s	1632 s	691 w	552 vw	1598 m, vCH$_3$COO

*vs, very strong; s, strong; m, medium; w, weak; vw, very weak.

The visible absorption spectra of all the complexes were observed in DMSO solution under anaerobic condition are shown in Table (1.15). The solution pH was approximately 4.84. Two absorption bands

were observed for all the complexes at around 780-800 nm and 595-609 nm due to d-d transition which are the characteristic of oxovanadium(IV) species[422,424].

The cumulative assignment of the spectroscopic results can be envisaged the following chemical structures of the complexes in Figure (1.28).
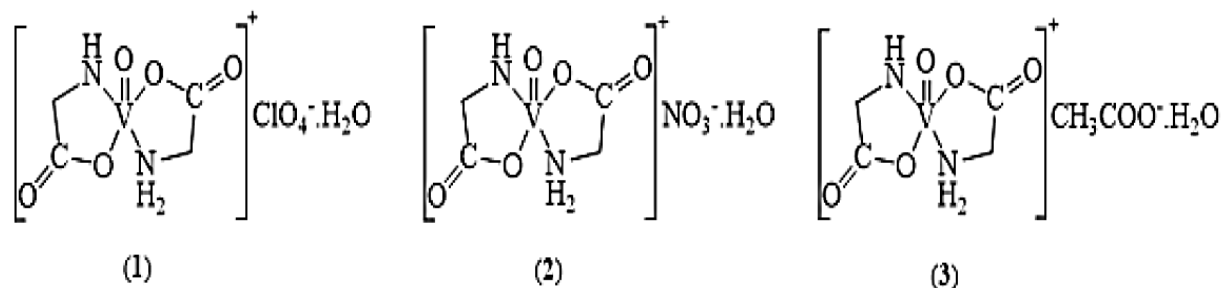
Figure (1.28): Proposed chemical structure of the complexes $[VIVO(GlyH)(Gly)]+ClO_4^-.H_2O$ (**1**), $[VIVO(GlyH)(Gly)]+NO_3^-.H_2O$ (**2**) and $[VIVO(GlyH)(Gly)]+CH_3COO^-.H_2O$ (**3**).

Assessments of antibacterial activities of biogenic chelator, glycine and their corresponding oxovanadium (IV) complexes were carried out against pathogenic bacteria *Shigella boydii*, *Shigella dysenteriae*, *Salmonella typhi* and *E coli* by disc diffusion method at three different concentrations (a: 2 mg/mL, b: 1 mg/mL and c: 0.5 mg/mL) and compared with the standard Ciprofloxacin (10 µg/disc) antibiotic disc. The results showed that the solvent, DMSO; salt, VOSO4; ligand, glycine as well as the complexes, $[VIVO(GlyH)(Gly)]^+ClO_4^{4-}.H_2O$, $[VIVO(GlyH)(Gly)]^+ NO^{3-}.H_2O$ and $[VIVO(GlyH)(Gly)]^+ CH_3COO^-.H_2O$, have no activity against the gram-negative bacteria *Salmonella typhi*, *Shigella dysenteriae*, *Shigella boydii* and *Escherichia coli* at the said concentrations. The results have been compared with commercially important bactericidal cipofloxacin. The inhibition by different complexes is also shown by Figure (1.29).
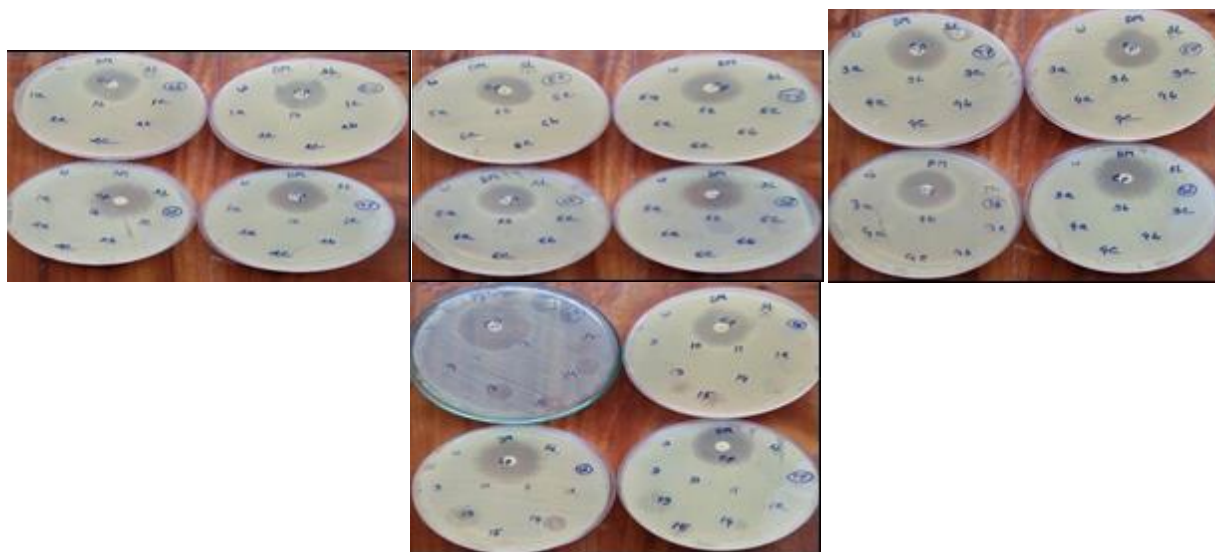
Figure (1.29): Antibacterial activity of complexes against *Salmonella typhi*, *Shigella dysenteriae*, *Shigella boydii* and *Escherichia coli*.

Study of Supun Katugampala and co-workers[425]

The study aimed to Synthesis, Characterization, and Antimicrobial Activity of Novel Sulfonated Copper-Triazine Complexes, which was summarized to Metallotriazine complexes possess interesting biological and medicinal properties, and the present study focuses on the synthesis, characterization, and antimicrobial activity of four novel copper-triazine derivatives in search of potent antibacterial and antifungal drug leads. In this study, 3-(2-pyridyl)-5,6-diphenyl-1,2,4-triazine-4,4′-disulfonic acid monosodium salt (L_1, ferrozine) and 3-(2-pyridyl)-5,6-di(2-furyl)-1,2,4-triazine-5,5′-disulfonic acid disodium salt (L_2, ferene) have been used as ligands to study the complexation towards copper(II). The synthesized complexes, $[CuCl_2(ferrozine)] \cdot 7H_2O \cdot MeOH$ (1), $[CuCl_2(ferrozine)_2] \cdot 5H_2O \cdot MeOH$ (2), $[CuCl_2(ferene)] \cdot H_2O \cdot MeOH$ (3), and $[CuCl_2(ferene)_2] \cdot H_2O \cdot MeOH$ (4), have been characterized spectroscopically, and preliminary bioassays have been carried out. FTIR spectroscopic data have shown that N=N and C=N stretching frequencies of complexes have been shifted towards lower frequencies in comparison with that of the ligands, confirming new bond formation between Cu and N, which in turn lowers the strength of N=N and C=N bonds. In addition, a bathochromic shift has been observed for UV-visible spectra of complexes (1), (2), (3), and (4). Furthermore, elemental analysis data have been useful to obtain empirical formulas of these complexes and to establish the purity of each complex. Complexes (1) and (2) have shown antibacterial activity for both *S. aureus* (ATCC® 25923) and *E. coli*

(ATCC® 25922) at 1 mg/disc concentration, and ferrozine has shown a larger inhibition zone against the clinical sample of *C. albicans* at 1 mg/disc concentration in comparison with the positive control, fluconazole.

The method of work followed by the researcher in this study, *Preparation of* [CuCl₂(ferrozine)]·7H₂O·MeOH (1), [CuCl₂(ferrozine)₂]·5H₂O·MeOH (2), [CuCl₂(ferene)]·H₂O·MeOH (3), and [CuCl₂(ferene)₂]·H₂O·MeOH (4). A solution of ferrozine in methanol was added to copper chloride dihydrate in methanol. Then the resulting mixture was stirred for 2 hours at room temperature. The Complexes were tested against Gram-positive *Staphylococcus aureus* ATCC® 25923 and Gram-negative *Escherichia coli* ATCC® 25922 bacterial species and a clinical isolate of *Candida albicans* as a fungal species. Antimicrobial assay was performed by a standard disk di.usion assay[426] where the inhibition zones were measured and expressed as a mean of three replicates. Gentamycin and fluconazole were used as positive controls, and methanol was used as the negative control.

The results of characterization for complexes involvement, FTIR data were recorded for dried crystals of ligands and complexes (1)–(4), and literature values were utilized where relevant[427]. The stretching frequency of the pyridine ring (νC=N) and stretching frequency of the triazine ring (νN=N) are considered mostly, because their values change upon formation of new bonds serving as good indicators of complex formation.

Stretching frequencies of N=N and C=N in complexes (1) and (2) have shifted to lower frequencies as expected, compared to those values of the free ferrozine ligand, due to σ donation of N lone pair which lowers strength of N=N and C=N bonds Table (1.14). Furthermore, a broad band around 3400–3300cm⁻¹ was observed due to OH groups from methanol or water. Similarly, stretching frequencies of N=N and C=N in complexes (3) and (4) were observed at lower frequencies in comparison with those of the free ferrozine ligand Table (1.16), and a broad band was observed around 3400–3300 cm⁻¹ due to OH groups of solvent.

Table (1.16): FTIR data comparison chart of complexes (**1**)–(**4**) in comparison with those of free ligands

	$\nu_{C=N}$ (cm^{-1})	$\nu_{N=N}$ (cm^{-1})
Ferrozine	1608	1503
Complex (1)	1596	1498
Complex (2)	1595	1498
Ferene	1589	1507
Complex (3)	1567	1499
Complex (4)	1570	1494

UV-Vis spectra of reactants and complexes (1, 2, 3, and 4) were recorded in methanol at room temperature. The absorption wavelengths of complexes (1)–(4) have shifted towards longer wavelengths (bathochromic shift) compared to the wavelengths of the reactants (copper, ferrozine, and ferene). Both ferrozine and ferene have aromatic ring systems and π-π* transitions are thus possible[428]. .ese results are in agreement with those previously reported for zinc complexes of ferene and ferrozine[429] where a bathochromic shift was observed for both mono and bis complexes in comparison with that of the free ligand.

Antimicrobial Activity for four complexes and ligands were studied in vitro for their antimicrobial activity against Gram-positive Staphylococcus aureus ATCC® 25923 and negative bacteria Escherichia coli ATCC® 25922, Inhibition zones were obtained by adding a concentration of 1 mg/disc, and the diameters of the zones are given in Table (1.17).

Table (1.17): Mean inhibition zone diameter at 1 mg/disc of complexes (1) and (2) and at 20 μg/disc of gentamicin.

	Mean inhibition zone diameter ± SEM (mm)	
	S. aureus ATCC® 25923	E. coli ATCC® 25922
Complex (1)	8.75 ± 0.75	7.50 ± 1.00
Complex (2)	7.00 ± 0.00	7.75 ± 0.25
Positive control (gentamicin)	26.00 ± 1.50	30.75 ± 0.75
Negative control	ND	ND

ND, not detected.

Analysis of the inhibition zone diameter revealed that only complex (1) and complex (2) show moderate antibacterial activity when compared to the positive control. It is interesting to see that ferrozine ligand demonstrates antifungal activity.

Antimicrobial activity reported here is of moderate value. Further studies are warranted to optimize this system for greater activity.

Study of Ting Liu and co-workers[430]

This research aimed to Synthesis, Structural Characterization, and Antibacterial Activity of Novel Erbium(III) Complex Containing Antimony, which was summarized to the novel 3D edta-linked heterometallic complex [Sb$_2$Er(edta)$_2$(H$_2$O)$_4$]NO$_3$·4H$_2$O (H$_4$edta = ethylenediaminetetraacetic acid) was

synthesized and characterized by elemental analyses, single-crystal X-ray diffraction, powder X-ray diffraction (XRD), Fourier transform infrared spectroscopy (FTIR), and thermal analysis.0ecomplex crystallizes in the monoclinic system with space group *Pm*. In the complex, each erbium(III) ion is connected with antimony(III) ions bridging by four carboxylic oxygen atoms, and in each $[Sb(edta)]^-$ anion, the antimony(III) ion is hexacoordinated by two nitrogen atoms and four oxygen atoms from the $edta^{4-}$ ions, together with a lone electron pair at the equatorial position. The erbium (III) ion is octacoordinated by four oxygen atoms from four different $edta^{4-}$ ions and four oxygen atoms from the coordinated water molecules. The carboxylate bridges between antimony and erbium atoms form a planar array, parallel to the (1 0 0) plane. There is an obvious weak interaction between antimony atom and oxygen atom of the carboxyl group from the adjacent layer. 0e degradation of the complex proceeds in several steps and the water molecules and ligands are successively emitted, and the residues of the thermal decomposition are antimonous oxide and erbium (III) oxide. The complex was evaluated for its antimicrobial activities by agar diffusion method, and it has good activities against the test bacterial organisms.

The method of work followed by the researcher in this study, Synthesis of $[Sb_2Er(edta)_2(H_2O)_4]NO_3 \cdot 4H_2O$. 2 mmol of $[Sb(Hedta)] \cdot 2H_2O$ was dissolved in hot distilled water, and the solution was heated to 95°C. Then, 2 mmol NH_4HCO_3 was gradually added to the above solution, and the solution was stirred for about 30 min. After cooling the solution to room temperature, 2 mmol $Er(NO_3)_3 \cdot 6H_2O$ was added to the above solution; in this case, the transparent solution was obtained. The mixture solution was held for a week, and the pink block crystals were isolated from the solution. The yield was about 58%.

The results of characterization for complexes involvement, the complex is stable in air and soluble in hot water and difficult to dissolve in most common organic solvents and slightly soluble in DMF. The molar conductance values of the complex in DMF and deionized water (10^{-3} mol·L^{-1} solution at 25°C) are 88.2 and 92.5 S·cm2·mol^{-1}, respectively. The results show that the complex belongs to 1:1 electrolyte nature[431].

Crystal Structure Analysis, the molecular structure of the title complex with atomic labeling scheme is shown in Figure (1.30). Crystallographic data and structure refinement parameters of the complex are given in Table (1.18)
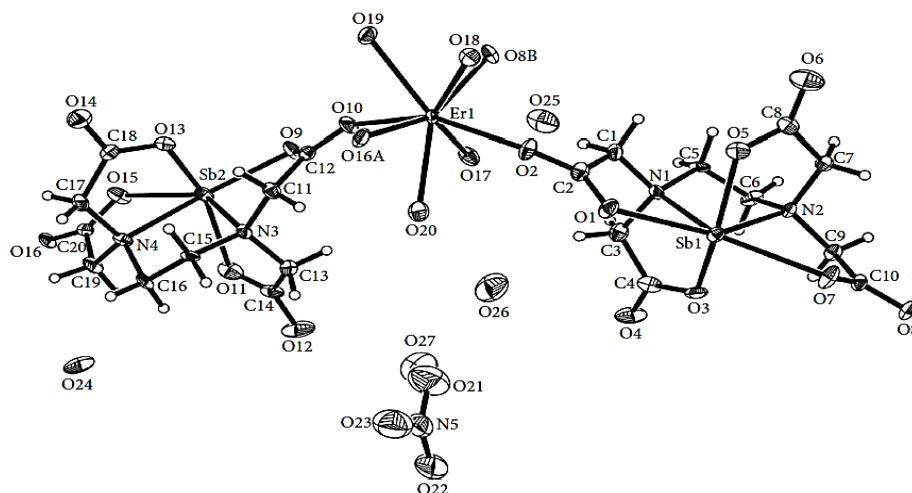
Figure (1.30): Thermal ellipsoid representation (at 50% probability) of molecular structure unit of the complex. All the H atoms are omitted for clarity. Symmetry codes: A $x - 1/2, -y, z - 1/2$; B $x + 1/2, -y + 1, z - 1/2$.

Table (1.18): Crystallographic data and structure re.nement parameters of the title complex

Empirical formula	$C_{20}H_{40}N_5O_{27}ErSb_2$	D_{calc} (g·cm^{-3})	2.278
Formula weight (g·mol^{-1})	1193.33	Absorption coefficient (mm^{-1})	4.043
T (K)	289(2)	F (000)	1162
Crystal system	Monoclinic	Crystal size (mm^3)	$0.48 \times 0.44 \times 0.20$
Space group	Pm	Theta range for data collection (°)	1.84 to 26.00
a (Å)	7.3790(10)	Limiting indices	$-9 \leq h \leq 9, -27 \leq k \leq 27, -13 \leq l \leq 13$
b (Å)	22.116(5)	Reflections collected/unique	7847/6826 [R(int) = 0.0209]
c (Å)	10.661(3)	Goodness-of-fit (GOF) on F^2	1.002
β (°)	90.55(2)	Final R indices [$I > 2\sigma(I)$]	$R_1 = 0.0392, wR_2 = 0.1051$
V (Å^3)	1739.7(7)	R indices (all data)	$R_1 = 0.0416, wR_2 = 0.1062$
Z	2	Largest diff. peak and hole (e·Å^{-3})	1.767 and −1.676

The FTIR spectrum of the title complex showed broad band at about 3426 cm^{-1} is due to ν(OH) vibration of the water molecule. .e frequency of the peak is higher than 3400 cm^{-1} showing that the oxygen atoms of the water molecule are coordinated to the metal ions[432]. The absorption peaks at 1593, 1402, and 1385 cm^{-1} may be from the asymmetric and symmetric stretching vibration in the carboxyl groups, respectively[433]. It is found that the absorption peak ν$_{as}$(COO$^-$) at 1690 cm^{-1} of Na$_2$H$_2$edta is shifted red to 1593 cm^{-1} and the absorption peak ν$_s$(COO−) at 1353 cm^{-1} of Na$_2$H$_2$edta is shifted blue to 1402 and 1385 cm^{-1} in the complex. The difference values [Δν (vas − vs) = 191 and 208 cm^{-1}] between the frequencies of the asymmetric and symmetric stretching vibration confirm that the oxygen atoms of carboxylic groups are coordinated to metallic ions by the monodentate mode and bidentate bridge mode in the complex[434], and it is in agreement with the crystal structure. .e weaker absorption peaks at about

1356 and 828 cm^{-1} may be from the stretching vibrations in the free nitrate ion. .is indicates that the nitrate ion is not coordinated to the metallic ions. The absorption peaks at 1082 and 1039 cm^{-1} may be from various stretching vibrations of the C–N and C–C bonds in the edta^{4-} ligand, respectively. In the far-infrared region, the frequency of the stretching vibration of the Sb–N bonds is 460 and 448 cm^{-1}, the frequency of the stretching vibration of the Sb–O bonds is 434 and 426 cm^{-1}, respectively. It may be reasonable to assign the peaks at 420 and 407 cm^{-1} to the stretching vibration of the Er–O bonds in the complex[435, 436].

Studying the thermal decomposition process of complexes is helpful to the understanding of the coordination structure of these complexes[437,438]. The TG curve of the complex in air atmosphere from room temperature to 800°C, data of possible thermal decomposition processes are listed in Table (1.19).

Table (1.19): Thermal decomposition data of the title complex

Reaction	Temperature (°C)	Mass loss (%)	
		m_{exp}	m_{theor}
$[Sb_2(edta)_2\text{-}\mu_4\text{-}Er(H_2O)_4]NO_3\cdot4H_2O$ $\downarrow -8H_2O$	70–220	12.00	12.08
$[Sb_2(edta)_2Er]NO_3$ $\downarrow -NO_2, -1/4O_2$	220–310	4.28	4.53
$[Sb_2(edta)_2Er]O_{0.5}$ $\downarrow -2(CH_2)_2NCH_2COO, -1/4O_2$	310–360	18.05	17.45
$(Sb\text{–}Sb)[N(CH_2COO)_3]_2(Er\text{–}Er)_{0.5}$ $\downarrow -2N(CH_2)_3, -2CO$	360–430	14.69	14.09
$(OSbO\text{–}OSbO)(CO)_4(OErO\text{–}OErO)_{0.5}$ $\downarrow -4CO, -3/4O_2$	430–510	11.36	11.40
$Sb_2O_3 + 0.5Er_2O_3$		39.62[a]	40.45[b]

[a]The experimental mass percent of the residue in the sample; [b]the calculated mass percent of the residue in the sample.

The first mass loss of 12.00% occurs between 70 and 220°C, corresponding to the gradual loss of the free water molecules and the coordinated water molecules (calculated as 12.08% for 8H$_2$O). Then, the sample will gradually lose the free nitrate ion at between 220 and 310°C and the corresponding mass loss of 4.28% (calculated as 4.53%). Between 310 and 360°C, two (CH$_2$)$_2$NCH$_2$COO groups in the complex are oxidized and decomposed, and meanwhile, one quarter oxygen molecules are lost, and the experimental mass loss (18.05%) is close to the calculated one (17.45%). The fourth step mass loss of the complex from 360 to 430°C is 14.69%, corresponding to the mass loss of two N(CH$_2$)$_3$ groups and two CO molecules (calculated as 14.09%) [437]. Upon further heating, the complex is decomposed completely between 430 and 510°C, and the mass loss of 11.36% in TG curve corresponds to lose the group of four CO molecules and threefourths of oxygen molecules (calculated as 11.40%). The remaining mass is almost constant until 510°C, and the .nal residues of the thermal decomposition of the

complex are the mixture of Sb_2O_3 and Er_2O_3, and the experimental result (39.62%) is in agreement with the result of theoretical calculation (40.45%). To check the residue, a certain mass of the complex is placed in an alumina crucible and heated in a mu«e furnace at 500°C for 2 h. Then the powder X-ray diffraction pattern of the pyrolysis products is recorded. Its characteristic peaks are consistent with the mixture of Sb_2O_3 and Er_2O_3. Therefore, the pyrolysis residues must be the mixture of Sb_2O_3 and Er_2O_3.

Antimicrobial Activity, the culture maintenance and preparation of inoculum were referenced by the literature method[439]. The antimicrobial activities of these compounds were determined qualitatively by agar diffusion method[440]. The inhibition was labeled as the diameter of bacteriostatic circle. A lawn of microorganisms was prepared by pipetting and evenly spreading inoculums (106-107CFU·cm^{-3}) onto agar set in petri dishes, using nutrient agar for the bacteria. Furacilinum was dissolved in DMSO, and penicillin, the title complex, and [Sb(Hedta)]·$2H_2O$ were dissolved in sterilized water. The Oxford cups were sticked on the previously inoculated agar surface and injected solution of the complex (0.15 mL) under sterile condition. The plates were incubated for 24 h at 37°C. .e antimicrobial activity was indicated by the presence of clear inhibition zones around the discs. Preliminary screening for antimicrobial activities of the complex was performed qualitatively using the disc diffusion assay in Table (1.20). Each of the compounds was tested three times and the average data were recorded. DMF exhibited no effect on the organisms tested. Furacilinum and penicillin were used as standard drugs, and their activities had been compared with the activities of the title complex. The complex yielded clear inhibition zones around the discs. The results show that the complex has significant antibacterial activities against five tested bacteria, and the antibacterial activities of the sequence are *Escherichia coli*, *Bacillus subtilis*, *Staphylococcus aureus*, *Salmonella typhi*, and *Staphylococcus epidermidis*, respectively. The complex has good antibacterial activity against *Escherichia coli* and *Bacillus subtilis*, and the diameter of inhibition zone of the complex is 26 and 22mm with the concentration of 1.0 mg·mL^{-1}. Meanwhile, the complex shows greater or equal activities against bacteria than the penicillin and furacilinum standard drugs.

Table (1.20): Antibacterial Activities of the title complex

Compound	Concentration (mg·mL^{-1})	Inhibition zone diameter (mm)				
		S. aureus	E. coli	S. typhi	B. subtilis	S. epidermidis
DMSO	—	—	—	—	—	—
[Sb(Hedta)]·$2H_2O$	1.0	14	17	13	14	12
[Sb_2(edta)$_2$-μ_4-Er(H_2O)$_4$]NO_3·$4H_2O$	1.0	17	26	16	22	16
Penicillin	1.0	15	18	17	19	18
Furacilinum	1.0	14	23	19	16	20

1.7 Objectives:

1- Synthesis some metal complexes with different amino acids and mixed amino acid as ligand such as Co (II) with glycine, serine, aspartic acid, and arginine, Cu (II) with glycine, Fe (III) with glycine, aspartic acid+arginine, and aspartic acid+arginine+ serine, Au (III) with glycine+aspragine, and serine+cysteine, Zn (II) with cysteine, and aspragine+leucine, and Ni (II) with leucine, and cysteine+leucine.

2- Characterization of some metal complexes.

3- To check the antibacterial activity of amino acid complexes against some types of bacteria.

Chapter Two

MATERIALS AND METHODS

MATERIALS AND METHODS

2.1 Materials

2.1.1 Chemicals and reagents

The chemicals used in the synthesis complexes are, cobalt (II) chloride hexa hydrate, iron (III) chloride hexa hydrate, cupper (II) sulfide, zinc (II) sulfide mono hydrate, nickel (II) chloride hexa hydrate, rock containing gold salts, aqua reiga solution (hydrochloric acid: nitric acid 3:1 molar ratio), hydrogen fluoride, sodium hydroxide, glycine, serine, arginine, aspartic acid, cysteine, leucine, asparagine, distill water and formic acid.

2.1.2 Instruments

Infrared spectra (IR spectra)

The IR spectra were recorded for amino acid complexes (as KBr discs) on infrared spectrophotometers, Shimadzu IR-435, and Perkin–Elmer FTIR in the region 4000–400 cm^{-1}.

Electronic spectra (UV/Vis- Spectroscopy)

Electronic spectra were recorded on a U.V-Vis. Spectrophotometer (Shimadzu, UV-1650PC-Spectrophotometer using dilute formic acid as a solvent at room temperature for amino acid complexes.

Conductivity measurement

Conductivity measurements for the amino acid complexes have been carried out using diluted formic acid as a solvent (10^{-3}M) at room temperature with conductivity Meter Model PCM3Jenway.

Thermo gravimetric analysis (TGA)

The absence and appear of coordinated water was established for amino acid complexes by thermo gravimetric analysis (TGA). TGA was carried out on a Perkin– Elmer model TGS-2 instrument.

X-Ray Diffraction (XRD)

The data were recorded at 25°C an automated Bruker SMART ABEX CCD diffractometer with Mo Kα X-ray source (λ= 0.71073 A°). Data reduction and absorption corrections were done using SAINT and SADABS software programs[441]. The structures were solved and refined using SHELX programs package[442]. Non hydrogen atoms were refined anisotropically. Hydrogen atoms were fixed at their calculated positions and refined using a riding model.

Energy dispersive X-ray (EDX)

EDX analysis were recorded by using LEOS430 scanning electron microscope coupled with energy dispersive X-ray analyzer model Oxford LINK ISIS. Samples were prepared by dispersing dry powder

on double sided conductive adhesive tape. Samples were coated with carbon by arc discharge method PCEDX. Samples were scanned in secondary electrons (SE) for morphology and back scattered electrons (BSE) mode for compositional image[443].

Atomic absorption spectroscopy

All gold determinations were performed using Perkin Elmer1100 B AAS with a graphite furnace, HGA (high graphite atomization) 700. The samples were charged into the tube with an autosampler AS-70 on the L'vov platform. The solutions for the establishment of the calibration curve (4, 8, 16 and 32 Ppm) were prepared using a nickel matrix modifier in an argon current. To obtain good signals for gold, a graphite furnace was selected with a temperature stabilized platform-STPF[444]. A stabilized temperature plat form furnace is not a piece of hard ware but a new concept that makes proper use of the existing equipment to reduce interferences to an absolute minimum. It includes the following feature:

a) Maximum power heating,

b) Atomization off the L'vov platform,

c) A minimal temperature difference of 1000ºC between thermal pretreatment and atomization,

d) Use of matrix modifiers,

 e) Gas stop during atomization,

 f) Peak area integration.

 2.2 Methods

Iron, copper, zinc, nickel, gold and cobalt amino acids complexes were synthesized, which include the interaction of some transition metal salts with some amino acids. Eight amino acid complexes were synthesized by the reaction between one type of amino acid with different transition metal salts by 2:1 molar ratio to produce the solid complexes $[ML_2.xH_2o]$ type, that include four amino acid complexes of cobalt(II) ions with glycine, serine, arginine, aspartic acid as ligands (Co-Gly, Co-Ser, Co-Arg, Co-Asp, respectively), two amino acids complexes of iron(III) and cupper(II) ions with glycine as ligand separately (Fe-Gly, Cu-Gly , acid complex respectively), one amino of zinc(II) ion with cysteine as ligand (Zn-Cys) and one amino acid complex of Nickle(II) ion with leucine as ligand (Ni-Leu). Five amino acid complexes were synthesized by the reaction between different type of mixed amino acids with different transition metal salts by 1:1:1 molar ratio to produce the solid complexes $[ML^1L^2.xH_2o]$ type, that include amino acid complexes of iron(III) ion with mixed ligand of (arginine+aspartic acid) Fe-(Arg+Asp), zinc(II) ion with mixed ligand of (Asparagine+Leucine), (Zn-(Asn+leu)), Nickle(II) ion with mixed ligand Leucine+ Cysteine (Ni-(leu+cys), two amino acids complexes of Gold(III) ion with

mixed ligand of (Cysteine+Serine) and (Asparagine+Glycine), (Au-(cys+ser)) and (Au-(Asn+Gly)), respectively), and one amino acid complexes was synthesized by the reaction between iron(III) ion with mixed ligand of (arginine+ aspartic acid+ serine) Fe-(Arg+Asp+Ser) by 1:1:1:1 molar ratio to produce the solid complexes $[ML^1L^2L^3.xH_2o]$ type. The solid complexes, were prepared following the procedure described in the literature,[443] aqueous solution of metal chlorides or metal sulfides and ligands were mixed under stirring and heated under reflux for about one hour, the PH of solution was adjusted to about 8-10 using sodium hydroxide. As a result of the complex formation process the acidity of the reaction mixtures reached PH 4-6 and the color change. The reaction product was cooled, filtered, dried and kept in a desicator over anhydrous $CaCl_2$.

2.2.1 Synthesis of Co.(Gly), Fe.(Gly), and Cu.(Gly) complexes

The complexes were prepared by following the procedure: 0.01 mol (0.75g) of glycine ligand. Was dissolved in 20 ml distilled water and for deprotonation of the amino acids 30% NaOH was added until the PH reach about 8-10.[443] Then 0.005 mol (1.1897, 1.3515, and 0.798) g of the $CoCl_2.6H_2O$, $FeCl_3.6H_2O$, $CuSO_4$ respectively; was dissolved in 10 ml of distilled water (separately), and was added to the deprotonated amino acid solution under stirring for about one hour. Until the color precipitate was formed, filtered off by filter paper, washed with distilled water for several times, and dried in air.

2.2.2 Synthesis of Co.(Asp), Co.(Arg), Co.(Ser) complexes

The complexes were prepared by following the procedure: 0.01 mol (1.31, 1.46, 0.93) g of aspartic acid, arginine and serine ligand respectively. Was dissolved in 20 ml distilled water (separately) and for deprotonation of the amino acids 30% NaOH was added until the PH reach about 8-10.[443] Then 0.005 mol (1.1897g) of the $CoCl_2.6H_2O$ was dissolved in 10 ml of distilled water, and was added to the deprotonated amino acid solution under stirring for about one hour. Until the color precipitate was formed, filtered off by filter paper, washed with distilled water for several times, and dried in air.

2.2.3 Synthesis of Zn.(Cys) complex

The complex was prepared by following the procedure: 0.01 mol (1.2116) g of cysteine ligand was dissolved in 20 ml distilled water, and for deprotonation of the amino acids 30% NaOH was added until the PH reach about 8-10.[443] Then 0.005 mol (0.8973g) of the $ZnSO_4.H_2O$ was dissolved in 10 ml of distilled water and added to the deprotonated amino acid solution under stirring for about one hour. Until the white precipitate was formed, filtered off, washed with distilled water for several times, and dried in air.

2.2.4 Synthesis of Ni.(Leu) complex

The complex was prepared by following the procedure: 0.01 mol (1.3118) g of leucine ligand. Was dissolved in 20 ml distilled water, and for deprotonation of the amino acids 30% NaOH was added until the PH reach about 8-10.[443] Then 0.005 mol (1.1884g) of the $NiCl_2.6H_2O$ was dissolved in 10 ml of distilled water, and was added to the deprotonated amino acid solution under stirring for about one hour. Until the green precipitate was formed, filtered off by filter paper, washed with distilled water for several times, and dried in air.

2.2.5 Synthesis of Fe(Arg)(Asp) complex

The complex was prepared following the procedure: 1 mmol (0.133g) of Aspartic acid was dissolved in 10 ml distilled water and for deprotonation of the Aspartic acid, 30% NaOH was added until the PH reach about 8-10[443]. Then 1 mmols of Arginine was dissolved in 10 ml distilled water and was added to the deprotonated Aspartic acid solution. Then 1 mmol (0.2703g) of the $FeCl_3.6H_2O$ was dissolved in 2 ml of distilled water, and added to the mixed amino acid solution under stirring for about one hour, left on heating until the solvent evaporated, washed with absolute ethanol several times, and dried in air.

2.2.6 Synthesis of Fe(Arg)(Asp)(Ser) complex

1 mmols (0.105, 0.133 and 0.174g) of serine, aspartic acid and arginine respectively; were dissolved in 10 ml distilled water, separately. And added the ligand solutions to each other, and for deprotonation of the mixture 30% NaOH was added until the PH reach about 8-10[443]. Then 1 mmol (0.7203g) of the $FeCl_3.6H_2O$ was dissolved in 2 ml of distilled water, and was added to the mixture of deprotonated amino acid solution under stirring for about one hour, heated until the solvent evaporated, washed with absolute ethanol several times, and dried in air.

2.2.7 Synthesis of Zn(Asn)(Leu) complex

The complex was prepared following the procedure: 0.005 mol (0.6605g) of Asparagine was dissolved in 10 ml distilled water and for deprotonation of the Asparagine, 30% NaOH was added until the PH reach about 8-10[443]. Then 0.005 mol of Leucine was dissolved in 10 ml distilled water and for deprotonation of the Asparagine, 30% NaOH was added until the PH reach about 8-10[443]. And was added to the deprotonated Asparagine solution. Then 0.005 mol (0.8973g) of the $ZnSO_4.H_2O$ was dissolved in 10 ml of distilled water, and added to the mixed amino acid solution under stirring for about one hour, Until the white precipitate was formed, filtered off by filter paper, washed with distilled water for several times, and dried in air.

2.2.8 Synthesis of Ni(Cys)(Leu) complex

The complex was prepared following the procedure: 0.005 mol (0.6058g) of Cysteine was dissolved in 10 ml distilled water and for deprotonation of the Cysteine, 30% NaOH was added until the PH reach about 8-10[443]. Then 0.005 mol (0.655g) of Leucine was dissolved in 10 ml distilled water and for deprotonation of the Leucine, 30% NaOH was added until the PH reach about 8-10[443]. And was added to the deprotonated Cysteine solution. Then 0.005 mol (0.8973g) of the $NiCl_2.6H_2O$ was dissolved in 10 ml of distilled water, and added to the mixed amino acid solution under stirring for about one hour, Until the green precipitate was formed, filtered off by filter paper, washed with distilled water for several times, and dried in air.

2.2.9 Synthesis of the gold complexes from the rock

2.2.9.1 Determination of gold in rock sample

Determined amount of gold in the rock by using atomic absorption spectrophotometer AAS. A laboratory method for the determination of gold in large (100 gram) samples has been developed for use in the study of the gold content of placer deposits and of trace amounts of gold in other geologic materials. In this method the sample is digested with hydrogen fluoride instead to bromine and ethyl ether, the gold is extracted into methyl isobutyl ketone, and the determination is made by atomic-absorption spectrophotometry. The lower limit of detection is 0.005 part per million in the sample. The few data obtained so far by this method agree favorably with those obtained by assay and by other atomic-absorption methods. About 25 determinations can be made per man-day. The digestion of rock sample was achieved following the procedure: 10 g of rock (Au) was dissolved in 40 ml hydrogen fluoride (HF) and heated in sand path in 350^OC even the sample was dried. The dryer sample was dissolved 25 ml aqua regia (hydrochloric acid 37%: nitric acid 65% (3:1)) and heated in sand path in $350^{\circ}C$ even the sample became in the form of a paste. The paste was transferred by less amount of hydrochloric acid 5% in a Teflon 100 ml of volumetric flask, 10 ml of methyl iso butyl ketone (MIBK) was added, shake about 20 min in the shaker, hydrochloric acid 5% was added until the solution reaches the end of the flask (not the mark).

2.2.9.2 Preparation of standard solution of gold

The three standard solution 10, 20, 30 ppm of gold was prepared by the following procedure: 1, 2, 3 ml respectively, was took from the 1000 ppm standard solution stock of gold in 100 ml volumetric flask, hydrochloric acid 5% was added until the solution reaches the mark.

2.2.9.3 Synthesis of Au(Cys)(Ser) complex

The complex was prepared following the procedure: 679.3 g of rock (Au) was dissolved in 1 L hydrogen fluoride (HF) and heated in sand path in 350^OC even the sample was dried. The dryer sample was dissolved 200 ml aqua regia (hydrochloric acid 37% : nitric acid 65% (3:1)) and heated in hot plate in 50^OC even the sample was dissolved completely (all gold in rock was change to $HAuCl_4$), sodium bi carbonate $NaHCO_3$ was added to the solution until the PH~7.0 to form sodium aurrate $Na(AuCl_4)$. 0.005 mol (0.6058g) of Cysteine was dissolved in 10 ml distilled water and for deprotonation of the Cysteine, 30% NaOH was added until the PH reach about 8-10[443]. Then 0.005 mol (0.465g) of Serine was dissolved in 10 ml distilled water and for deprotonation of the Serine, 30% NaOH was added until the PH reach about 8-10[443]. The deprotonated mixture of Cysteine and serine solution was added to sodium aurrate $Na(AuCl_4)$ under stirring for about one hour, Until the brown precipitate was formed, filtered off by filter paper, washed with distilled water for several times with water, and dried in air.

2.2.9.4 Synthesis of Au(Asn)(Gly) complex

The complex was prepared following the procedure: 679.3 g of rock (Au) was dissolved in 1 L hydrogen fluoride (HF) and heated in sand path in 350^OC even the sample was dried. The dryer sample was dissolved 200 ml aqua regia (hydrochloric acid 37%: nitric acid 65% (3:1)) and heated in hot plate in 50°C even the sample was dissolved completely (all gold in rock was change to $HAuCl_4$), sodium bi carbonate $NaHCO_3$ was added to the solution until the PH~7.0 to form sodium aurrate $Na(AuCl_4)$. 0.005 mol (0.6605g) of Asparagine was dissolved in 10 ml distilled water and for deprotonation of the Asparagine , 30% NaOH was added until the PH reach about 8-10[443]. Then 0.005 mol (0.375g) of Glycine was dissolved in 10 ml distilled water and for deprotonation of the Glycine, 30% NaOH was added until the PH reach about 8-10[443]. The deprotonated mixture of Asparagine and Glycine solution was added to sodium aurrate $Na(AuCl_4)$ under stirring for about one hour, Until the brown precipitate was formed, filtered off by filter paper, washed with distilled water for several times with water, and dried in air.

2.2.10 Microbial strains

The amino acid complexes were tested against the following microorganisms: *Escherichia coli*, *Pseudomonas aeruginosa, Staphylo coccus aureas, Entero coccus feacalis*. Antibacterial tests were then carried out by disc diffusion method.[445] Bacterial strains were cultured overnight at 37°C in agar.

Preparation of nutrient agar media, and muller hinton agar with blood media

Suspent 28 and 38g nutrient agar and muller hinton agar respectively, in 1000ml distilled water, heated to boiling to dissolve the media completely. Sterilize by autoclaving at 15 Ibs pressure (121°C) for 15 minute. 1ml of blood was mixed with muller hinton agar.

Antibacterial tests were then carried out by disc diffusion method,[445] the three types of bacteria (Escherichia coli, Pseudomonas aeruginosa, Staphylo coccus aureas), spread on nutrient agar media, and Entero coccus feacalis spread on muller hinton agar with blood media. The discs (6 mm in diameter) were impregnated with the 10, 20, 30, 40 µl/disc (1), (2), (3), (4) stock solution of 100 mg/ml respectively of amino acids complexes and placed on the oven at 37°C for 15 min to dried. Antibacterial activity was evaluated by measuring the zone of inhibition against the test organisms. All inhibitory tests were performed an average of four independent readings for each compound was recorded. Finally, Petri plates were incubated for 24 hours at 28 ± 2°C. The zone of inhibition was calculated in millimetres carefully. And calculate the zone diameter incident by 3mg for comparison between sensitivity of different amino acid complexes.

2.3 calculations

2.3.1 Calculation of the complexes [ML$_2$.XH$_2$O], and [MLL′.xH$_2$O] type synthesis

To synthesis amino acid complexes [ML$_2$.XH$_2$O] type will require weight per gram that equivalent 0.005 mols of transition metal salt and 0.01mols of amino acid (1:2 molar ratio), and a complexes [MLL′.xH$_2$O] type will require will require weight per gram that equivalent 0.005 mols of transition metal salt with 0.005mols from each amino acid (1:1:1 molar ratio). These calculations illustrated in Table (3.1).

Table (2.1) calculation for synthesis of complexes [ML$_2$.XH$_2$O], and [MLL′.xH$_2$O] type:

Compound	Rule	Molecular weight	Weight per g equivalent of 0.01 mol	Weight per g equivalent of 0.005 mol
Glycine C$_2$H$_5$NO$_2$	n = wt$_{(g)}$/M.wt	12×2+1×5+14×1+16×2= 75	0.01 × 75 = 0.75 g	0.005 × 75 = 0.375 g
Serine C$_3$H$_7$NO$_3$	Wt$_{(g)}$ = n × M.wt	12×3+1×7+14×1+16×3= 93	0.005 × 93 = 0.465 g	0.005 × 93 = 0.465 g
Arginine C$_6$H$_{14}$N$_4$O$_2$	M.wt ≡ Molecular weight of compound	12×6+1×14+14×4+16×2= 146	0.01 × 146 = 1.46 g	0.005 × 146 = 0.73 g
Aspartic acid	wt$_{(g)}$ ≡ weight per	12×4+1×7+14×1+16×4= 131	0.01 × 131 = 1.31 g	0.005 × 131 = 0.655 g

$C_4H_7NO_4$	gram			
Cysteine $C_3H_7NO_2S$	n ≡ number of mols	$12\times3+1\times7+14\times1+16\times2+32=$ 121	$0.01 \times 121 = $ 1.21 g	$0.005 \times 121 =$ 0.6058 g
Asparagine $C_4H_8N_2O_3$		$12\times4+1\times8+14\times2+16\times3=$ 132	$0.01 \times 132 = $ 1.32 g	$0.005 \times 132 =$ 0.6605 g
Leucine $C_6H_{13}NO_2$		$12\times6+1\times13+14\times1+16\times2=$ 131	$0.01 \times 131 = $ 1.31 g	$0.005 \times 131 =$ 0.6559 g
$CoCl_2.6H_2O$:		$58.93+35.5\times2+18\times6=$ 237.93	-	0.005×237.93 =1.1897 g
$CuSO_4$		$63.55+32+16\times4=$ 159.6	-	$0.005 \times 159.6 =$ 0.798 g
$FeCl_3.6H_2O$		$55.85+35.5\times3+18\times6=$ 270.3	-	$0.005 \times 270.3 =$ 1.3515 g
$ZnSO_4.H_2O$		$65.38+32+16\times4+18=$ 179.45	-	$0.005 \times 179.45 =$ 0.8973 g
$NiCl_2.6H_2O$		$58.69+35.5\times2+18\times6=$ 237.69	$0.01\times 237.93 =$ 2.3793 g	0.005×237.93 =1.1884 g

2.3.2 Calculations the Standard solutions of gold

To Prepared the 4, 8, 16, 32 ppm standard solution from 1000 Ppm standard solution stock, the calculated of compatible volume from stock, this shown in Table (2.2).

Table (2.2) calculation of gold standard solution

Concentration	Rule	Volume take from 1000 Ppm
4 Ppm	$M_1\times V_1=M_2\times V_2$	$1000\times V_1=4\times100$
	$M_1 \equiv$ molar concentration of solution before the dilution	$V_1=0.4ml$
8 Ppm	$M_2 \equiv$ molar concentration of solution after the dilution	$1000\times V_1=8\times100$
	$V_1 \equiv$ volume of solution before the dilution	$V_1=0.8ml$
16 Ppm	$V_2 \equiv$ volume of solution after the dilution	$1000\times V_1=16\times100$
		$V_1=1.6ml$
32 Ppm		$1000\times V_1=32\times100$
		$V_1=3.2ml$

Chapter Three

RESULTS AND DISCUSSION

RESULTS AND DISCUSSION

3.1 Determination of gold content in the rock sample

All gold determinations were performed using Perkin Elmer 1100B AAS with a graphite furnace, HGA (high graphite atomization) 700, the method of peak height measurement was selected. The use of an auto sampler is necessary for a series of samples. The selected instrumental conditions were: wavelength 242.8 nm slit 7 nm, lamp current 10 mA, integration time 5 s. of all parameters for the determination of gold by Atomic Absorption Spectroscopy (AAS) with a graphite furnace, the most important are the regime of furnace heating, time ramp and hold time temperature, as well as gas flow rate.[446] Using these conditions for the determination of the series of the standard solution and unknown sample of gold, these illustrated in Table (3.1), and plot the relationship of difference concentration against the absorption, which shown in Figure (3.1).

Table (3.1) absorption of gold standard solution and unknown rock sample:

Concentration per ppm	absorption
4	0.0845
8	0.1690
16	0.243
32	0.4216
unknown	0.391
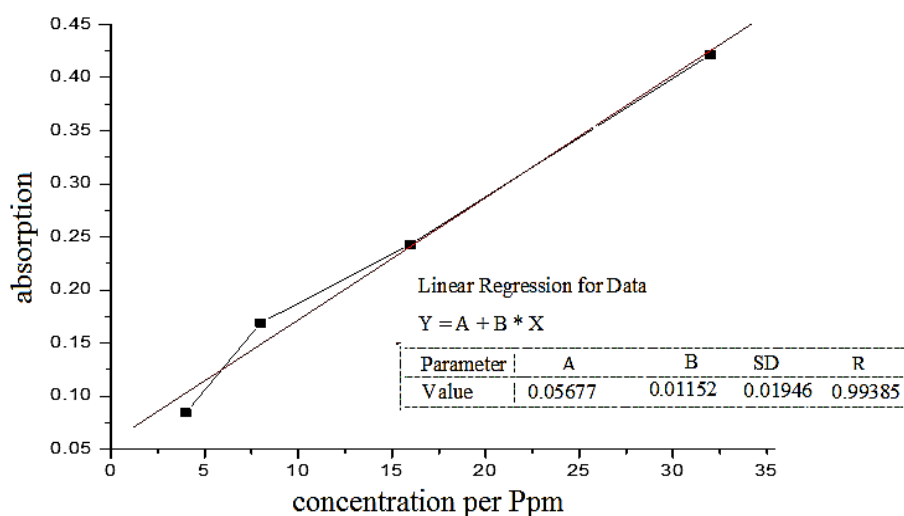
Figure (3.1) Plot of concentration against the absorption

Concentration of gold in rock sample

The experimental investigations were preceded by a trial of the direct determination of gold in geological sample by GF AAS; the sample was dissolved with acid in a Teflon vessel, the destruction of the silicate structure being achieved with HF. The gold content was determined by GFAAS and results was obtained by compared with the results of standard solution of gold, and finding gold content in the rock sample per gram, accordingly the necessary weight was calculated from the rock, which is equivalent to 0.005 moles of gold chloride $AuCl_3$ to interact with 0.005 moles of the amino acids, and the composition of the corresponding complexes by 1:1:1 molar ratio, these illustrated bellow:

$Y = A + B * X$ $\rightarrow$ $Y = 0.05679 + 0.01152 \times 0.391$ $\therefore$ $Y = 29$ ppm

$M_1 \times V_1 = M_2 \times V_2$ $\rightarrow$ $M_1 \times 20 = 29 \times 100$

$$M_1 = 145 \text{ Ppm} \equiv 145 \text{ mg/L}$$

$$0.145 \text{ g} \rightarrow 1000 \text{ ml}$$

$$X \text{ g} \quad \rightarrow 100 \text{ ml}$$

$\therefore$ $X = 0.0145$ g (Au) $\equiv$ 0.0145 g (Au) $\rightarrow$ 10 g (rock)

0.005 mols of AuCl3 to synthesis the gold complexes:

$$Wt \text{ (g)} = 0.005 \times 303.5 = \underline{1.5175} \text{ g}$$

197 Au: 106.5 Cl $\rightarrow$ 1.85:1 (Au:Cl) molar ratio

$$1.5175 \times 1.85 \div (1.85+1) = \underline{0.985} \text{ g (Au)}$$

$$10 \text{ g (rock)} \rightarrow 0.0145 \text{ g (Au)}$$

$$X \text{ g (rock)} \quad \rightarrow 0.985 \text{ g (Au)}$$

$\therefore$ $X = \underline{679.3 \text{ g (rock)}}$

From the calculation above found to be taken 679.3 g of the rock, which was equivalent to 0.005 moles of the Gold chloride $AuCl_3$

3.2 Physical analysis

Conductivity measurements for the amino acid complexes ($10^{-3}M$) in dilute formic acid as a solvent, diluted formic acid as a blank solution and, dithiocarbamate complex to evaluate the amino acid complexes, have been carried out at room temperature with conductivity Meter Model PCM3Jenway, which illustrated in Table (3.2).

Table (3.2) color and conductivity measurement of complexes:

complex	color	Concentration g/ml	Molar Conductance $(cm^2 ohm^{-1} mol^{-1})$
dithiocarbamate complex	-	1×10-3	76.9
Blank (formic acid)	-	2.44×10-3	36.5
Au (Asn.Gly)	Deep Brown	1×10-3	110.3
Au (Cys.Ser)	Deep Brown	1×10-3	116.4
Co.Gly	Reddish brown	1×10-3	Nil
Co.Ser	pink	1×10-3	Nil
Co.Asp	Pink	1×10-3	Nil
Co.Arg	Reddish brown	1×10-3	Nil
Fe(Gly)	Deep Brown	1×10-3	117.2
Fe(Arg+Asp)	Deep Brown	1×10-3	119.1
Fe(Arg+Asp+Ser)	Deep Brown	1×10-3	Nil
Cu.Gly	Blue	1×10-3	Nil
Zn.Cys	White	1×10-3	Nil
Zn.Asn.Leu	White	1×10-3	Nil
Ni.Leu	Green	1×10-3	Nil
Ni.Cys.Leu	Green	1×10-3	Nil

The molar conductivity of the dithiocarbamate complexes were measured in dimetylformamide (10^{-3}M) solvent indicates that theses complexe is 1:1 electrolyte. The corresponding amino acid complexes are soluble in formic acid but insoluble in warm DMF, THF, cyanomethane, benzene, dichloromethane, chloroform, DMSO, DMF+DMSO mixture and ethanol. Accordingly, the conductivity of the amino acid complexes were measured in concentrated formic acid and the value of the conductivity of formic acid is deducated.

3.2.1 Gold complexes

The conductivity of Au (Asn.Gly) and Au (Cys.Ser) complexes were measured, and the results obtain, indicate their 1:1 electrolytic nature. And the results obtain, indicate that the coordination sphere curries a negative charge, in the other word, two groups coordinated by negative charge and the other groups coordinated by lone pair electrons. This result was agreed with study of (Hamdi, *et al.*, 2013)[273], with different values of conductivity that deal with the gold complexes synthesized by difference ligand.

3.2.2 Cobalt complexes

Co.Gly, Co.Ser, Co.Asp, Co.Arg complexes, the conductivity values in formic acid were measured, and the results obtain, indicate that all ions involved in complex formation were coordinated with Co^{2+} ion, in the other word, two groups coordinated by negative charge and the other groups coordinated by

lone pair electrons (nonelectrolytes nature), that agreed with the conductivity result of the studies of (Reddy, *et al*, 2005)[287], (Rosu, *et al*, 2009)[310], and (Patil, *et al*, 2012)[319].

3.2.3 Iron complexes

The conductivity measurement of Fe (III) complexes showed, the Fe(Gly) and Fe(Arg+Asp) are 1:1 electrolytic nature that means the coordination sphere curries one negative charge, and the Fe(Arg+Asp+Ser) is nonelectrolyte nature, and the results obtain of Fe(Arg+Asp+Ser) complex, indicate that all ions involved in complex formation were coordinated with Fe^{3+} ion, in the other word, three groups coordinated by negative charge and the other groups coordinated by lone pair electrons (nonelectrolytes nature).

3.2.3 Copper, Zinc, and Nickel complexes

The Cu.Gly, Zn.Cys, Zn.Asn.Leu, Ni.Leu, and Ni.Cys.Leu complexes showed by molar conductivity measurement in formic acid are nonelectrolytes nature. And the results obtain, indicate that all ions involved in complex formation were coordinated with M^{2+} ion, in the other word, two groups coordinated by negative charge and the other groups coordinated by lone pair electrons. These results were agreed with the studies of (Reddy, *et al.,* 2005)[287], and (Rosu, *et al,* 2009)[310].

3.3 Energy dispersive x-ray spectra (EDX) study

The EDX profiles of Co.Gly, Co.Ser, Co.Asp, Co.Arg Au.(Asn.Gly), Au.(Cys.Ser), Fe(Gly), Fe(Arg+Asp), Fe(Arg+Asp+Ser), Cu.Gly, Zn.Cys, Zn.Asn.Leu, Ni.Leu, and Ni.Cys.Leu complexes confirmed the presence of O, C, N. the prominent nitrogen and oxygen clearly suggests to the functional group of amino acid ligand and metal ion peak presence indicated to formation of the complexes. And the percentage of each atom gives the number of ions in complex. These results had been summarized in Tables (3.3), (3.4), (3.5), (3.6), (3.7), (3.8), (3.9), (3.10), (3.11), (3.12), (3.13), (3.14), (3.15) and (3.16) respectively. The number of atoms for each complex was calculated according to their percentages shown by the apparatus where Co.Gly complex contains 4, 6, 1, and 2 ions of C, O, Co, and N, respectively, Co.Ser complex contains 6, 8, 1, and 2 ions of C, O, Co, and N, respectively, Co.Asp complex contains 8, 10, 1, and 2 ions of C, O, Co, and N, respectively, Co.Arg complex contains 12, 6, 1, and 8 ions of C, O, Co, and N, respectively, Au.(Asn.Gly) complex contains 6, 5, 1, 3 and 1 ions of C, O, Au, N and Cl, respectively, Au.(Cys.Ser) complex contains 6, 5, 1, 2, 1 and 1 ions of C, O, Au, N, S and Cl, respectively, Fe.Gly complex contains 4, 6, 1, 2 and 1 ions of C, O, Fe, N and Cl, respectively, Fe.(Arg+Asp) complex contains 10, 8, 1, 5 and 1 ions of C, O, Fe, N and Cl, respectively, Fe.(Arg+Asp+Ser) complex contains 13, 9, 1 and 6 ions of C, O, Fe and N, respectively, Cu.Gly

complex contains 4, 6, 1, and 2 ions of C, O, Cu, and N, respectively, Zn.Cys complex contains 6, 4, 1, 2 and 2 ions of C, O, Zu, N and S, respectively, Zn.Asn.Leu complex contains 7, 5, 1, 3 and 1 ions of C, O, Zu, N and S, respectively, Ni.leu complex contains 12, 6, 1, and 2 ions of C, O, Ni, and N, respectively. In addition, Ni.Cys.Leu complex contains 9, 6, 1, 1, and 2 ions of C, O, Ni, S, and N, respectively.

Table (3.3) EDX reading of Co.Gly complex:

Element	Result	Unit	3δ
O	39.18	%	0.215
Co	24.05	%	0.507
C	19.59	%	0.116
N	11.44	%	0.221
Trace element	5.584	%	0.320

Table (3.4) EDX reading of Co.Ser complex:

Element	Result	Unit	3δ
O	39.50	%	0.265
C	23.96	%	0.264
Co	19.59	%	0.132
N	9.32	%	0.210
Trace element	4.519	%	0.130

Table (3.5) EDX reading of Co.Asp complex:

Element	Result	Unit	3δ
O	44.62	%	0.283
C	26.77	%	0.109
Co	16.42	%	0.192
N	7.81	%	0.231
Trace element	4.378	%	0.145

Table (3.6) EDX reading of Co.Arg complex:

Element	Result	Unit	3δ
C	33.86	%	0.292
N	26.341	%	0.108
O	22.58	%	0.211
Co	13.85	%	0.107
Trace element	3.369	%	0.110

Table (3.7) EDX reading of Au.(Asn.Gly) complex

Element	Result	Unit	3δ
Au	43.97	%	0.066
C	17.85	%	0.005
O	16.05	%	0.036
N	9.365	%	0.011
Cl	7.914	%	0.030
Trace element	4.856	%	0.057

Table (3.8) EDX reading of Au.(Cys.Ser) complex:

Element	Result	Unit	3δ
Au	42.315	%	0.109
O	17.18	%	0.311
C	15.446	%	0.155
Cl	7.617	%	0.032
S	6.771	%	0.183
N	6.01	%	0.123
Trace element	4.66	%	0.145

Table (3.9) PCEDX reading of Fe(Gly)complex

Element	Result	Unit	3δ
O	35.428	%	0.127
Fe	20.610	%	0.446
C	17.710	%	0.175
Cl	13.100	%	0.210
N	10.332	%	0.245
Trace element	2.825	%	0.320

Table (3.10) EDX reading of Fe(Arg+Asp)complex

Element	Result	Unit	3δ
O	30.381	%	0.149
C	28.426	%	0.253
Fe	16.572	%	0.037
N	13.218	%	0.101
Cl	8.386	%	0.099
Trace element	3.064	%	0.320

Table (3.11) EDX reading of Fe(Arg+Asp+Ser) complex

Element	Result	Unit	3δ
C	33.6	%	0.164
O	31.013	%	0.120
N	18.077	%	0.210
Fe	12.03	%	0.135
Trace element	5.265	%	0.320

Table (3.12) EDX reading of Cu.Gly complex

Element	Result	Unit	3δ
O	39.69	%	0.208
Cu	26.28	%	0.581
C	19.84	%	0.124
N	11.56	%	0.021
S	1.57	%	0.008
Trace element	2.6004	%	0.035

Table (3.13) EDX reading of Ni.Leu complex

Element	Result	Unit	3δ
C	43.29	%	0.291
O	28.87	%	0.196
Ni	17.67	%	0.218
N	8.40	%	0.109
Trace element	1.824	%	0.242

Table (3.14) EDX reading of Ni.Cys.Leu complex

Element	Result	Unit	3δ
C	32.01	%	0.288
O	24.01	%	0.234
Ni	19.568	%	0.213
S	10.66	%	0.218
N	9.347	%	0.134
Trace element	4.416	%	0.045

Table (3.15) EDX reading of Zn.Cys complex

Element	Result	Unit	3δ
C	24.11	%	0.167
Zn	21.89	%	0.127
O	21.34	%	0.132
S	21.34	%	0.124
N	9.378	%	0.134
Trace element	1.764	%	0.145

Table (3.16) EDX reading of Zn.Asn.Leu complex

Element	Result	Unit	3δ
C	38.029	%	0.171
O	25.365	%	0.134
Zn	20.726	%	0.126
N	13.31	%	0.170
Trace element	2.646	%	0.165

3.4 Thermal Analysis

3.4.1 Cobalt complexes

Thermal Gravimetric Analysis (TGA) study for Cobalt complexes were investigated and recorded weight loss per mg against the temperature. The TGA curves of Co.Gly, Co.Ser, Co.Asp, and Co.Arg, Figures (3.2), (3.3), (3.4), and (3.5), respectively, revealed identical characteristic bands and little differences in temperature and weight loss. TGA curve for Co.Gly, Co.Ser, Co.Asp, and Co.Arg, complexes displays three stages of mass loss within the temperature range of 100–500°C. The first stage is at 110–180°C, corresponding to the dehydration of two moles of crystal water. The second stage occurs at around 200–320°C, corresponding to the loss of the volatile gases from decomposition of amino acid ligand. The third stage occurs at the temperature above to 450 °C. According to (Reddy, *et al*, 2005)[287], and (Rosu*, et al*, 2009)[310], such phenomenon was caused in the Co.Gly, Co.Ser, Co.Asp, and Co.Arg TGA complexes. 15.8% weight loss was reached for Co.Gly complex in temperature range 128-172ºC in the first stage, which corresponds to dehydration of the two moles of crystal water. The second stage involved weight loss of 30.4% in temperature range 220-26ºC, which corresponds to evaporation of CO_2, and NH_3 gases from the amino acid. The increase in weight associated in the 3th stage with temperature above 472^0C was due to oxidation of the cobalt ion to form cobalt oxide.

For Co.ser complex the weight loss of 11.8% was reached in the 1st stage at temperature range 122-165ºC corresponding to dehydration of two moles of the crystal water and 31.2% at 210-315ºC in the 2nd stage. The increase in weight associated in the 3th stage with temperature above 472^0C was due to oxidation of the cobalt ion to form cobalt oxide.

For Co.Asp complex the weight loss of 10.6% was reached in the 1st stage at temperature range 118-165ºC corresponding to dehydration of two moles of the crystal water and 25.6% at 240-259ºC in the 2nd stage. The increase in weight associated in the 3th stage with temperature above 471^0C was due to oxidation of the cobalt ion to form cobalt oxide.

For Co.Arg complex the weight loss of 9.4% was reached in the 1st stage at temperature range 133-179ºC corresponding to dehydration of two moles of the crystal water and 33.6% at 225-242ºC in the 2nd stage. The increase in weight associated in the 3th stage with temperature above 469^0C was due to oxidation of the cobalt ion to form cobalt oxide. These feature summarized in Table (3.17).

Table (3.17) Weight loss per mg against to the temperture per (°C) reading of Co.Gly, Co.Ser, Co.Asp, and Co.Arg complexes:

Co.Gly		Co.Ser		Co.Asp		Co.Arg	
Temp(°C)	Weight loss(mg)	Temp(°C)	Weight loss(mg)	Temp(°C)	Weight loss(mg)	Temp(°C)	Weight loss(mg)
128-172	0.8	122-195	0.59	118-165	0.53	133-179	0.47
220-261	1.52	210-315	1.56	240-259	1.25	225-242	1.68
462	Weight increased	459	Weight increased	471	Weight increased	469	Weight increased
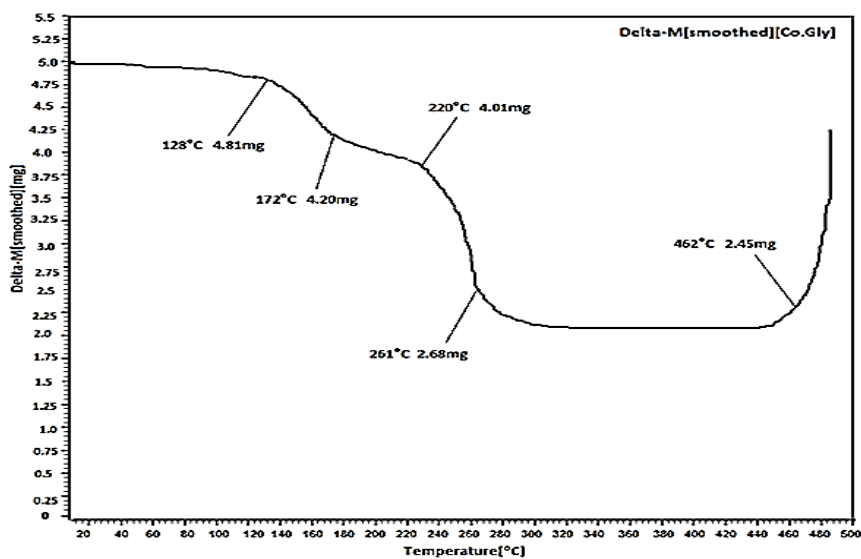
Figure (3.2) Thermal gravimetric curve of Co.Gly complex
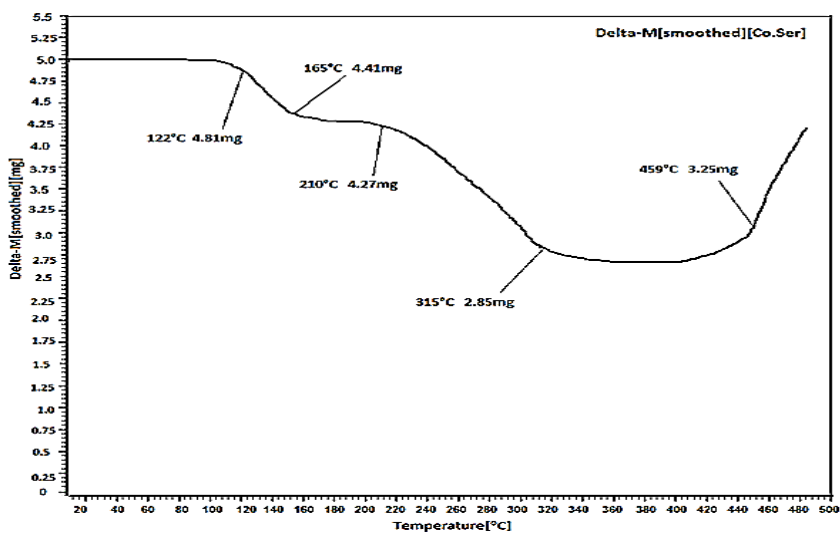
Figure (3.3) Thermal gravimetric curve of Co.Ser complex

138
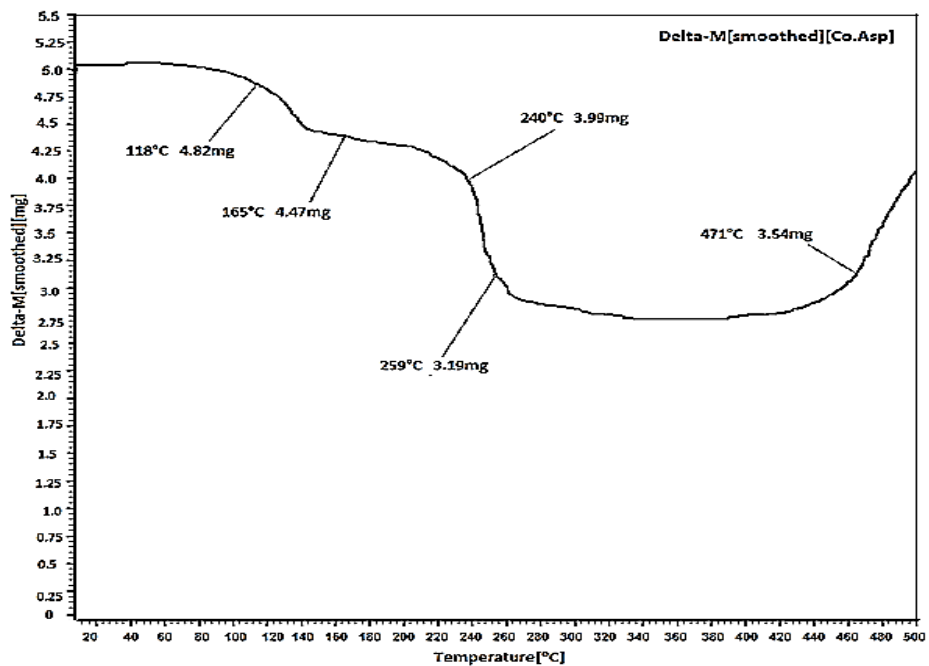
Figure (3.4) Thermal gravimetric curve of Co.Asp complex
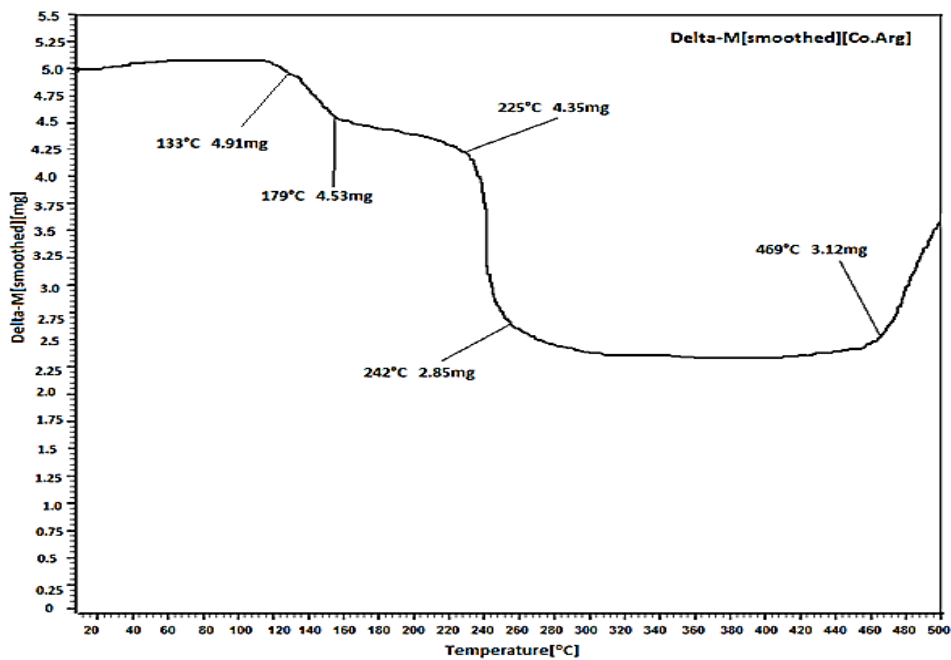
Figure (3.5) Thermal gravimetric curve of Co.Arg complex

139

3.4.2 Iron complexes

Fe(Gly), Fe(Arg+Asp), and Fe(Arg+Asp+Ser) complexes, Figures (3.6), (3.7), and (3.8), respectively, were investigated and recorded weight loss per mg against the temperature. The TGA curves of Fe.Gly, and mixed ligand Fe(Arg.Asp), showed same characteristic band in little difference in temperature and weight loss. TGA curve for Fe.Gly, and Fe(Arg.Asp) complexes displays two stages of mass loss within the temperature range of 100–500 °C. The first stage is at 100–180 °C, corresponding to the dehydration of two moles of crystal water. The second stage occurs at around 200–320 °C, corresponding to the loss of the volatile gases from decomposition of amino acid ligand. And the weight of the two complexes have been constant until the temperature reach 500°C, that indicate the Fe ion has not oxidation or decomposition occur. According to (Reddy, *et al*, 2005)[287], and (Rosu, *et al*, 2009)[310], such phenomenon was caused in the Fe(Gly) and Fe(Arg.Asp) TGA complexes. 16.4% weight loss was reached for Fe.Gly complex in temperature range 124-175ºC in the first stage, which corresponds to dehydration of the two moles of crystal water. The second stage involved weight loss of 31.8% in temperature range 224-272ºC, which corresponds to evaporation of CO_2, and NH_3 gases from the amino acid.

For Fe(Arg.Asp) complex the weight loss of 9.6% was reached in the 1st stage at temperature range 129-173ºC, corresponding to two moles of crystal water and 34.6% at 227-248 ºC in the 2nd stage. Another peak was evident (6.4%) at 248-264^{0}C also, which corresponds to evaporation carbon dioxide CO_2, and ammonium NH_3 gases from the amino acid. These results indicated the presence of two peaks in the second stage resulting from mixed amino acid.

But the TGA curve for Fe(Arg.Asp.Ser) complex displays one stage of mass loss within the temperature range of 200–320°C. 14.4% at 215-229ºC in the 1st stage. Another three peaks were evident (11.4%) at 229-250^{0}C, (14.6%) at 250-269^{0}C, and 17.2% at 269-320^{0}C also, which corresponds to evaporation carbon dioxide CO_2, and ammonium NH_3 gases from the decomposition of the amino acid. These feature summarized in Table (3.18).

Table (3.18) Weight loss per mg against to the temperture per (°C) reading Fe(Gly), Fe(Arg+Asp), and Fe(Arg+Asp+Ser) complexes:

Fe(Gly)		Fe(Arg+Asp)		Fe(Arg+Asp+Ser)	
Temp(°C)	Weight loss(mg)	Temp(°C)	Weight loss(mg)	Temp(°C)	Weight loss(mg)
124-175	0.82	129-173	0.48	215-229	0.72
224-272	1.59	227-248	1.73	229-250	0.57
		248-264	0.32	250-269	0.73
				269-230	0.86
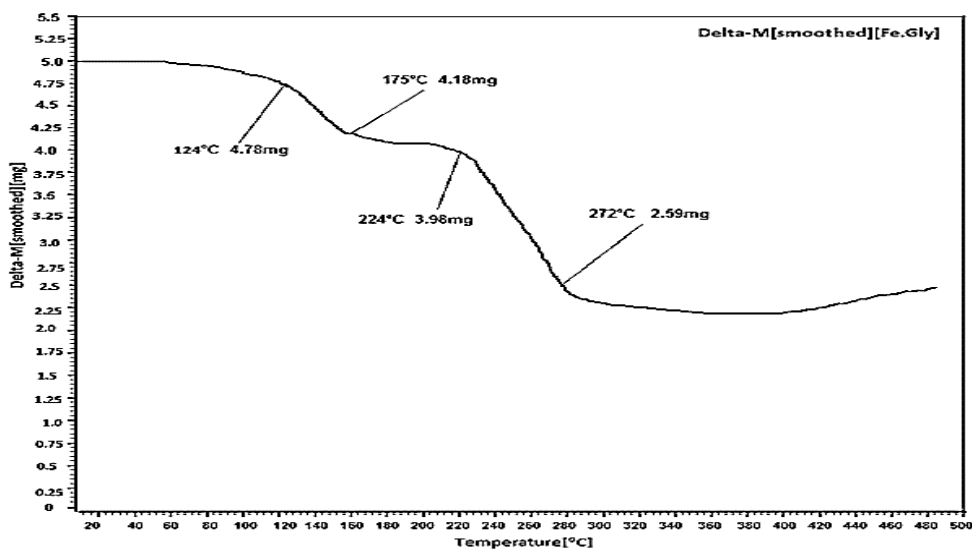
Figure (3.6) Thermal gravimetric curve of Fe.Gly complex
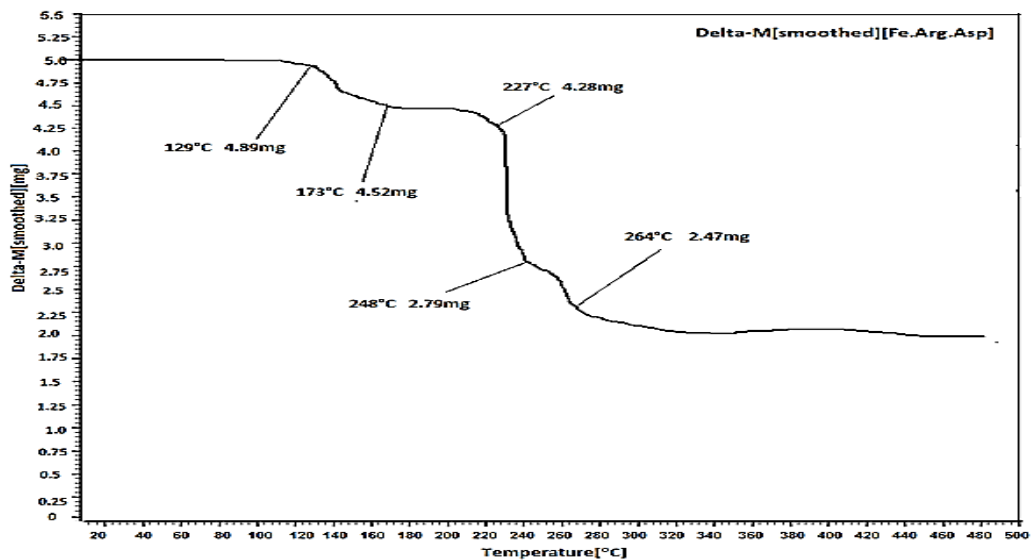
Figure (3.7) Thermal gravimetric curve of Fe(Arg.Asp) complex

141
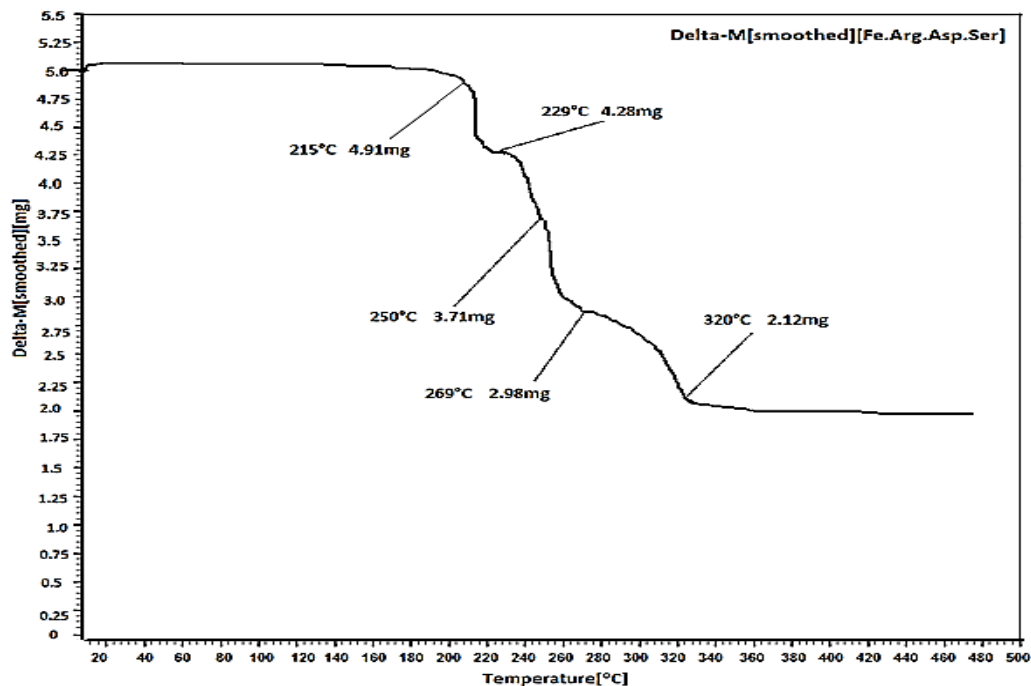
Figure (3.8) Thermal gravimetric curve of Fe(Asp.Arg.Ser) complex

3.4.3 Gold complexes

Au (III) complexes were investigated and recorded weight loss per mg against the temperature. The TGA curves of Au.(Asn.Gly) and Au.(Cys.Ser) complexes: figures (3.9) and (3.10) respectively, showed same characteristic band in little difference in temperature and weight loss. TGA curve for the two complexes displays one stage of mass loss within the temperature range of 200–270 °C, corresponding to the loss of the volatile gases from decomposition of amino acid ligand. According to (REDDY, *et al*, 2005)[287] (Rosu, *et al.,* 2009)[310], such phenomenon was caused in the Au.(Asn.Gly) and Au.(Cys.Ser) TGA complexes. For Au.(Asn.Gly) complex the weight loss of 13.6% was reached at temperature range 210-125°C, Another peak was evident (11.4%) at 245-255^{0}C also, which corresponds to evaporation carbon dioxide CO_2, and ammonium NH_3 gases from decomposition of the amino acid. These results indicated the presence of two peaks in the one stage resulting from mixed amino acid. And the weight of the two complexes has been constant until the temperature reach 500°C. These feature summarized in Table (3.19).

142

Table (3.19) Weight loss per mg against to the temperture per (°C) reading of Au.(Asn.Gly) and Au.(Cys.Ser) complexes:

Au.(Asn.Gly)		Au.(Cys.Ser)	
Temp(°C)	Weight loss(mg)	Temp(°C)	Weight loss(mg)
210-225	0.65	220-242	1.29
245-255	0.57	254-268	0.54
>255	Be constant	>268	Be constant
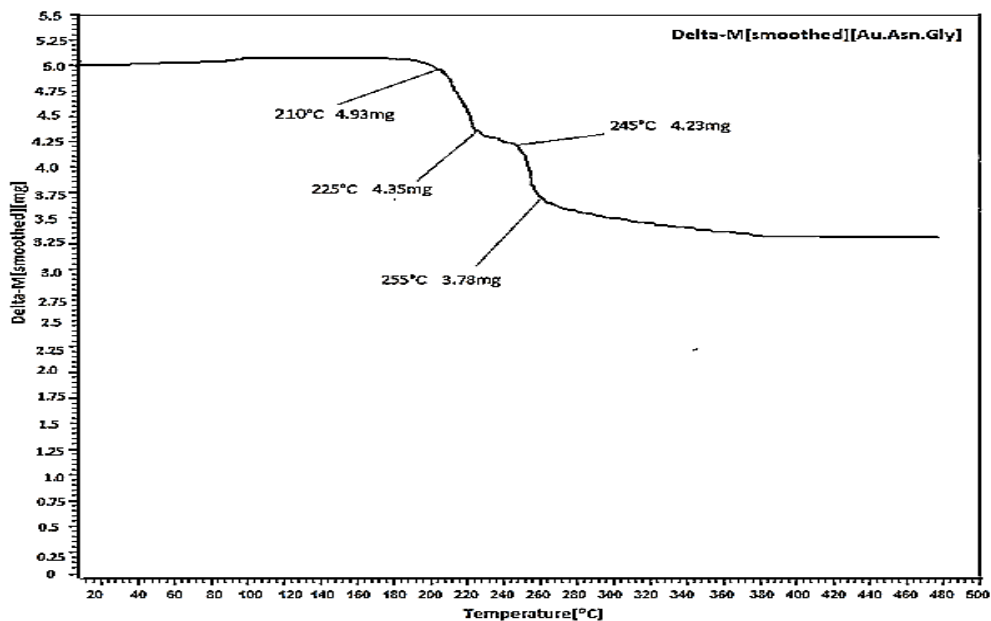
Figure (3.9) Thermal gravimetric curve of Au(Asn.Gly) complex
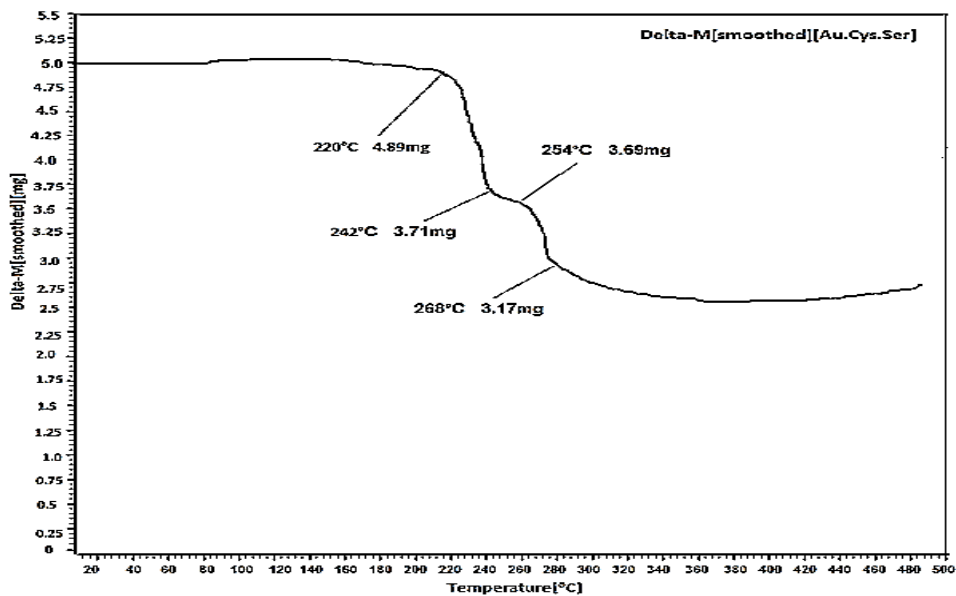
Figure (3.10) Thermal gravimetric curve of Au(Cys.Ser) complex

143

3.4.4 Nickel complexes

Thermal Gravimetric Analysis (TGA) for Ni.Leu, and Ni.(Cys+Leu), complexes Table (3.20), revealed identical characteristic bands and little differences in temperature and weight loss. TGA curve for the two complexes Figures (3.11), and (3.12) displays two stages of mass loss within the temperature range of 100–500 °C. The first stage is at 120–180°C, corresponding to the dehydration of two moles of crystal water and the second stage occurs approximately at 200–500 °C. According to (Rosu, *et al.,* 2009)[310], such phenomenon was caused in the Ni.leu and Ni.cys.leu TGA complexes. 11% weight loss was reached for Ni.leu complex in temperature range 156-188ºC in the first stage, which corresponds to dehydration of the two moles of crystal water. The second stage involved weight loss of 32% in temperature range 268-290 ºC, which corresponds to evaporation of CO_2, and NH_3 gases from the amino acid. Suddenly, the drop in weight associated with temperature range 472^0C was due to melting of Ni.Leu complex.

For Ni.cys.leu complex the weight loss of 11% was reached in the 1st stage at temperature range 119-160ºC corresponding to two moles of crystal water and 27% at 220-248 ºC in the 2nd stage. Another peak was evident (13%) at 280-300^{0}C also, which corresponds to evaporation carbon dioxide CO_2, and ammonium NH_3 gases from the amino acid. These results indicated the presence of two peaks in the second stage resulting from mixed amino acid. And at temperature approximately more than 300^{0}C, the weight will start to decrease in weight.

Table (3.20) Weight loss per mg against to the temperture per (°C) reading of Ni.Leu, and Ni.(Cys+Leu) complexes:

Ni.Leu		Ni.(Cys+Leu)	
Temp(°C)	Weight loss(mg)	Temp(°C)	Weight loss(mg)
156-188	0.55	119-160	0.59
268-290	1.60	220-248	1.36
>472	Melted	248-300	0.67
		>300	Steady decrease
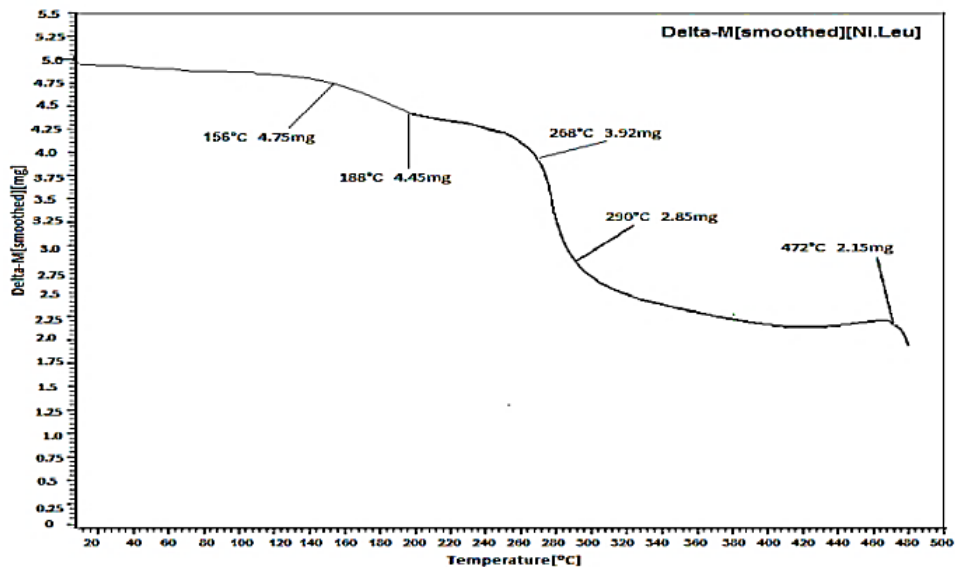
Figure (3.11) Thermal gravimetric curve of Ni.Leu complex
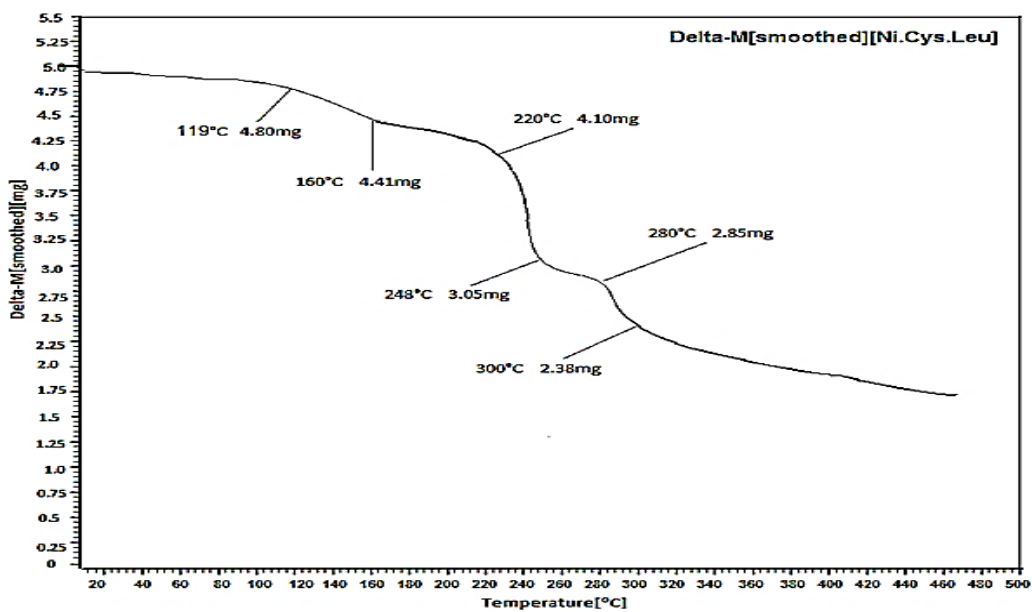
Figure (3.12) Thermal gravimetric curve of Ni(Cys.Leu) complex

3.4.5 Copper and Zinc complexes

Thermal Gravimetric Analysis (TGA) study for Zn.Cys, Zn.(Asn+Leu), and Cu.Gly complexes were investigated and recorded weight loss per mg against the temperature, Figures (3.13), (3.14), and (3.15), respectively, showed same characteristic band in difference in temperature and weight loss. TGA curve for Zn.Cys, and Zn.(Asn+Leu) complexes displays two stages of mass loss within the temperature range of 100–500 °C. The first stage is at 200–280°C, corresponding to the loss of the volatile gases from

145

decomposition of amino acid ligand. The second stage occurs at the temperature more than 280°C for Zinc complexes. According to (Reddy, *et al*, 2005)[287] (Rosu, *et al.,* 2009)[310], such phenomenon was caused in the Au.(Asn.Gly) and Au.(Cys.Ser) TGA complexes. 37% weight loss was reached for Zn.cys complex in temperature range 216-280ºC in the first stage, which corresponds to evaporation of CO_2, and NH_3 gases from the decomposition of the amino acid. The second stage involved an increase in weight by 19% in temperature range 280-341ºC, which corresponds to oxidation occur for Zn ion to form Zinc oxide. And the weight starts to decrease at a higher temperature than 341ºC.

For Zn.(Asn+Leu) complex the weight loss of 26% was reached in the 1st stage at temperature range 196-212ºC. Another peak was evident (29%) at 256-276^{0}C also, which corresponds to evaporation carbon dioxide CO_2, and ammonium NH_3 gases from the decomposition of the amino acid. These results indicated the presence of two peaks in the first stage resulting from mixed amino acid. The second stage involved an increase in weight by 24% in temperature range 298-366ºC, which corresponds to oxidation occur for Zn ion to form Zinc oxide. And the weight starts to decrease at a higher temperature than 366ºC.

TGA curve for Cu.Gly complex Figure (3.15), displays three stages of mass loss within the temperature range of 100–500 °C. The first stage is at 100–116 °C, corresponding to the dehydration of two moles of crystal water. The second stage occurs at around 116–244°C, corresponding to the loss of the volatile gases from decomposition of amino acid ligand. And the third stage occurs at around 244–280°C, which corresponds to oxidation occur for Copper ion to form copper oxide. According to (Reddy, *et al*, 2005)[287], and (Rosu*, et al*, 2009)[310], such phenomenon was caused in the Cu(Gly) TGA complex. 12.4% weight loss in an explosive way for Cu.Gly complex in temperature range 106-116ºC in the first stage, which corresponds to dehydration of the two moles of crystal water. The second stage involved weight loss of 27.6% in temperature range 116-184ºC, which corresponds to evaporation of CO_2, and NH_3 gases from the decomposition of the amino acid. The third stage involved an increase in weight by 20% in temperature range 244-280ºC, which corresponds to oxidation occur for Copper ion to form copper oxide. And the weight of the complex has been constant until the temperature reach 500°C. These feature summarized in Table (3.21).

Table (3.21) Weight loss per mg against to the temperture per (°C) reading of Zn.Cys, and Zn.(Asn+Leu) complexes:

Zn.Cys		Zn.(Asn+Leu)		Cu.Gly	
Temp(°C)	Weight loss(mg)	Temp(°C)	Weight loss(mg)	Temp(°C)	Weight loss(mg)
216-280	1.85	196-212	4.25	106-116	0.62
280-341	Gain 0.95 mg	256-276	3.70	116-184	0.93
>341	Steady decrease	298-366	Gain 1.2 mg	196-244	0.7
		>366	steady decrease	244-280	Gain 1mg
				> 280	Be constant
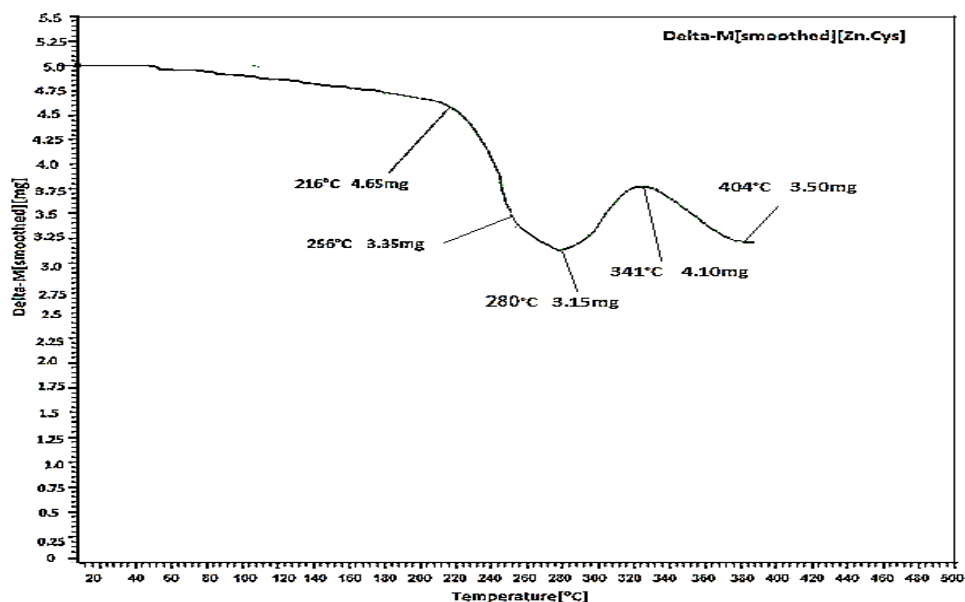
Figure (3.13) Thermal gravimetric curve of Zn.Cys complex
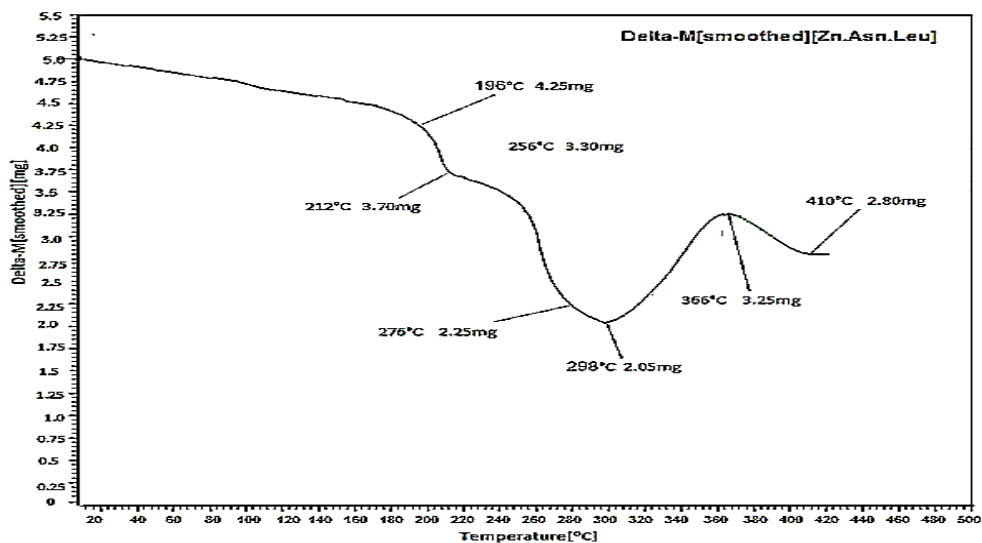
Figure (3.14) Thermal gravimetric curve of Zn(Asn.Leu) complex

147
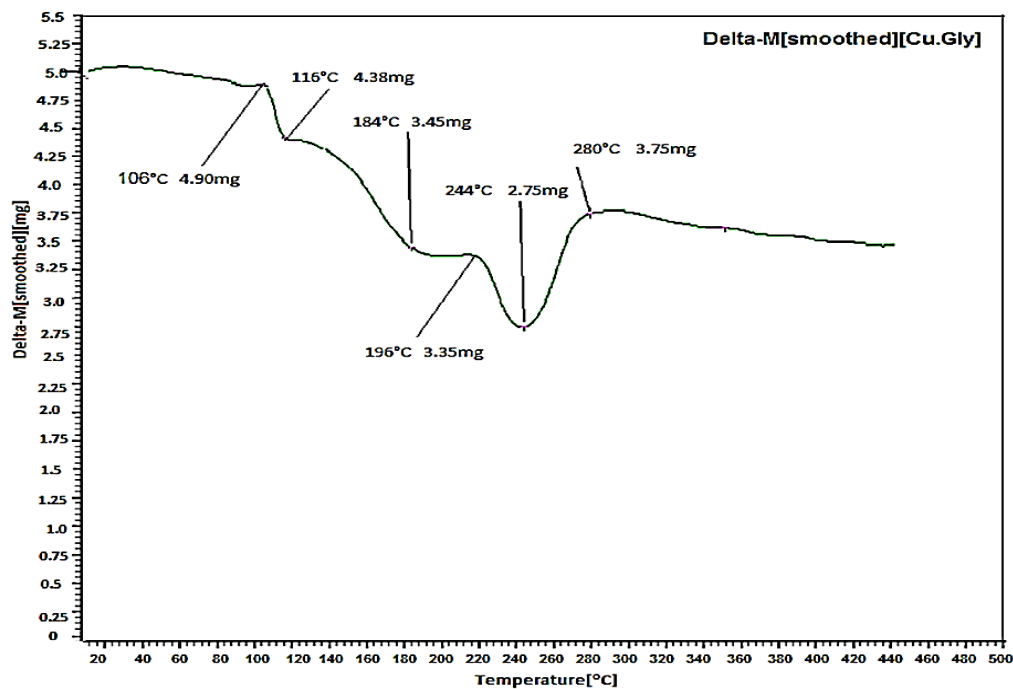
Figure (3.15) Thermal gravimetric curve of Cu.Gly complex

3.5 Infrared spectra

IR spectra were performed using [FT-IR] [ABB-MB 3000] spectrophotometer in the range (4000-400) cm^{-1} spectra were recorded as potassium bromide discs of amino acid complexes, which were showed a difference between the vibrational frequencies V_{as} (Coo-) at 1600 Cm^{-1} and V_s (Coo-) at 1400 Cm^{-1}, generally increase from the theoretical values of free amino acid when the M-O bond strength depending on the carboxylate coordination[406,447].Two very well resolved bands at 1500 cm^{-1} and 1610 cm^{-1} for V_s and V_{as} of bending vibration and broad peak at 3100 cm^{-1} for stretching vibration are an indication of the amino group to the metal ion[448,406]. Infrared spectra of the complexes were also measured in the region 400-700 cm^{-1} in order to identify frequencies related to M-O and M-N bands. The M-O frequencies were identified at rang (600–800) cm^{-1}. While M-N frequencies were identified at rang (400 – 600) cm^{-1}. These results are in agreement with literature value, being similar to other metal complexes with amino acid[449,406]. The v (O-H) stretching vibration do appear in the complexes at range (3450 – 3750) cm^{-1} suggesting the presence of the crystal and coordinated water. Table (3.22) describes the infrared spectra of the amino acid complexes.

3.5.1 Cobalt complexes

Co.Gly, Co.Ser, Co.Arg and Co.Asp complex spectra Figures (3.16), (3.17), (3.18), and (3.19) exhibit same characteristic band with difference in frequencies, the observed frequencies of the v_{asy} (COO⁻) were at (1647.28, 1604.84, 1631.85, and 1616.42) cm⁻¹, respectively, the v_{sy} (COO⁻) at (1415.81, 1400.38, 1485.09, and 1460.05) cm⁻¹, respectively. The absence of the uncoordinated vCOOH (1730-1775 cm⁻¹) in the IR spectra of Co^{2+} complexes indicates a clue for the coordination of the ligands to metal ions through the carboxylate anions[406]. The bands assigned due to the vCo-N at (443.85, 528.52, 451.36, and 430.65) cm⁻¹, respectively. The participation of the lone pairs of electrons on the N of the amino group in the ligand to the metals is supported by this band frequency observed the chelation of the Co^{2+} by the amino and carboxylate groups, The N-H stretching frequency at around (3271.41, 3430, 3568.46, and 3418.01) cm⁻¹, respectively, reduced on coordination, attributable to the reduction in bond order on coordination. vOH stretching bands at around (3564.6, 3465.02, 3637.90, and 3640.00) cm⁻¹ respectively, which eventually indicate the presence of crystal water molecule. and vN-H bending bands at around v_{sy} 1554.4, 1477.54, 1562.02, and 1510.02 cm⁻¹, respectively, and absent of the peak of v_{asy}.

3.5.2 Gold complexes

Au.(Asn.Gly), and Au.(Cys.Ser) complexes spectra Figures (3.20), and (3.21) exhibit same characteristic band with difference in frequencies, the observed frequencies of the v_{asy} (COO⁻) were at (1637.45, and 1627.81) cm⁻¹, respectively, the v_{sy} (COO⁻) at 1408.01 cm⁻¹, for Au.(Asn.Gly) complex and interference peak occur for Au.(Cys.Ser) complex. The absence of the uncoordinated vCOOH (1730-1775 cm⁻¹) in the IR spectra of Au^{3+} complexes indicates a clue for the coordination of the ligands to metal ions through the carboxylate anions. The two bands assigned due to the vAu-N, indicates a clue for the nitrogen involved in difference environment, which are at (540.03& 615.25 and 449.3 & 499.53) cm⁻¹, respectively. The participation of the lone pairs of electrons on the N of the amino group in the ligand to the metals is supported by this band frequency observed the chelation of the Au^{3+} by the amino and carboxylate groups, The N-H stretching frequency at around (3413.77, and 3415.70) cm⁻¹, respectively, reduced on coordination, attributable to the reduction in bond order on coordination. No bands appeared at more than 3400 cm⁻¹ for vOH stretching vibration, indicates there is no crystal water involved in Au^{3+} complexes, and vN-H bending bands at around v_{asy} (1588.02 and 1588.09) cm⁻¹, respectively, and v_{sy} at around (1460.01 and 1382.87) Cm⁻¹ respectively.

3.5.3 Iron complexes

For Fe.Gly, Fe.(Arg.Asp), Fe.(Arg.Asp.Ser) complexes, The IR- spectra Figures (3.22), and (3.23) and (3.24), exhibit same characteristic band with difference in frequencies, the observed frequencies of the v_{asy} (COO$^-$) were at (1631.67, 1645.17, and 1643.24) cm^{-1}, respectively, the v_{sy} (COO$^-$) at (1386.30, 1398.30, and 1425.30) cm^{-1}, respectively, are fairly in good agreement with the literature. The absence of the uncoordinated vCOOH (1730-1775 cm^{-1}) in the IR spectra of Fe^{3+} complexes indicates a clue for the coordination of the ligands to metal ions through the carboxylate anions. The bands assigned due to the vFe-N at (428.17, 441.67, and 418.52) cm^{-1}, respectively, also fairly resemble to the literature. The participation of the lone pairs of electrons on the N of the amino group in the ligand to the metals is supported by this band frequency observed the chelation of the Fe^{3+} by the amino and carboxylate groups, The N-H stretching frequency at around (3417.63, and 3419.56, and 3417.63) cm^{-1}, respectively, reduced on coordination, attributable to the reduction in bond order on coordination. vOH stretching bands of Fe.Gly, and Fe.(Arg.Asp) at around (3730.07, and 3743.57) cm^{-1} respectively, which eventually indicate the presence of crystal water molecule, and there is no band in this area for Fe.(Arg.Asp.Ser). That deal with no crystal water involved. and vN-H bending bands at around v_{asy} (1533.30, 1514.02, and 1626.90) cm^{-1}, respectively, and v_{sy} at around (1466.50, 1427.23, and 1512.09) Cm^{-1} respectively.

3.5.4 Copper complex

Cu.Gly spectra Figure (3.25), the observed frequencies of the v_{asy} (COO$^-$) was at 1682.00 cm^{-1}, the v_{sy} (COO$^-$) at 1303.94 cm^{-1}. The absence of the uncoordinated vCOOH (1730-1775 cm^{-1}) in the IR spectra of Cu^{2+} complexes indicates a clue for the coordination of the ligands to metal ions through the carboxylate anions. The bands assigned due to the vCu-N at 445.90 cm^{-1}. The participation of the lone pairs of electrons on the N of the amino group in the ligand to the metals is supported by this band frequency observed the chelation of the Cu^{2+} by the amino and carboxylate groups, The N-H stretching frequency at around 3409.81cm^{-1}, reduced on coordination, attributable to the reduction in bond order on coordination. vOH stretching band at around 3607.04cm^{-1}, which eventually indicate the presence of crystal water molecule, and vN-H bending band at around v_{asy} 1583.10 cm^{-1}, and v_{sy} at around 1554.69 Cm^{-1}.

3.5.5 Nickel complexes

The infrared spectra of the Ni.leu and Ni.cys.leu complexes, Figures (3.26), and (3.27) exhibit the observed frequencies v_{asy} (COO-) was at (1668.31, and 1668.31) cm^{-1}, respectively, and the v_{sy} (COO$^-$) at

(1359.72, and 1400.22) cm^{-1}, respectively, are fairly in good agreement with the literature. The absence of the uncoordinated vCOOH (1730-1775 cm^{-1}) in the IR spectra indicates a clue for the coordination of the ligands to metal ions through the carboxylate anions. The bands assigned due to the vNi-N at (447.45, and 443.60) cm^{-1}, respectively. The participation of the lone pairs of electrons on the N of the amino group in the ligand to the metals is supported by this band frequency observed the chelation of the Ni^{2+} by the amino and carboxylate groups, The N-H stretching frequency at around (3444.8, and 3427.27) cm^{-1}, respectively, reduced on coordination, attributable to the reduction in bond order on coordination. vOH stretching bands at around (3637.50, and 3639.43) cm^{-1}, respectively, which eventually indicate the presence of lattice water molecule. And vN-H bending bands at around v$_{asy}$ (1595.09, and 1596.95) cm^{-1} and v$_{sy}$ at around (1382.87, and 1504.37) cm^{-1}, respectively.

3.5.6 Zinc complexes

And the Zn.Cys, and Zn.(Asn.Leu) complexes spectra Figures (3.28), and (3.29) exhibit same characteristic band with difference in frequencies, the observed frequencies of the v$_{asy}$ (COO^{-}) were at (1681.90, and 1670.24) cm^{-1}, respectively, the v$_{sy}$ (COO^{-}) at (1404.08, and 1402.15) cm^{-1}, respectively, The absence of the uncoordinated vCOOH (1730-1775 cm^{-1}) in the IR spectra of Au^{3+} complexes indicates a clue for the coordination of the ligands to metal ions through the carboxylate anions. The two bands assigned due to the vZn-N, indicates a clue for the nitrogen involved in difference environment, which are at (449.38 and 498.6) cm^{-1}, respectively. The participation of the lone pairs of electrons on the N of the amino group in the ligand to the metals is supported by this band frequency observed the chelation of the Zn^{2+} by the amino and carboxylate groups, The N-H stretching frequency at around (3417.63, and 3415.70) cm^{-1}, respectively, reduced on coordination, attributable to the reduction in bond order on coordination. No bands appeared at more than 3400 cm^{-1} for vOH stretching vibration, indicates there is no crystal water involved in Au^{3+} complexes, and vN-H bending bands at around v$_{asy}$ (1598.88 and 1602.74) cm^{-1}, respectively, and v$_{sy}$ at around (1490.87 and 1490.87) Cm^{-1} respectively.

These general feature were investigated in all amino acid complexes, and were agreed with the result of IR-Spectra of the studies of Hamdi, and Mustafa, 2013[273], Reddy, *et al,* 2005[287], Alam, *et al,* 2009[289], Stanila, *et al,* 2011[299], Rosu, *et al,* 2009[310], Patil, *et al,* 2012[319], Al-Jeboori, and Al-shimiesawi, 2012[347], Tripathi *et al,* 2015[350], Qadir, *et al,* 2014[362], Hübner1, 2011[364], Aiyelabola, *et al.,* 2012[379], Rusu, *et al.,* 2009[389], and Islam, *et al.,* 2018[406].

Table (3.22) Important peaks appeared in the IR-Spectra of amino acid ligands and fourteen complexes

Compound	COO-		NH3+			M-O	M-N	O-H
	V_{asy}	V_{sy}	$Str_{(broad)}$	$Bend_{asy}$	$Bend_{sy}$			
Co.Gly	1647.28	1415.81	3271.41	-	1554.4	610	443.85	3564.6
Co.Ser	1604.84	1400.38	3430.00	-	1477.54	624.96	528.52	3465.02
Co.Arg	1631.85	1485.09	3568.46	-	1562.02	621.11	451.36	3637.90
Co.Asp	1616.42	1460.05	3418.01	-	1510.02	547.81	430.65	3640.00
Au.Asn.Gly	1637.45	1408.01	3413.77	1588.02	1460.01	669.25& 723.26	540.03 & 615.25	-
Au.Cys.Ser	1627.81	Over lab	3415.70	1588.09	1382.87	588.32& 625.09	449.3 & 499.53	-
Fe.Gly	1631.67	1386.30	3417.63	1533.30	1466.50	673.11	428.17	3730.07
Fe.Arg.Asp	1645.17	1398.30	3419.56	1514.02	1427.23	516.89	441.67	3743.57
Fe.Arg.Asp.Ser	1643.24	1425.30	3417.63	1626.90	1512.09	572.82	418.52	3741.65
Cu.Gly	1682.00	1303.94	3409.81	1583.10	1554.69	678.90	445.90	3607.04
Ni.Leu	1668.31	1359.72	3444.83	1595.09	1382.87	682.75	447.45	3637.50
Ni.Cys.Leu	1668.31	1400.22	3427.27	1596.95	1504.37	516.89	443.60	3639.43
Zn.Cys	1681.90	1404.08	3417.63	1598.88	1490.87	669.25	449.38	-
Zn.(Asn+Leu)	1670.24	1402.15	3415.70	1602.74	1490.87	682.30	498.6	-
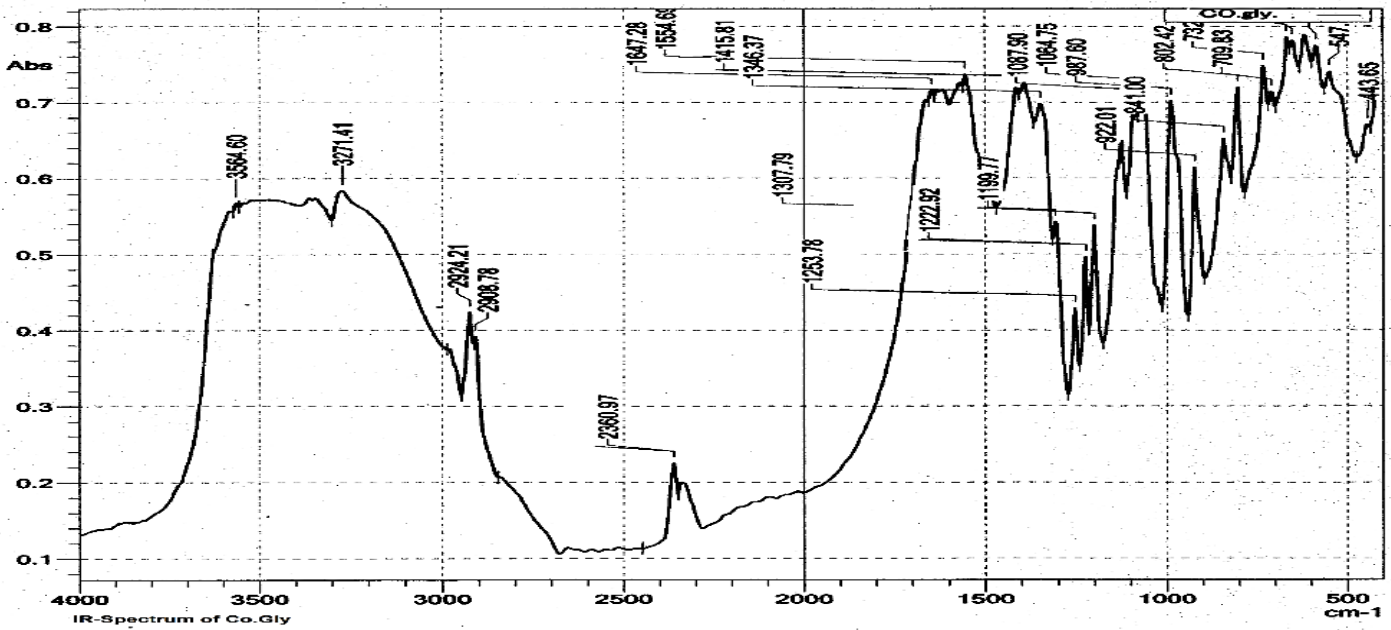
Figure (3.16) IR spectrum of Co.Gly complex

Figure (3.17) IR spectrum of Co.Ser complex

153
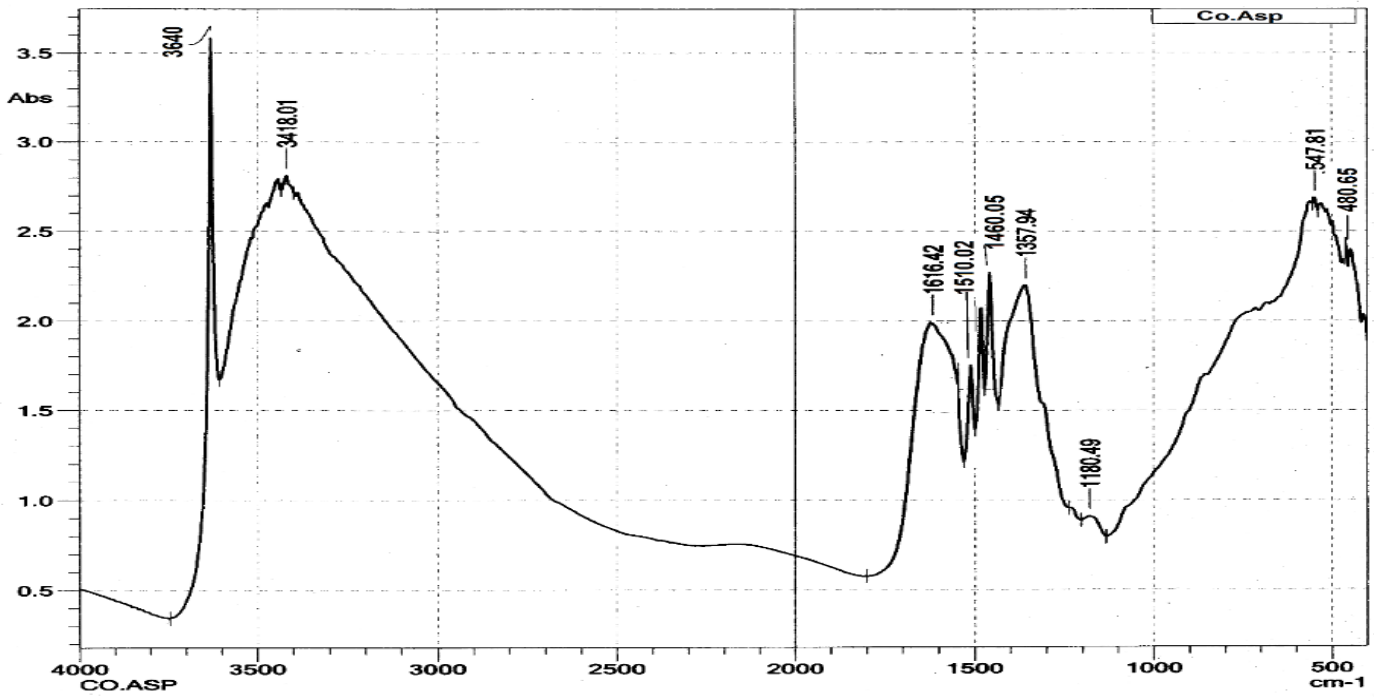
Figure (3.18) IR spectrum of Co.Asp compleX
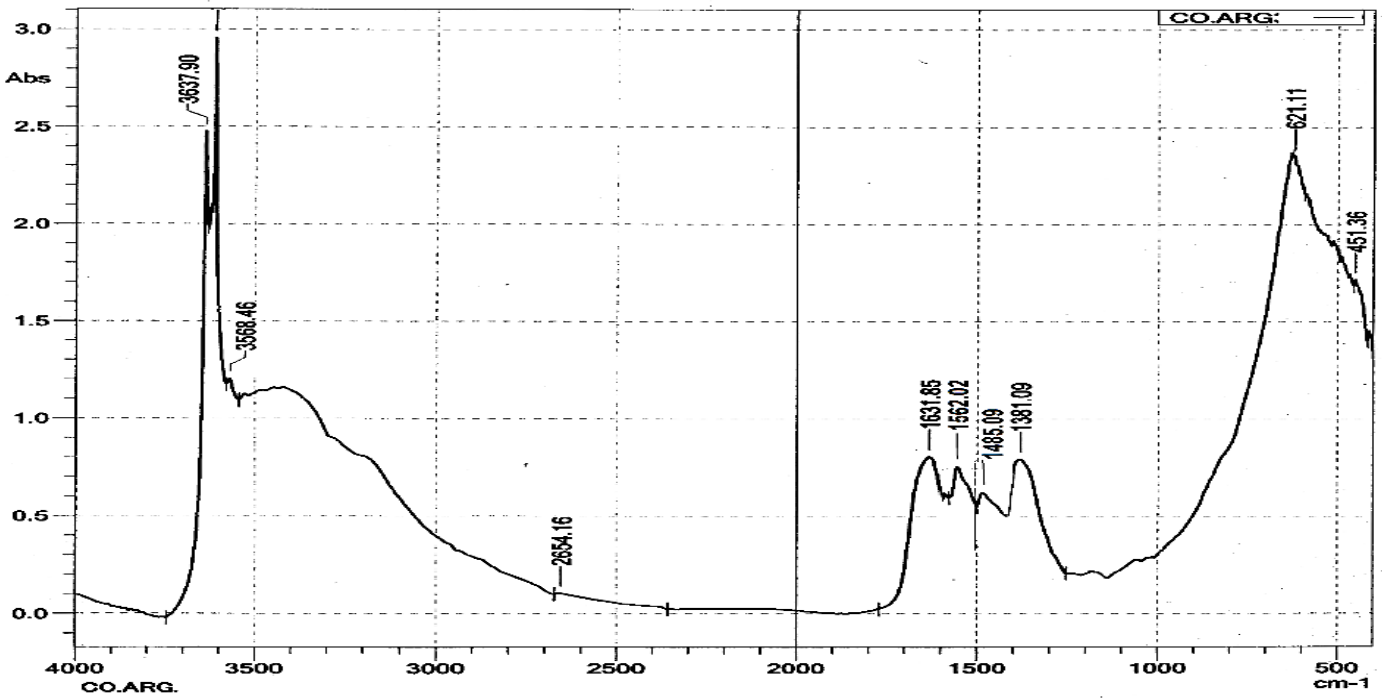
Figure (3.19) IR spectrum of Co.Arg complex

154
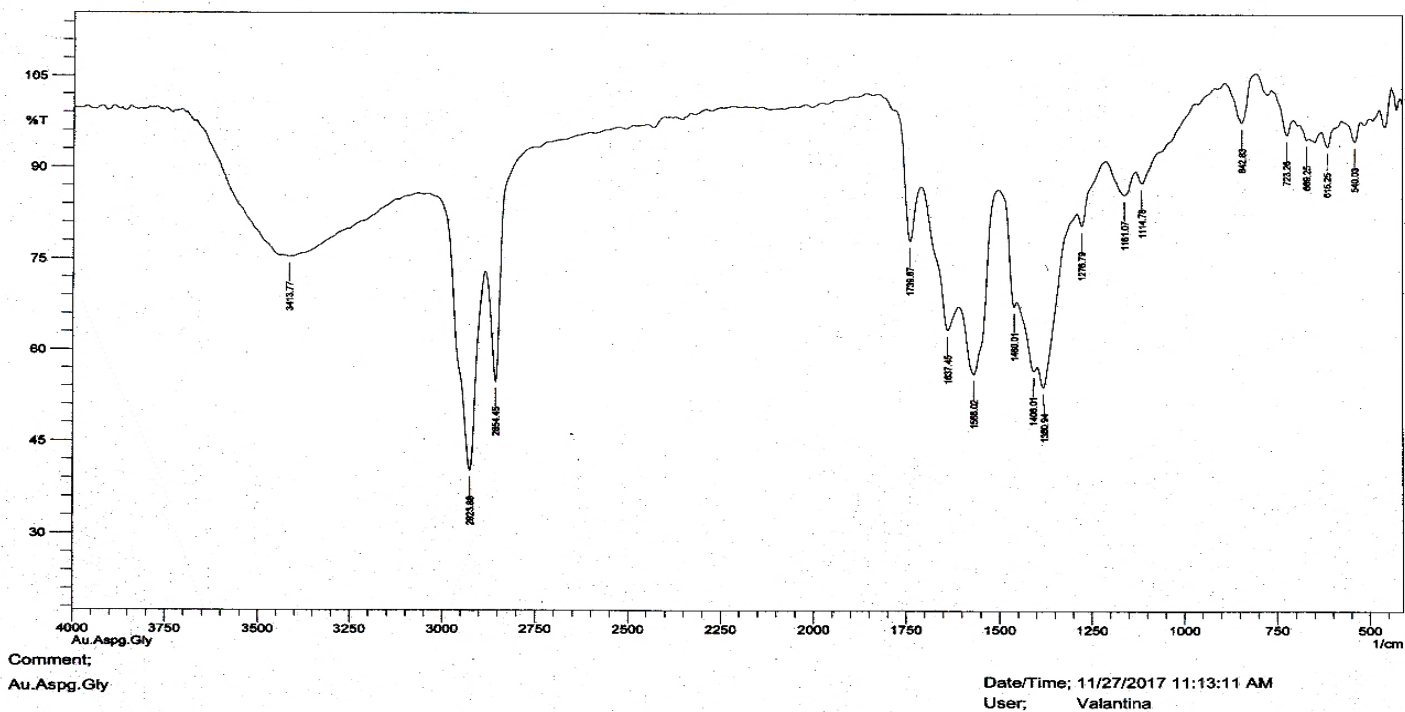
Figure (3.20) IR spectrum of Au.Asn.Gly complex
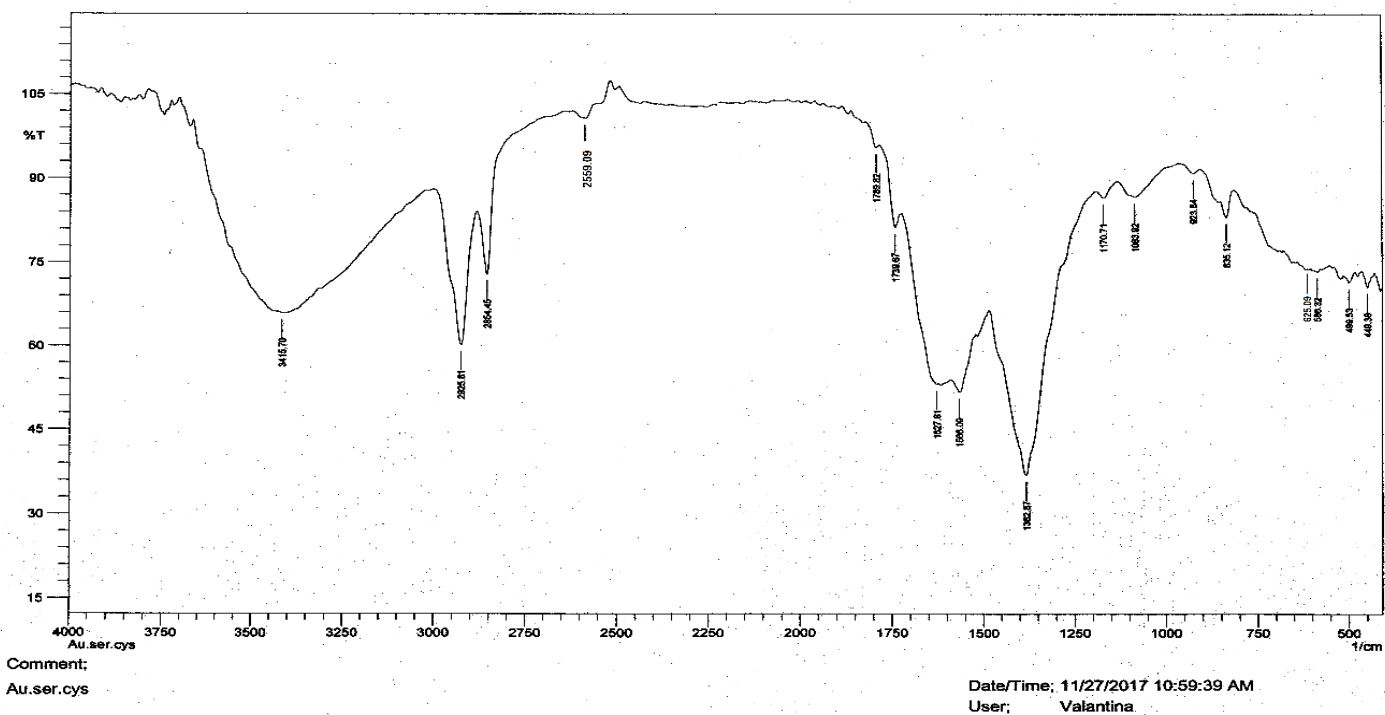
Figure (3.21) IR spectrum of Au.Cys.Ser complex

155
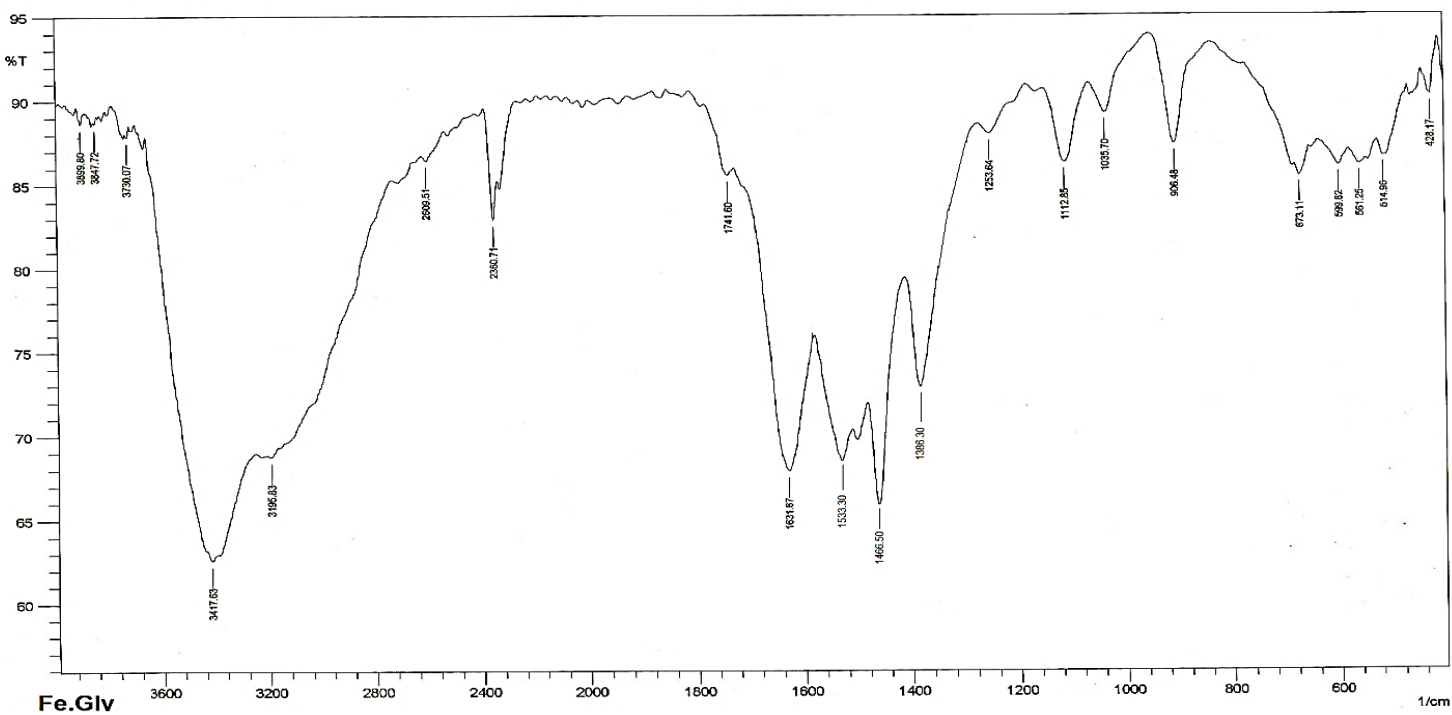
Figure (3.22) IR spectra of Fe.Gly complex
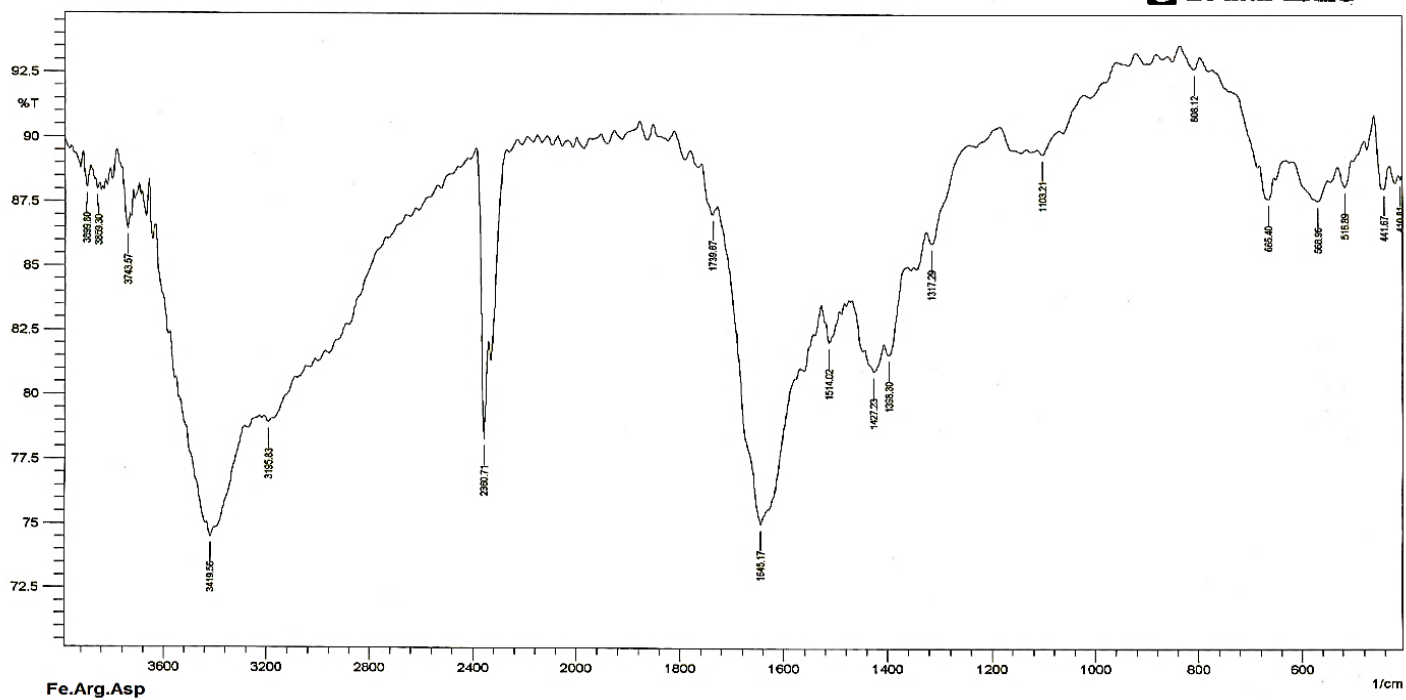
Figure (3.23) IR spectra of Fe.Arg.Asp complex

156
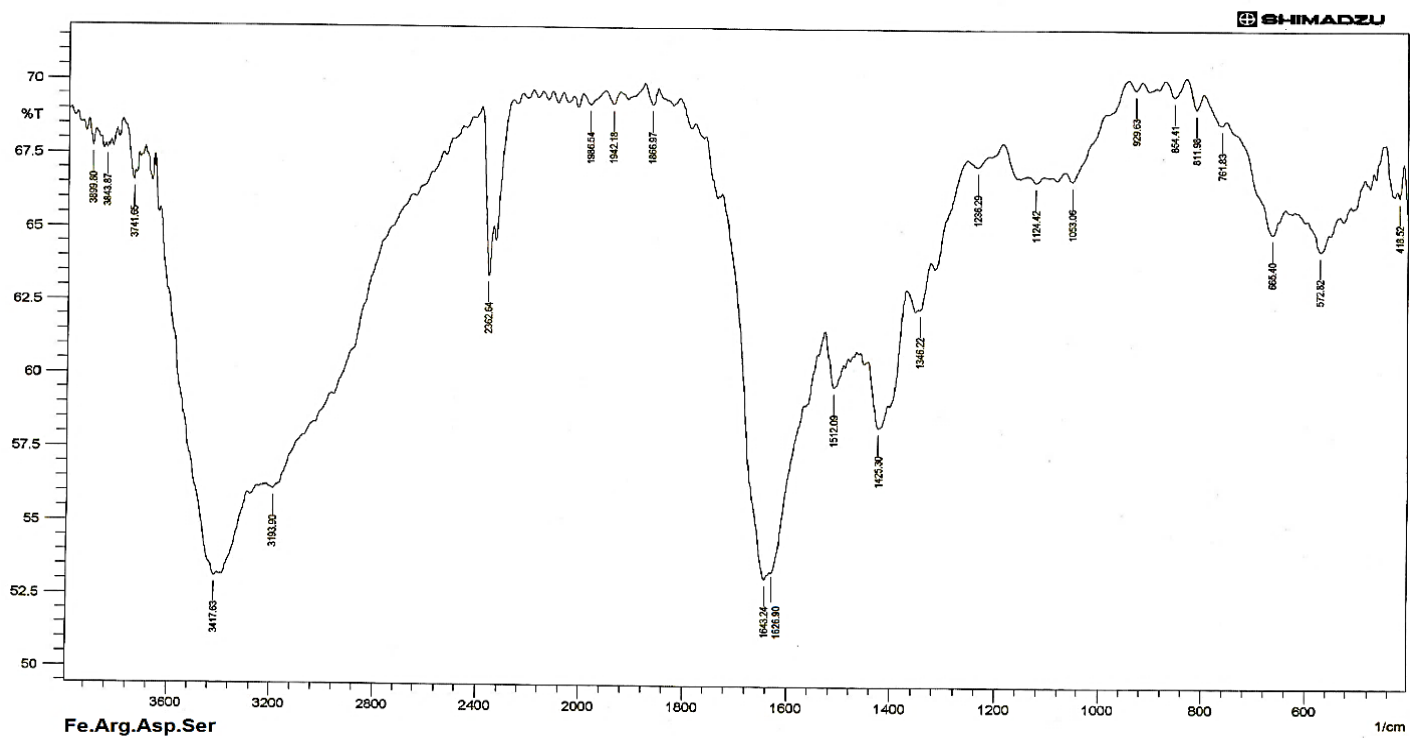
Figure (3.24) IR spectra of Fe.Arg.Asp.Ser complex
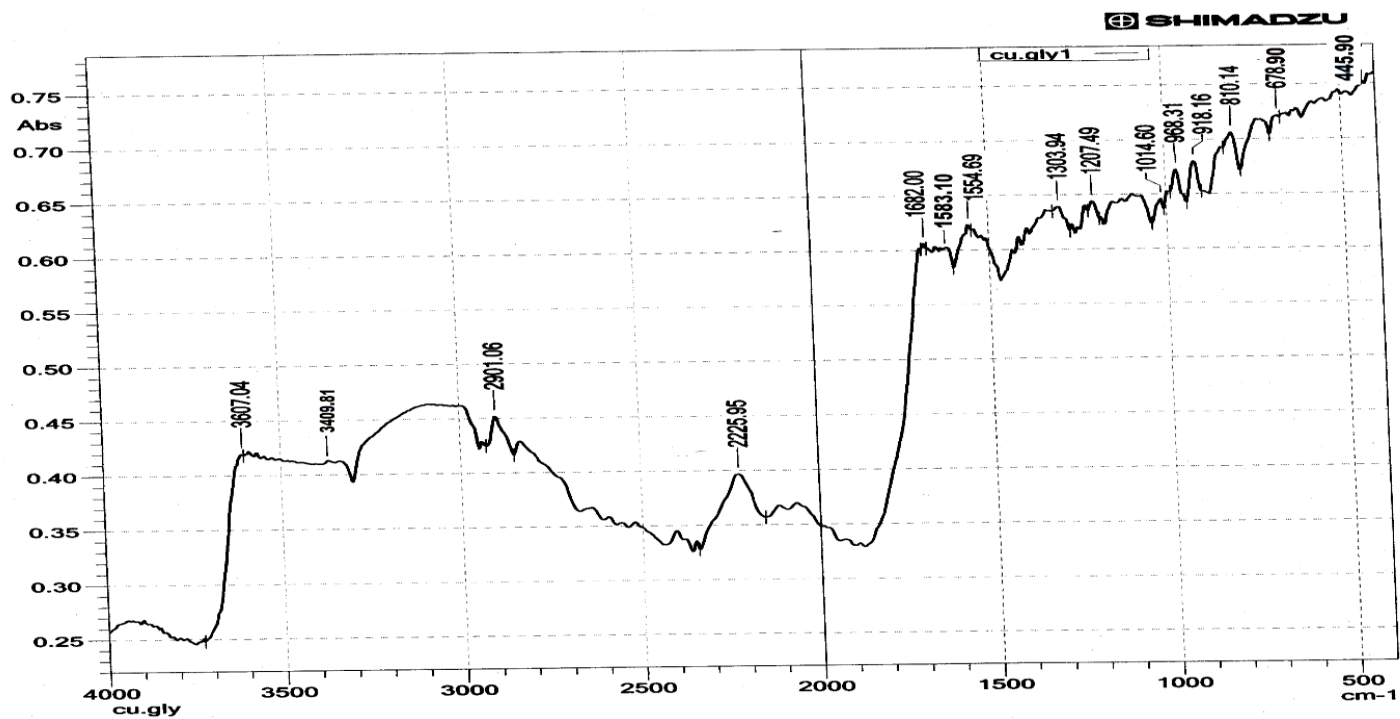
Figure (3.25) IR spectra of Cu.gly complex

157
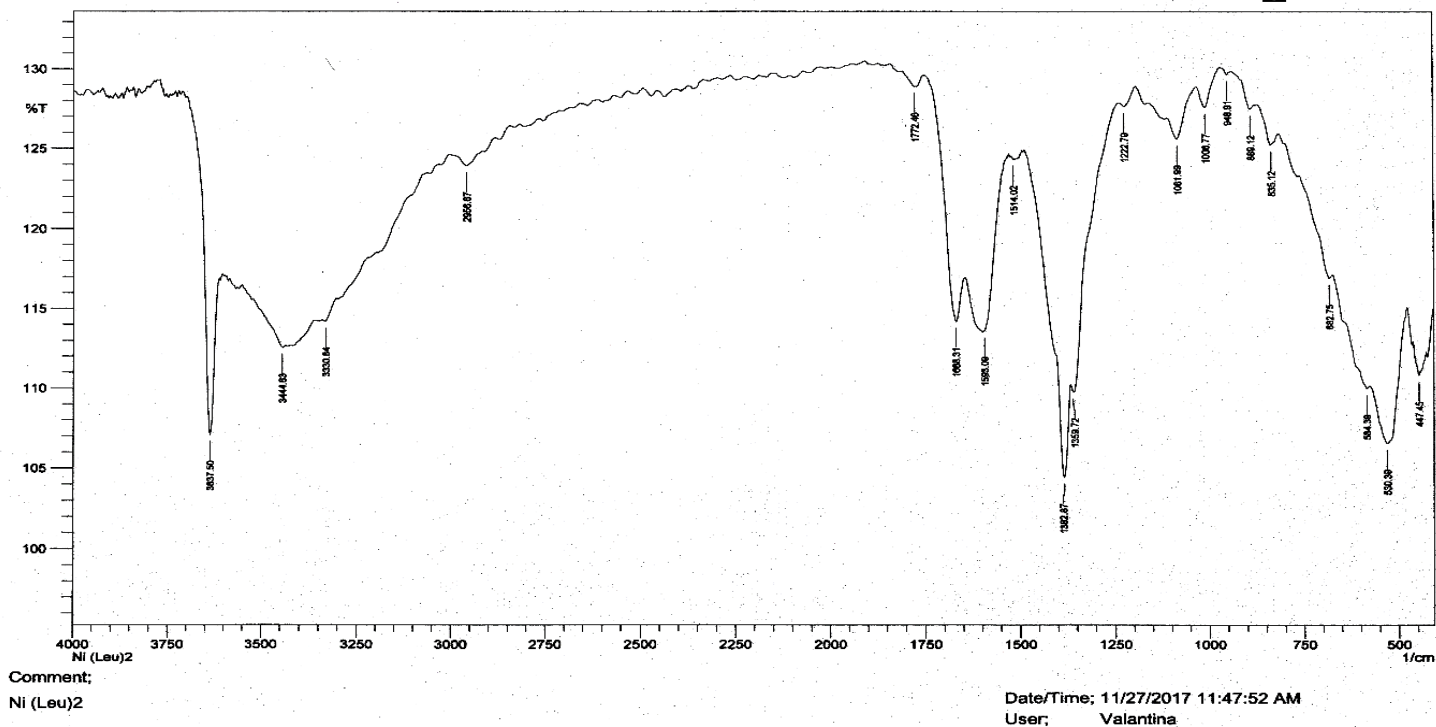
Figure (3.26) IR spectra of Ni.Leu complex
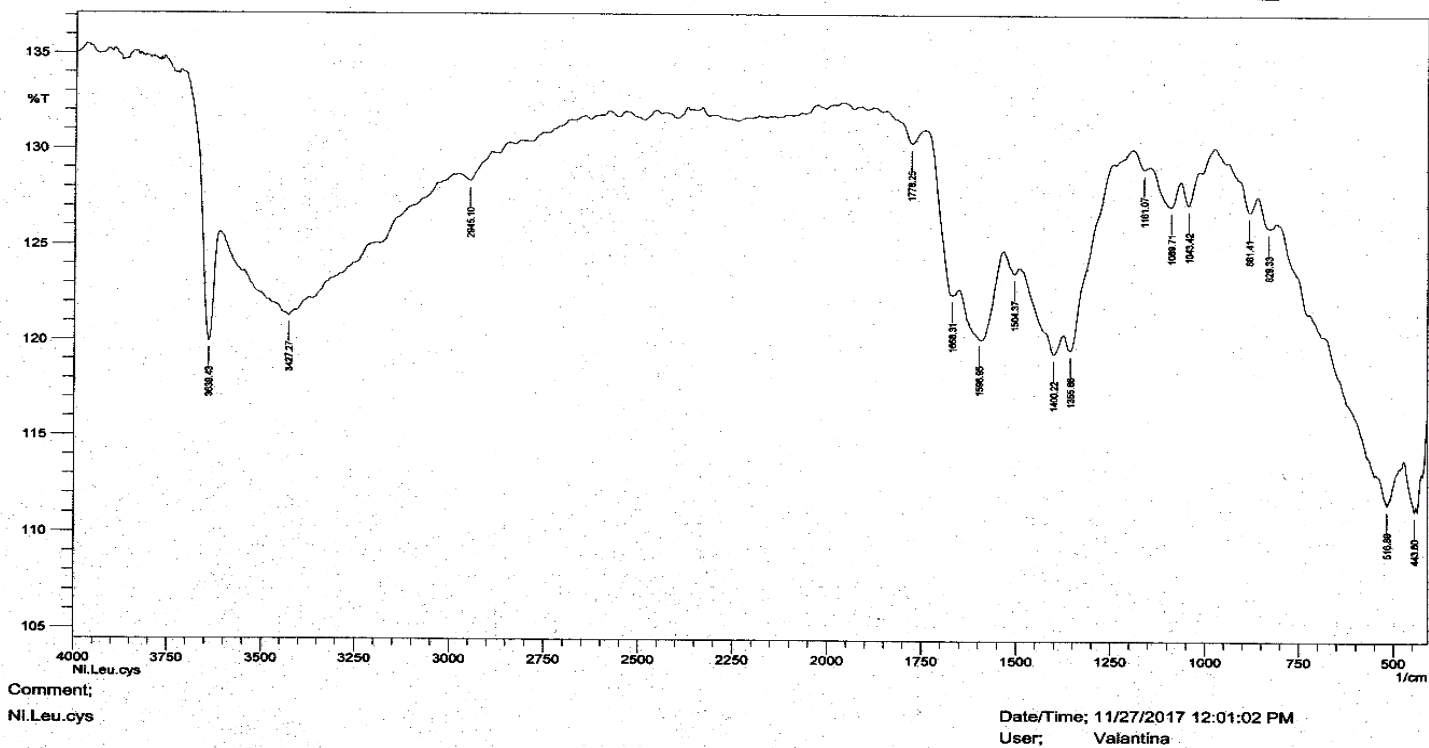
Figure (3.27) IR spectra of Ni.Cys.Leu comple

158
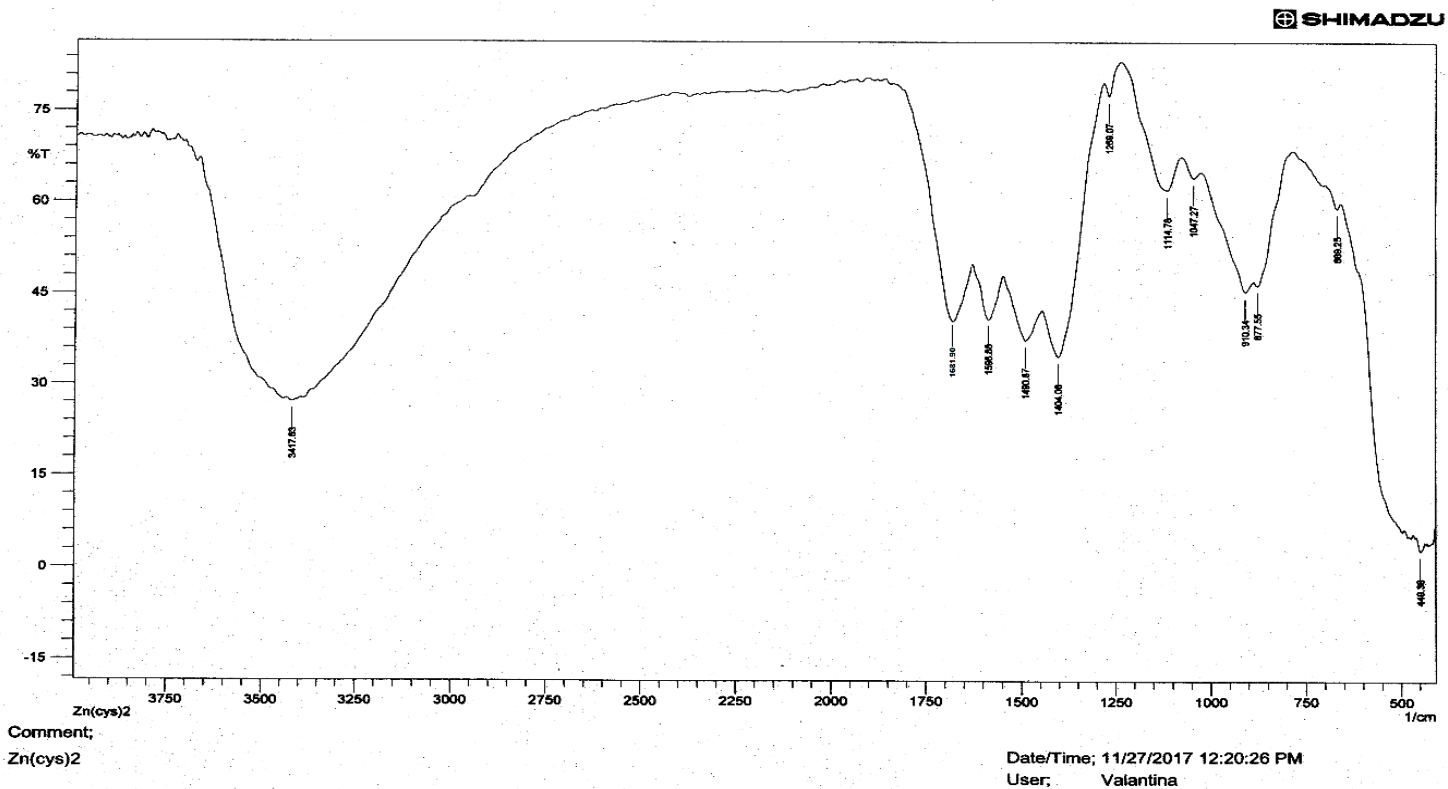
Figure (3.28) IR spectra of Zn.Cys complex
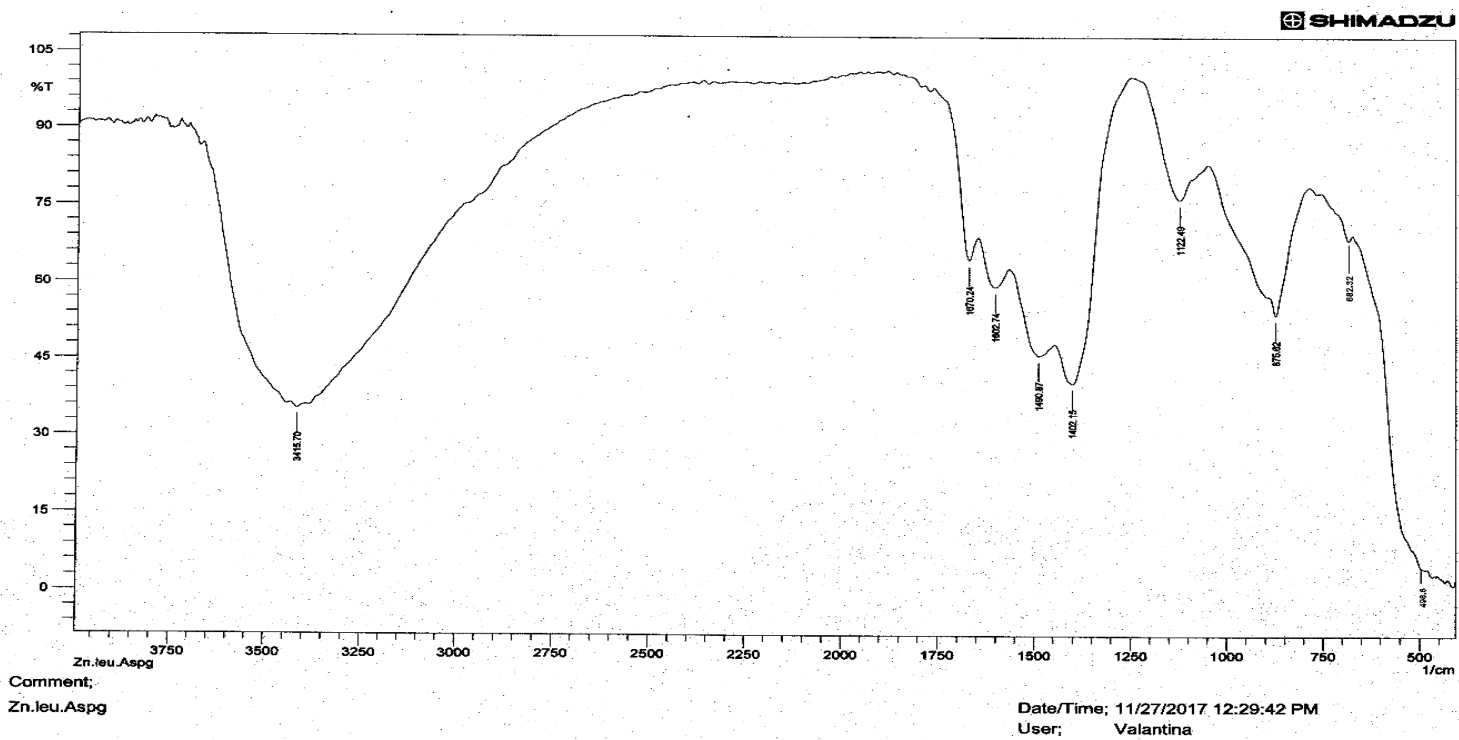
Figure (3.29) IR spectra of Zn.Asn.Leu complex

159

3.6 UV/Vis spectra study

3.6.1 Cobalt complexes

The features of the electronic spectra of the cobalt (II) complexes are very similar to each other. The electronic structures of cobalt (II) complexes with different ligands have been presented in the literature[450,451]. Based on the simplest model, three spin-allowed crystal field bands are expected. $^4A_2(F)$ → $^4T_2(F)$, $^4A_2(F)$ → $^4T_1(F)$, $^4A_2(F)$ → $^4T_1(P)$. And some absorption bands are observed. That attributed to charge transfer from the non-bonding orbitals of the oxygen atoms in the ligand to the cobalt (II) d orbitals. The last absorption bands are assigned to the $\pi \to \pi^*$ and n $\to \pi^*$ transitions of the ligand [452,453]. Table (3.23) the assignment of the characteristic wave lengths of the electronic transition of Co.Gly complex spectra figure (3.30) showed three transition bands at 246.00, 240.80, and 235.00 nm for $^4A_2(F)$ → $^4T_2(F)$, $^4A_2(F)$ → $^4T_1(F)$, $^4A_2(F)$ → $^4T_1(P)$, the charge transfer band is at 228.00 nm, and four bands at 218.80, 216.20, 213.80, and 202.80 due to $\pi \to \pi^*$ and n $\to \pi^*$ transitions of the glycine ligand. The Co.Ser complex spectra figure (3.31) showed three bands at 252.40, 245.80, and 240.40 nm for $^4A_2(F)$ → $^4T_2(F)$, $^4A_2(F)$ → $^4T_1(F)$, $^4A_2(F)$ → $^4T_1(P)$, the charge transfer band at 235.20 nm, and six bands at 232.80, 228.00, 218.80, 216.00, 211.20, and 205.00 due to $\pi \to \pi^*$ and n $\to \pi^*$ transitions of the serine ligand, That illustrated in Table (3.24). Co.Asp complex spectra Figure (3.32) showed three bands at 264.60, 260.80, and 256.00 nm for $^4A_2(F)$ → $^4T_2(F)$, $^4A_2(F)$ → $^4T_1(F)$, $^4A_2(F)$ → $^4T_1(P)$, the charge transfer band at 254.20 nm, and nine bands at 252.20, 245.40, 241.60, 234.80, 227.80, 218.80, 216.00, 210.80, and 204.60 due to $\pi \to \pi^*$ and n $\to \pi^*$ transitions of the aspartate ligand, that illustrated in Table (3.25). In addition Table (3.26) assignment of the characteristic wave lengths of the electronic transition of Co.Arg complex spectra Figure (3.33) showed three bands at 240.40, 234.80, and 228.00 nm for $^4A_2(F)$ → $^4T_2(F)$, $^4A_2(F)$ → $^4T_1(F)$, $^4A_2(F)$ → $^4T_1(P)$, the charge transfer band at 219.80 nm, and three bands at 213.80, 211.20, and 201.00 due to $\pi \to \pi^*$ and n $\to \pi^*$ transitions of the arginine ligand. The results of the electronic spectra of the cobalt (II) complexes were achieved in this research were agreed with the studies of Reddy, *et al*, 2005[287], Stanila, *et al*, 2011[299], Rosu, *et al,* 2009[310], Boruah 2012[313], Patil, *et al,* 2012[319], Al-Jeboori and Al-shimiesawi, 2012[347], Qadir, *et al,* 2014[362], Aiyelabola, *et a.l,* 2012[379], and Rusu, *et al.,* 2009[389].

Table (3.23) Electronic transitions occur in Co.Gly complex:

No	Wavelength	Abs
25	246.00	2.839
26	240.80	2.960
27	235.00	2.332
28	228.00	2.829
29	218.80	3.051
30	216.20	2.926
31	213.80	1.588
33	202.80	2.487

Table (3.24) Electronic transitions occur in Co.Ser complex:

No	Wavelength	Abs
23	252.40	0.376
24	245.80	0.781
25	240.40	1.909
26	235.20	2.871
27	232.80	1.038
28	228.00	2.855
29	218.80	2.675
30	216.00	2.888
31	211.20	2.725
32	205.00	2.963

Table (3.25) Electronic transitions occur in Co.Asp complex:

No	Wavelength	Abs
18	264.60	0.258
19	260.80	0.864
20	256.00	0.959
21	254.20	1.792
22	252.20	1.632
23	245.40	1.760
24	241.60	1.833
25	234.80	1.086
26	227.80	1.449
27	218.80	2.678
28	216.00	2.562
29	210.80	2.637
30	204.60	2.070

Table (3.26) Electronic transitions occur in Co.Arg complex:

| No	Wavelength	Abs
16	240.40	0.937
17	234.80	0.135
18	228.00	0.425
19	219.80	1.334
20	213.80	1.653
21	211.20	2.851
22	201.00	1.358

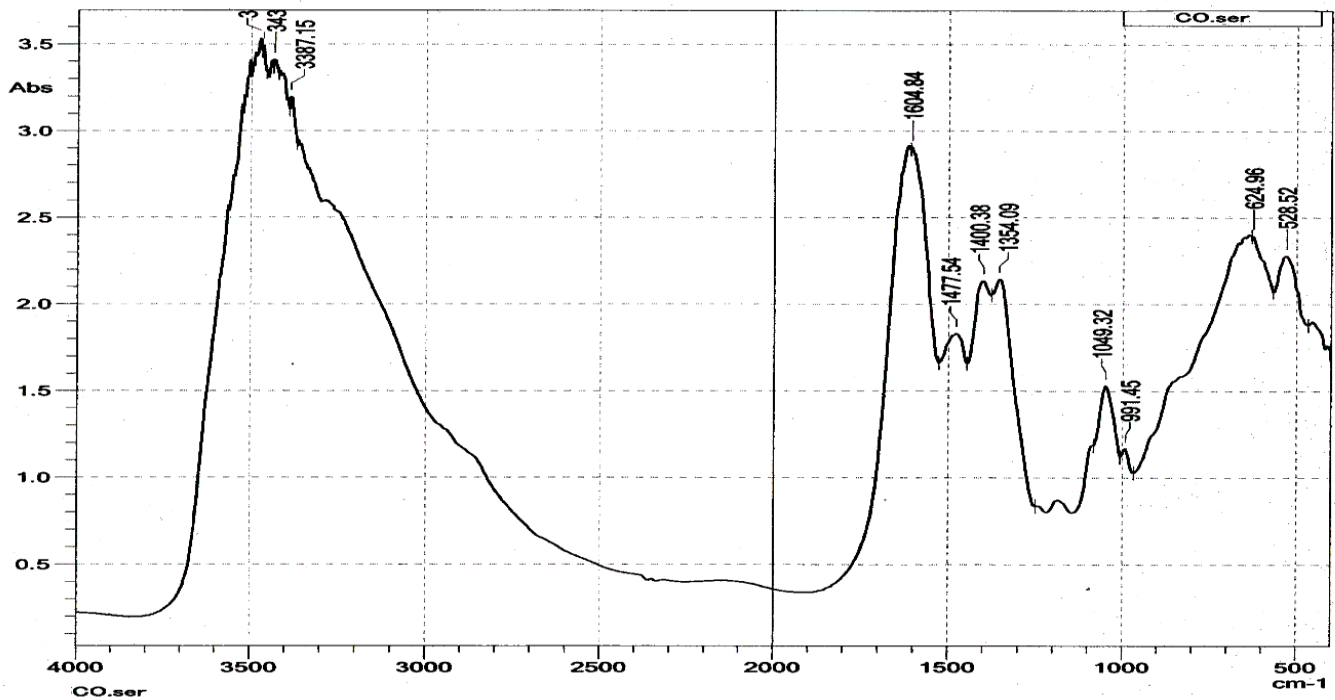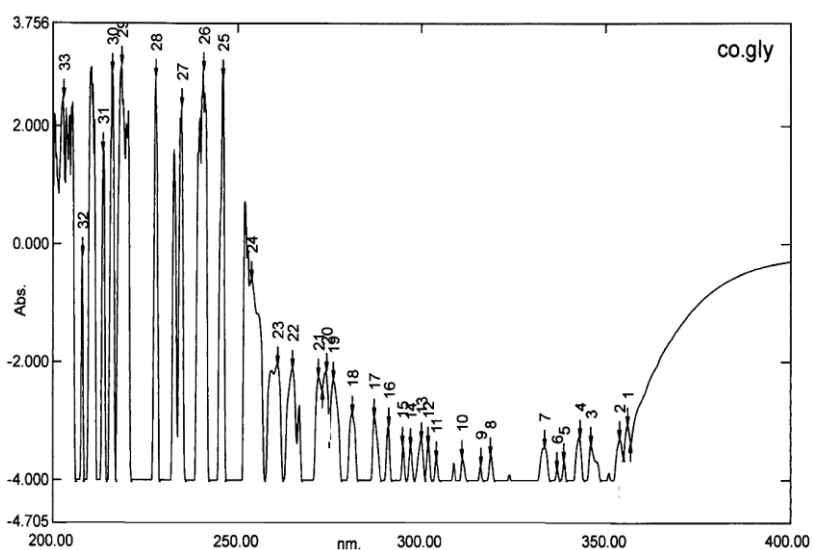

Figure (3.30) UV spectrum of Co.Gly complex
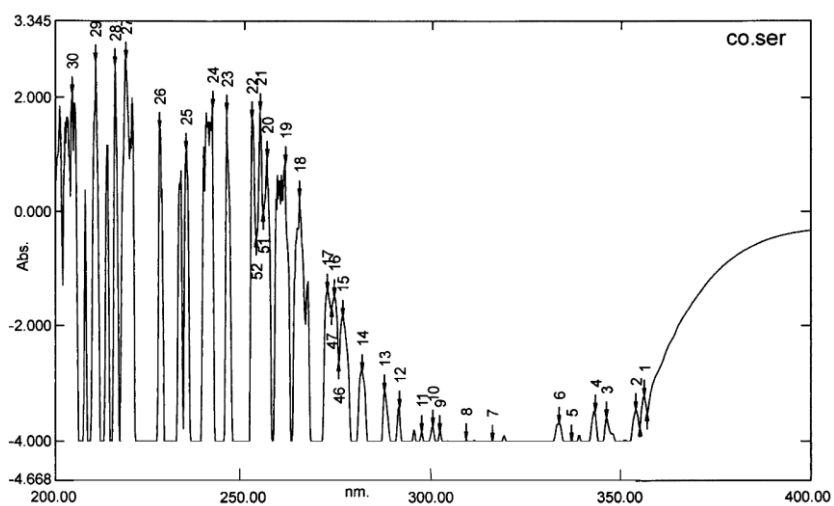
Figure (3.31) UV spectrum of Co.Ser complex

162
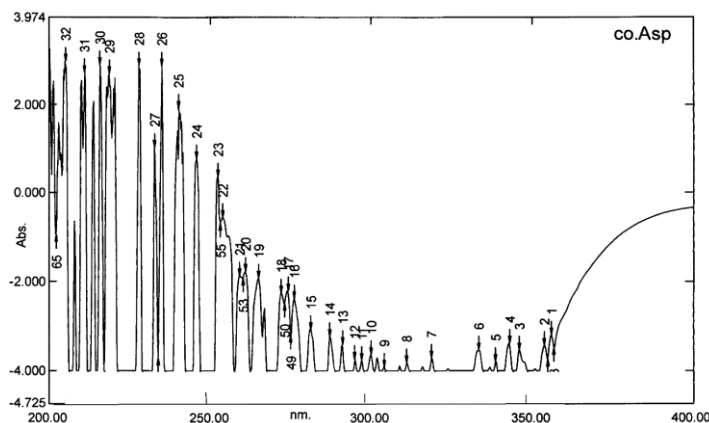
Figure (3.32) UV spectrum of Co.Asp complex
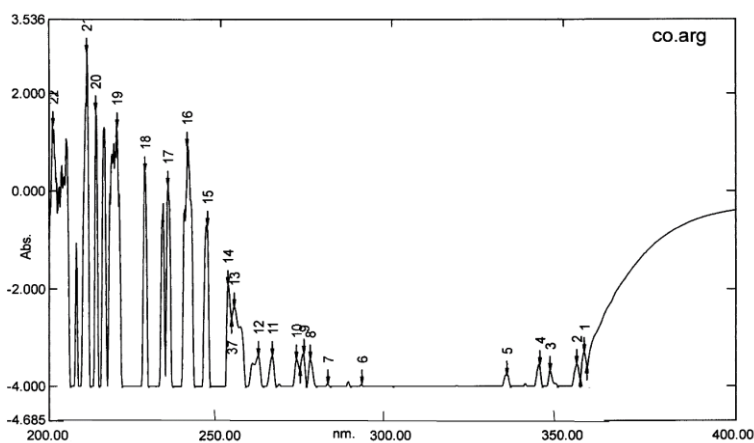
Figure (3.33) UV spectrum of Co.Arg complex

3.6.2 Iron complexes

Fe (III) complexes, only sextet term of the d^5 configuration octahedral geometry is the term ^6A_1g and does not split by the ligand field. Consequently, all the excited states have different spin multiplicity from the ground term and transition to them is forbidden. Many weak bands were observed and assigned as due to transition from ^6A_1g to ^4T_1g (G), $^4T_2g(G)$ and $^4Eg(G)$. And some absorption bands are observed. Which are attributed to charge transfer from the non-bonding orbitals of the oxygen atoms in the ligand to the iron (III) d orbitals, and absorption bands are assigned to the $\pi \rightarrow \pi^*$ and $n \rightarrow \pi^*$ transitions of the ligand [408,409]. Table (3.27) the assignment of the characteristic wave lengths of the electronic transition of Fe.Gly complex spectra Figure (3.34) showed three transition bands at 349.60, 344.60, and 339.00 nm due to transition from ^6A_1g to ^4T_1g (G), $^4T_2g(G)$ and $^4Eg(G)$, the charge transfer band was at 333.20 nm, and some transition in the region (201.2-327.4) nm due to $\pi \rightarrow \pi^*$ and $n \rightarrow \pi^*$ transitions of the glycine ligand. Fe.(Arg)(Asp) complex spectra figure (3.35) showed three transition

163

bands at 353.20, 345.60, and 342.00 nm due to transition from ^6A_1g to ^4T_1g (G), ^4T_2g(G) and ^4Eg(G), the charge transfer band was at 338.40 nm, and some transition in the region (210.60-333.8) nm due to $\pi \rightarrow \pi^*$ and n $\rightarrow \pi^*$ transitions of the aspartate and arginine ligands. These illustrated in table (3.28). In addition table (3.29) assignment of the characteristic wave lengths of the electronic transition of Fe.Arg.Asp.Ser complex spectra figure (3.36) showed three bands at (354.60, 351.00, and 348.60) nm due to transition from ^6A_1g to ^4T_1g (G), ^4T_2g(G) and ^4Eg(G), the charge transfer band was at 342.00 nm, and some transition in the region (210.80-338.80) nm due to $\pi \rightarrow \pi^*$ and n $\rightarrow \pi^*$ transitions of the arginine, aspartate, and serine ligands. The results of the electronic spectra of the cobalt (II) complexes were achieved in this research were agreed with the study of Al-Shaheen and Al-Mula, 2014[455].

Table (3.27) Electronic transitions occur in Fe.Gly complex:

No	Wavelength	Abs
1	349.60	3.976
2	344.60	3.994
3	339.00	4.000
4	333.20	4.000
5	327.40	4.000
6	323.00	4.000
7	315.80	4.000
8	314.40	4.000
9	308.80	4.000
10	301.80	4.000
11	301.80	4.000
12	297.20	4.000
13	291.40	4.000
14	284.40	4.000
15	276.40	4.000
16	272.40	4.000
17	269.80	4.000
18	263.20	4.000
19	260.00	4.000
20	256.40	4.000
21	253.40	4.000
22	238.60	3.556
23	236.20	4.000
24	231.80	3.770
25	221.00	3.759
26	210.60	3.660
27	201.20	4.000

164

Table (3.28) Electronic transitions occur in Fe.Arg.Asp complex:

No	Wavelength	Abs
4	353.20	2.222
5	345.60	4.000
6	342.00	3.626
7	338.40	3.147
8	333.80	3.337
9	319.60	3.602
10	316.60	3.242
11	308.60	1.967
12	304.20	2.423
13	301.80	3.673
14	291.20	3.166
15	287.20	2.957
16	282.00	2.300
17	275.60	3.285
18	265.60	2.807
19	259.00	3.629
20	252.20	3.358
21	245.40	3.178
22	240.60	2.937
23	235.00	2.995
24	233.00	2.127
25	228.00	2.481
26	218.40	3.348
27	215.80	2.528
28	213.80	2.450
29	210.60	2.650

Table (3.29) Electronic transitions occur in Fe.Arg.Asp.Ser complex:

No	Wavelength	Abs
2	354.60	1.541
3	351.00	1.692
4	348.60	3.186
5	342.00	3.283
6	338.80	3.233
7	333.20	3.628
8	319.40	3.193
9	316.20	3.270
10	311.60	4.000
11	308.80	3.228
12	303.80	2.460
13	299.00	3.229
14	295.20	1.651
15	291.20	2.181
16	282.00	2.838

17	373.60	4.000
18	271.80	4.000
19	264.20	2.786
20	259.00	3.202
21	252.40	2.606
22	245.80	2.759
23	240.20	3.302
24	233.20	2.437
25	220.00	2.946
26	213.60	1.373
27	210.80	2.877
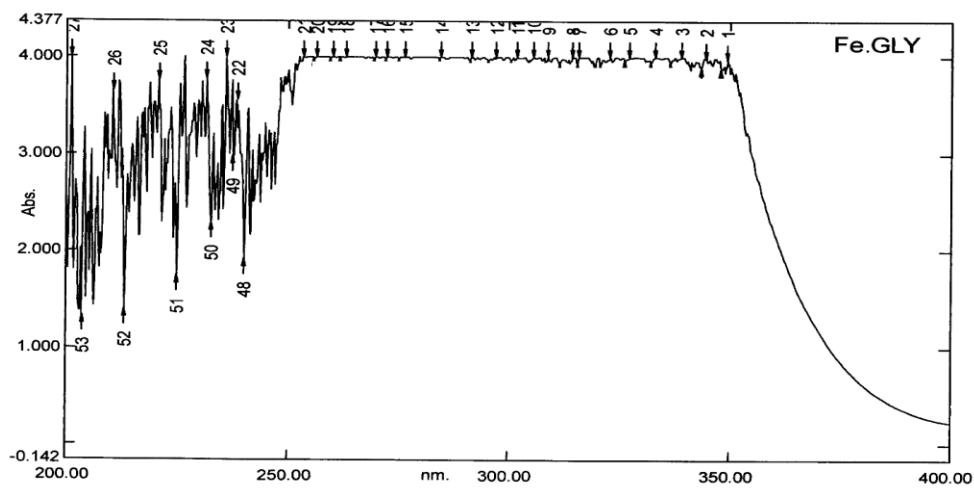
Figure (3.34) UV spectrum of Fe.Gly complex
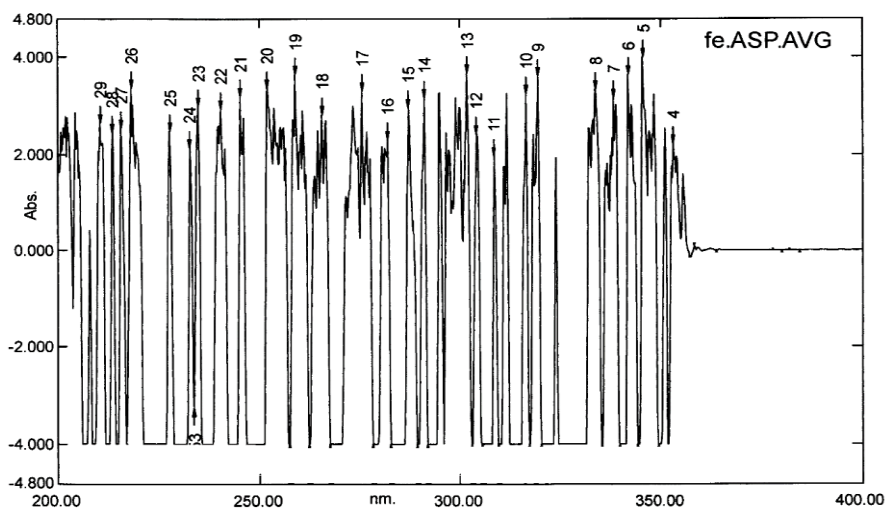
Figure (3.35) UV spectrum of Fe.Arg.Asp complex

166
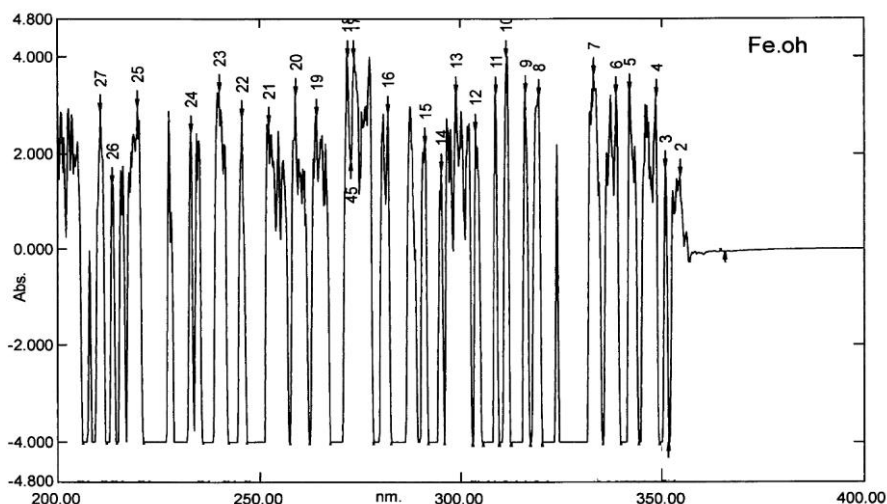
Figure (3.36) UV spectrum of Fe.Arg.Asp.Ser complex

3.6.3 Gold complexes

The electronic spectra of the prepared gold (III) complexes gave three absorption bands, These bands Can be assigned to $[^1A_1g \rightarrow {}^1A_2g]$ (v_1), $[^1A_1g \rightarrow {}^1B_1g]$, ($v_2$) and $[^1A_1g \rightarrow {}^1Eg]$ (v_3) transition respectively, the position of these bands are in agreement with low-spin square planar geometry for gold (III) complexes[456]. And some absorption bands are observed. Which are attributed to charge transfer from the non-bonding orbitals of the oxygen atoms in the ligand to the gold (III) d orbital. The last absorption bands are assigned to the n $\rightarrow$ σ*, $\pi \rightarrow \pi^*$ and n$\rightarrow \pi^*$ transitions of the ligand[457,458]. Table (3.30) the assignment of the characteristic wave lengths of the electronic transition of Au.(Asn.Gly) complex spectra Figure (3.37) showed three transition bands at (316.20, 311.60, and 308.80) nm for $[^1A_1g \rightarrow {}^1A_2g]$ (v_1), $[^1A_1g \rightarrow {}^1B_1g]$, ($v_2$) and $[^1A_1g \rightarrow {}^1Eg]$ (v_3), the charge transfer band is at 304.20 nm, and some transition band in the region (299.60- 210.8) nm due to the asparagine and glycine ligand. In addition Table (3.31) assignment of the characteristic wave lengths of the electronic transition of Au.(Cys.Ser) complex spectra Figure (3.38) showed three bands at (360.00, 356.00, and 347.40) nm due to transition from $[^1A_1g \rightarrow {}^1A_2g]$ (v_1), $[^1A_1g \rightarrow {}^1B_1g]$, ($v_2$) and $[^1A_1g \rightarrow {}^1Eg]$ (v_3), the charge transfer band was at 341.40 nm, and some transition in the region (205.00-338.40) nm due to $\pi \rightarrow \pi^*$ and n $\rightarrow \pi^*$ transitions of the cysteine and serine ligands. The results of the electronic spectra of the gold (III) complexes were achieved in this research were agreed with the study of Mikkat Zaghlool Hamdi, et al, 2013[273].

Table (3.30) Electronic transitions occur in Au.(Asn.Gly) complex:

No	Wavelength	Abs
10	316.20	1.022
11	311.60	3.647
12	308.80	3.577
13	304.20	2.570
14	299.60	3.279
15	295.20	3.236
16	290.60	3.276
17	286.80	3.273
18	280.60	4.000
19	275.60	4.000
20	272.20	3.659
21	266.40	3.584
22	260.20	3.582
23	253.80	4.000
24	252.00	3.660
25	245.40	3.137
26	241.00	3.408
27	234.80	2.564
28	233.00	3.306
29	228.20	2.906
30	218.40	3.679
31	216.20	3.638
32	213.80	2.877
33	210.80	3.707

Table (3.31) Electronic transitions occur in Au.(Cys.Ser) complex:

No	Wavelength	Abs
1	360.00	3.584
2	356.00	3.914
3	347.40	4.000
4	341.40	4.000
5	338.40	4.000
6	331.00	4.000
7	325.60	4.000
8	314.00	4.000
9	310.00	4.000
10	304.00	4.000
11	298.40	4.000
12	295.20	4.000
13	291.20	4.000
14	287.80	4.000
15	280.80	4.000
16	276.20	4.000

17	264.20	4.000
18	253.60	4.000
19	251.80	4.000
20	247.40	4.000
21	236.00	4.000
22	229.60	4.000
23	214.80	3.712
24	208.20	4.000
25	205.00	3.689
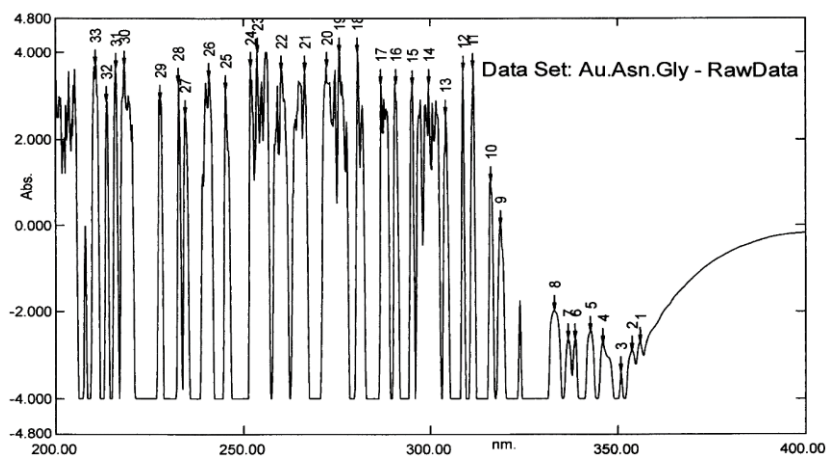
Figure (3.37) UV spectrum of Au.Asn.Gly complex
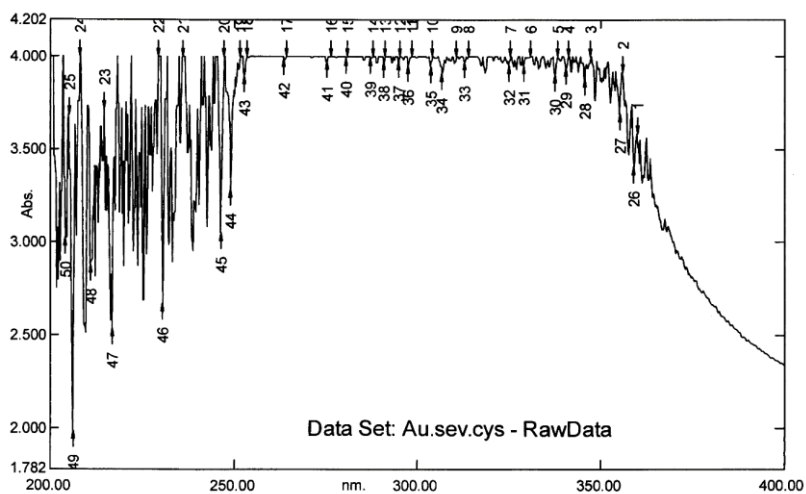
Figure (3.38) UV spectrum of Au.Cys.Ser complex

3.6.4 Nickel complexes

The electronic distribution of Ni (II) ion (d^8) is $t_2g^6 eg^2$, of these crystal field terms, ^3A_2g (F) is the ground state. Hence three spin allowed transitions are possible and the others are spin forbidden The three spin allowed transitions are: $^3A_2g(F) \rightarrow ^3T_1g(P)$, $^3A_2g(F) \rightarrow ^3T_1g(F)$ and $^3A_2g(F) \rightarrow ^3T_2g(F)$. And some absorption bands are observed. Which are attributed to charge transfer from the non-bonding orbitals of the oxygen atoms in the ligand to the Nickel (II) d orbitals. The last absorption bands are assigned to the $\pi \rightarrow \pi^*$ and $n \rightarrow \pi^*$ transitions of the ligand[457,458]. The assignment of the characteristic wave lengths of the electronic transition of Ni.Leu Figure (3.39), showed three bands at (339.60, 248.40, and 245.80) nm due to $^3A_2g(F) \rightarrow ^3T_1g(P)$, $^3A_2g(F) \rightarrow ^3T_1g(F)$ and $^3A_2g(F) \rightarrow ^3T_2g(F)$ transition, the charge transfer band was at 240.20 nm, and some transition in the region (233-201) nm due to $\pi \rightarrow \pi^*$ and $n \rightarrow \pi^*$ transitions of the cysteine and serine ligands. These illustrated in Table (3.32). And Ni.(Cys.Leu) spectra Figure (3.40), which was summarized in Table (3.33), showed three bands at (339.60, 241.00, and 229.40) nm due to $^3A_2g(F) \rightarrow ^3T_1g(P)$, $^3A_2g(F) \rightarrow ^3T_1g(F)$ and $^3A_2g(F) \rightarrow ^3T_2g(F)$ transition, the charge transfer band was at 226.20 nm, and three bands at 218.00, 215.40, and 207.60 nm due to $\pi \rightarrow \pi^*$ and $n \rightarrow \pi^*$ transitions of the asparagine and leucine ligands. These characteristic bands were agreed with the studies of Boruah 2012[313], Al-Jeboori *et al.*, 2012[347], and Aiyelabola, *et al*, 2012[379] of the previous studies.

Table (3.32) Electronic transitions occur in Ni.Leu complex:

No	Wavelength	Abs
1	339.60	0.008
2	248.40	0.001
3	245.80	0.010
4	240.20	0.070
5	233.00	0.066
6	229.20	0.118
7	225.80	0.080
8	223.80	0.062
9	220.20	0.078
10	215.00	0.333
11	207.00	0.403
12	201.00	0.550

Table (3.33) Electronic transitions occur in Ni.Asn.Leu complex:

No	Wavelength	Abs
1	339.60	0.001
2	241.00	0.082
3	229.40	0.105
4	226.20	0.075
5	218.00	0.095
6	215.40	0.379
7	207.60	0.658
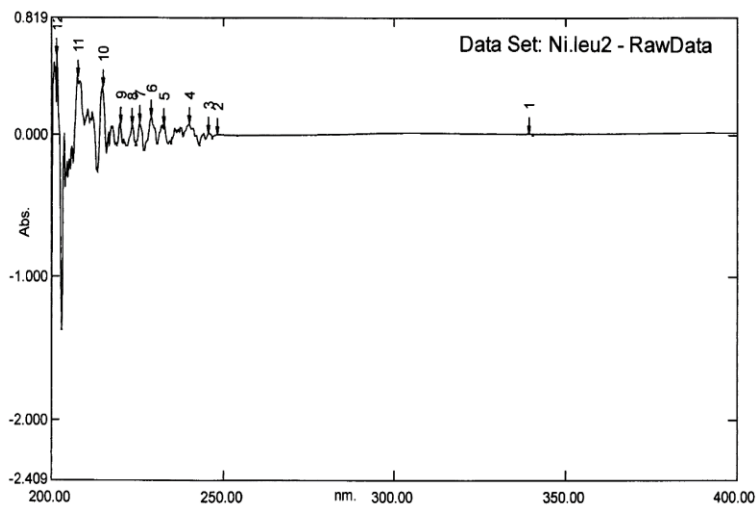
Figure (3.39) UV spectrum of Ni.Leu complex
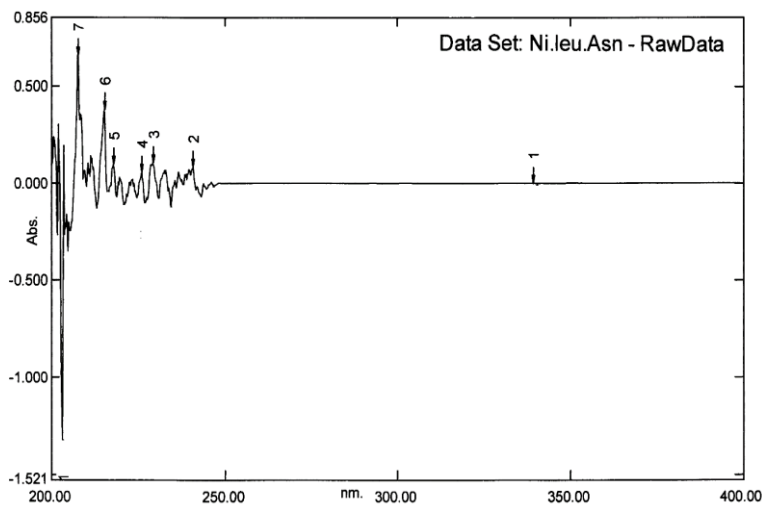
Figure (3.40) UV spectrum of Ni.Asn.Leu complex

3.6.5 Copper complex

In octahedral crystal field, the ground state electronic distribution of Cu^{2+} is $t_{2g}^6 e_g^3$ which yields ^2Eg term. The excited electronic state is $t_{2g}^5 e_g^4$ which corresponds to $^2T_{2g}$ term. Thus only one single

electron transition, i.e., $^2Eg \rightarrow {}^2T_2g$, is expected in an octahedral crystal field. Octahedral coordination is distorted either by elongation or compression of octahedron leading to tetragonal symmetry.

Normally, the ground state ^2Eg is split due to Jahn-Teller effect and hence lowering of symmetry is expected for Cu^{2+} ion, This state splits into ^2B_1g (dx^2-y^2) and $^2A_1g(dz^2)$ states in tetragonal symmetry and the excited term ^2T_2g also splits into $^2B_2g(dxy)$ and $^2Eg(dxz,dyz)$ levels. Thus, three bands are expected for tetragonal (C4v) symmetry[457,458], Accordingly Cu.gly complex Figure (3.41), showed three bands at (264.80, 258.60, and 254.60) nm, the band at 246.00 nm due to charge transfer from the non-bonding orbitals of the oxygen atoms in the ligand to the copper (II) d orbitals or vice versa, and some absorption bands are observed at (240.80, 235.20, 219.00, 216.00, 210.00, and 201.20) nm, these absorption bands are assigned to the $\pi \rightarrow \pi^*$ and n $\rightarrow \pi^*$ transitions of the glycine ligand. That illustrated in Table (3.34). These characteristic bands were agreed with the studies of Stanila, *et al,* 2011[299], Al-Jeboori *et al.*, 2012[347], Tripathi, *et al.,* 2015[350], Qadir, *et al.,* 2014[362], Hübner, *et al.,* 2011[364], Rodridues, *et al.*, 2017[374], Aiyelabola, *et al.,* 2012[379] of the previous studies of the Cu (II) complexes.

Table (3.34) Electronic transitions occur in Cu.Gly complex:

No	Wavelength	Abs
15	264.80	0.075
16	258.60	0.351
17	254.60	0.959
18	246.00	0.526
19	240.80	1.267
20	235.20	1.718
22	219.00	3.629
23	216.00	2.274
24	210.00	1.484
25	201.20	2.137
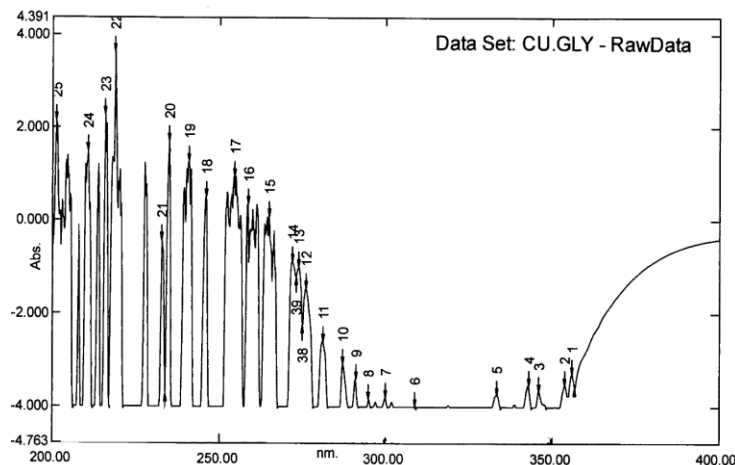
Figure (3.41) UV spectrum of Cu.Gly complex

3.6.6 Zinc complexes

Since the zinc (II) ion has d^{10} configuration, no d-d electronic transition, one absorption band was appeared could be assigned to a charge transfer transition. And some absorption bands are observed. Which are attributed to charge transfers from the non-bonding orbitals of the oxygen atoms in the ligand to the zinc (II) d orbitals or vice versa. The last absorption bands are assigned to the $\pi \to \pi *$ and n $\to \pi *$ transitions of the ligand[455,456]. Therefore, zinc (II) ion was tetrahedral geometry will be taking[459]. For Zn.cys complex spectra Figure (3.42) showed band at 232.00 nm of charge transfer, and three bands at (212.10, 209.02, and 206.30) nm due to $\pi \to \pi *$ and n $\to \pi *$ transitions of the cysteine ligand, these illustrated in Table (3.35). in addition Table (3.36) assignment of the characteristic wave lengths of the electronic transition of Zn.Asn.Leu complex spectra Figure (3.43) showed band at 245.00 nm of charge transfer, and six bands at (239.20, 233.60, 225.40, 214.20, 206.20, and 204.00) nm due to $\pi \to \pi *$ and n $\to \pi *$ transitions of the asparagine and leucine ligand. These characteristic bands were agreed with the studies of Reddy, *et al.,* 2005[287], Rosu, *et al.,* 2009[310], Al-Jeboori *et al.,* 2012[347] of the previous studies of the Zn (II) complexes.

Table (3.35) Electronic transitions occur in Zn.cys complex:

No	Wavelength	Abs
1	232.00	0.180
2	212.10	0.491
3	209.02	1.123
4	206.30	0.801

Table (3.36) Electronic transitions occur in Zn.Asn.Leu complex:

No	Wavelength	Abs
1	245.00	0.037
2	239.20	0.096
3	233.60	0.092
4	225.40	0.107
5	214.20	0.254
6	206.20	0.503
7	204.00	1.027
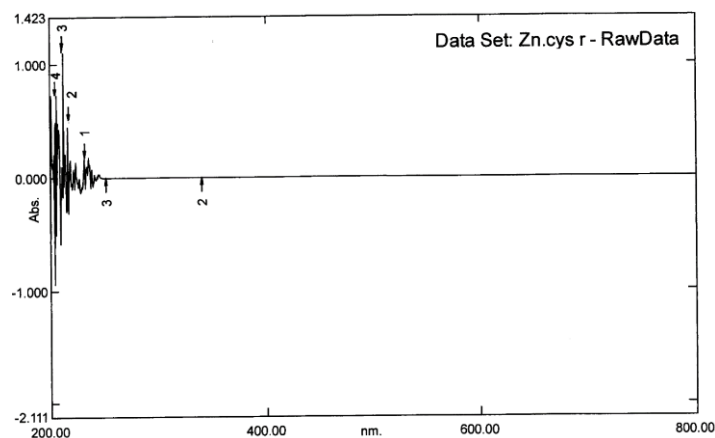
Figure (3.42) UV spectrum of Zn.cys complex
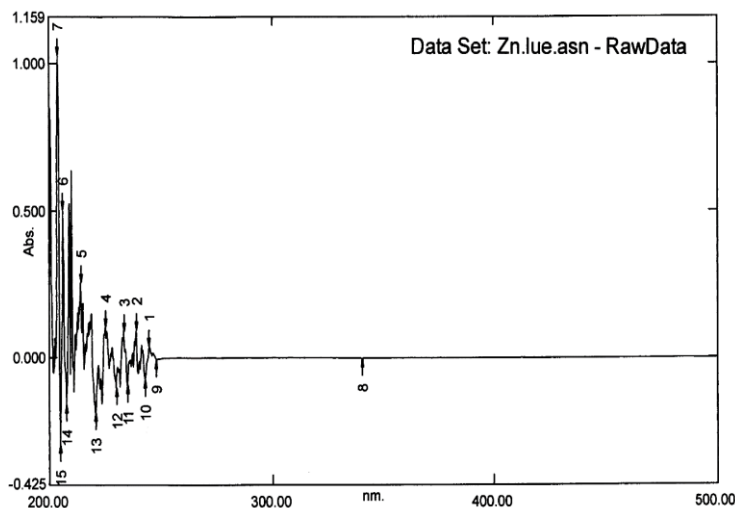
Figure (3.43) UV spectrum of Zn.Asn.Leu complex

3.7 X-ray Diffraction (XRD) study

The X-ray diffractogram of the two gold-amino acid complexes Au.(Asn.Gly) and Au.(Cys.Ser), four cobalt-amino acid complexes Co.Gly, Co.Ser, Co.Asp, and Co.Arg, three Iron-amino acid complexes Fe(Gly), Fe(Arg)(Asp), and Fe(Arg)(Asp)(Ser), two zinc-amino acid complexes Zn.Cys, Zn.(Asn)(Leu), two nickel-amino acid complexes (Ni.Leu, Ni.(Asn)(Leu), and one cupper-amino acid complex Cu.Gly complex were performed to obtain further evidence about the structure of the metal complexes. The diffractogram of the coordination amino acid complexs records more than 100 reflections between 0 to 80º (2θ) with maxima reflection at 2θ (10.14º) which corresponds to d (8.728Aº), According to (Chohan, *et al.,* 1998)[460] The X-ray pattern have been indexed by using computer software (PowdMoult 2.3

174

version), and the lattice constants a, b and c, Inter axial angle α, β, and γ for unit cell, molecular formula, molecular weight, and density values, of the gold, cobalt, iron, zinc, nickel, and copper complexes, were recorded and collected in Tables (3.37), (3.38), (3.39), (3.40), (3.41), and (3.42), respectively. Each diffractogram was well resolved into sharp reflux, that suggesting the amino acid complexes were monoclinic, and highly crystalline nature. These results were compatible to the result achieved in the studies of Yokota, et al, 2016[306], Tuna, *et al.,* 2003[461], Szalda., *et al.,* 2012[462], Telfer, *et al.,* 2001[463], Telfer, *et al.,* 2003[464], Telfer, *et al.,* 2014[465], Rowland, *et al.,* 2011[466], Provent, *et al.,* 2010[467], and Masood, *et al.,* 1998) [468].

Table (3.37) XRD study of Au.(Asn.Gly), and Au.(Cys.Ser) complexes:

		Au.(Asn.Gly)	Au.(Cys.Ser)
Molecular formula		$C_6 H_{11} Au O_5 N_3 Cl$	$C_6 H_{11} Au O_5 N_2 S Cl$
Crystal system		monoclinic	Monoclinic
Unit cell	a	5.1910 Å	5.1910 Å
	b	8.7480 Å	8.7480 Å
	c	14.4480 Å	14.4480 Å
	β	93.342°	91.632°
Molecular weight		437.5	455.5
Density per g/cm3		4.2582	4.4334

Table (3.38) XRD study of Co.Gly, Co.Ser, Co.Asp, and Co.Arg complexes:

		Co.Gly	**Co.Ser**	**Co.Asp**	**Co.Arg**
Molecular formula		$C_4H_{12}CoN_2O_8$	$C_6H_{16}CoN_2O_8$	$C_8H_{14}CoN_2O_{10}$	$C_{12}H_{34}CoN_8O_6$
Crystal system		monoclinic	monoclinic	monoclinic	monoclinic
Unit cell	a	9.200 A	9.5990 A	9.999 A	9.5080 A
	b	15.1230 A	15.3440 A	16.004 A	9.4280 A
	c	8.3210 A	8.9440 A	9.874 A	9.3090 A
	α	99.98°	100.47°	108.54°	78.86°
	β	111.78°	113.93°	118.32°	105.080°
	δ	79.56°	81.37°	89.76°	120.13°
Molecular weight		242.93	302.93	356.93	444.94
Density per g/cm3		1.087	1.356	1.597	1.304

Table (3.39) XRD study of Fe(Gly), Fe(Arg)(Asp), and Fe(Arg)(Asp)(Ser) complexes:

		Fe(Gly)	Fe(Arg)(Asp)	Fe(Arg)(Asp)(Ser)
Molecular formula		$C_4 H_{12} Fe O_6 N_2 Cl$	$C_{10} H_{25} Fe O_8 N_5 Cl$	$C_{13} H_{26} Fe O_9 N_6$
Crystal system		monoclinic	monoclinic	monoclinic
Unit cell	a	5.191 A	7.871 A	9.898 A
	b	8.748 A	9.978 A	10.543 A
	c	14.448 A	18.448 A	19.492 A
	α	-	-	-
	β	90.81°	94.81°	93.81°
	α	-	-	-
Molecular weight		275.35	434.35	465.84
Density per g/cm³		2.680	4.227	4.5336

Table (3.40) XRD study of Zn.Cys and Zn.Asn.Leu complexes:

		Zn.Cys	Zn.Asn.Leu
Molecular formula		C6H12 Zn N2 S2 O4	C10H18 Zn N3 O5
Crystal system		monoclinic	monoclinic
Unit cell	a	14.9178 Å	18.4178 Å Å
	b	9.8966 Å	10.3766 Å
	c	17.003 Å	17.5213 Å
	β	109.752 °	109.992 °
	α	-	108.872 °
Molecular weight		305.38	325.38
Density per g/cm³		1.914	2.0054

Table (3.41) XRD study of Ni.Leu and Ni.Cys.Leu complexes:

		Ni.Leu	Ni.Cys.Leu
Molecular formula		C12H28 Ni N2 O6	C9H22 Ni N2 O6 S
Crystal system		monoclinic	monoclinic
Unit cell	a	9.4390 Å	9.2340 Å
	b	9.998 Å	9.563 Å
	c	9.0076 Å	8.5676 Å
	α	78.250°	79.75°
	β	104 °	91 °
	γ	119°	92.54°
Molecular weight		354.69	286.69
Density per g/cm³		1.039	0.840

Table (3.42) XRD study of Cu.Gly complex:

		Cu.Gly
Molecular formula		C4H8 Cu N2 O4
Crystal system		monoclinic
Unit cell	a	15.4178 Å
	b	8.3366 Å
	c	16.4003 Å
	β	106.832 °
Molecular weight		211.55
Density per g/cm^3		1.328

3.8 Biological activity result

The antibacterial activity of amino acids complexes was investigated against isolated Gram positive strain (*Staphylo coccus aureas, Klebsiella pneumonia, and Entero coccus feacalis*), and gram negative (*Escherichia coli, Pseudomonas aeruginosa*). And take some commercial antibiotics sensitivity as standard drug, which were amoxyclav, gentamicin, cefotaxime, vancomycin, ciprofloxacin, co-trimoxazole, ceftriaxone, and ampicillin. The results presented in Table (3.43) and Figure (3.51), showed various degrees in antibiotic resistance. All bacterial species showed resistance to amoxyclav, cefotaxime, vancomycin (except *S. aureus*), and ampicillin. Among the tested bacterial isolates, the strongest antibacterial activities of antibiotics were obtained by vancomycin and gentamicin against *S. aureus*, with inhibition zones of 22 and 19 mm, respectively[469]. In Sudan, plant-based traditional medicine represents primary health care like extracts from *Capparis decidua* L. twigs[470]. In this study found the Antibacterial effects of twigs extracts showed different degrees of inhibition profiles against tested bacteria. The ethyl acetate extract showed the highest activity against *S. aureus* (21 mm), *B. subtilis* (20 mm) and *P.pneumoniae* (18 mm) while the n-butanol extract displayed best inhibition against *P.pneumoniae* (18 mm) and *E. coli* (16 mm). All extracts showed high antifungal activity against *A. niger* and *C. albicans* with inhibition zone ranged from 17 to 22 mm.

Antibacterial activity of amino acid complexes was evaluated by measured diameters of zone, which were occurred by four difference concentration, that illustrated in Tables (3.44), (3.45), (3.46), (3.47), and (3.48) for *Escherichia coli, Staphylococcus aureus, Pseudomonas aeruginosa, Enterococcus faecalis, and klebsiella pneumonia,* Figures (3.52), (3.53), (3.54), (3.55), and (3.56) respectively, the antibacterial activity of amino acid complexes was determined by the mean value of zone diameter, and estimated variability in zone diameter by stander deviation (SD), and Correlation Coefficient (*R*)(A single summary number that gives you a good idea about how closely one variable is related to another

variable) using computer software program (OriginPro 70), that illustrated in Tables (3.49), (3.50), (3.51), (3.52), and (3.53) of *Escherichia coli, Staphylococcus aureus, Pseudomonas aeruginosa, Enterococcus faecalis, and klebsiella pneumonia,* respectively.

According to antibacterial activity chart of standard drugs, that mentioned above, (0-12 mm ≡ R), (13-15 mm ≡ I), (16-22mm ≡ S), and (<22mm ≡ HS), all complexes of amino acid have a difference degree of inhibitory effect against gram positive and gram negative.

Cu.Gly complex has antibacterial activity to ward four bacteria's under tested, two bacteria's *Escherichia coli,* and *Staphylococcus aureus* showed sensitive and two bacteria's *Pseudomonas aeruginosa,* and *Enterococcus faecalis* showed high sensitive to Cu.Gly complex. That showed in Figure (3.57).

Cobalt complexes have different degrees of biological activity, *Escherichia coli* showed intermediate activity to ward Co.Gly, Co.Ser, and Co.Asp, while Co.Arg was sensitive, Co.Gly, Co.Ser, and Co.Arg were intermediate activity, and Co.Asp was sensitive to ward *Staphylococcus aureus*. *Pseudomonas aeruginosa* showed sensitive against all Cobalt complexes, in addition the bacteria of *Enterococcus faecalis* showed resistant to ward Co.Gly, and Co.arg, while the Co.Ser, and Co.Asp were sensitive. That showed in Figure (3.58).

Gold complexes showed strongest activity to ward bacteria's than stander drugs and other complexes, Au(Asn.Gly) was high sensitive against *Staphylococcus aureus*. *Pseudomonas aeruginosa,* and *klebsiella pneumonia,* while *Escherichia coli* showed resistant to this complex. In addition Au(cys.Ser) was high sensitive to *Staphylococcus aureus,* sensitive to *Pseudomonas aeruginosa* and *klebsiella pneumonia,* and resistant to *Escherichia coli.* That showed in Figure (3.59).

Two bacteria's *Escherichia coli and klebsiella pneumonia* showed intermediate, while two bacteria's *Staphylococcus aureus* and *Pseudomonas aeruginosa* showed sensitive to ward Fe.Gly complex. *Escherichia coli* and *Staphylococcus aureus* showed resistant, while *Pseudomonas aeruginosa,* and *klebsiella pneumonia* were intermediate activity against Fe(Arg.Asp) complex. In addition Fe(Arg.Asp.Ser) complex showed resistant to ward three bacterias *Escherichia coli, Staphylococcus aureus,* and *klebsiella pneumonia,* just it was sensitive to *Pseudomonas aeruginosa.* That showed in Figure (3.60).

Zn.Cys complex showed high sensitive to two bacteria's *Staphylococcus aureus,* and *Pseudomonas aeruginosa,* sensitive to *klebsiella pneumonia,* In addition the Zn(Asn.Leu) complex was high sensitive to ward two bacteria's *Staphylococcus aureus,* and *klebsiella pneumonia,* sensitive to ward

178

Pseudomonas aeruginosa, while *Escherichia coli was* resistant to ward Zinc complexes. That showed in Figure (3.61).

Two bacteria's *Escherichia coli and Staphylo coccusaure* showed resistance to Ni^{2+} complexes, while the Ni^{2+} complexes have strongest antibacterial activity to word *Pseudomonas aeruginosa*, and *Klebsiella pneumonia,* from the standard drug as used. That showed in Figure (3.62).

Table (3.43): Antibacterial sensitivity pattern of the test bacteria against 8 antibiotics

Antibiotic	Diameter of inhibition zone of antibiotic discs (mm)		
	E. coli	*S. aureus*	*P. aeruginosa*
Amoxyclav (10 µg)	7 (R)	9 (R)	0 (R)
Gentamicin (10 µg)	15 (I)	19 (S)	16 (S)
Cefotaxime (10 µg)	5 (R)	5 (R)	7 (R)
Vancomycin (10 µg)	0 (R)	22 (S)	0 (R)
Ciprofloxacin (30 µg)	11 (R)	12 (R)	8 (R)
Co-trimoxazole (30 µg)	10 (R)	6 (R)	9 (R)
Ceftriaxone (30 µg)	9 (R)	12 (R)	18.5 (I)
Ampicillin (10 µg)	(0) R	(0) R	(6.5) R

S, sensitive; R, resistant; I, intermediate
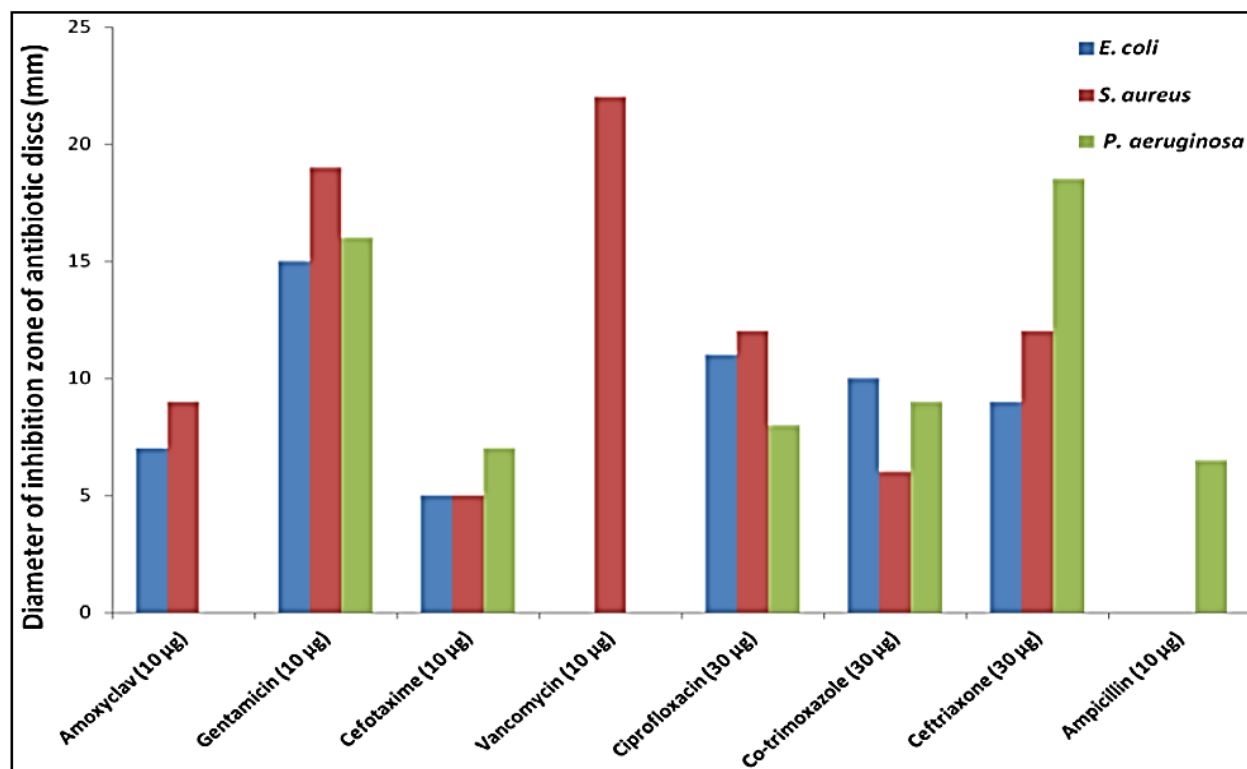
Figure (3.44): Antibacterial sensitivity pattern of the test bacteria against 8 antibiotics using disc diffusion technique.

179
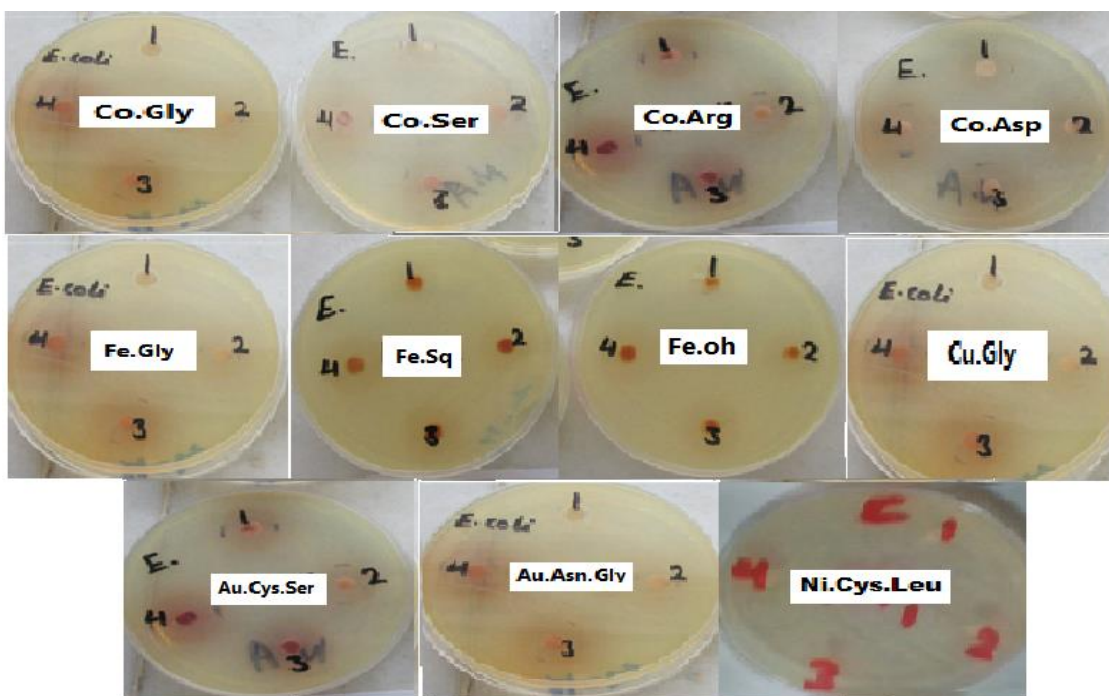
Figure (3.45) Antibacterial activity of amino acid complexes against *Escherichia coli*
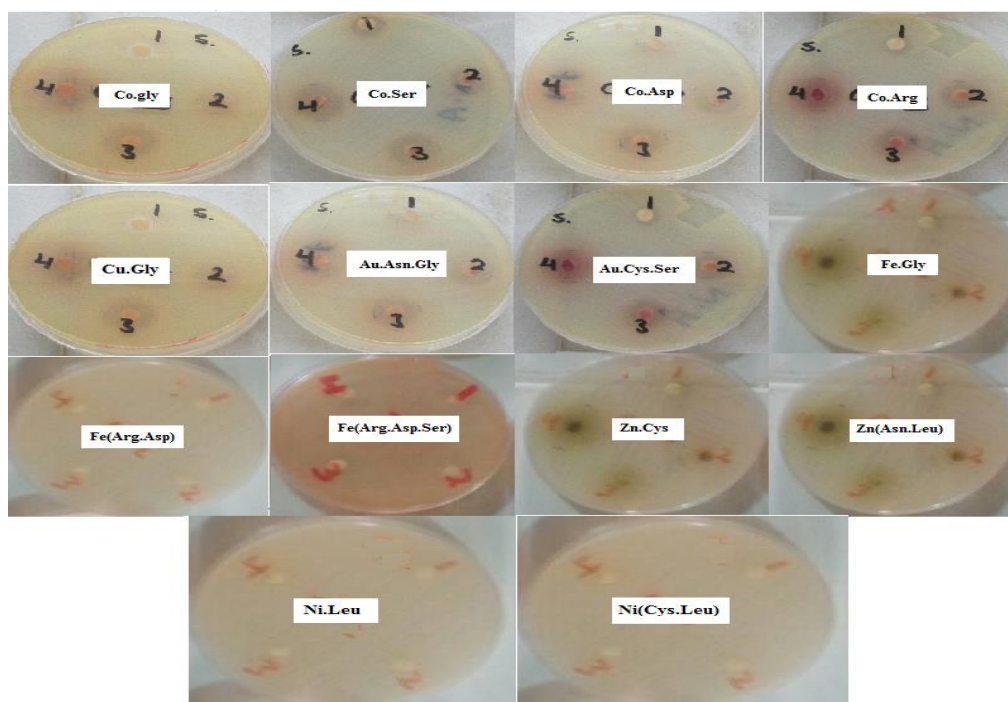
Figure (3.46) Antibacterial activity of amino acid complexes against *Staphylococcus aureus*
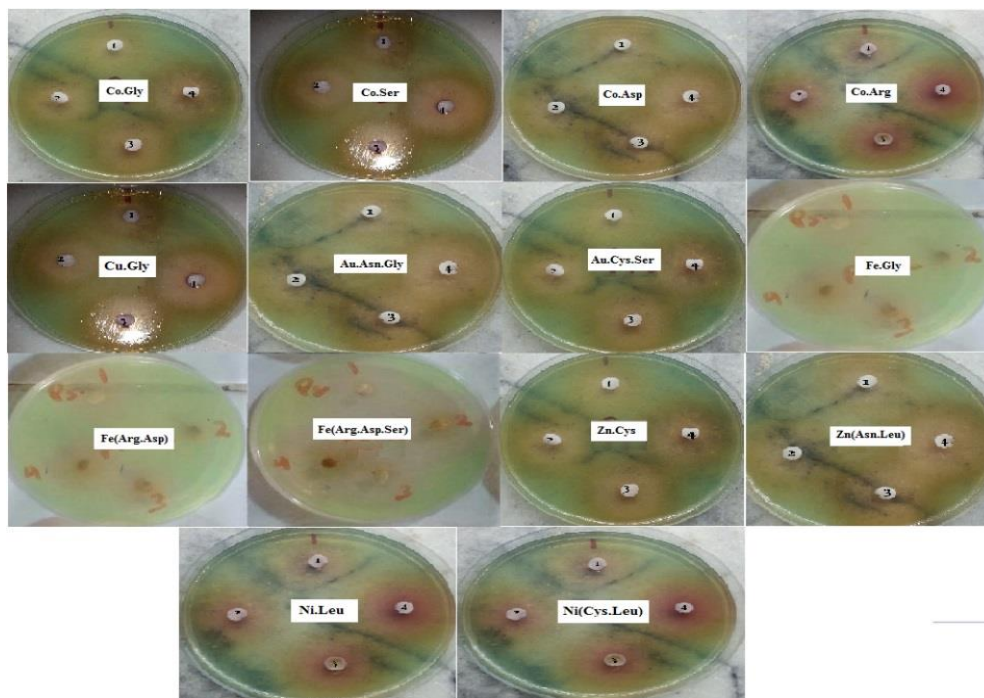
Figure (3.47) Antibacterial activity of amino acid complexes against *Pseudomonas aeruginosa*
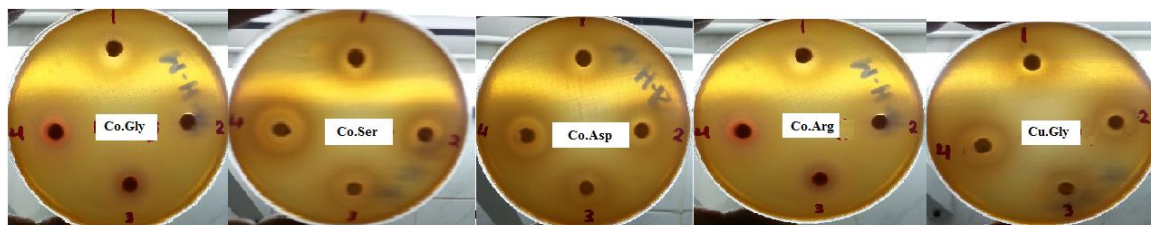
Figure (3.48) Antibacterial activity of amino acid complexes against *Enterococcus faecalis*
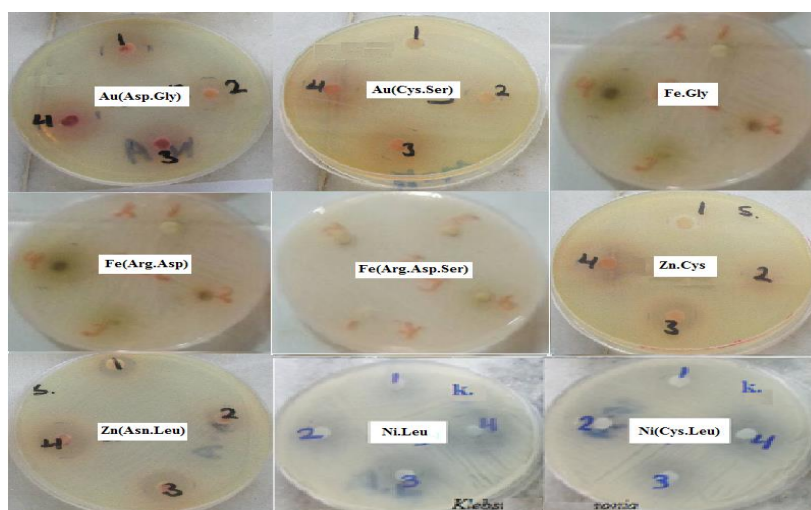
Figure (3.49) Antibacterial activity of amino acid complexes against *klebsiella pneumonia*

181

Table (3.44) Diameter of zone of four concentrations against *Escherichia coli*

Complex	Concentration per mg/ml	Diameter per mm
Co.Gly	2	10
	4	14
	6	16
	8	18
Co.Ser	2	12
	4	15
	6	17
	8	19
Co.Asp	2	16
	4	18
	6	20
	8	22
Co.Arg	2	14
	4	16
	6	18
	8	20
Cu.Gly	2	16
	4	18
	6	22
	8	28
Fe.Gly	2	8
	4	12
	6	16
	8	20
Fe.Arg.Asp	2	-
	4	-
	6	-
	8	7
Fe.Arg.Asp.Ser	2	-
	4	-
	6	8
	8	10
Au.Cys.Ser	2	12
	4	13
	6	15
	8	17
Au.Asn.Gly	2	7
	4	9
	6	11
	8	15
Ni.leu	2	7
	4	8
	6	9
	8	10
Ni.Cys.Leu	2	-
	4	-
	6	7
	8	9
Zn.Cys	2	9
	4	11
	6	13
	8	17
Zn.Asn.Leu	2	10
	4	12
	6	13
	8	16

Table (3.45) Diameter of zone of four concentrations against *Staphylococcus aureus*

Complex	Concentration per mg/ml	diameter
Co.Gly	2	10
	4	12
	6	15
	8	18
Co.Ser	2	12
	4	14
	6	16
	8	19
Co.Asp	2	15
	4	16
	6	17
	8	18
Co.Arg	2	10
	4	13
	6	15
	8	17
Cu.Gly	2	12
	4	15
	6	18
	8	23
Fe.Gly	2	13
	4	17
	6	20
	8	22
Fe.Arg.Asp	2	-
	4	-
	6	9
	8	11
Fe.Arg.Asp.Ser	2	6
	4	8
	6	10
	8	12
Au.Cys.Ser	2	31
	4	33
	6	35
	8	37
Au.Asn.Gly	2	26
	4	32
	6	34
	8	36
Ni.leu	2	8
	4	9
	6	11
	8	13
Ni.Cys.Leu	2	-
	4	-
	6	10
	8	14
Zn.Cys	2	22
	4	25
	6	28
	8	31
Zn.Asn.Leu	2	22
	4	24
	6	26
	8	28

Table (3.46) Diameter of zone of four concentrations against *Pseudomonas aeruginosa*

Complex	Concentration per mg/ml	diameter
Co.Gly	2	16
	4	18
	6	20
	8	22
Co.Ser	2	17
	4	19
	6	22
	8	25
Co.Asp	2	15
	4	18
	6	20
	8	24
Co.Arg	2	14
	4	16
	6	20
	8	22
Cu.Gly	2	18
	4	21
	6	25
	8	31
Fe.Gly	2	13
	4	17
	6	21
	8	25
Fe.Arg.Asp	2	11
	4	13
	6	17
	8	19
Fe.Arg.Asp.Ser	2	15
	4	17
	6	20
	8	25
Au.Cys.Ser	2	12
	4	16
	6	20
	8	24
Au.Asn.Gly	2	18
	4	22
	6	26
	8	28
Ni.leu	2	15
	4	19
	6	23
	8	29
Ni.Cys.Leu	2	20
	4	24
	6	26
	8	28
Zn.Cys	2	20
	4	23
	6	27
	8	30
Zn.Asn.Leu	2	13
	4	15
	6	19
	8	24

Table (3.47) Diameter of zone of four concentrations against *Enterococcus faecalis*

Complex	Concentration per mg/ml	diameter
Co.Gly	2	8
	4	10
	6	14
	8	16
Co.Ser	2	10
	4	14
	6	16
	8	18
Co.Asp	2	10
	4	12
	6	14
	8	17
Co.Arg	2	8
	4	10
	6	11
	8	13
Cu.Gly	2	16
	4	22
	6	28
	8	36

Table (3.48) Diameter of zone of four concentrations against *klebsiella pneumonia*

Complex	Concentration per mg/ml	diameter
Fe.Gly	2	11
	4	13
	6	16
	8	22
Fe.Arg.Asp	2	9
	4	12
	6	14
	8	18
Fe.Arg.Asp.Ser	2	8
	4	10
	6	13
	8	16
Au.Cys.Ser	2	14
	4	16
	6	18
	8	20
Au.Asn.Gly	2	11
	4	16
	6	22
	8	28
Ni.leu	2	18
	4	22
	6	28
	8	32
Ni.Cys.Leu	2	24
	4	26
	6	28
	8	32

	2	16
Zn.Cys	4	20
	6	24
	8	28
	2	22
Zn.Asn.Leu	4	28
	6	32
	8	38

Table (3.49) Mean, standard deviation, correlation coefficient and sensitivity of amino acid complexes Vs *Escherichia coli*:

Complex	Carve data			x′±SD	Sensitivity
	A ± Error	B ± Error	*R*		
Au (Asn.Gly)	4±0.9486	1.3±0.17321	0.98271	10.5±0.7746	R
Au (Cys.Ser)	10±0.47434	0.85±0.0866	0.98978	14±0.3873	I
Co.Gly	-5.77±1.465	0.743±0.099	0.9827	14.5±0.5854	I
Co.Ser	-8.542±1.033	0.8598±0.065	0.9943	15.75±0.335	I
Co.Asp	-12.00±0.00	1.00±0.00	0.00	17.0±0.00	S
Co.Arg	-14.00±0.00	1.00±0.00	1	19.00±0.00	S
Fe(Gly)	-2.00±0.00	0.50±0.00	1	14.00±0.00	I
Fe(Arg+Asp)	0.00±0.00	2.00±0.00	1	-	R
Fe(Arg+Asp+Ser)	0.00±0.00	2.00±0.00	1	-	R
Cu.Gly	-5.00±1.61	0.48±0.075	0.976	21.00±0.69	S
Zn.Cys	-4.30±1.27	0.743±0.099	0.9827	12.5±0.586	R
Zn.Asn.Leu	-7.92±1.823	1.013±0.14	0.9811	12.75±0.611	R
Ni.Leu	-12.00±0.00	2.00±0.00	1	8.5±0.00	R
Ni.Cys.Leu	0.00±0.00	2.00±0.00	1	-	R

Table (3.50) Mean, standard deviation, correlation coefficient and sensitivity of amino acid complexes Vs *Staphylococcus aureus*:

Complex	Carve data			x′±SD	Sensitivity
	A ± Error	B ± Error	*R*		
Au (Asn.Gly)	22.5±0.3873	1.8±0.0707	0.998	31.5±0.316	HS
Au (Cys.Ser)	29.00±0.00	1.00±0.00	1	34.00±0.00	HS
Co.Gly	-5.10±0.66	0.73±0.047	0.994	13.75±0.286	I
Co.Ser	-8.11±1.00	0.86±0.065	0.9943	15.00±0.334	I
Co.Asp	-28.00±0.00	2.00±0.00	1	16.00±0.00	S
Co.Arg	-6.82±0.05	0.91±0.06	0.994	13.05±0.334	I
Fe(Gly)	-6.74±1.26	0.65±0.069	0.989	18.00±0.466	S
Fe(Arg+Asp)	0.00±0.00	2.00±0.00	1	-	R
Fe(Arg+Asp+Ser)	-4.00±0.00	1±0.00	1	9.00±0.00	R
Cu.Gly	-4.27±0.92	0.545±0.052	0.991	17.00±0.426	S
Zn.Cys	-12.67±1.02	0.67±0.18	1	26.50±1.26	HS
Zn.Asn.Leu	-20.00±0.00	1.00±0.00	1	25.00±0.00	HS
Ni.Leu	-6.81±1.22	1.15±0.12	0.989	10.25±0.45	R
Ni.Cys.Leu	1.00±0.00	0.50±0.00	1	-	R

Table (3.51) Mean, standadr deviation, correlation coefficient and sensitivity of amino acid complexes Vs *Pseudomonas aeruginosa*:

Complex	Carve data			x′±SD	Sensitivity
	A ± Error	B ± Error	R		
Au (Asn.Gly)	15.00±0.95	1.7±0.17321	0.989	23.5±0.7746	HS
Au (Cys.Ser)	8.00±0.00	2±0.00	1	18.00±0.00	S
Co.Gly	-14.00±0.00	1.00±0.00	1	19.00±0.00	S
Co.Ser	-10.24±0.99	0.73±0.05	0.996	20.75±0.285	S
Co.Asp	-8.05±1.21	0.68±0.061	0.992	19.25±0.40	S
Co.Arg	-7.60±1.29	0.70±0.071	0.989	18.00±0.447	S
Fe(Gly)	-4.50±0.00	0.5±0.00	1	19.00±0.00	S
Fe(Arg+Asp)	-5.50±1.08	0.7±0.071	0.989	15.00±0.447	I
Fe(Arg+Asp+Ser)	-6.19±1.56	0.58±0.08	0.979	19.25±0.636	S
Cu.Gly	-5.78±1.23	0.45±0.05	0.987	23.75±0.492	HS
Zn.Cys	-9.66±0.62	0.59±0.024	0.998	25.00±0.186	HS
Zn.Asn.Leu	-4.28±1.24	0.523±0.068	0.983	17.75±0.57	S
Ni.Leu	-4.24±0.72	0.43±0.032	0.994	21.50±0.334	S
Ni.Cys.Leu	-13.20±2.44	0.74±0.098	0.982	24.50±0.585	HS

Table (3.52) Mean, standard deviation, correlation coefficient and sensitivity of amino acid complexes Vs *Enterococcus faecalis*:

Complex	Carve data			x′±SD	Sensitivity
	A ± Error	B ± Error	R		
Co.Gly	-3.4±0.077	0.70±0.07	0.989	12.00±0.45	R
Co.Ser	-5.77±1.46	0.74±0.099	0.982	14.50±0.585	I
Co.Asp	-6.39±0.87	0.86±0.065	0.994	13.25±0.334	I
Co.Arg	-7.92±1.15	1.23±0.11	0.992	10.50±0.392	R
Cu.Gly	-2.68±0.42	0.30±0.016	0.997	25.50±0.23	HS

Table (3.53) Mean, standard deviation, correlation coefficient and sensitivity of amino acid complexes Vs *klebsiella pneumonia*:

Complex	Carve data			x′±SD	Sensitivity
	A ± Error	B ± Error	R		
Au (Asn.Gly)	5±0.4743	2.85±0.086	0.999	24.25±0.3873	HS
Au (Cys.Ser)	11±0.4743	1.150.0866	0.994	17.25±0.3873	S
Fe(Gly)	-3.08±1.50	0.52±0.09	0.969	15.50±0.78	I
Fe(Arg+Asp)	-3.988±0.84	0.68±0.061	0.991	13.25±0.40	I
Fe(Arg+Asp+Ser)	-3.63±0.57	0.73±0.047	0.995	11.75±0.285	R
Zn.Cys	-6.00±0.00	0.50±0.00	1	22.00±0.00	S
Zn.Asn.Leu	-6.47±0.635	0.38±0.02	0.997	30.00±0.24	HS
Ni.Leu	-5.34±0.623	0.41±0.02	0.996	25.00±0.26	HS
Ni.Cys.Leu	-15.42±2.73	0.74±0.098	0.982	27.50±0.58	HS
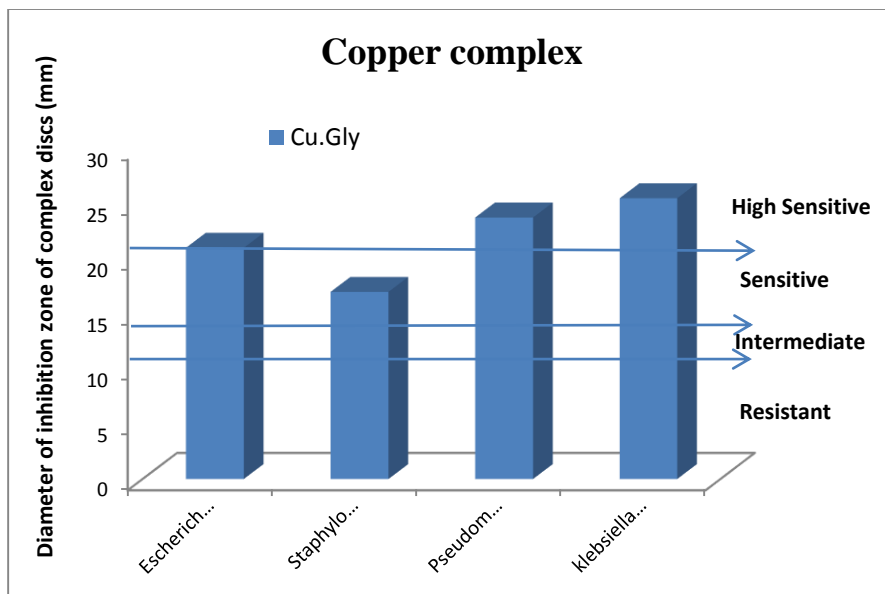
Figure (3.50): Antibacterial sensitivity pattern of the test bacteria against Cu.gly complex.
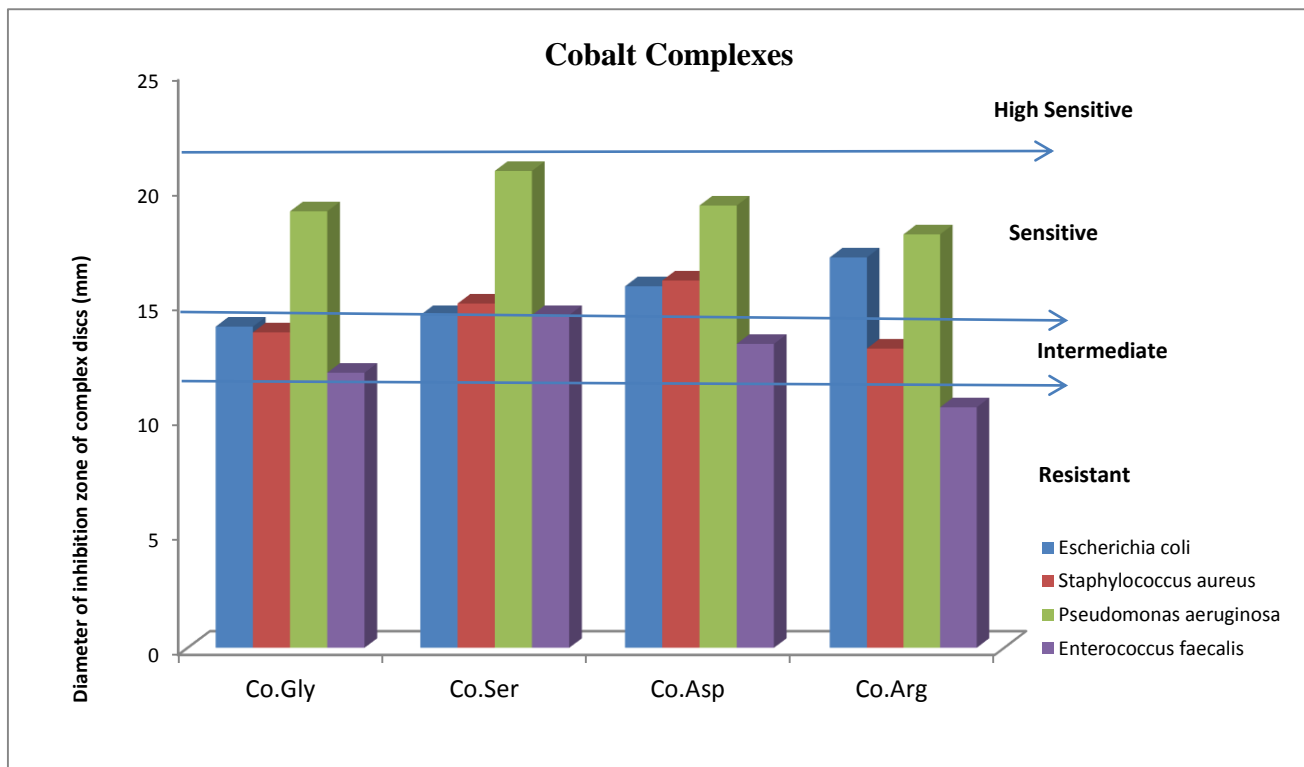
Figure (3.51): Antibacterial sensitivity pattern of the test bacteria against Cobalt complexes.

188
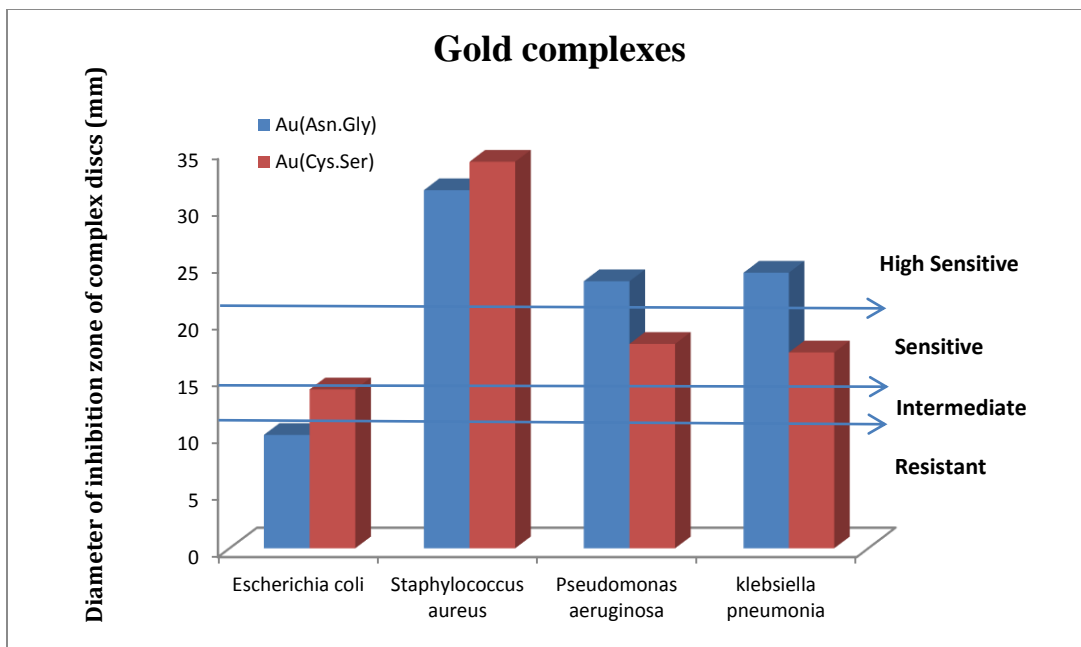
Figure (3.52): Antibacterial sensitivity pattern of the test bacteria against gold complexes.
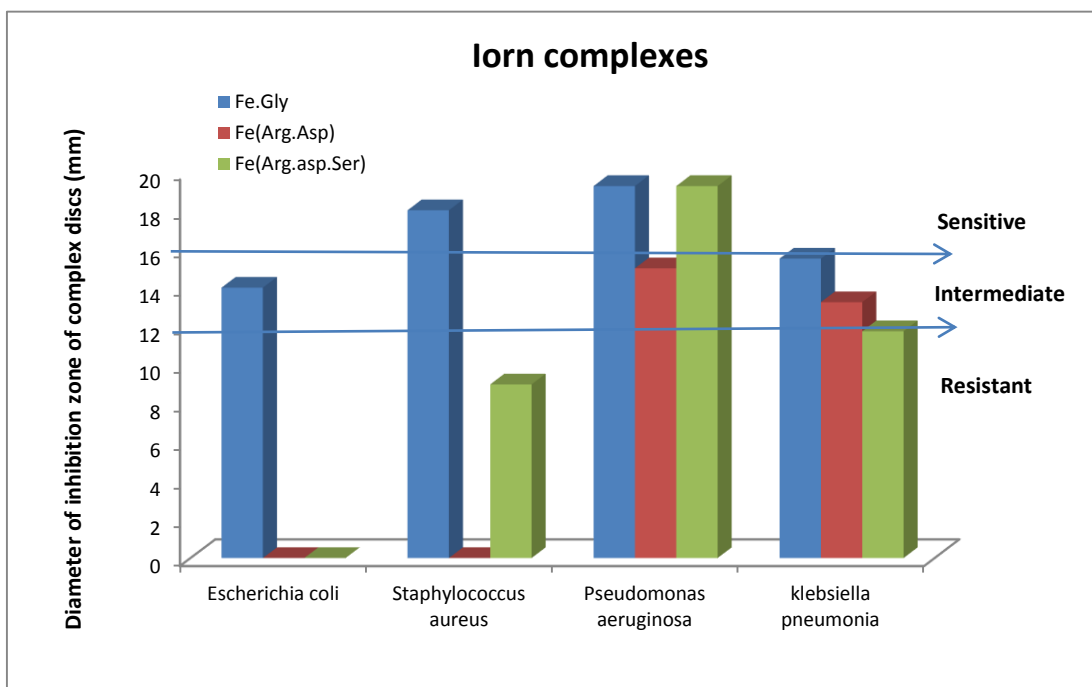
Figure (3.53): Antibacterial sensitivity pattern of the test bacteria against Iron complexes.
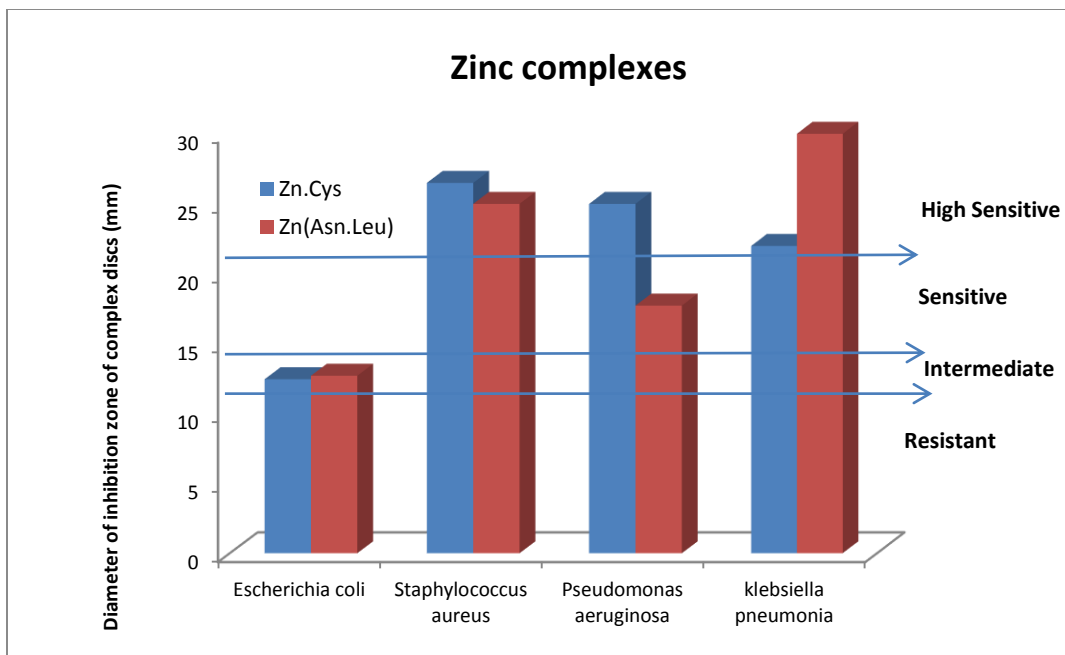
Figure (3.54): Antibacterial sensitivity pattern of the test bacteria against Zinc complexes.
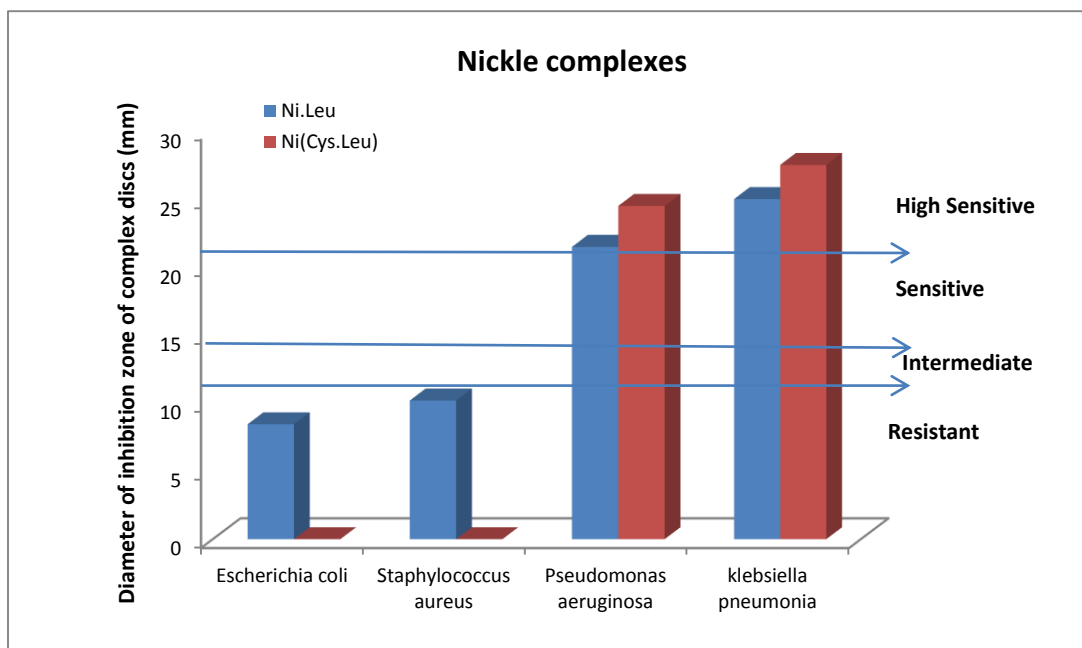
Figure (3.55): Antibacterial sensitivity pattern of the test bacteria against Nickle complexes.

3.9 Conclusion

Fourteen amino acid complexes of $[M(L)_2]Cl$ types of Cu (II) and Fe (III) ions with glycine, Fe.Gly and Cu.Gly, respectivly, Co (II) ion with glycine, serine, arginine, and aspartic acid, Co.Gly, Co.Ser, Co.Arg, Co.Asp, respectively, Ni (II) ion with Lucien, Ni.Leu, and Zn (II) ion with cysteine, Zn.Cys, and mixed amino acid ligands $[M(L)(L')]Cl$ types of Au (III) ion with asparagine+glycine, and cysteine+serine, Fe (III) ion with arginine+aspartic acid, Ni (II) ion with cysteine+leucin, and Zn (II) ion with asparagine+Lucien, Au.Asn.Gly, Au.Cys.Ser, Fe.Arg.Asp, Ni.Cys.Leu, , and Zn.(Asn+Leu), respectivly, and mixed amino acid ligands $[M(L)(L')(L'')]$ types of Co (II), Au (III), Fe (III), Cu (II), Ni (II), and Zn (II) ion $[M(L)_2]Cl$, $[M(L)(L')]Cl$, and $[M(L)(L')(L'')]$ types of Fe (III) ion with arginine+aspartic acid+serine Fe.Arg.Asp.Ser, were synthesized, by the reaction of a Metal Salts with a Ligands by 1:2, 1:1:1, and 1:1:1:1 molar ratio in basic media as catalyst to remove the proton from amino acid, and characterized by PCEDX, TGA, FTIR, UV/Vis, XRD, and electrical conductivity measurement.

Thermal gravimetric analysis of Co (II) complexes showed weight loss between 120-180°C, which equivalent to two moles of crystal water that agreement with result obtained from IR, EDX, and XRD analysis. The Electrical conductivity of the complexes can provide information about the number of ions involvement in the complexes in solution, which can give us a clear image about the structural geometry of the complexes, that showed the four complexes of Co (II) are non-electrolyte solution, (neutral complex) this indicated that coordination to Co through the two COO^- and two NH_2 groups, this proposal was supported by the IR-spectra of the complexes. As result as the complexes form are $[Co(gly)_2.(H_2O)_2]$ (a), $[Co(Ser)_2.(H_2O)_2]$ (b), $[Co(Asp)_2.(H_2O)_2]$ (c), $[Co(Arg)_2.(H_2O)_2]$ (d), respectively. This explained in Figure (3.63).
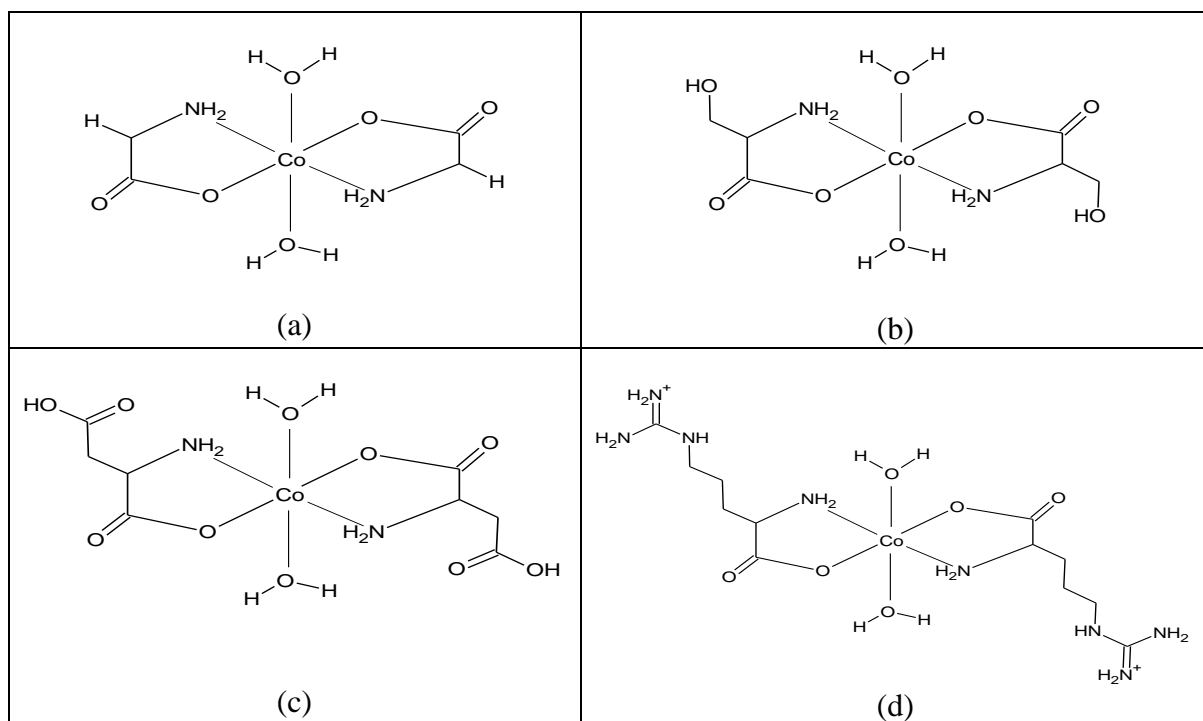
Figure (3.56): Structure of $[Co(Gly)_2.(H_2O)_2]$ (a), $[Co(Ser)_2.(H_2O)_2]$ (b), $[Co(Asp)_2.(H2O)_2]$ (c), and $[Co(Arg)_2.(H_2O)_2]$ (c) complex

Fe (III) complexes, the thermal gravimetric analysis of Fe.Gly and Fe.Arg.Asp complexes showed weight loss between 110-180°C, which equivalent to two moles of crystal water that agreed with result obtained from IR, EDX, and XRD analysis. And the electrical conductivity measurements were recorded of 2 mg/ml of complex solutions, showed the Fe.Gly and Fe.Arg.Asp complexes are electrolyte solution, 1:1 molar ratio this indicated that coordination to Fe (III) through the two COO⁻ and two NH_2 groups, and one mole of chloride ion containing out of the coordination sphere, and Fe.Arg.Asp.Ser complex is non-electrolyte solution, (neutral complex) this indicated that coordination to Fe through the two COO⁻ and two NH_2 groups, this proposal was supported by the IR-spectra, PCEDX, and XRD analysis of the complexes. As a result as the complexes form are $[Fe(gly)_2.(H_2O)_2]Cl$ (a), $[Fe(arg)(asp).(H_2O)_2]Cl$ (b), and $[Co(arg)(asp)(ser)]$ (c), This explained in Figure (3.64).

192
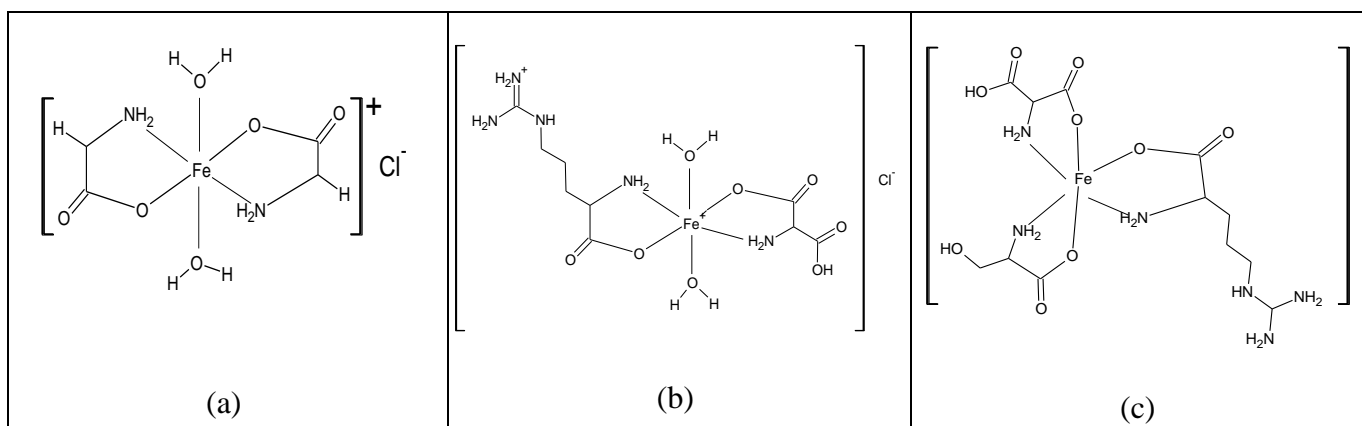
Figure (3.57): Structure of [Fe(Gly)$_2$.(H$_2$O)$_2$]Cl (a), [Fe(Arg)(Asp).(H$_2$O)$_2$]Cl, (b) [Fe(Arg)(Asp)(Ser)] (c), complexes

The two complexes of Au (III) are electrolyte solution, 1:1 molar ratio this indicated that coordination to Au $^{(III)}$ through the two COO$^-$ and two NH$_2$ groups, and one mole of chloride ion out of the coordination sphere, this proposal was supported by the IR-spectra, EDX, and XRD analysis of the complexes. As result as the complexes form take are squire planer geometry with two molecule of amino acid act as bidentate and one chloride ion lie out of coordination sphere, the two complexes are [Au(asn)(gly)]Cl (a), and [Au(cys)(Ser)]Cl (b). This explained in Figure (3.65).
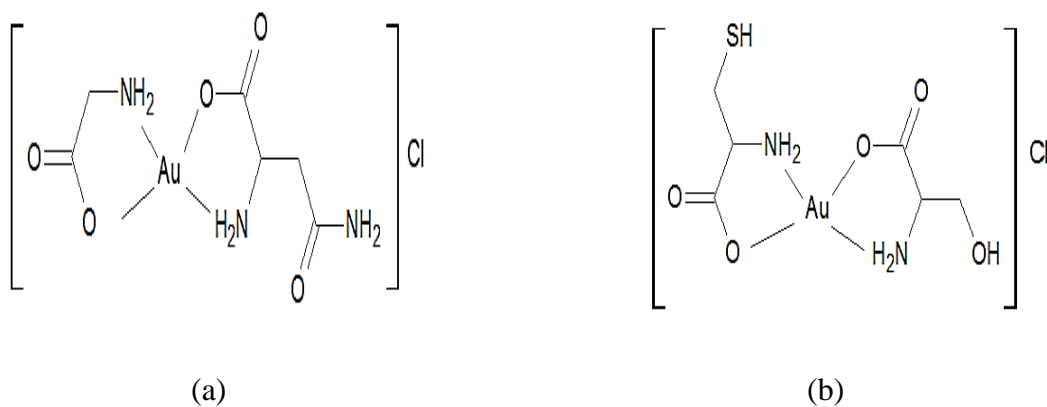
Figure (3.58) Structure of [Au(asn)(gly)]Cl (a), and [Au(cys)(Ser)]Cl (b) complexes

The Zn.cys and Zn.(Asn.Leu) complexes are non-electrolyte solution, (neutral complex) this indicated that coordination to Zn through the two COO$^-$ and two NH$_2$ groups, and absent peak of crystal water in thermal study, that indicate the two complexes have not contain water molecules, this proposal

193

was supported by the IR-spectra of the complexes. As result as the complexes are a tetrahedral geometry, which form are [Zn(cys)$_2$] (a), and [Zn(Asn).(Leu)] (b), respectively. This explained in Figure (3.66).
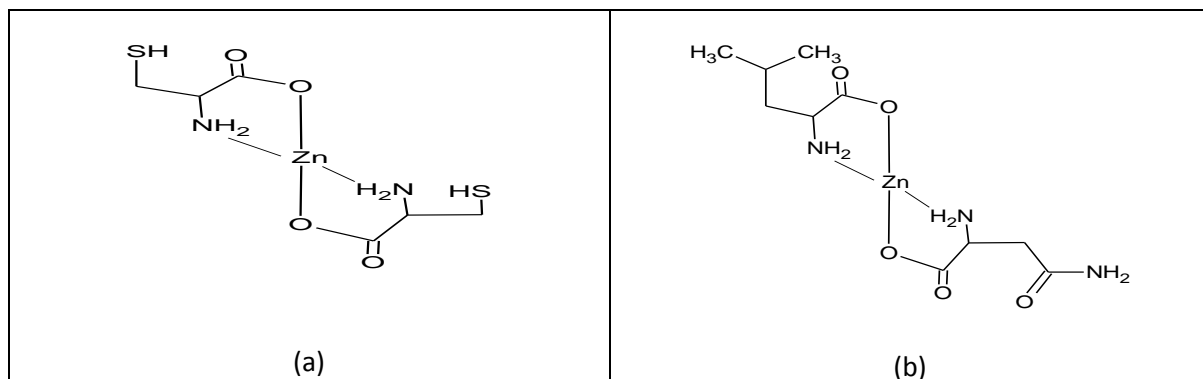
Figure (3.59) Structure of Zn(cys)$_2$, (a), and Zn(Asn)(Leu), (b) complex

The Ni.Leu, and Ni.Cys.Leu complexes are non-electrolyte solution, (neutral complex) this indicated that coordination to Ni through the two COO$^-$ and two NH$_2$ groups, this proposal was supported by the IR-spectra of the complexes. As a result as the complexes form are [Ni(leu)$_2$.(H$_2$O)$_2$] (a), and [Ni(cys)(leu).(H$_2$O)$_2$] (b), respectively. This explained in Figure (3.67).
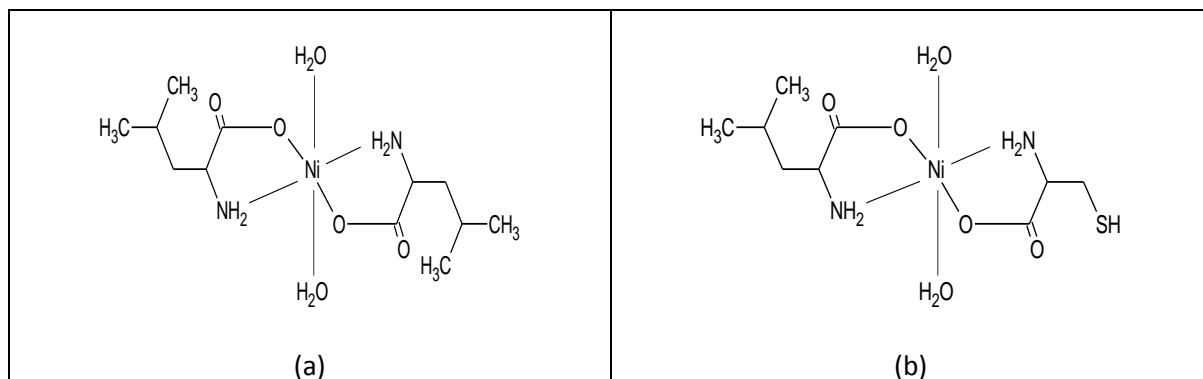
Figure (3.60) explain structure of Ni.Leu, (a), and Ni.Cys.Leu, (b) complex

Thermal gravimetric analysis of Cu (II) complex showed weight loss between 120-180°C, which equivalent to two moles of crystal water that agreement with result obtained from IR, PCEDX, and XRD analysis. The Electrical conductivity of the complexes showed the Cu (II) complex is non-electrolyte solution, (neutral complex) this indicated that coordination to Cu through the two COO⁻ and two NH_2 groups, this proposal was supported by the IR-spectra of the complexes. As result as the complexes form is [Cu(gly)$_2$.(H$_2$O)$_2$], This explained in Figure (3.68).
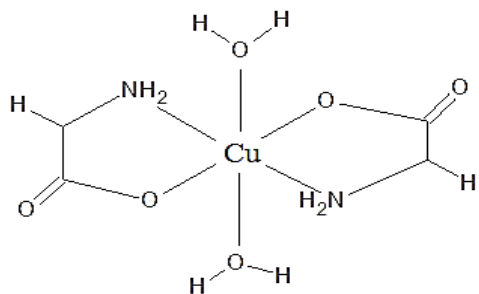
Figure (3.61) explain structure of Cu.gly complex

3.10 Recommendation

These compounds lead us to discovery novel and new antibiotics, that have no side effects and very safer for all patients. Therefore I want to highlight these compounds, to the competent authorities in order to upgrade the traditional antibiotics and replace them with antibiotics very safe for human health.

References:

1. Kabbani A.T., Hammud H.H., and Ghannoum A.M., (2007). Preparation and antibacterial activity of copper and cobalt complexes of 4-chloro-3-nitrobenzoate with a nitrogen donor ligand. Chem Pharm Bull 55(3):**446-450**.

2. Johari R., Kumar G., Kumar D., and Singh S., (2009). Synthesis and antibacterial activity of M (II) Schiff-Base complex. *J Ind Council Chem* 26(1):**23-27**.

3. S.J. Price, and P.J.Sadler, (1973). Gold drugs in frontiers in bioinorganic chemistry, Xavier, A.V., (Ed), VC+1 Publ. Weinhein, **pp376-388**.

4. O. M. Dhubhghaill and P. J. Sadler, (1993). Gold complexes in chemotherapy in metal complexes in chemotherapy, B. K. keppler (Ed) VCH Publ. Weinhein, pp **225-250**.

5. K. C. Dash and H. Schmidbar, (1982), Metal ions in biological systems, H. Sigel. Ed. Marcel Dekker, New York, p.**179**ff.

6. C. F. Shaw, (1999). Progress in chemistry, biochemistry and technology, Schmidbau r. H. Ed. Wiley, New York, P.259ff

7. P. J. Sadler and R. E. Sue, (1994). The chemistry of gold drugs", B.K. Keppler (Ed) VCH Publ. Weinhein, PP **115-127**.

8. V. Mariana, (2012), Structural studies of metal complexes with amino acids and biomarkers for use in diagnostic", Ph.D thesis, Babes-Bolyai University, Romania, website www.ubbcluj.ro

9. H. C. Freeman, (1973). Metal complexes of aminoacids and peptides, inorganig biochemistry, Eichhorn,G. L., Ed., Elsevier, Scientific, Amsterdam, (1), PP **121-166**.

10. H. Hossain, M. S. Islam, A. and Alam, T. Saltan, (2013) Synthsis, physicochemical studies and antimicrobial screening of metal complexes of Fe (III) and Au (III) with aminoacids, *Inter. J. Sci. and Tech.* Res., 2, 7.

11. N. Manav, A. K. Mishra and N.K. Kaushik, (2005), In vitroantitumour and antibacterial studies of some Pt(IV) dithiocarbamate complexes, Spectrochim Acta. Part A Molecular and Biomolecular spectroscopy, 65(1)**, 32**.

12. G.Hogrth, (2012), Metal dithiocarbamate complexes: chemistry and biological activity, Mini Rev. Med. Chem., 12(12), pp**1202-1215**.

13. K. Rajasekar, R. T. Ramchandramoorthy and A. Paulraj, (2012), Microwave assisted synthesis, structural characterization and biological activities of 4-aminoantipyrine and thiocyanate mixed ligand complexes, *Res.J. Pharmaceutical Sci.,* 1(4), pp **22-27**.

14. R. Bentley, (2005), Biochemistry and Molecular Biology Education, **33(4), 274**.

15. L. Roman, and O. Bârzu, (1979), Implicate biomedical combination complexes, Editor Dacia, p. **82**.

16. H. R. Kaback, (1997). A molecular mechanism for energy coupling in a membrane transport protein, the lactose permease of *Escherichia coli. Proc. Natl. Acad. Sci.,* **94**, 5539.

17. H. D. Ashmead, The Poles of Amino Acid Chelates in Animal Nutrition, Park Ridge Noyes 1993, **p. 457.**

18. R. Power, and K.Horgan, (2000). Biological chemistry and absorption of inorganic and organic metals, European Bioscience Centre, *Alltech. Inc., Dunboyne, Co. Meath, Ireland*.

19. M. Cátia Pereira, E. Beatriz Cabilio Guth, M. E. Sbrogio-Almeida, and A. Beatriz Castilho, (2001), Antibody response against *Escherichia coli* heat-stable enterotoxin expressed as fusions to flagellin. Microbiology, **147**, **861**.

20. Yek, E. C., Cintan, S., Topcuoglu, N., Kulekci, G., Issever, H., and Kantarci, A., (2010), Efficacy of amoxicillin and metronidazole combination for the management of generalized aggressive periodontitis. *J. Periodontol.* **81, 964–974**.

21. Ghayoumi, N. (2001).The use of metronidazole in the treatment of periodontal diseases. *J. West. Soc. Periodontol. Periodontal Abstr.* **49, 37–40**.

22. Bricker, S. L., Langlais, R.P.; and Miller, C.S. Oral Diagnosis, Oral Medicine and Treatment Planning, 2nded.; Hamilton, Ont.: London, UK, 2002; **p. 854**.

23. Katzung, B. G., Masters, S. B., and Trevor, A. J. (2012) Basic and Clinical Pharmacology, 12th ed., *Mc-Graw Hill Medical, Minneapolis, MN, USA*.

24. Klokkevold, P. R., Newman, M. G., Takei, H., Carranza, and F. A. Carranza's (2002), Clinical Periodontology, 9th ed.; *Saunders: Readfield, ME, USA*.

25. Kapoor, A., Malhotra, R., Grover, V., and Grover, D. (2012), Systemic antibiotic therapy in periodontics. *Dent. Res. J.* **9, 505–515.**

26. Pavia, M., Nobile, C. G., and Angelillo, I. F. (2003), Meta-analysis of local tetracycline in treating chronic periodontitis. *J. Periodontol*. **7, 916–932.**

27. Gilbert, A. (2004) Local tetracycline is an effective adjunct in the treatment of chronic periodontitis. Avid. Based Dent. **5, 67**.

28. Sinha, S., Kumar, S., Dagli, N., and Dagli, R.J. (2014), Effect of tetracycline HCl in the treatment of chronic periodontitis A clinical study. *J. Int. Soc. Prev. Community Dent*. **4, 149–153.**

29. Greenstein, G. (1993). The role of metronidazole in the treatment of periodontal diseases. *J. Periodontol.* **64, 1–15**.

30. Loesche, W.J., Schmidt, E., Smith, B.A., Morrison, E.C.; Caffesse, R.; and Hujoel, P.P. (1991), Effects of metronidazole on periodontal treatment needs. *J. Periodontol.* **62, 247–257.**

31. C. W. B. Berichte, (1871), 4, 40; translated by G. B. Kauffman, Classics in Coordination Chemistry, Part 2, Dover. New York, 1976, **pp. 75-93,**

32. S. M. Jorgensen, and Z. Anorg. Chem., (1899), 19, 109; translated by G. B. Kauffman, Classics in Coordination Chemistry, Part 2, **pp. 94-164**.

33. A. Werner, Z. *Anorg. Chem*., (1893), 3, 267m, B erichte, (1907), 40, 4817; 1911,44, 1887; 1914,47, 3087, A. Werner and A. Miolati, Z. Phys. Chem*.,* 1893, 12, 35; 1894, 14, 506, all translated by G. B. Kauffman, Classics in Coordination Chemistry, Part I , New York, 1968.

34. L. Pauling, *J. Chem. Soc.,* 1948, 1461; The Nature of the Chemical Bond, 3rd ed., Cornell University Press, Ithaca*,* NY, 1960, pp**. 145-182.**

35. J. S. Griffith and L. E. Orgel, ligand field theory. Q. Rev. Chem*. Soc.,* 1957, XI, **381.**

36. N. N. G reenwood and A. Earnshaw, (1984), The larger numbers depend on how the number of donors in organometallic compounds is counted; some would assign smaller coordination numbers because of the special nature of the organic ligands. Chemistry of the Elements, Pergamon Press, Elmsford*,* NY, **p. 1077**.

37. Pauling. (1941).The Nature of the Chemical Bond, pp. **145-182.**

38. Griftith and Orgel, op. cit.; L. E. Orgel, An Introduction to Transition-Metal Chemistry, Methuen, London, 1960.

39. H. Bethe, (1929). Splitting of Terms in Crystals. Ann. Phys., 1929, **3, 133.**

40. J. H. Van Vleck, (1932). Theory of the Variations in Paramagnetic Anisotropy among Different Salts of the Iron Group. Phys. Rev., 1932, **41, 208.**

41. J. H. Van Vleck,(1935). Valance strength and the magnetism of complex salts. *J. Chem. Phys.*, **3, 807**.

42. L. P. auling, The Nature of the Chemical Bond, 3rd ed., Cornell University Press, Ithaca*, NY,* 1960, Chapter 5.

43. P. N. Figgis and R. S. Nyholm, Inorganic chemistry. *J. Chern. Soc.,* (1959), 338, J. S. Griffith and L. E. Orgel, Q. Rev. *Chern. Soc.,* (1957), XI, **381.**

44. H. Beth e, splitting of terms in crystals. *Ann. Phys*., (1929), **3, 133.**

45. J. H. VanVleck, Electronic structures of transition metal complexes. *J. Chem. Phys*., 1935, **3, 807.**

46. Gary L. Miessler Donald A. Tarr, (1999). Inorganic Chemistry, Third Edition, 706 p **577-581, 592-597, 645-650, 695-701.**

47. J. E. House, (2008), Inorganic Chemistry, 850 p **645-650**.

48. Williams & Wilkins, a Wolters, Richard A. Harvey, Denise R. Ferrier. (2011). computer graphics, Michael Cooper, Lippincott Biochemistry. 5th ed, **vol 519 p 1-3.**

49. P. Naik, (2012), Essentials of Biochemistry First Edition, **vol 451 p 44-48**.

50. Victor W. Rodwell, David A. Bender, Kathleen M. Botham, Peter J. Kennelly, P. Anthony Weil, (2018). Harper Biochemistry, Thirtieth Edition, **vol 817 p 20-22.**

51. Nomenclature and Symbolism for Amino Acids and Peptides. IUPAC-IUB Joint Commission on Biochemical Nomenclature. 1983. Archived from the original on 9 October 2008. Retrieved 5 March 2018.

52. https://en.oxforddictionaries.com/definition/glycine

53. R.H.A. Plimmer (1912) [1908]. R.H.A. Plimmer; F.G. Hopkins, eds. The chemical composition of the proteins. Monographs on biochemistry. Part I. Analysis (2nd Ed.). London: Longmans, Green and Co. p. 82. Retrieved January 18, 2010.

54. Braconnot, H., (1820). "Sur la conversion des matières animales en nouvelles substances par le moyen de l`acide sulfurique" [On the conversion of animal materials into new substances by means of sulfuric acid]. *Annals Chem. de Phy*., 2nd series (in French). 13: 113–125. ; see **p. 114.**

55. MacKenzie, C., (1822). One Thousand Experiments in Chemistry: With Illustrations of Natural Phenomena; and Practical Observations on the Manufacturing and Chemical Processes at Present Pursued in the Successful Cultivation of the Useful Arts …. Sir R. Phillips and Company.

56. Boussingault (1838). "Sur la composition du sucre de gélatine et de lácide nitro-saccharique de Braconnot" [On the composition of sugar of gelatine and of nitro-glucaric acid of Braconnot]. *Comptes rendus (in French).* **7: 493–495.**

57. Horsford, E. N. (1847). Glycocoll (gelatine sugar) and some of its products of decomposition. *The American Journal of Science and Arts. 2nd series*. **3: 369–381.**

58.   Ihde, A. J. (1970). The Development of Modern Chemistry. Courier Corporation. ISBN 9780486642352.

59.   B. Jacob (1848). Jahres-Bericht über die Fortschritte der Chemie und Mineralogie (Annual Report on the Progress of Chemistry and Mineralogy). **vol. 47**. Tübigen, (Germany): Laupp. p. 654. From p. 654: "Er hat dem Leimzucker als Basis den Namen Glycocoll gegeben. 60.   Nye, Mary Jo (1999). Before Big Science: The Pursuit of Modern Chemistry and Physics, 1800-1940. Harvard University Press. ISBN 9780674063822.

61.   "glycine". Oxford Dictionaries. Retrieved 2015-12-06.

62.   Cahours, A. (1858). "Recherches sur les acides amidés, [Investigations into aminated acids]. Comptes rendus (in French). **46: 1044–1047**.

63.   O. Nduka, (2016). Modern Industrial Microbiology and Biotechnology. *CRC Press*. ISBN 9781439843239.

64.   Ingersoll, A. W., Babcock, S. H. (1932). Hippuric acid. Organic Syntheses. 12: 40.; Collective Volume, **2, p. 328**

65.   Wiley (2007). Kirk-Othmer Food and Feed Technology, 2 Volume Set. *John Wiley & Sons*. ISBN 9780470174487.

66. "Glycine Conference (prelim)". USITC. Archived from the original on 2012, Retrieved 2014.

67.   Drauz K., Grayson I., Kleemann A., Krimmer HP., Leuchtenberger, W., and Weckbecker C., (2007) Amino Acids in Ullmann's Encyclopedia of Industrial Chemistry, Wiley-VCH, Weinheim. doi:10.1002/14356007.a02_057.pub2

68. Hart, J. Roger (2005) "Ethylenediaminetetraacetic Acid and Related Chelating Agents" in Ullmann's Encyclopedia of Industrial Chemistry, Wiley-VCH, Weinheim.

69. Meléndez-Hevia, E., De Paz-Lugo, P., Cornish-Bowden, A., and Cárdenas M. L. (December 2009). A weak link in metabolism: the metabolic capacity for glycine biosynthesis does not satisfy the need for collagen synthesis. *Journal of Biosciences*. **34 (6): 853–72.**

70. Nelson, D. L.; and Cox, M. M. (2005), Principles of Biochemistry (4th ed.), New York: W. H. Freeman, pp. 127, 675–77, 844, 854, ISBN 0-7167-4339-6

71.   Hahn RG (1993). Dose-dependent half-life of glycine. Urological Research. 21 (4): 289–291. doi:10.1007/BF00307714. PMID 8212419.

72. Szpak, P. (2011). Fish bone chemistry and ultrastructure: implications for taphonomy and stable isotope analysis. *Journal of Archaeological Science*. **38(12):3358–3372.**

73. Liu Y., Zhang J. (2000). Recent development in NMDA receptors. *Chinese Medical Journal*. 74. Yusuke Shibui, Tadashi Miwa, Mayumi Yamashita, Keigi Chin, and Terutaka Kodama Yusuke Shibui, Safety (MSDS) data for glycine. The Physical and Theoretical Chemistry Laboratory Oxford University. 2005. Retrieved 2006.

75. Glycine from Japan and Korea (PDF). U.S. International Trade Commission. 2008. Retrieved 2014.

76. Kurtis F., Kamal P., Gregory L., Bill Willis, (2017). "Glycine Research Analysis". Examine.com.

77. Marilyn R. Abbott. (2007). Notice of Preliminary Determination of Sales at Less Than Fair Value: Glycine from India Federal Register **72: 62827.**

78. Stahl, S. S.; and Alsters, P. L. (2016). Liquid Phase Aerobic Oxidation Catalysis: Industrial Applications and Academic Perspectives. John Wiley & Sons. ISBN 9783527690152.

79. Glycine FCC IV | 56-40-6 | $C_2H_5NO_2$ | T&J Chemicals. Speciality Chemicals Supply | T&J Chemicals. Retrieved 2018.

80. Eaton S. J., Harakas G. N., Kimball R. W., Smith J. A., Pilot K. A., Kuflik M. T., and Bullard J. M., (2014). Formulation and Combustion of Glycerol–Diesel Fuel Emulsions. Energy & Fuels. **28 (6): 3940–3947**. doi:10.1021/ef500670d. ISSN 0887-0624.

81. Kvenvolden, K. A.; Lawless, J.; Pering, K.; Peterson, E.; F. Jose; P. Cyril; Kaplan, I. R.; and M. Carleton (1970). "Evidence for extraterrestrial amino-acids and hydrocarbons in the Murchison meteorite". *Nature*. 228 (5275): 923–926. Bibcode:1970Natur.228..923K. doi:10.1038/228923a0. PMID 5482102.

82. Reuters (2009). "Building block of life found on comet - Thomson Reuters 2009". Retrieved 2009.

83. European Space Agency (2016). "Rosetta's comet contains ingredients for life". Retrieved 2016.

84. Snyder L. E., Lovas F. J., and Hollis J. M., (2005). "A rigorous attempt to verify interstellar glycine". *Astrophys J*. 619 (2): 914–930. arXiv:astro-ph/0410335. Bibcode:2005ApJ...619..914S. 85. Staff. "Organic Molecule, Amino Acid-Like, Found In Constellation Sagittarius 27 March 2008 - Science Daily". Retrieved 2008.

86. David B. Hagtowiz "National Nutrient Database for Standard Reference". U.S. Department of Agriculture. Archived from the original on 2015. Retrieved 2009.

87. Nomenclature and symbolism for amino acids and peptides (IUPAC-IUB Recommendations (1983)", Pure Appl. Chem., **56 (5): 595–624, 1984**, *doi*:*10.1351/pac198456050595.*

88. Ueber die Bestandtheile der Seide. *Journal für praktische Chemie* **96**.

89. Serine. The Columbia Encyclopedia 6th ed. encyclopedia.com. Retrieved 22 October 2012.

90. Stryer L (1988). Biochemistry (3rd ed.). New York: W.H. Freeman. p. 580. ISBN 978-0-7167-1843-7.

91. Lehninger A.L., Nelson D.L., and Cox M.M., (2000). Principles of Biochemistry (3rd ed.). New York: W. H. Freeman. ISBN 1-57259-**153-6**.

92. Drauz K., Grayson I., Kleemann A., Krimmer H., Leuchtenberger W., and Weckbecker C., (2005). "Amino Acids". Ullmann's Encyclopedia of Industrial Chemistry. Weinheim: Wiley-VCH. doi*:*10.1002/14356007.a02_057.pub2.

93. Carter H. E., West H. D., (1940). "dl-Serine". Org. Synth., 20: 81.

94. Liu Y., Hill R. H., Arhem P., and von Euler G. (2001). "NMDA and glycine regulate the affinity of the Mg^{2+} block site in NR1-1a/NR2A NMDA receptor channels expressed in Xenopus oocytes". Life Sciences. **68 (16): 1817–26.**

95. Mothet J. P., Parent A. T., Wolosker H., Brady R. O., Linden D. J.,1 Ferris CD, Rogawski MA, and Snyder S.H., (2000). "D-serine is an endogenous ligand for the glycine site of the N-methyl-D-aspartate receptor*"*. Proceedings of the National Academy of Sciences of the United States of America. **97(9): 4926–31.**

96. Takarada T., Hinoi E., Takahata Y., and Yoneda Y., (May 2008). "Serine racemase suppresses chondrogenic differentiation in cartilage in a Sox9-dependent manner". *Journal of Cellular Physiology.* **215 (2): 320–8.**

97. Ma M. C., Huang H. S., Chen. Y.S., and Lee S. H., (Nov 2008). "Mechanosensitive N-methyl-D-aspartate receptors contribute to sensory activation in the rat renal pelvis". Hypertension. **52 (5): 938–44**.

98. Ghasemi M., Rezania F., Lewin J., Moore K. P., and Mani A. R. (Jun 2010). "d-Serine modulates neurogenic relaxation in rat corpus cavernosum". Biochemical Pharmacology. **79 (12): 1791–6.**

99. de Koning T.J., (April 2006). "Treatment with amino acids in serine deficiency disorders". *Journal of Inherited Metabolic Disease*. **29 (2): 347–351.**

100. Tabatabaie L., Klomp L. W., Berger R., and de Koning T. J., (March 2010). "L-serine synthesis in the central nervous system: a review on serine deficiency disorders". Mol Genet Metab. **99 (3): 256–262.**

101. Balu D. T., Li Y., Puhl M. D., Benneyworth M. A., Basu A. C., Takagi S., Bolshakov V. Y., and Coyle J. T., (Jun 2013). "Multiple risk pathways for schizophrenia converge in serine racemase knockout mice, a mouse model of NMDA receptor hypofunction". Proceedings of the National Academy of Sciences of the United States of America. **110 (26): 2400–9.**

102. Dunlop R. A., Cox P. A., Banack S. A., and Rodgers K. J., (2013), "The non-protein amino acid BMAA is misincorporated into human proteins in place of L-serine causing protein misfolding and aggregation". PLOS ONE. **8 (9): 75376.**

103. Singh S. P., and Singh V., (Oct 2011). "Meta-analysis of the efficacy of adjunctive NMDA receptor modulators in chronic schizophrenia". *CNS Drugs*. **25 (10): 859–85**.

104. Madeira C., Lourenco M. V., Vargas-Lopes C., Suemoto C. K., Brandão C. O., Reis T., Leite R. E., Laks J., Jacob-Filho W., Pasqualucci C. A., Grinberg L. T., Ferreira S. T., and Panizzutti R., (May 5, 2015). "d-serine levels in Alzheimer's disease: implications for novel biomarker development". Translational Psychiatry. **5 (5): e561.**

105. IUPAC-IUBMB Joint Commission on Biochemical Nomenclature. "Nomenclature and Symbolism for Amino Acids and Peptides". Recommendations on Organic & Biochemical Nomenclature, Symbols & Terminology etc. Archived from the original on 2007. Retrieved 2007.

106. Glasel, J. A.; and Deutscher, M. P. (1995). Introduction to Biophysical Methods for Protein and Nucleic Acid Research. *Academic Press*. p. 456. ISBN 9780080534985.

107. Tapiero H., Mathé G., Couvreur P., and Tew KD (2002). "L-Arginine". (review). Biomedicine & Pharmacotherapy. **56 (9): 439–445.**

108. Wu G., Jaeger L. A., Bazer F. W., and Rhoads J. M., (2004). "Arginine deficiency in preterm infants: biochemical mechanisms and nutritional implications". (review). *The Journal of Nutritional Biochemistry*. **15 (8): 442–51.**

109. "Drugs and Supplements Arginine". Retrieved 2015.

110. S. Annalynn (1998). Dietitian's Handbook of Enteral and Parenteral Nutrition. Jones & Bartlett Learning. p. 76. ISBN 9780834209206.

111. Apel, Frank (2015). "Biographie von Ernst Schulze" (PDF). Retrieved 2017.

112. S. Ernst; and S. Ernst (1887). "Ueber das Arginin" [On arginine]. *Zeitschrift für physiologische Chemie.* 11 (1–2): **43–65.**

113. S. Ernst; and W. Ernst (1897). "Ueber ein Spaltungsproduct des Arginins" [On a cleavage product of arginine]. Berichte der Deutschen Chemischen Gesellschaft (in German). 30: 2879–2882. The structure for arginine is presented on p. **2882.**

114. Schulze, E.; and Winterstein, E. (1899). "Ueber die Constitution des Arginins" [On the constitution of arginine]. Berichte der Deutschen Chemischen Gesellschaft (in German). 32: **3191–3194.**

115. Cohen, J. B. (1919). Organic Chemistry for Advanced Students, Part 3 (2nd ed.), New York, USA: Longmans, Green & Co. **p. 140.**

116. Sörensen, S.P.L. (1910). "Über die Synthese des dl-Arginins (α-Amino-δ-guanido-n-valeriansäure) und der isomeren α-Guanido-δ-amino-n-valeriansäure"" [On the synthesis of racemic arginine (α-amino-δ-guanido-n-valeric acid) and of the isomeric α-guanido-δ-amino-n-valeric acid]. Berichte der Deutschen Chemischen Gesellschaft (in German). **43: 643–651.**

117. Ignarro, L. J., (2000). Nitric Oxide: Biology and Pathobiology. Academic Press. **p. 189.** 118. Borlase, B. C. (1994). *Enteral Nutrition.* Jones & Bartlett Learning. **p. 48.**

119. F. l. R. Allan; and B. Stephanie (2012). A Biochemical Approach to Nutrition. Springer Science & Business Media. p. 45. ISBN 9789400957329.

120. Nutrient Requirements of Dogs. National Academies Press. 1985. **p. 65.**

121. W. Ann; and B. Kara (2015). Nutrition and Disease Management for Veterinary Technicians and Nurses. *John Wiley & Sons.* p. 232. ISBN 9781118811085.

122. Spano, M. A.; Kruskall, L. J.; and Thomas, D. T. (2017). Nutrition for Sport, Exercise, and Health. Human Kinetics. p. 240. ISBN 9781450414876.

123. W. R. Ross; and Z. Sherma (2012). Bioactive Dietary Factors and Plant Extracts in Dermatology. Springer Science & Business Media. p. 75. ISBN 9781627031677.

124. Morris S.M., (2004). "Enzymes of arginine metabolism". (review). *The Journal of Nutrition.* 134 (10 Suppl): 2743S–2747S, discussion 2765S–2767S.

125. M. Claudio; and F. Christian (2015). The Metabolic Challenges of Immune Cells in Health and Disease. *Frontiers Media* SA. p. 17. ISBN 9782889196227.

126. Stechmiller J.K., Childress B., and Cowan L., (2005). "Arginine supplementation and wound healing". (review). Nutrition in Clinical Practice. **20 (1): 52–61.**

127.   Witte MB, Barbul A (2003). "Arginine physiology and its implication for wound healing". (review). Wound Repair and Regeneration. **11 (6): 419–23.**

128.   Andrew PJ, Mayer B (1999). "Enzymatic function of nitric oxide synthases". (review). Cardiovascular Research. **43 (3): 521–31.**

129.   Gokce N (2004). "L-arginine and hypertension". (review). *The Journal of Nutrition.* 134 (10 Suppl): 2807S–2811S, discussion 2818S–2819S. doi:10.1093/jn/134.10.2807S. PMID 15465790.

130.   Rajapakse NW, De Miguel C, Das S, and Mattson D.L., (2008). "Exogenous L-arginine ameliorates angiotensin II-induced hypertension and renal damage in rats". (primary). Hypertension. **52 (6): 1084–90.**

131.   Dong J.Y., Qin L.Q., Zhang Z., Zhao Y., Wang J., Arigoni F., and Zhang W. (2011). "Effect of oral L-arginine supplementation on blood pressure: a meta-analysis of randomized, double-blind, placebo-controlled trials". review. *American Heart Journal.* **162 (6): 959–965.**

132.   Mathews, C. K.,; Van Holde, K. E.; and Ahern, K. G. (2000). Biochemistry (3rd ed.). *San* Francisco, Calif.: Benjamin Cummings. **p. 180**. ISBN 0805330666. OCLC 42290721.

133.   Barnes, and Michael R. (2007). Bioinformatics for Geneticists: A Bioinformatics Primer for the Analysis of Genetic Data. John Wiley & Sons. **p. 326**. ISBN 9780470026199.

134.   Kleanthous, Colin (2000). Protein-protein Recognition. Oxford University Press. **p. 13**. 135. Griffiths, John R.; and Unwin, Richard D. (2016). Analysis of Protein Post-Translational Modifications by Mass Spectrometry. John Wiley & Sons. ISBN 9781119250883.

136.   U.S. National Library of Medicine (2009) Growth hormone stimulation test.

137.   Alba-Roth J., Müller O.A., Schopohl J., and von Werder K., (1988). "Arginine stimulates growth hormone secretion by suppressing endogenous somatostatin secretion". *The Journal of Clinical Endocrinology and Metabolism*. **67 (6): 1186–9.**

138.   Kanaley J.A., (2008). "Growth hormone, arginine and exercise". Curr Opin Clin Nutr Metab Care. **11 (1): 50–4.**

139.   Forbes S.C., Bell G.J., (2011). "The acute effects of a low and high dose of oral L-arginine supplementation in young active males at rest". Appl Physiol Nutr Metab*. **36 (3): 405–11.***

140.   Gui S., Jia J., Niu X., Bai Y., Zou H., Deng J., Zhou R., (2014). "Arginine supplementation for improving maternal and neonatal outcomes in hypertensive disorder of pregnancy: a systematic review". (review). *Journal of the Renin-Angiotensin-Aldosterone System*. **15 (1): 88–96.**

141. "Nomenclature and Symbolism for Amino Acids and Peptides". IUPAC-IUB *Joint Commission on Biochemical Nomenclature.* 1983. *Archived* from the original on 2008. Retrieved 2018.

142. G. Voet, Judith; W. Pratt, and Charlotte (2016). Fundamentals of biochemistry: life at the molecular level. ISBN 9781118918401. OCLC 910538334.

143. Berzelius J.J.*,* Öngren O.G., (1839). Traité de chimie (in French). 3. Brussels: A. Wahlen et Cie. p. 81. Retrieved (2015).

144. Plimmer R., (1912) [1908]. Plimmer R., Hopkins F., eds. The chemical composition of the proteins. Monographs on Biochemistry. Part I. Analysis (2nd ed.). London: Longmans, Green and Co. p. 112. Retrieved 2010.

145. "Nomenclature and symbolism for amino acids and peptides (IUPAC-IUB Recommendations 1983)", Pure Appl. Chem., **56 (5): 595–624**, 1984.

146. Dunn M.S., and Smart B.W., (1950). "DL-Aspartic Acid". Organic Syntheses. 30: 7.*;* Collective **Volume, 4, p. 55.**

147. Lehninger A. L., Nelson D. L., and Cox M.M., (2000). Principles of Biochemistry (3rd ed.). *New York: W. H. Freeman. ISBN* 1-57259-153-6.

148. Chen P.E., Geballe M.T., Stansfeld P.J., Johnston A.R., Yuan H., Jacob A.L., Snyder J.P., Traynelis S.F., Wyllie D.J., (2005). "Structural features of the glutamate binding site in recombinant NR1/NR2A N-methyl-D-aspartate receptors determined by site-directed mutagenesis and molecular modeling". Molecular Pharmacology. **67 (5): 1470–84.**

149. Ferrier, D. R. (2013). Biochemistry. Lippincott Williams & Wilkins. ISBN 9781451175622.

150. Cynober, L. A., (2003). Metabolic & Therapeutic Aspects of Amino Acids in Clinical Nutrition, Second Edition. *CRC Press*. ISBN 9780203010266.

151. Silva V.R., Belozo F.L., Micheletti T.O., Conrado M., Stout J.R., Pimentel G.D., and Gonzalez A.M., (2017). "β-hydroxy-β-methylbutyrate free acid supplementation may improve recovery and muscle adaptations after resistance training: a systematic review". Nutrition Research. **45: 1–9.**

152. Wilkinson D.J., Hossain T., Hill D.S., Phillips B.E., Crossland H., Williams J., Loughna P., Churchward-Venne T.A., Breen L., Phillips S.M., Etheridge T., Rathmacher J.A., Smith K., Szewczyk N.J., and Atherton P.J., (2013). "Effects of leucine and its metabolite β-hydroxy-β-methylbutyrate on human skeletal muscle protein metabolism". *The Journal of Physiology*. **591 (11): 2911–2923.**

153. Winter, Ruth (2009). A consumer's dictionary of food additives (7th ed.). New York: Three Rivers Press. ISBN 0307408922.

154. Institute of Medicine (2002). "Protein and Amino Acids". Dietary Reference Intakes for Energy, Carbohydrates, Fiber, Fat, Fatty Acids, Cholesterol, Protein, and Amino Acids. *Washington, DC:* The National Academies Press. **pp. 589–768.**

155. National Nutrient Database for Standard Reference. U.S. Department of Agriculture. Archived from the original on 2015. Retrieved 2009.

156. L. Combaret, (2008). Human Nutrition Research Centre of Clermont-Ferrand. "A leucine-supplemented diet restores the defective postprandial inhibition of proteasome-dependent proteolysis in aged rat skeletal muscle". *Journal of Physiology* 569, issue 2**, p. 489-499.**

157. Verhoeven S., Vanschoonbeek K., Verdijk L.B., Koopman R., Wodzig W.K., Dendale P., and van Loon L.J., (2009). "Long-term leucine supplementation does not increase muscle mass or strength in healthy elderly men". *The American Journal of Clinical Nutrition*. **89 (5): 1468–75.**

158. Hartman A.L., Santos P., O'Riordan K.J., Stafstrom C.E., and Marie Hardwick J. (2015). "Potent anti-seizure effects of D-leucine". Neurobiology of Disease. **82: 46–53.**

159. Fontana L., Cummings N.E., Arriola Apelo S.I., Neuman J.C., Kasza I., Schmidt B.A., Cava E., Spelta F., Tosti V., Syed F.A., Baar E.L., Veronese N., Cottrell S.E., Fenske R.J., Bertozzi B., Brar H.K., Pietka T., Bullock A.D., Figenshau R.S., Andriole G.L., Merrins M.J., Alexander C.M., Kimple M.E., and Lamming D.W., (2016). "Decreased Consumption of Branched-Chain Amino Acids Improves Metabolic Health". Cell Reports. **16 (2): 520–530.**

160. Lynch C.J., and Adams S.H., (2014). "Branched-chain amino acids in metabolic signalling and insulin resistance". *Nature Reviews. Endocrinology*. **10 (12): 723–36.**

161. Caron A., Richard D., Laplante M., (2015). "The Roles of mTOR Complexes in Lipid Metabolism". *Annual Review of Nutrition*. **35: 321–48.**

162. Cummings N.E., Williams E.M., Kasza I., Konon E.N., Schaid M.D., Schmidt B.A., Poudel C., Sherman D.S., Yu D., Arriola Apelo S.I., Cottrell S.E., Geiger G., Barnes M.E., Wisinski J.A., Fenske R.J., Matkowskyj K.A., Kimple M.E., Alexander C.M., Merrins M.J., and Lamming D.W., (2017). "Restoration of metabolic health by decreased consumption of branched-chain amino acids". *The Journal of Physiology*.

163. White P.J., Lapworth A.L., An J., Wang L., McGarrah R.W., Stevens R.D., Ilkayeva O., George T., Muehlbauer M.J., Bain J.R., Trimmer J.K., Brosnan M.J., Rolph T.P., and Newgard C.B, (2016). "Branched-chain amino acid restriction in Zucker-fatty rats improves muscle insulin sensitivity by

enhancing efficiency of fatty acid oxidation and acyl-glycine export". Molecular Metabolism. **5 (7): 538–51.**

164. Badawy A.A., Lake S.L., and Dougherty D.M. (2014). "Mechanisms of the pellagragenic effect of leucine: stimulation of hepatic tryptophan oxidation by administration of branched-chain amino acids to healthy human volunteers and the role of plasma free tryptophan and total kynurenines". *International Journal of Tryptophan Research*. **7: 23–32.**

165. Elango R., Chapman K., Rafii M., Ball R.O., and Pencharz P.B., (2012). "Determination of the tolerable upper intake level of leucine in acute dietary studies in young men". *The American Journal of Clinical Nutrition*. **96 (4): 759–67.**

166. Rasmussen B., Gilbert E., Turki A., Madden K., and Elango R., (2016). "Determination of the safety of leucine supplementation in healthy elderly men". Amino Acids. **48 (7): 1707–16**.

167. Etzel M.R., (2004). "Manufacture and use of dairy protein fractions". *The Journal of Nutrition*. **134 (4): 996S–1002S.**

168. Kim J.H., Lee C., Lee M., Wang H., Kim K., Park S.J., Yoon I., Jang J., Zhao H., Kim H.K., Kwon N.H., Jeong S.J., Yoo H.C., Kim J.H., Yang J.S., Lee M.Y., Lee CW., Yun J., O.h S.J., Kang J.S., Martinis S.A., Hwang K.Y., Guo M., Han G., Han J.M., and Kim S. (2017). "Control of leucine-dependent mTORC1 pathway through chemical intervention of leucyl-tRNA synthetase and RagD interaction". Nature Communications. **8 (1): 732.**

169. Jewell J.L., Russell R.C., and Guan K.L. (2013). "Amino acid signalling upstream of mTOR". *Nature Reviews Molecular Cell Biology*. **14 (3): 133–9.**

170. Sancak Y., Peterson T.R., Shaul Y.D., Lindquist R.A., Thoreen C.C., Bar-Peled L., and Sabatini D.M., (2008). "The Rag GTPases bind raptor and mediate amino acid signaling to mTORC1". Science. 320 (5882): **1496–501.**

171. Wolfson R.L., Chantranupong L., Saxton R.A., Shen K., Scaria S.M., Cantor J.R., and Sabatini D.M., (2016). "Sestrin2 is a leucine sensor for the mTORC1 pathway". Science. **351 (6268): 43–8.**

172. Saxton R.A., Knockenhauer K.E., Wolfson R.L., Chantranupong L., Pacold M.E., Wang T., Schwartz T.U., and Sabatini D.M., (2016). "Structural basis for leucine sensing by the Sestrin2-mTORC1 pathway". Science. **351 (6268): 53–8.**

173. Chantranupong L., Wolfson R.L., Orozco J.M., Saxton R.A., Scaria S.M., Bar-Peled L., Spooner E., Isasa M., Gygi S.P., and Sabatini D.M., (2014). "The Sestrins interact with gatro to negatively regulate the amino-acid-sensing pathway upstream of mTORC1". Cell Reports. **9 (1): 1–8.**

174. Wilson J.M., Fitschen P.J., Campbell B., Wilson G.J., Zanchi N., Taylor L., Wilborn C., Kalman D.S., Stout J.R., Hoffman J.R., Ziegenfuss T.N., Lopez H.L., Kreider R.B., Smith-Ryan A.E., and Antonio J., (2013). "International Society of Sports Nutrition Position Stand: beta-hydroxy-beta-methylbutyrate (HMB)". *Journal of the International Society of Sports Nutrition.* **10 (1): 6.**

175. Zanchi N.E., Gerlinger-Romero F., Guimarães-Ferreira L., de Siqueira Filho M.A., Felitti V., Lira F.S., Seelaender M., and Lancha A.H., (2011). "HMB supplementation: clinical and athletic performance-related effects and mechanisms of action". Amino Acids. **40 (4): 1015–1025.**

176. Kohlmeier M., (2015). "Leucine". Nutrient Metabolism: Structures, Functions, and Genes (2nd ed.). Academic Press. **pp. 385–388.**

177. Rosenthal J., Angel A., and Farkas J., (1974). "Metabolic fate of leucine: a significant sterol precursor in adipose tissue and muscle". *Am. J. Physiol.* **226 (2): 411–8.**

178. "KEGG Reaction: R10759". Kyoto Encyclopedia of Genes and Genomes. Kanehisa Laboratories. Archived from the original on (2016). Retrieved 2016.

179. Mock D.M., Stratton S.L., Horvath T.D., Bogusiewicz A., Matthews N.I., Henrich C.L., Dawson A.M., Spencer H.J., Owen S.N., Boysen G., and Moran J.H., (2011). "Urinary excretion of 3-hydroxyisovaleric acid and 3-hydroxyisovaleryl carnitine increases in response to a leucine challenge in marginally biotin-deficient humans". primary source. *The Journal of Nutrition.* **141 (11): 1925–1930.**

180. "KEGG Reaction: R04137". Kyoto Encyclopedia of Genes and Genomes. Kanehisa Laboratories. Archived from the original on (2016). Retrieved (2016).

181. "Homo sapiens: 4-hydroxyphenylpyruvate dioxygenase reaction". MetaCyc. SRI International. 2012. Retrieved 2016.

182. "Leucine metabolism". Brenda. Technische Universität Braunschweig. Archived from the original on 2016. Retrieved 2016.

183. Nelson, D. L.; and Cox, M. M., "Lehninger, Principles of Biochemistry" 3rd Ed. worth Publishing: New York, 2000. ISBN 1-57259-153-6.

184. Vauquelin L.N., and Robiquet P.J. (1806). "La découverte d'un nouveau principe végétal dans le suc des asperges". *Annales de Chimie (in French).* 57: 88–93.

185. R.H.A. Plimmer (1912) [1908]. R.H.A. Plimmer; F.G. Hopkins, eds. The chemical composition of the proteins. *Monographs on biochemistry.* Part I. Analysis (2nd ed.). London: Longmans, Green and Co. **p. 112**. Retrieved 2010.

186. Robiquet, P.J., (1809). "Analyse de la racine de réglisse" [Analysis of licorice root]. *Annales de Chimie et de Physique* (in French). **72 (1): 143–159.**

187. Plisson, A. (1828). "De l'indentité de l'asparagine avec l'agédoïte" [On the identity of asparagine with agédoïte]. *Journal de Pharmacie et des Sciences Accessoires* (in French). **14 (4): 177–182.**

188. Harvey Wickes Felter, M.D. and John Uri Lloyd (1898). "Glycyrrhiza (U. S. P.)—Glycyrrhiza". King's American Dispensatory. Henriette's Herbal Homepage.

189. Boutron-Charlard; and Pelouze (1833). "Ueber das Asparamid (Asparagin des Herrn Robiquet) und die Asparamidsäure" [On asparamide (the asparagine of Mr. Robiquet) and aspartic acid]. *Annalen der Chemie* (in German). **6: 75–88. p. 80.**

190. Liebig, Justus (1833). "Ueber die Zusammensetzung des Asparamids und der Asparaginsäure" [On the composition of asparamide [asparagine] and aspartic acid]. *Annalen der Chemie* (in German). **7: 146–150**. **p. 149.**

191. Piria, and Raffaele (January 1846). "Studi sulla costituzione chimica dell' asparagina e dell' acido aspartico" [Studies of the chemical constitution of asparagine and aspartic acid]. *Il Cimento* (in Italian). **4: 55–73.**

192. Plimmer, and R. H. Aders (1912). The Chemical Constitution of the Proteins. Part I: Analysis (2nd ed.). London, England: Longmans, Green and Co. **p. 112.**

193. Kolbe, and Hermann (1862). "Ueber die chemische Constitution des Asparagins und der Asparaginsäure" [On the chemical constitution of asparagine and aspartic acid]. *Annalen der Chemie* (in German). **121: 232–236.**

194. Piutti, A. (1886). "Ein neues Asparagin" [A new asparagine]. Berichte der Deutschen Chemischen Gesellschaft (in German). **19: 1691–1695.**

195. Grimaux, and Edouard, (1875). "Recherches synthetiques sur le groupe urique" [Synthetic investigations of the uric group]. Bulletin de la Société Chimique de Paris. 2nd series (in French). **24: 337–355. p. 352.**

196. Piutti, Arnaldo (1888). "Sintesi e costituzione delle asparagine" [Synthesis and constitution of asparagine]. Gazzetta Chimica Italiana (in Italian). **18: 457–472.**

197. B. Robert, W. Eric, G. Linda, S. Peter; H. Clare; H. Fiona; B. Michael; and R. Daniel (2010). "Chapter 5: Systems Biology of Cell Organization". Biology (Canadian ed.). United States of America: McGraw-Hill Ryerson. pp. 105–106. ISBN 978-0-07-074175-1.

198. Ruzzo, E.K.,(2013). "Deficiency of asparagine synthetase causes congenital microcephaly and a progressive form of encephalopathy". Neuron. **80 (2): 429–41.**

199. B. Patricie; and A. Markus (1999). "The dolichol pathway of N-linked glycosylation". Biochimica et Biophysica Acta *(BBA)* - General Subjects. **1426 (2): 239–257.**

200. I. Barbara, and C. Sarah E (1999). "Effect of N-linked glycosylation on glycopeptide and glycoprotein structure". Current Opinion in Chemical Biology. **3 (6): 643–9.**

201. Patterson, Marc C., (2005). "Metabolic Mimics: The Disorders of N-Linked Glycosylation". Seminars in Pediatric Neurology. **12 (3): 144–51.**

202. Nelson, D. L., Cox, and M. M.; (2000), Lehninger, Principles of Biochemistry. 3rd Ed. Worth Publishing: New York. ISBN 1-57259-153-6.

203. "cystine". Encyclopædia Britannica. 2007. Encyclopædia Britannica Online. 27 July 2007 www.britannica.com/eb/article-9028437/cystine

204. Gortner, R. A.; W. F. and Hoffman, W. F. (1941). "l-Cystine". Organic Syntheses.; Collective Volume, **1, p. 194.**

205. M.A. Aslaksena; O.H. Romarheima; T. Storebakkena; A. Skrede (28 June 2006). "Evaluation of content and digestibility of disulfide bonds and free thiols in unextruded and extruded diets containing fish meal and soybean protein sources*".* Animal Feed Science and Technology. **128 (3–4): 320–330.**

206. Gahl, William A.; Thoene, Jess G.; Schneider, Jerry A. (2002). "Cystinosis". *New England Journal of Medicine.* **347 (2): 111–121.**

207. H. J. M. Bowen, (1976) Trace Elements in Biochemistry, 2nd ed. London: Academic Press.

208. F. H. Nielsen, and J. R. Hunt, (1989) Trace elements emerging as important in human nutrition. In: P. J. Stumbo, (Ed.), Proceedings of the Fourteenth National Databank Conference, Iowa City: University of Iowa, **p135-143.**

209. R. M. Douglas, H. Hemilä, E. Chalker, and B. Treacy, (2007) Vitamin C for preventing and treating the common cold. *The Cochrane Database of Systematic* Reviews, 3: CD000980.

210. D. L. Heiserman, (1992) Element 30: Zinc Exploring Chemical Elements and their Compounds, New York: TAB Books, **p122.**

211. S. Zevenhoven, and K. Kilpinen, (2001) Trace Elements, Alkali Metals, Berlin: Springer, **p8-1 to 8-30.**

212. W. B. Connie, S. R. Christine, (2009) *Handbook of Clinical Nutrition and Aging,* New York: Springer, **p151.**

213. C. D. Berdanier, J. T. Dwyer, and E. B. Feldman, (2007*)* Handbook of Nutrition and Food, Boca Raton, Florida: CRC Press.

214. H. Ensminger, and J. E. Konlande, (1993) Foods & Nutrition Encyclopedia, 2nd ed. *Boca Raton, Florida: CRC Press*, **p2368-2369.**

215. J. Osredkar, and N. Sustar, (2011) Copper and zinc, biological role and significance of copper/zinc imbalance*, Journal of Clinical Toxicology*, **p3: 1-18**.

216. S. Prasad, (2003) Zinc deficiency: Has been known of for 40 years but ignored by global health organisations, *British Medical Journal*, **326(7386): 409-410**.

217. L. Plum, L. Rink, and H. Haase, (2010) The essential toxin: Impact of zinc on human health, *International Journal of Environ Research Public Health*, **7(4): 1342-1365.**

218. S. C. Burjonrappa, and M. Miller, (2012) Role of trace elements in parenteral nutrition support of the surgical neonate, *Journal of Pediatric Surgery*, **47: 760-771.**

219. Z. S. Lassi, B. A. Haider, and Z. A. Bhutta, (2010) Zinc supplementation for the prevention of pneumonia in children aged 2 months to 59 months, *The* Cochrane Database of Systematic Reviews, 12: CD005978.

220. H. H. Sanstead, C. J. Frederickson, and J. G. Penland, (2000) Zinc nutriture as related to brain, *Journal of Nutrition*, **130: 140S-146S.**

221. C. A. Heyneman, (1996) Zinc deficiency and taste disorders, Annals of Pharmacotherapy, 30: 186-187.

222. W. Maretm, and H. H. Sandstead, (2006) Zinc requirements and the risks and benefits of zinc supplementation, *Journal of Trace Elements in Medicine and Biology*, **20: 3-18.**

223. S. Prasad, (2004) Zinc deficiency: İts characterization and treatment, *Metal İons in Biological Systems*, 41: 103-137.

224. WHO Contributors, (2007) The Impact of Zinc Supplementation On Childhood Mortality And Severe Morbidity, Geneva, Switzerland: World Health Organization.

225. W. M. Haynes, (2014) CRC Handbook of Chemistry and Physics, Internet Version 2015, 95th ed. Boca Raton, FL: CRC Press/Taylor and Francis.

226. C. R. Hammond, (2004) The elements. İn: Handbook of Chemistry and Physics, 81st ed. Boca Raton: CRC Press.

227. W. H. Rayner, (2007) Jewelry Making Through History: An Encyclopedia, Westport, C.T., Greenwood Publishing Group, p56.

228. National Research Council, Food Nutrition Board, (1980) Copper. In: Recommended Dietary Allowances, Washington, D.C: NRC/NAS, **p151-154.**

229. N. E. Hellman, and J. D. Gitlin, (2002) Ceruloplasmin metabolism and function*, Annual* Review of Nutrition, **22: 439-458.**

230. P. J. O. Brien, and W. R. Bruce, (2009) Endogenous Toxins: Targets for Disease Treatment and Prevention, Vol. 2. Toronto: John Wiley & Sons**, p405-406.**

231. M. C. Linder, L. Wooten, P. Cerveza, S. Cotton, R. Shulze, and N. Lomeli, (1998) Copper transport, *American Journal of Clinical Nutrition*, **67(5)**: 965S-971S.

232. M. Roger, (2011) The Minerals You Need, USA: Safe Goods Publishing, p 21.

233. R. Uauy, M. Olivares, and M. Gonzalez, (1988) Essentiality of copper in humans, *Journal of Clinical Nutrition*, **67(5): 952-959.**

234. M. Angelova, S. Asenova, V. Nedkova, and R. Koleva-Kolarova, (2011) Copper in the human organism, *Trakia Journal of Sciences*, **9(1): 88-98**.

235. C. T. Jeremias, L. B. David, and J. Royden, (2006) Severe ataxia, myelopathy, and peripheral neuropathy due to acquired copper deficiency in a patient with history of gastrectomy JPEN, *Journal of Parenteral and Enteral Nutrition*, **30: 446-450.**

236. H. Kodama, and C. Fujisawa, (2009) Copper metabolism and inherited copper transport disorders: Molecular mechanisms, screening, and treatment, Metallomics, **1(1): 42-52.**

237. S. G. Kaler, C. J. Liew, A. Donsante, J. D. Hicks, S. Sato, and J. C. Greenfield, (2010) Molecular correlates of epilepsy in early diagnosed and treated Menkes disease, *Journal of International Medicine and Dentistry*, **33(5): 583-589.**

238. T. Aoki, Y. Yamaguchi, and N. Shimizu, (1996) Copper deficiency and its treatment from the point of view of copper metabolism in the body, Pediatrics of Japan, **37: 317-329.**

239. M. Wessling-Resnick, (2014) Iron. In: A. C. Ross, B. Caballero, R. J. Cousins, K. L. Tucker, R. G. Ziegler, (Ed.), Modern Nutrition in Health and Disease, 11th ed. Baltimore, MD: Lippincott Williams & Wilkins, **p176-88.**

240. Tsugutoshi, (2004) Copper deficiency and the clinical practice, *Japan Medical Association Journal,* **47: 365-370.**

241. R. D. Crichton, and G. Bo, P. Geisser, (2008) Iron Therapy With Special Emphasis on Intravenous Administration, 4th ed. Bremen: UNI-MED.

242. Food and Nutrition Board, Institute of Medicine, National Academy of Sciences, (2001) Dietary Reference Intakes for Vitamin A, Vitamin K, Arsenic, Boron, Chromium, Copper, Iodine, Iron, Manganese, Molybdenum, Nickel, Silicon, Vanadium, and Zinc, Washington, DC: National Academy Press.

243. P. J. Aggett, (2012) Iron. In: J. W. Erdman, I. A. Macdonald, S. H. Zeisel, editors. *Present Knowledge in Nutrition*, 10th ed. Washington, DC: Wiley-Blackwell, **p506-520.**

244. L. E. Murray-Kolbe, and J. Beard, (2010) Iron. In: P. M. Coates, J. M. Betz, M. R. Blackman, G. M. Cragg, M. Levine, J. Moss, J. D. White, (Ed.), Encyclopedia of Dietary Supplements, 2nd ed. London and New York: Informa Healthcare, **p432-438.**

245. R. Casiday, and F. Regina, (2007) Iron Use and Storage in the Body: Ferritin and Molecular Representations, St. Louis, USA: Department of Chemistry, Washington University.

246. R. C. Hider, X. Kong, (2013) Iron: Effect of overload and deficiency. In: A. Sigel, H. Sigel, R. K. O. Sigel, (Ed.), *I*nterrelations between Essential Metal Ions and Human Diseases, Metal Ions in Life Sciences, Vol. 13. Ch. 8. Dordrecht: Springer, **p229-294.**

247. World Health Organization, (2008) Worldwide Prevalence of Anaemia 1993-2005: WHO Global Database on Anaemia, Geneva: World Health Organization.

248. E. S. Wintergerst, and S. Maggini, D. H. Hornig, (2007) Contribution of selected vitamins and trace elements to ımmune function, Annals of Nutrition and Metabolism, **51(4): 301-323.**

249. S. R. D'Souza, and A. George, (2007) Restless legs syndrome in Indian patients having iron deficiency anemia in a tertiary care hospital, Sleep Medicine, **8(3): 247-251**.

250. F. S. Al-Fartusie, A. T. Marzook, and T. S. Morad, (2012) Study of some trace elements and antioxidant vitamins in sera of Iraqi women with toxoplasmosis, *Al-Mustansiriyah Journal of Science,* **23(3): 199-206.**

251. S. S. Chauhan, R. Thakur, and G. D. Sharma, (2008) Nickel: İts availability and reactions in soil, *Journal of Industrial Pollution Control*, **24(1): 57-62.**

252. S. Kasprzak, F. W. Sunderman, and K. Salnikow, (2003) Nickel carcinogenesis, Mutation Research*,* **533: 67-97.**

253. R. K. Sharma, and M. Agarwal, (2005) Biological effects of heavy metals: An overview, *Journal of Environmental Biology*, **26(2): 301-313.**

254. B. Virginia, (1953) Axel fredrick cronstedt, *Journal of Chemical Education*, **30(5): 247-251.**

255. K. S. Kasprzak, (1987) Nickel, advances in modern environ, Toxicology, **11: 145-183.**

256. R. M. Welch, (1981) The biological significance of nickel, *Journal of Plant Nutrition*, **3(1-4): 345-356.**

257. M. Anke, L. Angelow, M. Glei, M. Müller, and H. Illing, (1995) The biological importance of nickel in the food chain. *Fresenius Journal of Analytical Chemistry*, **352(1-2): 92-96.**

258. M. Anke, B. Groppel, H. Kronemann, and M. Grün, (1983) Nickel.an essential element. International Agency for Research on Cancer Scientific Publications, **(53): 339-365.**

259. M. Poonkothai, and S. Vijayavathi, (2012) Nickel as an essential element and a toxicant, *International Journal of Engineering, Science and Technology* **1(4); 285-288.**

260. M. Sydor, and D. B. Zamble, (2013) Nickel metallomics: General themes guiding nickel homeostasis. In: B. Lucia, (Ed.), Metallomics and the Cell. *Metal Ions in Life Sciences*, Vol. 12. Ch. 11. Dordrecht: Springer.

261. K. Salniko, T. Davidson, Q. Zhang, L. C. Chen, N. Su, and M. Costa, (2003) The involvement of hypoxia inducible transcription factor 1 dependent pathway in nickel carcinogenesis, Cancer Research. **63: 3524 -3530.**

262. IPCS (International Programme on Chemical Safety), (1992) Environmental Health Criteria 108: Nickel, Geneva: World Health Organization.

263. J. P. Thyssen, A. Linneberg, T. Menné, and J. D. Johansen, (2007) The epidemiology of contact allergy in the general population-prevalence and main findings, Contact Dermatitis, **57(5): 287-299.**

264. J. J. Hostynek, and H. I. Maibach, (2002) Nickel and the Skin, Boca Raton*: CRC Press*, p1-**249.**

265. D. G. Barceloux, (1999) Nickel, Clinical Toxicology, **37(2): 239-258.**

266. B. Mühlethaler, J. Thissen, (1969) Smalt, Studies in Conservation, **14(2): 47-61.**

267. C. Mandeville, and H. Fulbright, (1943) The energies of the rays from Sb122, Cd115, Ir192, Mn54, Zn65, and Co60, Physical Review, **64(9-10): 265-267.**

268. J. Emsley, (2001) Manganese. Nature's Building Blocks*: An A-Z* Guide to the Elements, Oxford, UK: Oxford University Press, **p249-253.**

269. C. E. Housecroft, and A. G. Sharpe, (2008) Inorganic Chemistry, 3rd ed. Harlow: Prentice Hall, **p305-306.**

270. K. M. Unice, A. D. Monnot, S. H. Gaffney, B. E. Tvermoes, K. A. Thuett, D. J. Paustenbach, and B. L. Finley, (2012) Inorganic cobalt supplementation prediction of cobalt levels in whole blood and urine using a biokinetic model, Food and Chemical Toxicology, **50, 2456-2246.**

271. V. Battaglia, A. Compagnone, A. Bandino, M. Bragadin, C. A. Rossi, F. Zanetti, S. Colombatto, M. A. Grillo, and A. Toninello, (2009) Cobalt induces oxidative stress in isolated liver mitochondria responsible for permeability transition and intrinsicapoptosis in hepatocyte primary cultures, *The International Journal of Biochemistry and Cell Biology*, **41: 586-594.**

272. N. Lombaert, D. Lison, P. Van Hummelen, and M. K. Volders, (2008) In vitro expression of hard metal dust (WC-Co) responsive genes in human peripheral blood mononucleated cells, Toxicology and Applied Pharmacology, **227: 299-312.**

273. M. Z. Hamdi., and I. A. Mustafa, (2013), Mixed ligand complexes of gold (III) with some amino acids and dithiocarbamates or dithiophosphates, *Science Journal of Analytical Chemistry*, 1, No. 2, 2013, **pp. 21-27.**

274. A. Vogel, "A text book of practical organic chemistry". ELBS: London, pp499–501(1968).

275. F. F. Jian, Q. Hao, X. Hang, L. Lu, and X. Wang, (2000), "Structure of bis(o,o-diisopropyldithiophosphato-S,S′)(1,10- phenanthroline N1,N10) zinc(II) complex, [Zn(phen)(S$_2$P(OiPr)$_2$)$_2$]", *J.Chem.Crytallog*. 30, 7, **pp469- 472.**

276. W.J. Geary, (1971)"The use of conductivity measurements in organic solvents for characterization of coordination compounds", Coord. Chem. Rev., **7, 81.**

277. J.M. Tunney, A.J. Blake, E.S.Davies, J. Mcmater, C.Wilson and C.D. Garner, (2006), "Synthesis and structure of gold(III) complexes of asymmetric dithiolene ligands "*Polyhedron*., **25, 2,P. 591.**

278. A. Manohar, K. Ramalingam, and K. Karpagavel, (2012) "Mixed ligand complexes involving bis(dithiocarbamato)nickel(ii) and phosphorus donors: synthesis, spectral, thermal studies and bas investigations" *Inter.J. Chem.Tech. Res*., 4, (4), **pp1383-1391.**

279. A. J. Odola and J. A.O. Woods, (2011), Synthesis, characterization and antimicrobial activity studies of new nickel(ii) mixed ligand complexes of disubstituted dithiocarbamates with ethylsalicylaldiminate" Scholars Research Library, Archives of Applied Science Research, 3 (4)**pp 463-470.**

280. L. Giovagnini, C. Marzano, F. Bettio and D. Fregona, (2005), Mixed complexes of Pt(II) and Pd(II) with ethylsarcosinedithiocarbamate and 2-/3-picoline as antitumor agents", *J. Inorg. Biochem.* **99, (11), 2139‑2150.**

281. L. Szucova, Z. Travnıcek and J. Marek, (2003) O,O Dialkyldithiophosphato and O-alkyldithiophosphato nickel(II) complexes with bidentate P-donor ligands*, Polyhedron* 22 pp **1341-/1348.**

282. L. Bolundut, I. Haiduc, E. Ilyes, G KociokKhun, K. C. Molloy and S. GmezRuiz, (2010)" Hydrogen bond supramolecular selfassembly in nickel(II) dithiophosphates, Ni[S2P(OR)2]2, R = sec-Bu, iso-Bu, and their bis(pyrazole) adducts", Inorg. Chim. Acta. 363, **pp 4319‑4323.**

283. F. Jian, K. Jiao, Q.Wang and H.Wang, (2004), Synthesis and crystal structure of trans bis(o,odiisopropylthiophosphoryl-1Himidazole- N_3)bis(o,odiisopropyldithiophosphato)   nickel(II) complex: Ni[N_3ImSP(OiPr)$_2$]$_2$ [S$_2$P(OiPr)$_2$]$_2$ (Im= imidazole; iPr= isopropyl)", *J. Chem. Crystallo.*, **34, (2).**

284. A. K. Molodkin, N. Ya. Esina, O. I. Andreeva, and M. Konde, (2008), Mixed-Ligand Platinum(IV) Complexes with amino acids and cytosine*, Russi. J. Inorg*. Chem., **53, (8), 1295‑1303.**

285. M. B.Tarallo, A. J. C. Filho, E. D. Vieira, A. Monge, C.Q. Leite, F.R.Pavan, G. Borthagaray, D. Gambino, and M. H. Torre, (2009), Research of new mixed-chelate copper complexes with quinoxaline N1,N4-dioxide derivatives and alanine as ligands, potential antimycobacterial agents".**97,(1),80-89.**

286. A. Caubet, V. Moreno, E. Moins and C. Miravitiies, (1992), Methionine and histidine Pd (II) and Pt(II) complexes: crystal structures and spectroscopic properties, *J. Inorg. Biochem*., **48, 135-152**

287. P. R. Reddy, M. R. and P. Manjula, (2005), Synthesis and characterization of mixed ligand complexes of Zn(II) and Co(II) with amino acids: Relevance to zinc binding sites in zinc fingers, *J. Chem. Sci.*, 117, No. 3, May 2005, **pp. 239–246.**

288. Geary W. J. (1971). The use of conductivity measurements in organic solvents for the characterisation of coordination compounds. *J. Coord. Chem.* Rev. **(7). 81.**

289. M. M. Alam, S. M. M. Rahman, M. M. Rahman, and S. M. S. Islam, (2010), Simultaneous Preparation of Facial and Meridional Isomer of Cobalt-Amino acid Complexes and their Characterization, *journal of scientific research, J.sci.Rse*. **2 (1), 91-98.**

290. G. B. Kauffman, M. Karbassi, E. Kyuno, W. J. Birdsall, and P. E. A. Kylanpaa, (1989). Simultaneous Preparation of Facial and Meridional Isomer of Cobalt-Amino Acid Complexes and their Characterization. Inorg. Synthesis **25, 135**.

291. A. J. Saraceno, I. Nakagawa, S. Mizushima, Columba Curran, and J. V. Quagliano, (1958), Infrared absorption spectra of in organic coordination complexes. *J. Am. Chem. Soc.* **80, 5018**.

292. H. A. Begum, E. Ahmed, K. M. A. Malik, and M. A. Quyser, (1994), Simultaneous Preparation of Facial and Meridional Isomer of Cobalt-Amino Acid Complexes and their Characterization. Dhaka Univ. J. Sci**. 42, 9.**

293. H. Kuroya and Tsuchida, (1940), Inorganic reaction mechanism. *Chem. Soc. J. pn.* **15, 427.**

294. R. G. Neville and George Gorin, (1956), Cysteine complexes with cobalt (III) ion. *J. Am. Chem. Soc*. **78, 4891.**

295. R. S. Young, (1960), Cobalt, It's Chemistry, Metallurgy, and uses (*Reinhold Publ. Corp.*,).

296. E. Larsen and S. F. Mason*,* (1966), Hydroxo bridge complexes of chromium (III), and cobalt (III), *J. Chem. Soc*. A, **313.**

297. Batiu C., Jelic C., Leopold N., Cozar O., and David L., (2005). Spectroscopic investigations of new Cu(II), Co(II), Ni(II) complexes with γ-L-glutamyl amide as ligand. *J Mol Struct* 744-747:325-330.

298. H. A. Begum, E. Ahmed, K. M. A. Malik, and M. A. Quyser, (1994), Simultaneous Preparation of Facial and Meridional Isomer of Cobalt-Amino Acid Complexes and their Characterization. Dhaka Univ. J. Sci. **42, 9.**

299. A. Stanila, C. Braicu, S. Stanila, and R. M. Popi, (2011), Antibacterial Activity of Copper and Cobalt Amino Acids Complexes, *journal of Notulae Botanicae Horti AgrobotaniciCluj-Napoca*, **39(2):124-129.**

300. Stanila A, Marcu A, Rusu D, Rusu M, and David L., (2007). Spectroscopic studies of some copper (II) complexes with amino acids. *J. Mol Struct* **834:364-368.**

301. Marcu A., Stanila A., Cozar O., and David L., (2008). Structural investigations of some metallic complexes with threonine as ligand. *J. Optoelectron Adv. M.* **10(4):830-833.**

302. P.N.Radivojsa, N.Juranic, M.B.Celap, K.Tarituni and K.Saito, Polyhedreon, **10, 2717** (1991).

303. P. Genova, T. Varadinova, R. Alexandrova, S. Trifunovic, and P. Radivojsa, (2001), Cytotoxicity of Co(III) complexes of arginine, **Vol. 8, No. 4.**

304. M. B. Celap, M. J. Malinar, P. N. Radivojsa , and L. *j. Solujic, borg*. @nth., 23, 91 (1985).

305. Markovic, M., Judas, N. and Sabolovic, J. (2011) Combined Experimental and Computational Study of cis-Trans Iso- merism in Bis(L-Valinato)Copper(II). Inorganic Chemistry*, **50, 3632-3644.**

306. M. Yokota, S. Kikuchi, J. Sen, T. Kamei, and N. Doki1, (2016), Cu(II) Complex of L-Leucine Favor a Different Type of Crystal Structure from Cu(II)-L-Val and Cu(II)-L-Ile, Advances in Chemical Engineering and Science, 6, 62-66 Published Online 2016 in Sci. Res.

307. Fawcett, T.G., Ushay, M., Rose, J.P., Lalancette, R.A., Potenza, J.A. and Schugar, H.J. (1979) Molecular Structures of the Copper-Amino Acid Complexes Bis(L-Leucinato)Copper(II) and Bis(D,L-2-Aminobutyrato)Copper(II). Inorganic Chemistry, 18, 327-332.

308. Weeks, C.M., Cooper, S. and Norton, D.A. (1969) The Crystal Structure of the Copper (II) Complex of L-Isoleucine. Acta Crystallographica, B25, **443-450.**

309. Nair M., Arasu T.P., Pillai S.M. and Natarajai, C. (1993). Complex combinations of transition metals with mixed ligand. *J. Chem. Soc., Dalton Trans.,* **917.**

310. T. Rosu, M. Negoiu, C. Dobrogeanu, T. Ruse T. Rosu, M. Negoiu, C. Dobrogeanu, and T. Ruse, 2009, Complex combinations of transition metals with mixed ligand, Analele Universitâţii din Bucureâti – Chimie, Anul XII (serie nouâ), **vol. I-II, pag. 109–116.**

311. Lever, A. B. P. (1984) Inorganic Electronic Spectroscopy, *Elsevier, Amsterdam*.

312. K. Ozutsumi and H. Ohtaki, (1984) Advances in Inorganic Chemistry. Bull. *Chem.Soc*. (Japan), **57, 2605.**

313. D. Boruah, (2012), Interaction of Cobalt(II) and Nickel(II) ions with Amino acids in Aqueous solution: A Spectrophotometric Study, *International Journal of Scientific and Research Publications,* 2, Issue 8, 2012 1 ISSN **2250-3153.**

314. J. D. Lee, Concise Inorganic Chemistry, 5th ed., *Blackwell Science* Ltd., 1996.

315. D. Feakins, R. D. O. Neill, W. E. Waghorne and A. *J. I. Ward*, (1982).

Interaction of Cobalt(II) and Nickel(II) ions with Amino acids in Aqueous solution: A Spectrophotometric Study *J. Chem. Soc. Fara. Trans. I.,* 1982, **78, 143.**

316. M. Castillo and E. Ramrez, Complexes of selected transition metal ions with N-modified glycine as ligand. Trans. Metal. , 1984, **9, 268.**

317. Y. B. Yakolev and V. G. Ushakova, Russ.(1983). Thallium interactions in biological fluids. A potentiometric investigation of dimethylthallium complex equilibria with some typical amino acids *J. Inorg. Chem*., **28(8), 1217.**

318. N. Raman, R.Y. Pitchaikani and A. Kulandaisamy, (2001), Synthesis, characterization and biological activity of mixed ligand Co(II) complexes of schiff base 2-amino-4-nitrophenol-n-salicylidene with some amino acidsProc. Indian Acad. Sci. (Chem. Sci .), 2001, 113(3), 183-189.

319. A. R. Patil, K. J. Donde, S. S. Raut, V. R. Patil and R. S. Lokhande (2012), Synthesis, characterization and biological activity of mixed ligand Co(II) complexes of schiff base 2-amino-4-nitrophenol-n-salicylidene with some amino acids, *Journal of Chemical and Pharmaceutical Research*, 4(2):1413-1425

320. I. Sakiyan, E. Logoglu, S. Arslan, N. Sari and N. Sakiyan, "Biometals. (2004) Antimicrobial activities of N-(2- hydroxy-1-naphthalidene)-amino acid(glycine, alanine, phenylalanine, histidine, tryptophane) Schiff bases and their manganese(III) complexes", Kluwer Academic pub.; Netherlands, 17(2), 115-120.

321. A.R. Patil, K.J. Donde, S.S. Raut, V.R Patil and R.S. Lokhande, (2011), *J. Pharm. Reser*., 4(7), 2256-2260.

322. S. Gaur, and B. Sharma (2003), Synthesis, characterization and thermal studies of Co(II), Ni(II), Cu(II) and Zn(II) complexes of some Schiff bases derived from 4-amino-3-mercapto-6-methyl-5-oxo-1,2,4 triazine. *J. Indan Chem. Soc*., **8, 841-842.**

323. S. Panda, R. Mishra, A.K. Panda and K.C. Satpathy, (1989), Synthesis, Characterization, and Antibacterial Studies of Mixed Ligand Dioxouranium Complexes with 8-Hydroxyquinoline and Some Amino Acids. *J. Ind. Chem. Soc*., **66, 472-474.**

324. V. S. Shivankar, R.B. Vaidya, S. R. Dharwadkar and N. V. Thakkar, (1989), A bioinorganic study of some cobalt (II) schiff base complexes of variously substituted hydroxyl benzaldimines. Syn. Reac. Inorg. Metal-Org. Chem ., 2003, **33(9), 1597-1622.**

325. K. Nakamoto, Y. Morimoto and A.E. Martell, (1961), Synthesis, X-ray structure and antimycobacterial activity of silver complexes with a-hydroxycarboxylic acids. *J. Am. Chem. Soc.*, **83, 4528-4532.**

326. Z. H. Chohan, M. Arif, M.A. Akhtar and C. T. (2006), Bioinorganic Chemistry and Applications Supuran*, Hindavi Publishing Corporation , , **1-13.**

327. B.T. Thaker, K.R. Surati, P. Patel and S.D. Parmar, J. Iran. Chem. Soc ., 2006, 3(4), 371-377.

328. E. Sinn and C.M. Harris, (1969), Coord. Chem. Rev**., 4(4), 391-422.**

329. S.B. Kalia, K. Lumba, G. Kaushal and M. Sharma, (2007), *Indian. J. Chem.,* 46A, **1233-1239.**

330. A.P. Mishra and M. Khare, (2000), Synthesis, Structural, and Biological Studies of Some Schiff Bases and Their Metal Complexes. *J.Indian Chem. Soc*., **77(8), 367-370.**

331. A. I. Vogel, "A Text Book of Quantitative Inorganic Analysis", 3rd Ed.; ELBS, Longman Green: London, 1961, **415-456.**

332. F. Tuna, G. Clarkson, N.W. Alcock and M.J. Hannon, (2003). The effect of phenyl substituents on supramolecular assemblies containing directly linked bis-pyridylimine ligands: synthesis and structural characterisation of mononuclear nickel(ii) and dinuclear silver(i) and cobalt(iii) complexes of (2-pyridyl)phenylketazine. Dalton Trans., 2003, **2149-2155.**

333. D.J. Szalda, C. Creutz, D. Mahajan and N. Sutin, (1983), Comprehensive Coordination Chemistry II: From Biology to Nanotechnology. *Inorg. Chem*., 22(17), **2372-2379.**

334. S. G. Telfer, G. Bernardinelli and A. F. Williams, (2001), The Use of Electrospray Mass Spectrometry to Determine Speciation in a Dynamic Combinatorial Library for Anion Recognition. Chem. Commun ., **1498-1499.**

335. S.G. Telfer, R. Kuroda and T. Sato, (2003), Stereoselective formation of dinuclear complexes with anomalous CD spectra. Chem. Commun ., **1064-1065.**

336. S.G. Telfer, T. Sato, T. Harada, R. Kuroda, J. Lefebvre and D.B. Leznoff, (2004), Synthesis, Structure and Reactivity of Paramagnetic Iron (II) and Iron (III) Amidodiphosphine Complexes. Inorg. Chem**., 43(20), 6168- 6176.**

337. J. M. Rowland, M. M. Olmstead and P. K. Mascharak, (2002), Synthesis and Assessment of CO Release Capacity of Manganese Carbonyl Complexes Derived from Rigid α-Diimine Ligands of Varied Complexity. *Inorg. Chem*., **41(6), 1545-1549.**

338. C. Provent, G. Bernardinelli, A.F. Williams and N. Vulliermet, (2001), *Eur. J. Inorg. Chem.*, 1963-1967.

339. M. A. Masood, E. J. Enemark and T. D. P. Stack, (1998), Ligand Self-Recognition in the Self-Assembly of a [{Cu(L)}2]2+ Complex: The Role of Chirality. Angew Chem Int Ed Engl., **37, 928-932.**

340. I. Sakyan, E. Logoglu, S. Arslan, N. Sari and N. Akiyan, (2004), Metal-Based Antibacterial and Antifungal Agents: Synthesis, Characterization, and In Vitro Biological Evaluation of Co(II), Cu(II), Ni(II), and Zn(II) Complexes with Amino Acid-Derived Compounds. Biometals., **17(2), 115-120.**

341. J. L. McLauglin, C. J. Chang and D. L. Smith, (1991), "Bench top' bioassay for the discovery of bioactive natural products: an update. In: Atta-ur-Rahman", Ed. I Amsterdam, The Netherlands: Elsevier Science., **9, 383-409.**

342. V. K. Patel, A. M. Vasanwala and C. N. Jejurkar, (1989), Synthesis and biological screening of novel 2-morpholinoquinoline nucleus clubbed with 1,2,4-oxadiazole motifsIndian. *J. Chem.*, 28A, 719-721.

 343. Z. H. Chohan, M. Praveen and A. Ghaffar, (1997), Metal-Based Drugs, **4(5), 267-272.**

344. Z.H. Chohan, A.K. Misbahul and M. Moazzam, (1988), Synthesis, Characterisation and Biological Activity of Chiral Mixed Ligand Ni(II) Complexes. *Indian J. Chem.*, **27(A), 1102-1104.**

345. M.T. Madigan, J.M. Martinko and J. Parker, (1997), "Microbial growth control. In Biology of Microorganisms", 8th Ed.; Prentice-Hall: New Jersey, **397-429.**

346. T. Vemralinov, L. Arpadjan, J. Beattie J., (2006), Cobalt Methionine complex as feed additive in buffaloes in selected districts of Punjab, Pakistan. Acta Pharm . **56, 105-112.**

347. F. H. A. Al-Jeboori and T. A. M. Al-Shimiesawi, (2013), Synthesis and investigation of complex formation between amino acid (glycine) and various metal ion by using spectroscopic methods, *Journal of Chemical and Pharmaceutical Research*, **5(11):318-321.**

348. C. Batiu, C. Jelic, N. Leopold, O. Cozar, and L. David, (2005), Spectroscopic investigations of new Cu(II), Co(II), Ni(II) complexes with γ-L-glutamyl amide as ligand. *J. Mol. Struct*, **325-330, 744-747.**

349. Eskander M. F., Khalil T. E., Werner R., Haase W., Svoboda I., and Fuss H. (2000), Synthesis, Characterization of Some Complexes of Copper (II) with L-Asparginine, L-Histidine, L-Lysine. Polyhedron, **19, 949–958.**

350. I. P. Tripathi and A. Kamal, (2015), Synthesis, Characterization of Some Complexes of Copper (II) with L-Asparginine, L-Histidine, L-Lysine, *American Journal of Advanced Drug Delivery,* **3(1):095-103.**

351. Reddy P. S., and Reddy K. H. (2000), *Polyhedron* **19, 1687–1692.**

352. U. car, I., Bulut, A., and Büyükgüngüor O., (2007), *J. Phys. Chem. Solids*, **68, 2271–2277.**

353. Eskander, M. F., Khalil, T. E., Werner, R., Haase, W., Svoboda, I., and Fuss, H. (2000), Synthesis, Spectral, Electrochemical Analysis and Screening for α-Glucosidase Inhibition of Some Complexes of Copper (II) with Amino acids. Polyhedron, **19, 949–958.**

354. Rabindra Reddy P., Radhika M. and Manjula., (2005), Synthesis and characterization of mixed ligand complexes of Zn(II) and Co(II) with amino acids: Relevance to zinc binding sites in zinc fingers. *J. Chem. Sci*., **117, 3, 2005, 239–246.**

355. K. Nakamato, and J. Kieft, (1967), Synthesis, Spectral and Electrochemical analysis of Copper(II) complexes with L-threonine, L-tyrosine, L-tryptophane and L-histidine. **29, 2561-2568.**

356. G. Maracotrigiano, L. Menabue and G.C. Pellaani, (1975), Synthesis and Characterization of Complexes of [(N,N --Bis(2- Hydroxy Ethyl) Glycine] with Some Metal Salts. *J. Inorg. Nucl. Chem.,* **47, (11), 2431.**

357. M. Kothar and D. H. Busch, (1996), Synthesis, Spectral, Electrochemical Analysis and Screening for α-Glucosidase Inhibition of Some Complexes of Copper (II) with Amino acids. *Inorg. Chem.,* **8, 2276.**

358. Fessenden, R.J. and Fessenden, (1990), *J. S. Organic chemistry, Harness and Nabie Inc.,* **1048.**

359. Nakamoto, K., Wiley Interscience, New York, 2009, **66-74.**

360. Elzahany, E.A., Hegab, K.H., Safaa, K.H. and Youssef, N.S., (2008), Synthesis, characterization and antimicrobial activities of some metal (II) amino acids' complexes. *Australian Journal of Basic and Ap-plied Sciences,* **2, 210-220.**

361. Donald, L.P., M.L. Gary, S.K. George and R.V. James, (2009). Introduction to Spectroscopy, Brooks*/Cole, USA.*

362. M. A. Qadir, M. Ahmed, A. Ahmad, S. Naz, S. A. A. S. Tirmazi, R. Khan, I. Hussain and R. Waseem, (2014), Synthesis of Metal Complexes with Amino Acids for Animal Nutrition, Global Veterinaria 12 (6): **858-861**, 2014, ISSN 1992-6197.

363. J. Hurov, T. Stappenbeck, C. Zmasek, L. White, S. Ranganath, J. Russell, A. Chan, and K. Murphy, (2001), *H. Piwnica-Worms, Mol Cell Biol*., **21, 3206.**

364. M. Hübner, I. Hauer1, C. Muller, D. Rusu, K. Botond, and L. David1 2011, spectroscopic studies of copper (II) complexes with some amino acid as ligand, Analele Universităţii de Vest din Timişoara **Vol. LV, P 77-85** Seria Fizică,

365. I. Tinoco, K. Sauer, and J. C. Wang, (1995), Physical Chemistry: *Principles and Applications in Biological Sciences,* Third Edition, Prentice Hall: New Jersey, **p. 86.**

366. G. Socrates, (2001), Infrared and Raman Characteristic Group Frequencies: *Tables and Charts, third edition, Wiley, Chichester.*

367. L. J. Bellamy, (1975), The Infra-red Spectra of Complex Molecules, Wiley, New York, **p. 83.**

368. D. Xiee, J. G. Park, M. Faddak, J. Zhao, and H. Khanjoun, (2006), Spectroscopic studies of copper (II) complexes with some amino acid as ligand. *Journal of Biomaterials Applications*, **21, 147.**

369. B. L. Silva, P. T. C. Freire, F. E. A Melo, I. Guedes, Araújo Silva, Mendes Filho, and A. J. D Moreno, (1998), *Brazilian Journal of Physics*, **28, 19.**

370. W. Kemp, Organic Spectroscopy, (1984), MacMillan Publisher Ltd, London, p. 186.

371. G. Mohamed, and N. El-Gamel, (2004), Spectrochimica Acta Part A: Molecular and Biomolecular Spectroscopy, **60 (13), 3141.**

372. E. Prenesti, S. Berto, and P. G. Daniele, (2003), Spectrochimica Acta*, 59, 201.**

373. Rayms K. A., Olson K.E., Mcgaw M., Oray C., Carlson J.O., and Beaty B. J. (1998). Effect of heavy metals on *Aedes aegypti* (Diptera:Culicidae) larvae. Ecotoxicol Environ Saf **39: 41-47.**

374. T. A. D. Rodrigues, E. J. DE Arruda, M. F. Fernandes, C. T. DE Carvalho, A. R. Limaand I. Cabrini, (2017), Copper II - polar amino acid complexes: toxicity to bacteria and larvae of Aedes aegypti, Anais da Academia Brasileira de Ciências*, 89(3 Suppl.): **2273-2280.**

375. BARAN E.J., WAGNER C.C., TORRE M.H., KREMER E., and KÖGELER P., (2000). Vibrational spectra of the Cu (II) complexes of aspartic and glutamic acids. *Acta Farm Bonaer* **19: 231-234.**

376. Brumano G., (2008). Biotecnologia aplicada ao valor nutricional dos alimentos. *Rev Elet Nutri* **5: 707-721.**

377. Ponnusamy L., XU N., Nojima S., Wesson D.M., Schal C., and Apperson C.S., (2008). Identification of bacteria and bacteria-associated chemical cues that mediate oviposition site preferences by Aedes aegypti. Proc Nat Acad Sc USA 105: **9262-9267.**

378. Nomiya, K. and Yokoyama, H. (2002) Synthesis, crystal structures anti antimicrobial activities of polymeric silver (I) complexes with three amino-acids [aspartic acid (H2asp), glycine (Hgly) and asparagines (Hasn)]. *Journal of Chemical Society, Dalton Transaction*, **2483-2490.**

379. T.O. Aiyelabola, I. A. Ojo, A. C. Adebajo, G. O. Ogunlusi, O. Oyetunji, E. O. Akinkunmi, and A. O. Adeoye, (2012), Synthesis, characterization and antimicrobial activities of some metal(II) amino acids' complexes, Advances in Biological Chemistry, **2, 268-273.**

380. Youssef, N. S. and Hegab, K. H. (2005) Synthesis and Characterization of Some Transition Metal complexes of thiosemicarbazones derived from 2-acetylpyrrole and 2- acetylfuran. Synthesis and Reactivity in Inorganic and Metal-Organic Chemistry, **35, 391-399.**

381. Osowole, A. (2011) Synthesis, characterization and mag- netic and thermal studies on some metal(II) thiophenyl schiff base complexes. *International Journal of Inorganic Chemistry*, 1-7.

382. Greenwood, N. N. and Earnshaw, A. (1997) Coordination compounds. *Butterworth-Heinemann, Hong Kong,* **1060- 1090.**

283. Fessenden, R. J. and Fessenden, J. S. (1990) Organic chemistry. *Harness and Nabie Inc.,* **1048.**

384. Nakamoto, K. (2009) Complexes of amino acids. *In: K.* Nakamoto, Ed., Infrared and Raman Spectra of Inorganic and Coordination Compounds*,* Wiley Interscience, New York, **66-74.**

385. Elzahany, E. A., Hegab, K. H., Safaa, K. H. and Youssef, N. S. (2008) Synthesis, characterization and biological activity of some transition metal complexes with Schiff Bases derived from 2-formylindole, salicyladehyde and N-amino rhodanine. *Australian Journal of Basic and Ap-plied Sciences*, **2, 210-220.**

386. Fahmideh, S., Lotf, A.S. and Shahriar, G. (2010) Synthe-sis, characterization and anti-tumour activity of Fe(III) schiff base complexes with unsymmetric tetradentate ligands. Bulletin of Chemical Society of Ethiopia**, 24, 193- 199.**

387. Konstantinovic, S., Radovanovic, C., Cakic, Z. and Vasic, V. (2003) Synthesis and characterization of Cd (II), Ni (II), Cu (II) and Zn (II) complexes with 3-salicylidenehydra- zono-2-indolinone. *Journal of the Serbian Chemical Society*, **68, 641-647.**

388. URL http://wwwchem.uwimona.edu.jm/lab_manuals/ c31lex1.html.

389. D. Rusu, A. Stanila, I. O. Marian, C. O. Marian, M. Rusu, and R. Lucaciu, (2009), Synthesis and Characterization of Some Cobalt (II) Complexes with Amino Acids Having Biological Activities, Rev. Chim. (Bucureti), 60, Nr. 9 **p 939-943.**

390. BURGER, K., (1973), Coordination Chemistry: Experimental Methods, Akademiai Kiado, Budapest, **p.23.**

391. Stefan, L.S., (1994,), Synthesis and Characterization of Some Cobalt (II) Complexes with Amino Acids Having Biological Activities *J. Therm. Anal*., 42, **p.1299.**

392. Shengli J., Mian J., Sanoing C., and Rongzu H., (2001), J. Thermal Analysis and Cal.*,* 66, **p.423.**

393. Batiu, C., Jelic, C., Leopold, N., Cozar, O., and David, L., (2005), Synthesis and characterisation of bismuth (III) vanadate. *Journal of Molecular Structure,* 744-747, p.325.

394. SOCRATES G., (2001), Infrared and Raman Characteristic Group Frequencies: Tables and Charts, 3rd edition, *Wiley, Chichester*, **p.173**

395. SCHRADER, B., (1995), Infrared and Raman Spectroscopy, Methods and Applications, VCH, Weinheim, **p. 220.**

396. Malandrinos G., Dodik., and Louloudim., (2000), Inorg. Chem., **79, p.21.**

397. Zolezzi, S., Decinti, A, and Spodine, D., (1999), Syntheses and characterization of copper (II) complexes with Schiff-base ligands derived from ethylenediamine, diphenylethylenediamine and nitro, bromo and methoxy salicylaldehyde. Polyhedron **18, p.897.**

398. M. M. S. Saif, A. A. Al-Fakih and M. A. M. Hassan, (2017), Antibacterial activity of selected plant (Aqueous and methanolic) extracts against some pathogenic bacteria, *Journal of Pharmacognosy and Phytochemistry* **6(6): 1929-1935.**

399. Parekh J., and Chanda S., (2006), In-vitro Antimicrobial Activities of Extracts of *Launaea procumbens* Roxb. (Labiateae), *Vitis vinifera* L. (Vitaceae) and *Cyperus rotundus* L. (Cyperaceae). *African Journal of Biomedical Research*. **9(2):89-93.**

400. Benlafya K., Karrouchi K., Charkaoui Y., El karbane M., and Ramli Y., (2014), Antimicrobial activity of aqueous, ethanolic, methanolic, cyclohexanic extracts and essential oil of *Nigella sativa* seeds. *Journal of chemical and Pharmaceutical Research*. **6(8):9-11.**

401. CLSI (Clinical and Laboratory Standards Institute). Methods for Dilution Antimicrobial Susceptibility Tests for Bacteria that Grow aerobically; Approved Standard, 10th edn. National Committee for Clinical Laboratory Standards, Wayne, USA, (2015), **88.**

402. Essawi T, and Srour M., (2015), Screening of some Palestinian medicinal plants for antibacterial activity. *Journal of Ethnopharmacology*. **70:343-349.**

403. Valgas C., de-Souza S. M., Smânia E. F. A., and Smânia A. Jr. (2007), Screening methods to determine antibacterial activity of natural products. *Brazilian Journal of Microbiology*. **38:369-380.**

404. Olano I., Alonso-Paz E., Cerdeiras M.P., Fernandez J., Ferreira F., and Moyna P., (2011), Screening of the Uruguayan medicinal plants for anti-microbial activity. Journal of Ethnopharmacology (Part II). **53:111-115.**

405. Lister P. D., Wolter D.J., and Hanson N.D., (2009), Antibacterial-resistant *Pseudomonas aeruginosa*: Clinical impact and complex regulation of chromosomally encoded resistance mechanisms. Clinical Microbiology Reviews. **22(4):582-610.**

406. M. K. Islam, Md. Nuruzzaman, R. I. Ripon, Md. Shalauddin, F. B. Biswas, M. M. Hossain, M. R. Islam, and S. Khan, 2018, Synthesis, Characterization and Bioactivities of Some Novel Oxovanadium (IV) Glycinato Complexes, *European Scientific Journal* Vol.14, No.21 ISSN: 1857 − 7881 (Print) e - ISSN **1857- 7431.**

407. Temitayo, A., Isaac, O. and Olugbena, A. (2012). Structural and antimicrobial studies of coordination compounds of phenylalanine and glycine. *J. Chem.*, *4*(2), 49-59.

408. Negoiu, M., Rosu, T., Saramet, I. and Matei, C. A. (2016). Complexes of Cu(II) and Mn(II) with acylated amino acids derived from glycine and α-alanine. **Analele Universitătii din Bucuresti- Chimie, Anul XIV (serie nouă), I-II, 129-133.**

409. Osunlaja, A. A., Ndahi1 N. P. and Ameh, J. A. (2014). Synthesis, physico-chemical and antimicrobial properties of Co(II), Ni(II) and Cu(II) mixed-ligand complexes of dimethylglyoxime - Part I. *Afr. J. Biotechnol.*, **8(1), 4-11.**

410. Chidambaram, M. V. and Bhattacharya, P. K. (2009). *J. Indian Chem. Soc.,* **47, 881.**

411. Di Bernardo, P., Tomat, G., Zanonata, P., Portanova, R. and Tolazzi, M. (2012). Thermodynamics of vanadyl (IV)-carboxylate complex formation in aqueous solution. **Inorg. Chim. Acta, 145(2), 285-288.**

412. Tomiyasu, H. and Gordon, G. (2014). Stability constants for the oxovanadium(IV)-glycine system in aqueous solution. *J. Coord. Chem.*, **3, 47-56.**

413. Fabian, I. and Nagypal. I. (2016). NMR relaxation studies in solutions of transition metal complexes VI. equilibria and proton exchange processes in aqueous solutions of VO^{2+} glycine system. *Inorg. Chim. Acta*, **62, 193-199.**

414. Sharma, R. (2013). Synthesis, characterization and antimicrobial activity of bis(γ aminobutyrohydroxomate)oxovanadium (IV). *Asain J. Adv. Basic Sci*., **1(1), 45-50.**

415. Islam, M. K., Kanamori, K. and Hossain, M. M. (2016). Synthesis and spectroscopic properties of the first homoleptic histidine complex of vanadium (IV) [VIVO(L-his)(L-Hhis)]ClO4.H2O. *J. Bangladesh Chem. Soc.*, **24(1), 1-8.**

416. Sharma, S. and Sharma, N. (2013). Synthesis, characterization, electrochemistry and antimicrobial activities of bis(hydroxamato)oxidovanadium (IV) complexes. **Chem. Sin., 4(3),108-119.**

417. Amit, R., Y., Vijaya, V. D. and Anand, S. A. (2015). Synthesis, characterization, electrical and biological studies of VO (IV), MoO2 (VI), WO2 (VI), Th (IV) and UO2 (VI) complexes with hydrazone ligand. **Rev. Roum. Chim., 55(9), 537- 542.**

418. Agarwal, R. K., Chakraborti, I. and Sharma, S. K. (2014). Synthesis and characterization of oxovanadium(iv) complexes of schiff-bases derived from 4-aminoantipyrine. *Polish J. Chem.*, **68(6), 1085-1092.**

419. Nakamoto, K. (2013). Complexes of amino acids. Infrared and raman spectroscopy of inorganic and coordination compounds: applications in coordination, organometallics and bioinorganic chemistry. John 6th Ed.; Wiley and Sons: United states. **67-69**.

420. Miller, F. A. and Wilkins, C. H. (2014). Infrared spectra and characteristic frequencies of inorganic ions, their use in qualitative analysis. Anal. Chem., *24***(8), 1253-1294.**

421. Ackarmann, M. N. (2003). Infrared spectrometry of inorganic salts a general chemistry experiment. *J. Chem. Edu.*, *47***, 69-70.**

422. Rangel, M., Tamura, A., Fukushima, C. and Sakurai, H. (2008). In vitro study of the insulin-like action of vanadyl-pyrone and -pyridinone complexes with a $VO(O_4)$ coordination mode. *J. Biol. Inorg. Chem.*, *6***(2), 128-132.**

423. Klich, P. R., Daniher, A. T., Challen, P. R., McConville, D. B. and Youngs, W. J. (2016). Vanadium (IV) Complexes with Mixed O,S Donor Ligands. Syntheses, structures, and properties of the anions Tris(2-mercapto-4 methylphenolato)vanadate(IV) and Bis(2-mercaptophenolato) oxovanadate(IV). Inorg. Chem., *35***(2), 347-356.**

424. Katoh, A., Taguchi, K., Okada, H., Harata, M., Fujisawa, Y., Takino, T. and Sakurai, H. (2010). Synthesis of Oxovanadium Complexes and Their Apoptosis-Inducing Activity in Leukemia Cells. Chem. Lett., *29***(8), 866.**

425. S. Katugampala, I. C. Perera, C. Nanayakkara, and T. Perera, (2018), Synthesis, Characterization, and Antimicrobial Activity of Novel Sulfonated Copper-Triazine Complexes, Hindawi Bioinorganic Chemistry and Applications *Volume*, Article ID 2530851, 7 pages.

426. Institute CaLS, "Methods for dilution antimicrobial susceptibility tests for bacteria that grow aerobically; approved standard—seventh edition," in *M7–A7,* Clinical and Laboratory Standards Institute, *Wayne, PA, USA*, 2006.

427. V. B´ereau and J. Marrot, (2015), "Coordination studies of 5,6- diphenyl-3-(2-pyridyl)-1,2,4-triazine towards Zn2+ cation. Synthesis and characterization by X-ray diffraction and spectroscopic methods," Comptes Rendus Chimie, vol. 8, no. 6-7, **pp. 1087–1092.**

428. D. Eastwood, R. L. Lidberg, and M. S. Dresselhaus, (2015), "Ultraviolet-visible fluorescence spectroscopy of selected polyaromatic hydrocarbons and organometallics on hexagonal graphite and boron nitride," Chemistry of Materials, **vol. 6, no. 2, pp. 211–215.**

429. N. Abeydeera, I. C. Perera, and T. Perera, "Synthesis, characterization, and BSA-binding studies of novel sulfonated zinc-triazine complexes," **Bioinorganic Chemistry and Applications,** vol. 2018, Article ID 7563820, 7 pages, 2018.

430. T. Liu, R. G. Yang, and G. Q. Zhong, (2018), Synthesis, Structural Characterization, and Antibacterial Activity of Novel Erbium(III) Complex Containing Antimony, **Hindawi Bioinorganic Chemistry and Applications,** Article ID 4313197, 9 pages, https://doi.org/10.1155/2018/4313197.

431. W. J. Geary, (2016), " The use of conductivity measurements in organic solvents for the characterisation of coordination compounds," **Coordination Chemistry Reviews, vol. 7, no. 1, pp. 81–122.**

432. K. Nakamoto, (2013), Infrared and Raman Spectra of Inorganic and Coordination Compounds, John Wiley & Sons Inc., New York, NY, USA, 6th edition.

433. H. P. Xiao, S. Aghabeygi, W. B. Zhang, (2017), "A new Zn (II) twodimensional coordination polymer, $\{[Zn(\mu\text{-}4,4'\text{-bipy})(1,4\text{-ndc}) (H_2O)_2]\cdot(H_2O)\}n$ (4,4′-bipy = 4,4′-bipyridine and 1,4-ndc = 1,4-naphthalenedicarboxylate)," *Journal of Coordination Chemistry*, **vol. 61, no. 22, pp. 3679–3686.**

434. G. Q. Zhong, J. Shen, Q. Y. Jiang, and K. B. Yu, (2017), "Synthesis and structural determination of a novel heterometallic complex $[Sb_2(edta)_2\text{-}\mu4\text{-}Co(H_2O)_2]\cdot5.15H_2O$," *Chinese Journal of Chemistry*, **vol. 29, no. 12, pp. 2650–2654, 2011**.

435. J. Shen, Q.,Y. Jiang, G.,Q. Zhong, Y.,Q. Jia, and K.-B. Yu, (2012), "Synthesis, crystal structure and thermal decomposition of a novel 3D heterometallic Sb(III)-Pr(III) complex $[Sb2\text{-}\mu4\text{-}(EDTA)_2Pr(H_2O)5]NO_3\cdot4H_2O$," **Acta Chimica Sinica, vol. 65, no. 16, pp. 1588–1592.**

436. J. Wang, X.,D. Zhang, Z. R. Liu, and W. G. Jia, (2016), "Synthesis and structural determination of binuclear nine-coordinate $(NH_4)_4[Yb_2(dtpa)_2]\cdot9H_2O$," *Journal of Molecular Structure*, **vol. 613, no. 1-3, pp. 189–193.**

437. G. Q. Zhong, J. Shen, Q. Y. Jiang, Y. Q. Jia, M. J. Chen, and Z. P. Zhang, (2015),"Synthesis, characterization and thermal decomposition of SbIII-M-SbIII type trinuclear complexes of ethylenediamine-N,N,N′,N′-tetraacetate (M: Co(II), La(III), Nd(III), Dy(III))," *Journal of Aermal Analysis and Calorimetry*, **vol. 92, no. 2, pp. 607–616.**

438. J. Shen, B. Jin, Q. Y. Jiang, G. Q. Zhong, Y. M. Hu, and J.C. Huo, (2012), "Synthesis, characterization, and magnetic properties of heterometallic trinuclear complex with Sb(III) and Ho(III)," Inorganica Chimica Acta, **vol. 385, pp. 158–163**.

439. Y.C. Guo, Y.Q. Feng, Z. P. Qiao, S. Y. Chen, and S. Z. Huang, (2014), "Syntheses, crystal structures and antibacterial activities of dithiocarbamate complexes [M(MeBnNCS2)3], M (II) Sb(III), Bi(III)," *Chinese Journal of Inorganic Chemistry*, **vol. 30, no. 5, pp. 1031–1037.**

440. A. C. Ekennia, D. C. Onwudiwe, L. O. Olasunkanmi, A. A. Osowole, and E. E. Ebenso, (2015), "Synthesis, DFTcalculation, and antimicrobial studies of novel Zn(II), Co(II), Cu(II), and Mn(II) heteroleptic complexes containing benzoylacetone and dithiocarbamate," Bioinorganic Chemistry and Applications, vol. 2015, Article ID 789063, 12 pages.

441. Saint (ver. 6.02), Shelxtl (6.10), Sadabs (ver. 2.03) (Bruker AXS Inc., Madison, Wisconsin, USA) 2002.

442. Sheldrick M., SHELX-97, program for Crystal Structure Solution and Refinement *(*University of Gottingen, Gottingen, Germany) 2006.

443. Blaschke, R., (2014), Signals excited by the scanning beam, in Electron Microscopy in Mineralogy, edited by H. R. Wenk, (Springer-Verlag, Berlin-Heidelberg) **488-493.**

444. P. Elmer, (1984), Analytical Techniques for Graphite Furnace Atomic Absorption Spectrometry.

445. Pal S., Kyung T.Y., and Myong S.J., (2012). Does the antibacterial activity of silver nanoparticles depend on the shape of the nanoparticle? A study of the gram-negative bacterium Escherichia col. Appl Environ Microbiol **73(6):1712-1720**.

446. N. PETROVI, D. BUELAN, S. COKI and B. NE, (2001),The determination of the content of gold and silver in geological samples, *J. Serb. Chem. Soc. 66*(1)45–52.**

447. S. Nagae, M. Ushijima, S. Hatono, J. Imai; S. Kasuga, H. Matsuura, Y. Itakura, and Y. Higashi. (2011), Chemical and Biological Properties of *S*-1-Propenyl-l-Cysteine in Aged Garlic Extract. *Planta Med.* **60(3), 214-217.**

448. P. Mejnikov, P. Corbi, and C. Aguila. (2013)*,* Synthesis and investigation of complex formation between amino acid (glycine) and various metal ion by using spectroscopic methods *J. Alloys comp*. **307(1-2), 179-183.**

449. C. Batiu; C. Jelic, N. Leopold, O. Cozar; and L. David, (2014), Testing of some synthetic derivatives of L-glutamic acid as inhibitors of soil urease activity. *J. Mol. Struct*. **325-330, 744-747.**

450. Shishkin, V.N., Kudrik, E.V., and Shaposhnikov, G.P., (2010), Synthesis and some properties of transition metal complexes with octa(sulfophenyl)tetrapyrazinoporphyrazine. *Russ. J. Coord. Chem.* **31, 516–520. 37.**

451. Conarmond, J., plunere, P., Lehn, J.M., Agnus, Y., Louis, R., Kahn, O., and Badarous, M. (2014), Dinuclear copper (II) cryptates of macrocyclic ligands: Synthesis, crystal structure, and magnetic properties. Mechanism of the exchange interaction through bridging azido ligands. *J. Am. Chem. Soc.* **104, 6330–6340.**

452. Nassirinia, N., and Sadeghi, N., Amani, S., (2008), Two new alkoxo-bridged dinuclear cooper (II) complexes with 3-aminopyrazidine-2-carboxylic acidas ligand. *J. Coord. Chem*. **61, 796–801.**

453. Rodríguez, A., Sousa-Pedrares, A., García-Vázquez, J.A., and R. A. Sousa, J. (2009), Electrochemical synthesis and characterization of zinc(II) complexes with pyrimidine-2-thionato ligands and their adducts with N,N donors. Polyhedron **28, 2240–2248.**

455. Al-Shaheen J. Amira Al-Mula A. Miaa, (2014), Schiff Base Complexes of Fe (III) Derived from Amino Acids, *Research Journal of Chemical Sciences,* **4(8), 25-32.**

456. J. M. Tunney, A. J. Blake, E. S. Davies, J. Mcmater, C. Wilson and C. D. Garner, (2006) "Synthesis and structure of gold(III) complexes of asymmetric dithiolene ligands "Polyhedron., **25, 2,P. 591.**

457. Nassirinia, N., Sadeghi, N., and Amani S., (2006), Two new alkoxo-bridged dinuclear gold(III)complexes with 3-aminopyrazidine-2-carboxylic acidas ligand. *J. Coord. Chem.* **61, 796–801.**

458. Rodríguez, A., Sousa-Pedrares, A., García-Vázquez, J.A., and R. A. Sousa J. (2014), Electrochemical synthesis and characterization of gold(III)complexes with pyrimidine-2-thionato ligands and their adducts with N,N donors. Polyhedron **28, 2240–2248.**

459. J. S. Griffith, *"Theory of Transition Metal Ions",* (1964) Cambridge University Press, Oxford.

460. Chohan, Zahid H., Praveen M and Ghaffer A., (1998), Synth. React. Inorg. Met. Org. Chem. **28. 1673.**

461. F. Tuna, G. Clarkson, N. W. Alcock and M. J. Hannon, , (2003), The effect of phenyl substiuents on supramolecular assemblies containing directly linked bis-pyridylimine ligands: synthesis and structural characterisation of mononuclear nickel (ii) and dinuclear silver(i) and cobalt(iii) complexes of (2-pyridyl) phenylketazine, *Dalton Trans*., 2149-2155 .

462. D. J. Szalda, C. Creutz, D. Mahajan and N. Sutin, (2012), Synthesis and Structural Analysis of Powder Complex of Tris(bipyridine)cobalt(II) Trifluoromethanesulfonate Octahydrate. Inorg. Chem ., 22(17), 2372-2379.

463. S.G. Telfer, G. Bernardinelli and A.F. Williams, (2001). Diastereospecific synthesis of amino-acid substituted 2,2′-bipyridyl complexes. *Chem. Commun .,* 1498-1499.

464. S.G. Telfer, R. Kuroda and T. Sato, (2003). CD spectra of polynuclear complexes of diimine ligands: theoretical and experimental evidence for the importance of internuclear exciton coupling. Chem. Commun ., 2003, 1064-1065.

465. S. G. Telfer, T. Sato, T. Harada, R. Kuroda, J. Lefebvre and D. B. Leznoff, (2014), Effect of non-covalent interaction on the diastereoselective self-assembly of Cu(ii) complexes containing a racemic Schiff base in a chiral self-discriminating process. Inorg. Chem ., 43(20), 6168- 6176.

466. J. M. Rowland, M. M. Olmstead and P. K. Mascharak, (2011), Low-spin [M (II) (L)$_2$] and [M (III) (L)$_2$]+ (M = Fe and Co) complexes of tridentate azo-containing pyridine/pyrazine amide ligands: structures, properties and redox potential correlations. *Inorg. Chem*., 41(6), 1545-1549.

467. C. Provent, G. Bernardinelli, A.F. Williams and N. Vulliermet, (2010), *Eur. J. Inorg. Chem*, 1963-1967.

468. M. A. Masood, E. J. Enemark and T. D. P. Stack, (1998), Structure and Reactivity Studies of a Nonsymmetric One-Electron Oxidized Cu Bis-phenoxide Complex. *Angew Chem Int Ed Engl.*, 37, 928-932.